The importance of plant-derived lipids for arbuscular mycorrhiza symbiosis and other plant-microbe interactions

Andreas Marius Keymer

Dissertation der Fakultät für Biologie der Ludwig-Maximilians-Universität München

München, 2019

Dissertation eingereicht am: 15. Januar 2019

Tag der mündlichen Prüfung: 10. April 2019

Erstgutachter: Prof. Dr. Caroline Gutjahr
Zweitgutachter: Prof. Dr. Martin Parniske

Eidesstattliche Erklärung:

Ich versichere hiermit an Eides statt, dass die vorgelegte Dissertation von mir selbstständig und ohne unerlaubte Hilfe angefertigt ist.

München, den 9. Januar 2019

Andreas Keymer

Erklärung

Hiermit erkläre ich, dass die Dissertation nicht ganz oder in wesentlichen Teilen einer anderen Prüfungskommission vorgelegt worden ist. Ich habe mich nicht anderweitig einer Doktorprüfung ohne Erfolg unterzogen.

München, den 9. Januar 2019

Andreas Keymer

Table of Content

I. List of Abbreviations

ABC	ATP Binding Casette
ACS	Acetyl-Coenzym A Synthase
ACP	Acyl-acyl Carrier Protein
AM	Arbuscular Mycorrhiza
AMF	Arbuscular Mycorrhiza Fungus
AMS	Arbuscular Mycorrhiza Symbiosis
AMT	Ammonium Transporter
At	*Arabidopsis thaliana*
BCP1	Blue Copper Protein1
BF	Bright Field
CaM	Calmodulin
Ca^{2+}	Calcium Ion
CBX1	CTTC Motif-Binding Transcription Factor 1
CCaMK	Calcium- and Calmodulin- dependent protein Kinase
CNGC	Cyclic Nucleotide-gated Channel
COs	Chitin Oligomers
CSG	Common SYM(biosis) Genes
DAG	Diacylglycerol
DGDG	Digalactosyldiacylglycerols
dis	*disorganized*
DMI	Doesn't Make Infection
EHM	Extra-haustorial Membrane
ER	Endoplasmic Reticulum
ERF	Ethylene Response Factor
ERM	Extraradical Mycelium
ET	Ethylene
ETI	Effector-triggered Immunity
EV	Extracellular Vesicle
EXO	Exocyst
FA	Fatty Acid
FAME	Fatty Acid Methyl Ester
FAS	Fatty Acid Synthase
FATM	Fatty Acid Thioesterase M
GA	Gibberellic Acid
GC	Gas Chromatography
GFP	Green Fluorescent Protein
GPAT	Glycerol 3-phosphate Acyltransferase
HMGR	3-Hydroxy-3-Methylglutaryl Coenzyme A Reductase
Hpa	*Hyaloperonospora arabidopsidis*
HR	Hypersensitive Response
IRM	Intraradical Mycelium
JA	Jasmonic Acid

LCOs	Lipochitooligosaccharides
Lj	*Lotus japonicus*
LPA	Lysophosphatic Acid
LHC	Light Harvesting Complex
MAG	Monoacylglycerol
MCA	Medicago truncatula calcium ATPase
MGDG	Monogalactosyldiacylglycerol
MIG	Mycorrhiza Induced GRAS
MS	Mass Spectrometry
MST	Monosaccharide Transporter
Mt	*Medicago truncatula*
NFP	Nod Factor Perception
NFR	Nod Factor Receptor
NIN	Nodule Inception
NLS	Nuclear Localization Signal
NMR	Nuclear Magnetic Resonace
NUP	Nucleoporins
PAM	Peri-arbuscular Membrane
PAS	Peri-arbuscular Space
PPA	Pre-penetration Apparatus
PTI	Pattern-triggered Immunity
PA	Phosphatidic Acid
PC	Phosphatidylcholine
PCR	Polymerase Chain Reaction
PE	Phosphatidylethanolamine
PI	Phosphatidylinositol
Pi	Phosphate
PS	Phosphatidylserine
PT	Phosphate Transporter
RAD1	Required for Arbuscule Development 1
RAM2	Reduced Arbuscular Mycorrhiza 2
red	*reduced and degenerated*
RNS	Root Nodule Symbiosis
RNAi	RNA interference
ROS	Reactive Oxygen Species
SA	Salicylic Acid
SL	Strigolactone
STR	Stunted Arbuscules
SYMRK	Symbiosis Receptor Kinase
TAG	Triacylglycerol
VAMP	Vesicle-Associated Protein
YFP	Yellow Fluorescent Protein
WGA	Wheat Germ Agglutinin
WRI	Wrinkeled

II. List of Publications

Research Paper:

- **Keymer A**#, Pimprikar P#, Wewer V, Huber C, Brands M, Bucerius SL, Delaux PM, Klingl V, von Roepenack-Lahaye E, Wang TL, Eisenreich W, Dörmann P, Parniske M, Gutjahr C (2017). Lipid transfer from plants to arbuscular mycorrhiza fungi. **eLife** 6. pii: e29107. # These authors contributed equally to the work

- Brands M, Wewer V, **Keymer A**, Gutjahr C, Dörmann P (2018). The *Lotus japonicus* acyl-acyl carrier protein thioesterase FatM is required for mycorrhiza formation and lipid accumulation of *Rhizophagus irregularis.* **Plant Journal,** DOI: 10.1111/tüj.13943.

- **Keymer A,** Huber C, Eisenreich W, Gutjahr C (2018). Tracking lipid transfer by fatty acid isotopolog profiling from host plants to arbuscular mycorrhiza fungi. **Bio-Protocol** 8(7): e2786

Review:

- **Keymer A,** Gutjahr C (2018). Cross kingdom lipid transfer in arbuscular mycorrhiza symbiosis and beyond. **Current Opinion in Plant Biology** 44: 137 - 144

III. Declaration of contribution of co-author

Paper I: Lipid transfer from plants to arbuscular mycorrhiza fungi

Reference: **Keymer A**#, Pimprikar P#, Wewer V, Huber C, Brands M, Bucerius SL, Delaux PM, Klingl V, von Roepenack-Lahaye E, Wang TL, Eisenreich W, Dörmann P, Parniske M, Gutjahr C (2017). Lipid transfer from plants to arbuscular mycorrhiza fungi. **eLife** 6. pii: e29107. # These authors contributed equally to the work

A. Keymer designed, performed and analyzed most of the experiments, created figures and contributed to the conception of this study except the following.

P. Pimprikar identified the mutation in the *RAM2* gene by map-based cloning and Sanger sequencing (Figure supplement 3 and 4 corresponding to Figure 1), imaged the arbuscule phenotype of *ram2* and performed the complementation of *ram2* (Figure 1B), visualized the activity of *DIS* and *RAM2* promoter (Figure 2A and 2B; Video 1, 2, 3, 4, 5 and 6) and provided cDNA samples for qPCR analysis in Figure 6. V. Wewer, M. Brands, E. Roepenack-Lahaye and Prof P. Dörmann performed mass spectrometry for lipid profiling (Figure 4E, Figure 5 including corresponding supplemental Figures 1-3 and 5 -11 and Figure 7). C. Huber and Prof. W. Eisenreich performed isotopolog profiling (Figure 8 including corresponding supplemental Figures 2 – 4). S. Bucerius and M. Parniske identified the mutation in the *DIS* gene by map-based cloning and Next Generation sequencing, imaged the arbuscule phenotype and performed complementation of *dis* (Figure 1A and corresponding supplemental Figure1). Technician V. Klingl supported some experiment by cloning, hairy root transformation and cDNA preparation under the supervision of A. Keymer. PM. Delaux performed phylogenic and syntheny analysis of DIS (Figure 3 including the corresponding Figure 3). Prof. M. Parniske contributed to the concept and materials of this study and editing of the manuscript. Prof. C. Gutjahr conceived the study, designed experiments, supervised the study, and wrote the manuscript.

Signature of co-first-author:

Andreas Keymer

Signature of co-first-author:

Dr. Priya Pimprikar

Signature of the supervisor:

Prof. Dr. Caroline Gutjahr

Paper II: The *Lotus japonicus* acyl-acyl carrier protein thioesterase FatM is required for mycorrhiza formation and lipid accumulation of *Rhizophagus irregularis*

Reference: Brands M, Wewer V, **Keymer A**, Gutjahr C, Dörmann P (2018). The *Lotus japonicus* acyl-acyl carrier protein thioesterase FatM is required for mycorrhiza formation and lipid accumulation of *Rhizophagus irregularis.* **Plant Journal,** DOI: 10.1111/tüj.13943.

A. Keymer designed, performed, analyzed and created figures for the following experiments:

- Imaging of *fatm* stunted arbuscule phenotype (Figure 2)
- Genetic complementation of *fatm* (supplemental Figure S2)

A. Keymer further contributed to editing the manuscript.

Signature of the supervisor:

Prof. Dr. Caroline Gutjahr

Manuscript I: Defective lipid biosynthesis of *Arabidopsis thaliana* perturb colonization by the biotrophic pathogen *Hyaloperonospora arabidopsidis*

Reference: **Keymer A.**, Brands M., Banhara A., Dörmann P, Parniske M., Gutjahr C. (2018). Defective lipid biosynthesis of *Arabidopsis thaliana* perturbs colonization by the biotrophic pathogen *Hyaloperonospora arabidopsidis*

A. Keymer designed, performed and analyzed most of the experiments, created figures, wrote the manuscript and contributed to the conception of this study except the following.

M. Brands and Prof. P. Dörmann performed lipid profiling (Figure 3). A. Banhara performed cell death measurements on *kasI* (Figure 2D) and contributed to materials and methods of this study. Prof. M. Parniske contributed to the concept and materials of this study. Prof. C. Gutjahr conceived the study, designed experiments, supervised the study and edited the manuscript.

Signature of the supervisor:

Prof. Dr. Caroline Gutjahr

IV. Summary

Ever since their origin, plants have been associated with diverse microorganisms, above as well as below ground. Particularly widespread and therefore prominent is the plant interaction with arbuscular mycorrhiza fungi (AMF). Arbuscular mycorrhiza (AM) is an ancient mutualistic symbiosis between most land plants and obligate biotrophic fungi of the *Glomeromycotina.* The key feature of this plant-microbe association is the reciprocal nutrient transfer between both organisms.

Nutrient exchange in AM symbiosis (AMS) has been studied already for decades and mineral nutrients such as phosphate, ammonia and sulfate were identified as important commodities transferred from the fungus to the plant. Vice versa, hexoses have been found to be translocated from the plant to the fungus as reward. This nutrient swap has great impact on health, physiology and overall performance of the host plant. It also has effects at a much larger scale on global carbon cycles and the sustainment of complex ecosystems such as tropical rainforests.

AMF colonize plant roots via an intraradical hyphal network and insert arbuscules, which are highly branched tree-shaped structures, in single inner cortical root cells. The arbuscule and its host cell represent the main interface of this association and thereby the core element, at which nutrient transfer takes place. The host plant is in control of AM root colonization by the fungus, as a range of plant mutants is available, which perturb root colonization. A number of plant AM mutants, exhibit a similar AM-phenotype, with a reduced percentage of root length colonization and a perturbed arbuscule morphology, which is characterized by small, less branched and stunted arbuscules.

The two *Lotus japonicus* mutants *dis* (*disorganized arbuscule*) and *ram2* (*reduced arbuscular mycorrhiza*)*,* which are impaired in the establishment of AMS, have been identified via a forward genetics screen. Both, *DIS* and *RAM2,* are AM-specific fatty acid/lipid biosynthesis genes in *Lotus japonicus*. *DIS* encodes a β-keto-acyl ACP synthase I (KASI), crucial for fatty acid chain elongation from C4 to C16 and *RAM2* encodes glycerol-3-phosphate acyltransferase 6 (GPAT6), which acts bifunctionally by catalyzing dephosphorylation as well as acylation of glycerol-3-phosphate (G3P) in order to produce sn2-monoacylglycerol (MAG).

In this doctoral thesis, both genes were characterized in-depth, concerning function, expression and requirement for the symbiosis. I was able to show that AM-competent

host plants harbor an AM-specific lipid biosynthesis machinery in their genomes, which is used to produce lipids exclusively in arbuscule containing cells. Strikingly, I revealed that these lipids are transported to the obligate biotrophic fungus for its nourishment. Via application of $^{13}C_6$-glucose to colonized plants, followed by isotopolog profiling, I could show that plant-derived lipids are transported to the fungus in colonized *L. japonicus* wildtype plants. In contrast, lipid transport was perturbed in both lipid biosynthesis mutants, *dis* and *ram2,* and in the AM-specific ABCG half-transporter mutant *str* (*stunted arbuscules*). In addition, I collaborated with the laboratory of Peter Dörmann (University of Bonn) in the characterization of the AM-specific fatty acid thioesterase FatM, which terminates fatty acid chain elongation by hydrolysis of the acyl-ACP thioester bond. FatM is a further essential component of the AM-exclusive fatty acid/lipid biosynthesis machinery in arbuscocytes (arbuscule-containing cells) and acts in the same pathway with DIS and RAM2.

Literature suggests that the dependence on host lipids or lipid parasitism occur in a range of interorganismic associations with participants from almost all kingdoms. By investigating the influence of plant-derived lipids on the detrimental association of *Arabidopsis thaliana* with the oomycete *Hyaloperonospora arabidopsidis (Hpa),* this thesis goes beyond the boundaries of AM research. *Hpa*-infected *Arabidopsis thaliana* mutants, which carry their mutations in *KASI* and *GPAT6*, that are homologs of *DIS* and *RAM2,* exhibited severe impairment in colonization by and development of *Hpa*. These results hint towards a prominent role of plant-derived lipids also for oomycete-plant interactions.

V. Zusammenfassung

Seit ihrem Ursprung sind Pflanzen mit unterschiedlichen Mikroorganismen sowohl über- als auch unterirdisch vergesellschaftet. Weit verbreitet und daher von besonderer Bedeutung ist die Interaktion von Pflanzen mit arbuskulären Mykorrhiza Pilzen (AMP). Die arbuskuläre Mykorrhiza (AM) ist eine evolutionär alte Symbiose, die zwischen den meisten Landpflanzen und den obligat-biotrophen Pilzen der *Glomeromycotina* ausgebildet wird. Das Hauptmerkmal dieser Pflanzen-Mikrobien-Interaktion ist der reziproke Nährstoffaustausch zwischen beiden Organismen.

Der Nährstoffaustausch der arbuskulären Mykorrhiza Symbiose (AMS) wird bereits seit Jahrzenten erforscht. Hierbei wurden mineralische Nährstoffe wie Phosphat, Ammonium und Sulfat als wichtige Stoffe identifiziert, die von dem Pilz zur Pflanze transportiert werden. Als Gegenleistung wurden Hexosen ausfindig gemacht, die in entgegengesetzter Richtung von der Pflanze zum Pilz transportiert werden. Dieser Nährstoffhandel wirkt sich erheblich auf die Gesundheit, die Physiologie und das allgemeine Leistungsvermögen der Wirtspflanze aus. In einem jedoch noch größeren Ausmaß beeinflusst dieser Nährstoffaustausch außerdem globale Kohlenstoffkreisläufe und die Erhaltung komplexer Ökosysteme, wie die der tropischen Regenwälder.

AMP besiedeln die Pflanzenwurzeln durch ein intraradikales Hyphennetzwerk und kolonisieren zusätzlich einzelne Wurzelzellen des inneren Kortex durch die Ausbildung von Arbuskeln (hoch-verzweigte baumförmige Strukturen). Die Schnittstelle zwischen Arbuskel und Wirtszelle stellt das Kernstück der Symbiose dar, da an dieser der Nährstoffaustausch stattfindet. Wie die Existenz einer Reihe von Pflanzenmutanten, welche die Wurzelkolonisierung beeinträchtigen, zeigt, kontrolliert die Wirtspflanze die Kolonisierung durch den Pilz. Einige pflanzliche AM-Mutanten weisen einen ähnlichen AM-Phänotypen auf, der durch eine reduzierte Wurzelkolonisierungsrate und eine gestörte Arbuskelmorphologie (kleine, gering-verzweigte und verkümmerte Arbuskeln) gekennzeichnet ist.

In einem klassisch-genetischen Screen wurden die beiden *Lotus japonicus* Mutanten *dis* (*disorganized arbuscules*) und *ram2* (*reduced arbuscular mycorrhiza*), welche in der Ausbildung der AMS beeinträchtigt sind, identifiziert. *DIS* und *RAM2* sind beides AM-spezifische Fettsäure- bzw. Lipidbiosynthese Gene in *Lotus japonicus. DIS* kodiert für eine β-Keto-Acyl-ACP Synthase I (KASI), die für die Verlängerung der

Fettsäurekette von C4 nach C16 entscheidend ist, während *RAM2* für eine Glycerol-3-Phosphat Acyltransferase 6 (GPAT6) kodiert, die durch die Katalyse der Dephosphorylierung und der Acylierung von Glycerol-3-phosphat (G3P) bifunktional wirkt, um sn2-Monoacylglycerol (MAG) herzustellen.

In dieser Doktorarbeit wurden beide Gene betreffend Funktion, Expression und deren Notwendigkeit für die Symbiose charakterisiert. Es konnte herausgefunden werden, dass AM-kompetente Wirtspflanzen einen AM-spezifischen Lipidbiosyntheseweg besitzen, der genutzt wird, um Lipide ausschließlich in Arbuskel-enthaltenden Zellen zu produzieren. Außerdem konnte gezeigt werden, dass diese Lipide zum obligat-biotrophen Pilz für dessen Ernährung transportiert werden. Durch die Auswertung der Isotopolog-Profile nach der Zugabe von $^{13}C_6$-Glukose zu kolonisierten Pflanzen, konnte gezeigt werden, dass in kolonisierten *Lotus japonicus* Wildtyp-Pflanzen pflanzliche Lipide zum Pilz transportiert werden. Im Gegensatz dazu war der Lipidtransport in beiden Lipidbiosynthesemutanten, *dis* und *ram2,* sowie in der AM-spezifischen ABCG Halb-Transporter Mutante *str* (*stunted arbeuscues*) beeinträchtigt. Drüber hinaus wurde in Kollaboration mit dem Labor von Peter Dörmann (Universität Bonn) die AM-spezifische Fettsäure-Thioesterase FatM charakterisiert, welche die Verlängerung der Fettsäurenkette mittels Hydrolyse der Acyl-ACP Thioester Bindung beendet. FatM ist eine weitere essentielle Komponente des AM-exklusiven Fettsäure-/Lipidbiosyntheseweges in Arbuskozyten (Arbuskel-enthaltende Zellen) und agiert im selben Signalweg wie *DIS* und *RAM2*.

Die Fachliteratur legt nahe, dass die Abhängigkeit von Wirtslipiden bzw. das Phänomen des Lipid-Parasitismus für eine Reihe von interorganismischen Vereinigungen mit Vertretern aus fast allen Reichen bekannt ist. Durch die Erforschung des Einflusses pflanzlich-abstammender Lipide auf die schädliche Interaktion von *Arabidopsis thaliana* mit dem Oomyceten *Hyaloperonospora arabidopsidis* (*Hpa*), geht diese Arbeit über die AM-Forschung hinaus. *Hpa*-infizierte *Arabidopsis* Mutanten, die Mutationen in *KASI* bzw. *GPAT6* (Homologe von *DIS* bzw. *RAM2*) tragen, wiesen eine starke Beeinträchtigung sowohl in der Kolonisierung als auch in der Entwicklung von *Hpa* auf. Diese Ergebnisse deuten auf eine bedeutende Rolle pflanzlicher Lipide auch für Oomyceten-Pflanzen-Interaktionen hin.

VI. Introduction:

1. Plant-microbe interaction

Plants are not axenic independent organisms but are hosts for a diverse community of microorganisms (fungi, archaea, oomycetes, bacteria etc.) (Müller et al. 2016). In fact, plants have been associated with microorganisms (so called plant-microbiota) ever since their origin hundreds of million years ago (Busby et al. 2017). These interactions, present above as well as below ground, occur either attached to or inside of plant tissue and cover the whole spectrum from beneficial symbioses to plant diseases (Bary 1879). Within these diverse interorganismic associations, both partners have successfully coevolved with each other. Plant hosts do not only communicate with a broad range of microorganisms but are able to discriminate between beneficial and pathogenic interactions. Pathogenic microbes provoke devastating effects on plant health and lead to economically significant crop loss every year (Salanoubat et al. 2002; Dean et al. 2012). Whereas, favorable plant-microbe interactions have compelling advantageous impact on plant nutrition, defense and growth (Compant, Clément, and Sessitsch 2010; Mendes et al. 2011; Friesen et al. 2011; Selosse et al. 2014). Therefore, research efforts focusing on mutualistic plant-microbe interactions play a key role to develop urgently needed microbe-based solutions for a sustainable future agriculture and forest management (Sessitsch and Mitter 2014; Busby et al. 2017).

Microbes inhabit the rhizosphere, which defines the millimeters of soil in direct contact with the plant root, stick on the leaf respectively root surface (phylloplane/ rhizoplane) or colonize the endosphere of leaves and roots. These spheres and planes represent discriminating and determining environments for plant-microbiota and herein resulting ecological and biological processes (Bais et al. 2006).

Soil is considered as a particularly complex and diverse habitat. With millions of species and billions of individual organisms found within the soil of a single ecosystem, it represents one of the largest biodiversity reservoirs on Earth (Bardgett and van der Putten 2014). The foundation of the soil food web is shaped by microbes, who significantly contribute to the functioning of ecosystems (Brussaard 1997; Nielsen et al. 2015). Fungi and bacteria represent the majority of soil microbes and account for most of belowground biomass (Fierer et al. 2009).

2. Arbuscular mycorrhiza symbiosis

2.1 A living fossil of root endosymbiosis

Among the soil-living plant-microbiota, arbuscular mycorrhiza fungi (AMF) are a remarkable example of mutualistic fungal organisms. According to fossil findings and phylogenetic analyses, AMF have successfully coevolved with their host plants about 400-500 million years ago, coinciding with the plant colonization of terrestrial environments (Parniske 2000; Martin 2017; Brundrett and Tedersoo 2018). AMF have an enormous host-range as they form a mutualistic interaction with over 80 % of all land plants (Smith and Read 2008; Spatafora et al. 2016). This makes AM symbiosis (AMS) the most abundant and pervasive terrestrial symbiosis (Fitter 1996).

Over the years AMF have undergone a vivid time of taxonomic revisions, which illustrates the difficulty in resolving the earliest branches in fungal genealogy. Using ribosomal DNA-based phylogenies, Schüßler et al. placed them in the *Glomeromycota* phylum, a sister group of the *Dikarya* (Schüßler et al. 2001). Whereas, a more recent phylum-level phylogenetic classification of zygomycete fungi, based on genome-scale data, placed AMF in the subphylum *Glomeromycotina*, closely related to *Mortierellomycotina* (Spatafora et al. 2016).

AMF harbor some distinct features in terms of age, lifestyle and genetic make-up. Being morphologically unaltered since 400-500 million years, these fungi could be addressed as “living fossils” (Parniske 2008). Their hyphal network is coenocytic, usually aseptate and characterized by a cytoplasm with hundreds of nuclei. In accordance, AMF produce multinucleated spores (Kamel et al. 2016; Lanfranco et al. 2016). Some mating-related processes have been reported and latest findings demonstrated that AMF can generate genetic diversity via internuclear recombination in a dikaryotic life stage (Corradi and Brachmann 2017; Chen et al. 2018). Albeit, spores are able to germinate in absence of their partner, AMF rely on a photoautotrophic host to complete their life cycles. As such, they are obligate biotrophs.

Although, most plants do not depend entirely on the association to AMF and are able survive on their own, plants in symbiosis with *Glomeromycotinan* fungi benefit substantially. Numerous scientific studies have shown that arbuscular mycorrhiza symbiosis (AMS) significantly supports plant growth and strengthens resistance against biotic as well as abiotic stresses (Auge 2001; Ruiz-Lozano 2003; Gohre and

Paszkowski 2006; Liu et al. 2007; Gianinazzi et al. 2010; Pérez-de-Luque et al. 2017; Smith et al. 2011). Particularly these plant promoting features embody great potential in order to reduce fertilizer and pesticide usage for a more sustainable crop production and further fuel the need for onward in-depth research on arbuscular mycorrhiza symbiosis (Berruti et al. 2016).

2.2 Arbuscular mycorrhiza development

The name arbuscular mycorrhiza has originated from the Latin word “arbuscula” meaning “little tree” and a combination of the Greek words “myces“ (fungus) and “rhiza” (root). As the term already suggests, the prime developmental feature of this association is a fungal derived tree-shaped structure: the arbuscule. Arbuscule generation is the result of a successful fungal colonization of the plant root. The colonization process is fully and tightly controlled by the plant and can be separated into distinct steps by fungal progression through the host root (Gutjahr and Parniske 2013).

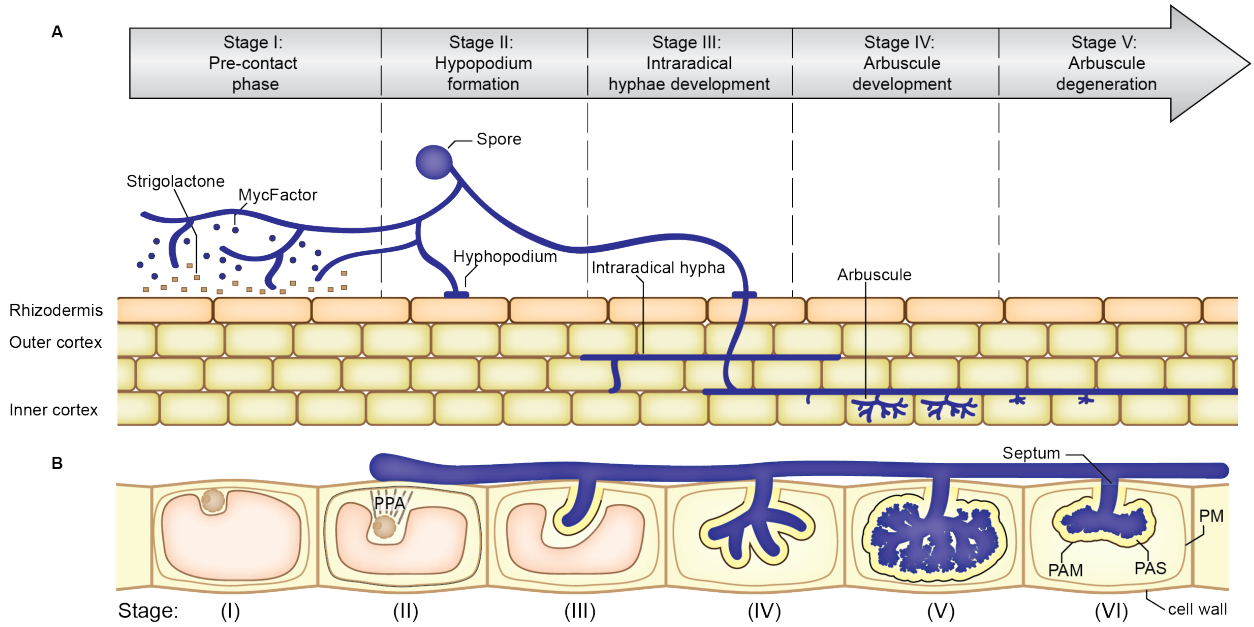

Figure 1: (A) Schematic representation of the root colonization process by arbuscular mycorrhiza fungi, dissected in five distinct stages. (B) Schematic representation of seven stages of arbuscule development inside a cortical root cell. (Figure modified from Pimprikar and Gutjahr 2018)

i) *Pre-contact phase* – Reciprocal recognition

Colonization of the root by AM fungi is initiated via chemical cross-talk in the pre-contact phase (MacLean et al. 2017). In phosphate deficient conditions, the plant exudes strigolactone (SL), a carotenoid-derived plant hormone (Yoneyama et al. 2007; Yoneyama et al. 2012; Kretzschmar et al. 2012; Al-Babili and Bouwmeester 2015). SLs are perceived by the fungus and trigger enhanced metabolic activity (Tsuzuki et al. 2016). This results in accelerated spore germination, hyphal branching and fungal growth towards the plant root (Buée et al. 2000; Akiyama et al. 2005; Besserer et al. 2006; Besserer et al. 2008). How exactly SLs are perceived is still not fully understood. But calcium signaling might play a significant role, as intracellular calcium levels change quickly in fugal hyphae upon SL perception (Moscatiello et al. 2014). In addition to SLs, N-acetylglucosamine (GlcNAc), which is exported via the plasma membrane harbored transporter NOPE1, has been identified as another bioactive molecule to initiate the establishment of AMS in maize and rice (Nadal et al. 2017). To answer to the plant-derived chemical cocktail, also AMF synthesize chemical signaling molecules. The so-called Myc-factors are produced by activated AMF to act as symbiotic cues, which induce repetitive calcium oscillations in root cells (Maillet et al. 2011). Myc-factors represent a cocktail of sulphated and non-sulphated lipochitooligosaccharides (S-LCO and NS-LCO) as well as the short-chain chitooligosaccharides (CO) (Maillet et al. 2011; Genre et al. 2013). Apparently, individual host plants differ in their recognition capability of Myc-LCOs and Myc-COs, which implies the existence of plant species specific Myc-factor receptor combinations (Sun et al. 2015). In addition to calcium spiking, Myc-factor perception leads to drastic gene expression changes, starch accumulation and root branching of the host (Kosuta et al. 2003; Oláh et al. 2005; Navazio et al. 2007; Kosuta et al. 2008; Gutjahr et al. 2009; Kuhn et al. 2010; Chabaud et al. 2011; Maillet et al. 2011; Bonfante and Genre 2015). All these events taking place inside the plant root prime physical interaction and fungal accommodation in the following phases.

ii) *Pre-penetration phase* – Hyphopodium formation

Mutual acquaintance leads to fungal growth towards the plant root and first physical interaction of both partners. Upon hyphal attachment on the root surface, the hyphal

tip differentiates and forms an attachment structure, the hyphopodium. In response to chemical and mechanical signals emanating from the fungal structure, drastic rearrangements inside the adjacent plant cell take place. First, the nucleus of the cell migrates directly underneath the position of the hyphopodium, then leaves that position in order to traverse the vacuole. The second nuclear migration across the cell lumen is accompanied by the assembly of the pre-penetration apparatus (PPA) (Genre et al. 2005; Genre et al. 2009). The PPA represents an intracellular accommodation structure, which is produced by the plant ahead of hyphal entry into the cell in order to predetermine and guide the fungal colonization of the root (Genre et al. 2005; Genre et al. 2008). The PPA resembles a cytoplasmic bridge across the vacuole, which is surrounded by cytoskeletal microtubules and microfilaments, a lager quantity of ER membranes as well as Golgi vesicles, polymorphic mitochondria and plastids, which are associated to this specific structure (Bonfante and Genre 2008). The nucleus moves ahead of the growing PPA. PPA formation erupts dramatic changes in the metabolic activity and a complete reorganization of a fully differentiated cortical cell that accomplishes functional trafficking service of the entire cellular machinery in order to enable AM establishment. Interestingly, this radical rearrangement process seems to be completely reversible (Sieberer et al. 2012).

iii) *Intraradical hyphae development* – Root endosphere entry

After the PPA has successfully formed and spans the whole cell width, hyphal ingress into the root cell takes place (Genre et al. 2005). Although, the exact entry position varies between different host plants, AMF always form a hyphopodium to enter the root. In case of *Lotus japonicus,* the hypha enters the rhizodermis between two adjacent cells, whereas in *Medicago truncatula,* the entering hypha grows through one rhizodermal cell (Bonfante et al. 2000; Genre et al. 2005). In any case, it seems that the fungus must at least once passage a cell intracellularly to be able to progress into the inner cortex. The intracellular traverse might be a plant request to control fungal colonization of the cortex. Once the fungus has reached the inner cortical cells, the hypha starts to spread longitudinally and colonizes single inner cortical cells (Demchenko et al. 2004).

iv) *Arbuscule development* – Inner cortical cell colonization

The arbuscule is a differentiated highly-branched tree-like hyphal structure, which is formed upon fungal colonization of single inner cortical root cells (Pimprikar and Gutjahr 2018). Both, the fungal arbuscule and the arbuscule accommodating cortical cell (arbuscocyte) constitute together the core component and main symbiotic interface of this mutualistic association (Parniske 2008; Lanfranco et al. 2012).

Two distinct characteristic types of hyphal progression and arbuscule insertion in the inner cortex have been described for AMF (Bonfante and Genre 2008). However, also intermediate patterns are known (Dickson 2004). The type of colonization is determined by both, fungus and host plant. The *Paris*-type is characterized by intracellular hyphal progression. The fungus transverses longitudinal the inner cortical cells and subsequently produces an arbuscule. The *Arum*-type, mostly seen in colonized legumes including *L. japonicus,* is defined by intercellular hyphal spread in the apoplast, which is followed by selective arbuscule colonization of distinct cells (Bonfante and Genre 2008).

The *Arum*-type arbuscule development takes place in five stages. Analogous to hyphal root entry and progression, also arbuscule formation requires significant rearrangements of the accommodating cell, which is controlled by the host.

Prior to hyphal entry, nuclear migration and PPA formation in the arbuscocyte is reported (stage I). Stage II is initiated by hyphal entry. Although, the hypha penetrates the plant cell wall, the host plasma membrane does not rupture but rather invaginates. This implies that neither the fungal hypha nor the formed arbuscule is ever in direct contact with the plant cytoplasm. Accordingly, hyphal entry and arbuscule branching triggers synthesis of a specific plant-derived membrane, the peri-arbuscular membrane (PAM). This membrane continually envelops the fungal arbuscule and enables the separation of the fungus from the plant cytoplasm (Remy et al. 1994; Harrison 2005). The PAM composition differs from the plasma membrane composition explicitly as it harbors a specific set of PAM-localized proteins (Pumplin and Harrison 2009; Roth et al. 2018). Enveloped by the PAM, the developing arbuscule further branches and subsequently matures (stage III & IV). The first arising branches of the differentiating hypha are lower-order branches and define the birdfoot-stage, which is denoting for a maturing arbuscule (III) (Gutjahr and Parniske 2013). When the arbuscule is matured and fully branched it almost fills out the entire housing cortical

cell (IV). The mature arbuscule can be subdivided into two PAM domains - the trunk and branch domain. Both domains can be distinguished in regard of their protein composition (Gutjahr and Parniske 2013).

Extensive branching of the arbuscule demands a rapid *de novo* synthesis of the PAM. Experimental data suggest that exocytosis plays a significant role in arbuscule formation (Zhang et al. 2010; Genre et al. 2012; Gutjahr et al. 2012). For example, PAM-localized exocytotic vesicle-associated membrane proteins (VAMPs) seem to be indispensable for arbuscule formation (Ivanov et al. 2012). Besides PAM formation, cellular reorganizing processes to accommodate the symbiotic interface include vacuolar fragmentation, proliferation of plastids and mitochondria around this structure as well as the actin and microfilament-based formation of a basket-like structure around the arbuscule. Moreover, ER and Golgi vesicle aggregate around the PAM and the nucleus moves from the cell periphery underneath the arbuscule center (Bonfante-Fasolo 1983; Fester et al. 2001; Lohse et al. 2005; Pumplin and Harrison 2009).

A mature arbuscule is maintained for 2-5 days before degradation is initiated (Alexander et al. 1988; Kobae and Hata 2010). The short arbuscule lifetime leads to a high turnover and to a constant and simultaneous formation and degradation of arbuscules in the colonized root. Arbuscule degradation (stage V) is characterized by collapse of the branch domain, shrinking of the arbuscule and disconnection of the senescing arbuscule from the hyphal network via introduction of a septum (Gutjahr and Parniske 2013). On the plant side, degradation of the arbuscule goes along with degeneration of the PAM including its anchored proteins and increase of peroxisomes around the collapsing arbuscule (Pumplin and Harrison 2009). Peroxisomes might either be involved in recycling processes of the PAM or protect the plant cell from reactive oxygen species. Degeneration of the arbuscule and the reprogramming of the arbuscocyte is structured and organized in order to ensure the survival of the plant cell. Considering this massive rearrangement processes upon arbuscule formation including costly practices such as organelle and membrane synthesis, the short lifetime of arbuscules is hard to explain and still remains an open question. One could argue that the high turnover ensures a tight regulation, which facilitates the high efficiency of this symbiosis for both mutualistic partners and protects the host plant against fungal cheaters (Gutjahr and Parniske 2017).

2.3 Signal transduction in arbuscular mycorrhiza symbiosis

Successful accommodation of AMF inside the root requires the activation of a signaling cascade that results in transcriptional reprogramming of the host cell. This cascade, which facilitates signal transduction from the plasma membrane to the nucleus is not exclusively required for AM colonization but is also coopted by the evolutionary younger root nodule symbiosis (RNS) (Oldroyd 2013). RNS is a mutualistic interaction of members from the legume family and nine additional plant families with nitrogen-fixing bacteria like rhizobia or species of the actinobacterial genus *Frankia* (Griesmann et al. 2018). The plant host accommodates the bacteria in a unique organ, the nodule. Rhizobia colonize these nodules, differentiate and fix nitrogen via its conversion to ammonium, which is available for the host (Kistner and Parniske 2002; Oldroyd and Downie 2008).

Both endosymbioses depend on so-called common symbiosis genes (CSG). These CSG are decisive for integration and transduction of symbiotic signals from the plasma membrane to the nucleus. CSG are functionally conserved in many plant species, for example in rice, what also indicates their existence prior to the diversification of angiosperms (Markmann et al. 2008; Gutjahr et al. 2008). Moreover, homologs of these genes are also present in bryophytes and in the green algae order Charales, which supports the hypothesis that the CSGs evolved in plants prior to land colonization (Wang et al. 2010; Delaux et al. 2013). The AM phenotype of all CSG defective mutants is characterized by early block of fungal colonization in the outer cell layers, which explains the early and fundamental role of CSGs in AM development (Kistner et al. 2005). Besides the existence of this cascade, also CSG-independent AM-signaling components have been discovered, which highlight the existence of additional and exclusive AM-signaling cascades (Kosuta et al. 2003; Siciliano et al. 2007; Gutjahr et al. 2008; Kuhn et al. 2010; Gutjahr et al. 2015).

i) Signal integration

The precise plant receptor for Myc-factor perception and signal integration remains still elusive. Though, some evidence suggests it is a putative member of the LysM family (Op den Camp et al. 2011; Zhang et al. 2014; Miyata 2014; Buendia et al. 2015). In addition, another plasma membrane-anchored protein, the receptor-like kinase

SYMRK/DMI2 (SYMBIOSES RECEPTOR KINASE/DOESN'T MAKE INFECTIONS 2), is required for AM and RNS (Stracke et al. 2002; Gherbi et al. 2008; Markmann et al. 2008; Antolín-Llovera et al. 2014). Perinuclear calcium oscillations triggered by Myc-factor perception mark the initialization of the common symbiosis signaling cascade. Downstream of Myc factor perception, the signal responsible for perinuclear calcium oscillations is transmitted to the nucleus in order to create nuclear calcium spiking. Several channels, which are required for signal integration have been identified in the nuclear envelope. The three cyclic nucleotide gated channels CNGC15 a, b and c are permeable for Ca^{2+} and its respective mutants are perturbed in AM-symbiosis (Charpentier et al. 2016). CASTOR and POLLUX in *Lotus*, respectively DMI1 in *Medicago,* act as counter ion channels for potassium (Charpentier et al. 2008; Venkateshwaran et al. 2012). MCA8 is a Ca^{2+}-dependent ATPase (Capoen et al. 2011) and NUP85, NUP133 and NENA form the nuclear pore complex whose exact roles are yet not fully understood but possibly could be involved in second messenger signal integration (Kanamori et al. 2006; Saito et al. 2007; Groth et al. 2010; Binder and Parniske 2013). Furthermore, mevalonate, synthesized via HMGR1, is apparently sufficient to trigger Ca-spiking. As such, mevalonate represents a second messenger in signal transduction (Kevei et al. 2007; Venkateshwaran et al. 2015).

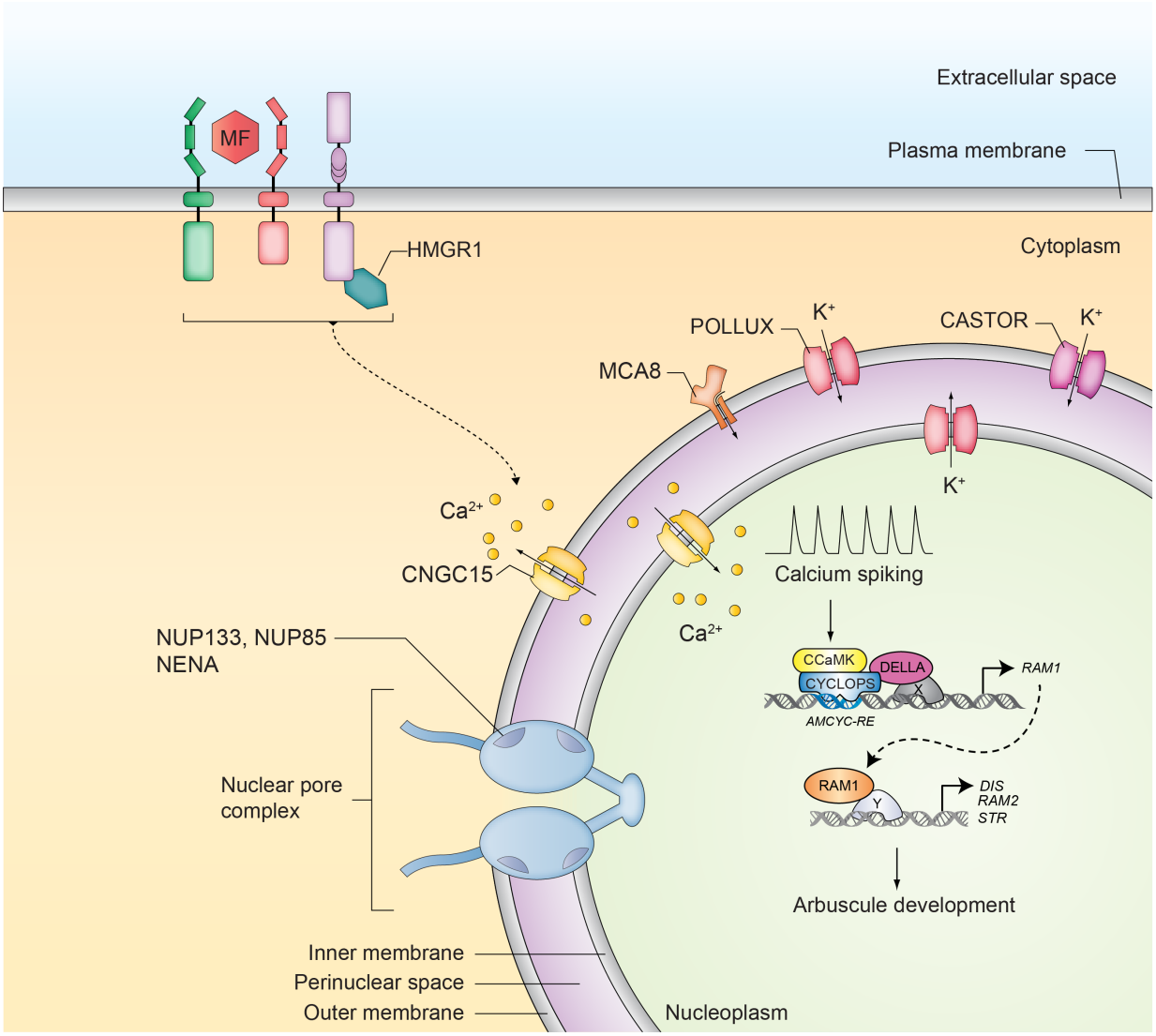

Figure 2: Schematic overview of AM signal transduction upon Myc factor perception via the common symbiosis signaling pathway in a root cell (Figure modified from Singh and Parniske 2012).

ii) Signal decoding and transcriptional response

The calcium- and calmodulin-dependent serine/threonine protein kinase CCaMK constitutes a decoder for symbiotic calcium spiking in the nucleus. CCaMK is one of the core components of the common symbiosis proteins (CSP) (Miller et al. 2013). As a consequence, *ccamk/dmi3* mutants are neither able to form mutualistic associations with rhizobia nor with AMF but show normal symbiotic calcium oscillations (Levy et al. 2004; Mitra et al. 2004; Kistner et al. 2005; Gutjahr et al. 2008). Additionally, to the kinase domain, CCaMK contains three EF hands and a calmodulin binding domain. Upon calmodulin and calcium binding, the kinase is released from its auto inhibition (Miller et al. 2013). The key significance of CCaMK as symbiotic signaling decoder is

evident, as a mayor part of Myc-LCO seems to be dependent on CCaMK (Czaja et al. 2012; Camps et al. 2015). Moreover, ectopic expression of an autoactive version of NLS-CCaMK^{314}, which contains only the kinase domain, is sufficient for induction of cytoplasmic aggregations, simulation of PPA-like structures in cortical cells and to induce AM marker gene expression in non-colonized roots (Takeda et al. 2012; Takeda et al. 2015). A direct phosphorylation target of CCaMK is the transcriptional activator CYCLOPS/IPD3 in *Lotus/Medicago* (Zipfel and Oldroyd 2017; Singh et al. 2014).

CYCLOPS is a DNA-binding transcriptional activator. Its activity is determined by phosphorylation of two serine residues within the N-terminal regulatory domain (Yano et al. 2008; Messinese et al. 2007; Singh et al. 2014). In *L. japonicus* and *O. sativa cyclops* mutants are able to host internal hyphae but not arbuscules, whereas in *Medicago* mutants, fungal colonization is only affected by a reduced percentage of colonization, which implies that *Medicago* harbors a further activator in addition to IPD3 downstream of DMI3 (Yano et al. 2008; Gutjahr et al. 2008; Horváth et al. 2011; Jin et al. 2018). If CCaMK can be seen as master decoder of nuclear calcium oscillations in AMS as well as in RNS, CYCLOPS can be attributed as master regulator for both associations. Activated by CCaMK, CYCLOPS is not only able to induce *NIN (NODULE INCEPTION)* expression, a RNS specific transcriptional regulator, but CYCLOPS accomplishes also the promoter activation of the AM-specific transcription factor RAM1 (REDUCED ARBUSCULAR MYCORRHIZA 1) by direct binding of DNA (Singh et al. 2014; Pimprikar et al. 2016). Strikingly, recent research has shown that CYCLOPS interacts with DELLA in heterologous systems and that DELLA is able to amplify the transactivation potential of CYCLOPS on the AM-specific *RAM1* promoter as well as on promoters of the two nodulation important genes *NIN* and *ERN1* (Pimprikar et al. 2016; Jin et al. 2016).

della1della2 mutants in *Medicago* are perturbed in AMS and root nodule symbiosis (Floss et al. 2013; Jin et al. 2016), which highlights the importance of DELLLA proteins as common symbiosis protein. DELLAs have first been known to act as repressors for gibberellic acid (GA) signaling, but later qualified themselves as important regulators for crosstalk between hormone and biotic signaling cascades (Peng and Harberd 1993; Alvey and Harberd 2004; Gallego-Bartolomé et al. 2012; Davière and Achard 2013). DELLA proteins belong to the family of GRAS proteins. They are degraded by the 26S proteasome upon perception of GA after polyubiquitination, which enables the induction of changes in gene expression (Davière and Achard 2016). GA-dependence

for AM development was identified early in *Pisum* and later also seen for root nodule symbiosis in *Lotus* (El Ghachtouli et al. 1996; Maekawa et al. 2009). Bioactive GA treatment on colonized *Medicago* and *Lotus* plants abolishes arbuscule formation even if intraradical hyphae are formed (Floss et al. 2013; Takeda et al. 2015; Pimprikar et al. 2016). These findings propose a positive role of DELLA for arbuscule generation. Both, overexpression of a GA-resistant DELLA protein as well as treatment with a GA biosynthesis inhibitor trigger *RAM1* induction, which suggests DELLA acting downstream or at least in the same hierarchy as CYCLOPS (Park et al. 2015; Floss et al. 2013; Pimprikar et al. 2016). Therefore, DELLA is characterized as the most-downstream component of the CSSP known so far.

To accommodate root symbionts such as AMF or rhizobia, severe transcriptional reprogramming needs to be achieved by the plant (Breakspear et al. 2014; Roux et al. 2014; Camps et al. 2015; Handa et al. 2015; Hohnjec et al. 2015). Thus, the main function of the common symbiosis genes (CSG) might be to initialize these transcriptional changes. Additionally, specificity in transcriptional adaptation to result either in AMS or RNS needs to be ensured. A study testing the transcriptional plant response upon specific Nod/Myc-factor treatments showed that indeed upon CSG activation AM/RNS specificity of the plant transcriptional answer is warranted (Czaja et al. 2012). This implies that in addition to the common symbiosis signaling cascade other signaling pathways facilitate the decisive specificity for both associations.

iii) AM specific signaling downstream of common SYM signaling cascade

Intensive research on transcriptional regulators identified four important representatives for AMS establishment in *Petunia, Medicago* and *Lotus.* RAM1, RAD1 (REQUIRED FOR ARBUSCULE DEVELOPMENT 1), MIG1 (MYCORRHIZA INDUCED GRAS 1), which belong like DELLAs and NSP1 to the large family of plant-specific GRAS transcription factors, and the ERF/AP2 domain containing transcription factor ERF1 (ETHYLENE RESPONSE FACTOR 1)/WRI15b (WRINKLED 5b) are all indispensable for the regulation of arbuscule development and branching (Bolle 2004; Gobbato et al. 2012; Devers et al. 2013; Park et al. 2015; Xue et al. 2015; Rich et al. 2015; Heck et al. 2016; Pimprikar et al. 2016; Luginbuehl et al. 2017; Pimprikar and Gutjahr 2018). Knock-out mutations or artificial RNAi based silencing of these

regulators perturb arbuscule formation, which results in stunted arbuscules in the respective mutants.

Several studies in different plant species were performed on RAM1, which make RAM1 to the best characterized regulator so far (Rich et al. 2017). *ram1* mutants are significantly less colonized by the fungus and exhibit a severe arbuscule phenotype (Pimprikar et al. 2016; Rich et al. 2015; Park et al. 2015). Characterized by only the trunk domain or crude branches, the arbuscules in *ram1* fail to produce high-order branches. Upon fungal colonization *RAM1* is highly expressed and the promoter seems to be particularly active in colonized root zones (Gobbato et al. 2012; Gobbato et al. 2013; Park et al. 2015; Rich et al. 2015; Pimprikar et al. 2016). Various downstream located genes seem to be depended on *RAM1* expression. For example, expression of *VAPYRIN* and *EXO70I*, required for PAM formation, the AM-specific transporters encoding genes *STR, PT4* and *AMT2.2* and expression of genes crucial for lipid biosynthesis are abolished in *ram1* of *Medicago* and *Petunia* (Gobbato et al. 2012; Park et al. 2015; Bravo et al. 2017; Xue et al. 2015; Rich et al. 2015; Luginbuehl et al. 2017). Intriguingly, in *ram1* of *L. japonicus,* unlike to *Medicago* and *Petunia,* induction of some AM-marker genes like *SbtM1, BCP1, STR, RAM2* or *PT4* is not completely abolished*,* which evinces species-specific transcriptional regulation and redundancy in *L. japonicus* at the level of RAM1. Nevertheless, this redundant factor X is obviously insufficient to support arbuscule maturation (Pimprikar and Gutjahr 2018). This suggests that indeed targets of RAM1 regulation are responsible for the *ram1* phenotype (Pimprikar et al. 2016). Furthermore, ectopic overexpression of *RAM1* in absence of the fungus induces many AM-marker genes significantly (Pimprikar et al. 2016). Notably, the *RAM1* promoter is activated by direct CYCLOPS-binding to an AM-specific *cis* element (AMCYC-RE) within the promoter region and *RAM1* overexpression restores arbuscule formation in *cyclops* (Pimprikar et al. 2016). All in all, these findings pinpoint RAM1 as a main player and as the entry point into AM-specific transcriptional regulation downstream of DELLA and CYCLOPS.

A whole bouquet of transcription-factor (TF) encoding genes, foremost members of the GRAS family, seem to be activated upon arbuscule formation (Xue et al. 2015; Rich et al. 2015; Gaude et al. 2012; Rich et al. 2017). GRAS proteins are prone to interact with each other and to form heterocomplexes (Hirano et al. 2017). Several interactions of symbiotic GRAS proteins have been already shown – although, almost exclusively only in heterologous systems (MacLean et al. 2017). RAM1 interacts in yeast and *Nicotiana*

benthamiana with considerable other GRAS proteins involved in AM symbiosis (Pimprikar and Gutjahr 2018). Confirmation of this interactions *in situ* is a required next step, but the already obtained results indicate the importance of GRAS TFs and hint towards a putative highly complex connectivity in AMS transcriptional wiring.

2.4 Nutrient exchange

Arbuscular mycorrhiza is no exception but rather default state for AM-competent plants in nature (Smith and Smith 2011). The driving force and key argument for *Glomeromycotina* fungi and plants to invest their energy in the establishment of this interaction is the reciprocal exchange of nutrients (Roth and Paszkowski 2017). As studies, focusing on competitive mycorrhiza performance of different fungal strains suggest, this reciprocal nutrient exchange seems to follow a cooperative and bilateral rewarding principle, which is called “biological market” (Kiers et al. 2011). Analogous to an economic market, both partners likely interact with multiple partners and exchange commodities to their mutual benefit, which prevents enslavement and ensures the evolutionary stability and success of AMS (Kiers et al. 2011). Yet, the concept of reciprocal fair trade seems to falter in mixed plant culture experiments (Walder et al. 2012).

On large scale, AMS nutrient exchange is a significant factor for global nutrient cycles, ecology, evolution and the physiology of plants (Redecker et al. 2000; Marschner et al. 1995; Allen et al. 2003; Read and Perez-Moreno 2003). The fungus delivers mineral nutrients and water taken up from the soil to the plant and receives about 20 % of photosynthetically fixed carbon as a trade-off (Smith et al. 2011; Roth and Paszkowski 2017).

However, plants are able to monitor the nutrient availability in the soil and control the degree of fungal colonization with respect to their nutrient status (Carbonnel and Gutjahr 2014). For example, AM development is repressed in high phosphate (Pi) conditions (Braunberger et al. 1991; Balzergue et al. 2010; Breuillin et al. 2010). Yet, the plant’s decision to promote or repress AM colonization is not only dictated by Pi availability but rather seems to follow Liebig’s law of the minimum as the suppressive effect of high Pi conditions is overcome by nitrogen (N) shortage or, to a lesser degree, by shortage of mineral nutrients like potassium, calcium or iron (Nouri et al. 2014; Gutjahr and Parniske 2017).

The exact mechanisms to control AM development via nutrient signaling are still elusive (Gutjahr and Parniske 2013). Studies highlight the plant being head of control as it determines arbuscule lifetime. For example, AM-specific phosphate transporter mutants in rice and *Medicago* exhibit low colonization and an increased number of stunted arbuscules as result of an accelerated arbuscule turnover (Javot et al. 2007; Yang et al. 2012). However, it remains unclear when and why the plant initiates arbuscule turnover. Possibly also the fungus might induce the turnover via active signaling.

In general, arbuscule lifetime is controlled cell autonomously and can vary between individual arbuscules (Kobae et al. 2010). Although, the exact signaling pathway for arbuscule degeneration is still unknown, studies by Floss et al. illustrated that the GRAS transcription regulators MYB1, NSP1 and DELLA are involved by triggering expression of hydrolase genes (Floss et al. 2017). It is conceivable that the relatively short lifetime of an arbuscule is an efficient mechanism to control arbuscule performance and ensure throughout nutrient exchange (Gutjahr and Parniske 2017).

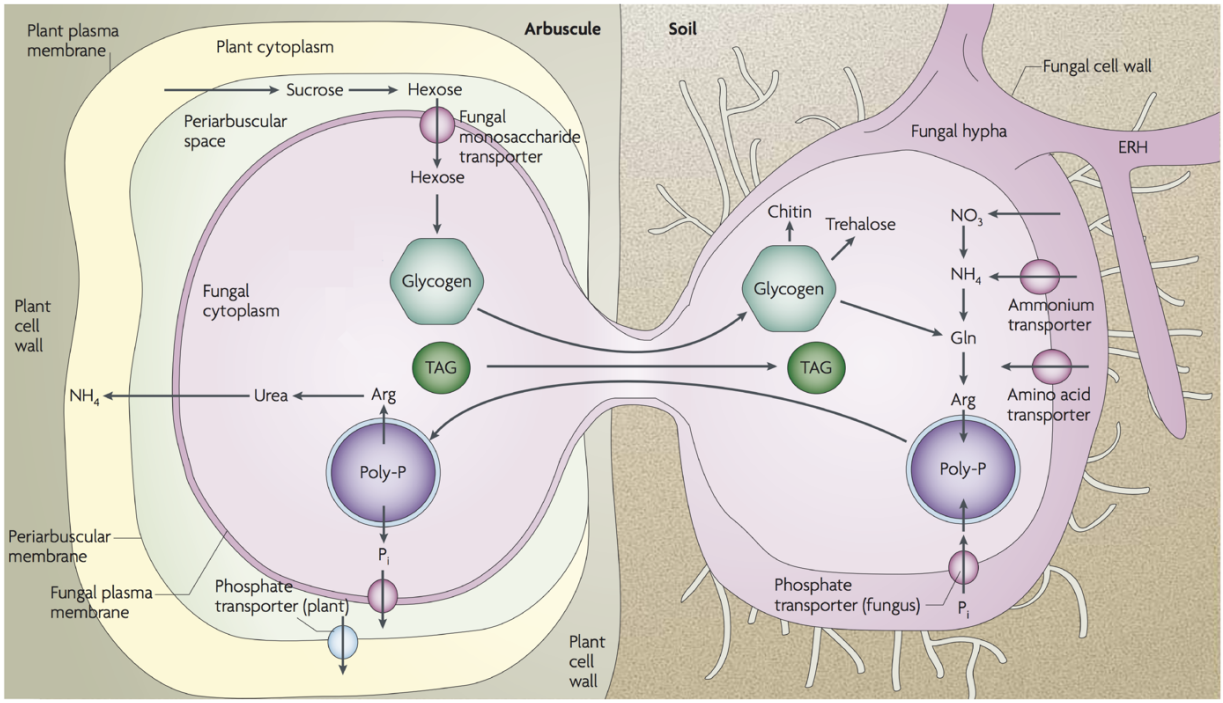

Figure 3: Metabolic fluxes and long-distance transport in arbuscular mycorrhiza symbiosis (modified Figure from Parniske 2008)

i) Transfer from fungus to plant

Root colonization by AMF significantly improves the nutrient status of the plant by suppling its host with a variety of mineral nutrients (Marschner and Dell 1994). The cocktail of fungal cargo consists of macronutrients essential for plant health. Phosphate, nitrogen and sulfate are transported in substantial amounts from the fungal extraradical mycelium to the colonized roots (Harrison et al. 2002; Tanaka and Yano 2005; Leigh et al. 2008; Allen and Shachar-Hill 2009; Casieri et al. 2012). The dense and widespread extraradical hyphal network of AMF massively enhances the uptake capacity for nutrients in the soil compared to plant roots (Javot et al. 2007). The network's absorbing surface area extends easily beyond the nutrient depletion zone, which is formed around roots.

Phosphorus is a major macronutrient and limiting factor for plant growth and predominately occurs as the dihydrogen ion phosphate ($H_2PO_4^-$; Pi) in soil. Soluble Pi, which is uptake-ready is low-abundant in soil and due to phosphate's low mobility, Pi depletion zones emerge rapidly (Schachtman et al. 1998; Nussaume et al. 2011). To overcome Pi starvation, plants have developed several strategies, which also includes physiological responses but nevertheless foremost association with AMF. Interestingly, AMF might not only transport Pi directly to the plant but also be able to induce the expression and secretion of plant acid phosphatases to enhance direct plant uptake (Ezawa et al. 2005).

However, almost the entire plant Pi uptake can be of AMF contribution (Poirier and Bucher 2002; Smith et al. 2004). Little is known about AMF strategies to exploit unavailable Pi from the soil. Possibly, they are able to mineralize organic P (Shibata and Yano 2003; Feng 2003). For example, *Rhizophagus clarus* releases acid phosphatase from its extraradical hyphae for hydrolysis of Pi and its mobilization (Sato et al. 2015). Also, a bacterial contribution for soil phosphorus utilization might be likely. Fungal Pi uptake is facilitated by $Pi:H^+$ symporters (PTs), which are expressed in the extraradical mycelium (ERM) (Harrison and Buuren 1995; Maldonado-Mendoza et al. 2001; Benedetto et al. 2005; Xie et al. 2016). Once taken up by the ERM, Pi is converted into long polyphosphate chains (polyP) inside vacuoles and then translocated to the IRM via either cytoplasmic streaming or a vacuolar network (Ezawa et al. 2003; Solaiman et al. 1999; Olsson et al. 2002; Uetake et al. 2002; Hijikata et al. 2010). Synchronous and equivalent uptake of positive charged cations like Na^+, K^+,

Ca^{2+} and Mg^{2+} into the fungal mycelium takes place to cope with the massive accumulation of negative charged polyP and to maintain a neutral charged fungal cell (Kikuchi et al. 2014). Translocated to the IRM, polyP is hydrolyzed by phosphatases and subsequently phosphate is released into the acidic periarbuscular space (PAS), which is formed between PAM and fungal membrane (Kojima and Saito 2004). Strikingly, expression of PTs at the arbuscule might allow reabsorption of Pi from the PAS and therefore control nutrient transport homeostasis (Benedetto et al. 2005; Balestrini et al. 2007; Fiorilli et al. 2013; Xie et al. 2016).

Diverse labeling studies confirmed that nitrogen is taken up from soil and sent to the plant by AMF in addition to phosphate. Into the ERM, nitrogen is ingested in inorganic forms – nitrate (NO_3^-) and preferentially ammonium (NH_4^+) – as well as organic forms like glycine and glutamic acid (Ames et al. 1983; Govindarajulu et al. 2005; López-Pedrosa et al. 2006; Bago et al. 1996; Hawkins et al.2000). Once taken up, the different nitrogen sources are converted into arginine, which is then translocated along the coenocytic fungal hyphae to the IRM (Govindarajulu et al. 2005). Inside the IRM, ammonium is released from its carbon backbone and similarly to phosphate translocated into the PAS via an unknown mechanism (Govindarajulu et al. 2005; Cruz et al. 2007; Lanfranco et al. 2018).

For both macronutrients, PAM-localized plant uptake-transporters are known and have been extensively studied for many years. AM-specific phosphate transporters like PT4 in *Medicago* and PT11 in rice, all belonging to the phosphate symporter family Pht1, have been identified in various plant species (Harrison et al. 2002; Paszkowski et al. 2002; Rausch et al. 2001; Tamura et al. 2012; Yang et al. 2012; Poirier and Bucher 2002). Interestingly, in a phylogenetic tree of Pht1 transporters, all AM-specific proteins cluster in a separate AM-host plant exclusive clade (Hong et al. 2012; Yang et al. 2012). This already indicate the specific determination of AM-specific Pht1 transporters. AM-specific *PT* genes have been described to be specifically expressed in arbuscocytes. However, *PT4* promoter activity for *Lotus* and *Medicago* has also been reported in root tips under Pi starvation (Volpe et al. 2015). *Medicago* PT4 and its homologs exclusively localize to the branch-domain of the PAM (Harrison, Dewbre, and Liu 2002; Kobae and Hata 2010; Tamura et al. 2012). *PT4* knock-out mutations or RNAi-mediated silencing cause accelerated arbuscule turnover and premature arbuscule degeneration, which points out the importance of Pi transport for AMS maintenance (Javot et al. 2007; Yang et al. 2012; Volpe et al. 2015; Xie et al. 2016).

Strikingly, this premature degeneration phenotype is eliminated when colonized *pt4* plants are under nitrogen starvation (Javot et al. 2011; Breuillin-Sessoms et al. 2015). Labelling studies imply that ammonium might be the nitrogen containing compound sent to the plant (Govindarajulu et al. 2005; Cruz et al. 2007). Hence, plant ammonium transporters of the AMT family, which are induced upon mycorrhization and localized to the PAM have been discovered in many plant species (Gomez et al. 2009; Kobae and Hata 2010; Koegel et al. 2013; Breuillin-Sessoms et al. 2015).

Also, proton ATPases have been identified in *Medicago* and *N. tabacum,* which are exclusively expressed in arbuscuocytes (Gianinazzi-Pearson et al. 2000; Krajinski et al. 2014). Proton ATPase activity provides the energy for active membrane transport by generating an electrochemical gradient via proton transfer. ATPase *ha1* mutants in rice and *Medicago* exhibit a stunted arbuscule phenotype and abolished nutrient transfer, which highlights the importance of arbuscocyte expressed ATPase provided energy for nutrient uptake from the PAS across the PAM inside the plant cell (Krajinski et al. 2014; Wang et al. 2014).

Furthermore, PAM-harbored proteins have been identified, which are believed to act as transceptors for phosphate and ammonium. Transceptors constitute transporters that are rather assigned to nutrient sensing than transporting (Popova et al. 2010; Yang, Grønlund, et al. 2012; Breuillin-Sessoms et al. 2015; Volpe et al. 2015; Xie et al. 2016). Their presence implies that both nutrients are decisive components of arbuscule lifetime regulation, which emphasizes the arbuscule not only as the key interface of nutrient transfer but also as determining structure for AMS maintenance (Gutjahr and Parniske 2017). Reciprocal sensing of both partners as critical component for AM maintenance is further supported by the identification of a PAM-harbored Serin/Threonine receptor-like kinase (ARK1) in rice and maize (Roth et al. 2018). Colonized *ark1* mutants produce mature arbuscules but exhibit a significantly reduced number of fungal vesicles and a concomitant reduction in total root length colonization (Roth et al. 2018), which further indicates the requirement of continuous communication between both partners, even after arbuscule maturation.

ii) Transfer from plant to fungus

The host plant does not only benefit from AMF but also rewards the fungal nutrient delivery by the supply of photosynthetically fixed carbon to the fungus in return (Smith

and Read 2008). AMF require large amounts of energy in form of carbon building blocks to produce their extended hyphal networks for soil exploration. The entire carbon demand of AMF depends on the host plant, which determines the fungal obligate biotrophic lifestyle. As mentioned earlier, one fifth of photosynthetically fixed plant carbon is transferred to the fungus. Approximately 5 billion tons of carbon per year is thought to be consumed by AMF, which sequesters atmospheric carbon dioxide to the soil organic carbon and thus impacts global carbon cycles substantially (Bago et al. 2000; Parniske 2008).

The carbon drain, arising upon arbuscular mycorrhiza associations, influences plant carbon balance heavily. Mycorrhiza colonization increases the carbon sink strength, which results in a redirection of photo assimilates towards the root and especially accumulation of sugars and lipids in colonized roots (Wright, Read, and Scholes 2002). Accordingly, sucrose synthases and invertases are transcriptionally upregulated upon AMS and impairment of these enzymes exhibits AM-specific phenotypes in diverse plant species (Blee and Anderson 1998; Wright et al. 2002; Hohnjec et al. 2003; Schaarschmidt et al. 2006; Baier et al. 2010).

The transferred cargo of plant carbon to the fungal partner has been studied for decades. Already a while ago, detailed labelling and tracer-based NMR studies demonstrated that plants transfer hexoses to the fungus (Shachar-Hill et al. 1995; Pfeffer et al. 1999; Solaiman et al. 1999; Bago et al. 2000; Douds et al. 2000). Supporting the importance of hexose transfer, a mycorrhiza-induced fungal hexose transporter MST2 with high transport activity for glucose is essential for arbuscule development and quantitative root colonization as shown by host-induced gene silencing (Helber et al. 2011).

However, the main carbon storage form in AMF are lipids, particularly triacyglycerols (TAGs), and not carbohydrates (Trépanier et al. 2005). Consistent with this, lipid droplets are highly abundant in all fungal structures (like hyphae, vesicles, spores and arbuscules) and have been identified as transport vehicles for the plant-derived carbon cargo inside the fungus, in addition to glycogen (Bago et al. 2002; Bago et al. 2003).

Although, *de novo* fatty acid (FA) biosynthesis has only been observed in colonized roots but neither in the ERM nor in spores, it has long been assumed that plant derived hexoses are the exclusive plant cargo and serve as precursors for fungal lipid biosynthesis (Pfeffer et al. 1999; Trépanier et al. 2005). Furthermore, arbuscule development is escorted by activation of a cohort of lipid biosynthesis genes in the

arbuscule containing cell (Gaude et al. 2012; Gaude et al. 2012) Studies on recently available whole genome sequences of AMF *Rhizophagus irregulars, Rhizophagus clarus, Gigaspora margarita* and *Gigaspora rosea* have not revealed genes encoding multi-domain cytosolic FA synthase subunits, typically crucial for *de novo* fatty acid synthesis in fungi and animals (Wewer et al. 2014; Ropars et al. 2016; Salvioli et al. 2016; Tang et al. 2016; Kobayashi et al. 2018). Hence, it is hard to imagine the fungus is capable producing sufficient amounts of FAs by itself, even if fungal genomes do possess enzymatic machinery for higher chain length FA elongation and desaturation (Wewer et al. 2014; Trépanier et al. 2005). All these findings have exposed FAs or lipids as potential cargo to transfer carbon from plant to fungus in addition to carbohydrates.

3. Obligate biotrophy of filamentous microbes

Plant interacting biotrophic microbes establish long-term relationships with their host in order to complete their life cycles. As being entirely dependent on its host, biotrophs need to engender colonization and interaction strategies to maintain living-host association for their own survival. Mendgen and Hahn defined microbial characteristics like highly developed infection structures, limited secretory activity – especially of lytic enzymes, long-term suppression of host defense and a specialized interface structure as hallmarks of biotrophy (Mendgen and Hahn 2002). AMF share all the mentioned properties and are accordingly attributed as obligate biotrophs (Bago and Bécard 2002; Kloppholz et al. 2011; Tisserant et al. 2013). AMF have been shown to scavenge nutrients via their specialized haustoria, the arbuscules, they release effectors that might contribute to suppress host-defense and their genomes lack several key genes like FAS synthase or lytic enzymes as evolutionary adaption to their obligate biotrophic lifestyle (Tisserant et al. 2013; Kobayashi et al. 2018; Sędzielewska Toro and Brachmann 2016). However, biotrophy is no question of mutualism or parasitism. Thus, comparable to AMF, pathogenic filamentous biotrophs such as powdery mildews, downy mildews, rust or smut fungi cannot be cultivated in absence of their hosts, produce specialized interface structures for host manipulation and overall share distinct features of biotrophy with AMF (Mendgen and Hahn 2002; Kuhn et al. 2016; Baxter et al. 2010).

How the host is able to differentiate between beneficial and harmful microbes still remains largely elusive. One could assume that especially biotrophic pathogens might face higher resistance and greater plant-defense obstacles to infect their hosts in order to complete their lifecycle than beneficial microbes like AMF do. Thus, the competence of pathogens like the oomycete *Hyaloperonospora arabidopsidis* (*Hpa*) to establish and maintain a true biotrophic interaction with *Arabidopsis thaliana* can be accounted as a paramount example of microbial biotrophy, which harbors great potential to elucidate essential features of obligate biotrophic plant-microbe interactions. Interestingly, genomes of the pathogenic biotrophs like *Hpa* or *Blumeria graminis* reveal not only a significant reduction of genes but also accompanied specialization like gene-reshuffling as trade-offs to the microbe's obligate biotrophic lifecycle (Spanu et al. 2010; Baxter et al. 2010). Though, these evolutionary genome adaptations harden the host dependence of microbes, they contribute to a better host adaption, reduce energy cost and thus finally promote the individual fitness of the microbe.

4. Oomycetes - A vast group of pathogens

Oomycetes comprise a versatile lineage of eukaryotic organisms, which colonize all environments (Thines 2018). Fossil findings indicate that a number of oomycetes emerged as endophytes of land plants approximately 300-350 million years ago (Krings et al. 2011). Oomycete lifestyles range from biotrophy to necrotrophy and from obligate to facultative pathogenesis (Judelson 2017). Although, sharing some distinct features like hyphal growth and proliferation via spores, oomycetes do not belong to the *Mycota* but to the kingdom of *Straminipila,* which means that they are more related to diatoms and brown algae than to true fungi (Dick 2001). A major discrimination between true fungi and oomycetes is the nature of the cell wall. Whereas fungal walls are chitin based, oomycete cell walls consist of cellulose (Slusarenko and Schlaich 2003). Furthermore, many representatives exhibit motile biflagellate zoospores, which illustrates that oomycetes most likely evolved in a marine environment (Thines and Kamoun 2010). Several oomycetes species have evolved into highly effective pathogens infecting a broad host range of eukaryotes like *Alveolata, Animalia, Mycota, Straminipila* and *Plantae* (Thines and Kamoun 2010). Plant parasitism has evolved independently in three lineages of ooymcetes (Thines and Kamoun 2010). Well-known plant pathogens like *Phytophtora, Phytium* as well as *Hyaloperonospora* species

comprise the major group of *Peronosporaceae* whose members cause economically important crop losses (Coates and Beynon 2010; Judelson 2017).

4.1 *Hyaloperonospora arabidopsidis* (*Hpa*) – Life cycle

H. arabidopsidis is one of 700 powdery mildew species within the *Peronosporaceae* and one the few filamentous microbes, which is able to infect the well-established model plant *Arabidopsis* (Koch and Slusarenko 1990; Kamoun et al. 2015). Therefore, the *Hpa-Arabidopsis* association is meaningful to study biotrophic microbe-host interactions. *Hpa* is most infective in cold (around 10 °C) and moist conditions. Its life cycle starts with an asexual conidiospore, which germinates on top of a plant leaf and produces an attachment structure, named appressorium, on the leaf surface - usually at the junction of two neighboring epidermal cells. This leads to hyphal penetration into the plant tissue. The hypha inserts between the neighboring cells. Next, a haustorium is introduced in at least one of these epidermal plant cells. After the first haustorial insertion the hypha starts branching inside the intercellular space of the mesophyll. Subsequently, the hyphal network embeds digit-like haustoria into single mesophyll cells. Analogous to arbuscules of AMF, the oomycetal haustoria do not break but invaginate the plant cell membrane. Thus, haustoria are always surrounded by a plant-derived extrahaustorial membrane (EHM), which is newly formed (Mims et al. 2004). Conidiophores, asexual reproduction organs, develop from hyphal tips in substomatal cavities. Approximately seven days post infection, the mature conidiophores emerge through stomata and form tree-shaped sporangiophores, which carry asexual conidiospores. Sexual reproduction is initiated by interlacing hyphae, which form oogonia and paragynous antherida in the leaf/cotyledon. Oogonia subsequently produce sexual oospores. Oospores are able to survive the winter and germinate in favorable conditions to initiate a new life cycle (Koch and Slusarenko 1990; Mauch-Mani and Slusarenko 1993; Slusarenko and Schlaich 2003; Soylu and Soylu 2003).

4.2 Oomycete-plant interaction – The arms race

Plants and pathogens constantly co-evolve. Individual plants are in favor of selection, which are least susceptible to infection of detrimental microbes. Simultaneously pathogens are selected by their means to evade host defense. This results in a

constant arms race of both opponents. The defense arsenal of plants is quite complex and hierarchically ordered. It includes processes such as pattern-triggered immunity (PTI), which is initiated upon plant perception of pathogen-associated molecular pattern (PAMPs) or perception of plant-derived damage-associated molecular pattern (DAMPs), and microbial effector-triggered immunity (ETI). Both mechanisms involving hypersensitive response (HR) but also local as well as systemic immune responses, which are interconnected with other physiological processes and comprise reactive oxygen species (ROS) and hormones like salycilic acid (SA), ethylene (ET) or jasmonic acid (JA) (Jones and Dangl 2006; Caillaud et al. 2013; Asai et al. 2014; Boller and Felix 2009). To evade the plant defense machinery, oomycetes secrete effector proteins into the plant cell apoplast or cytoplasm. The most common effectors are the RxLR-type proteins. An N-terminal signal peptide and a RxLR (or RxLR-EER) motif facilitate secretion and host uptake and a C-terminal domain harbors the effector activity (Asai et al. 2014; Baxter et al. 2010). Besides effectors, probably diverse pathogen-derived biomolecules are involved to support infection and suppress host immunity. For example, reciprocal small RNA (sRNA) translocation between plant and microbes in order to induce gene silencing was first observed in the grey mold causing fungus *Botrytis cinerea* infecting tomato and *Arabidopsis* (Weiberg et al. 2013; Cai et al. 2018). It is highly likely that sRNA trafficking is a more widespread phenomenon and thus might also be a component of the elaborate infection arsenal of *Hpa*.

4.3 Host nutrient reliance of *Peronosporaceae*

There is little doubt that oomycetal haustoria represent the key exchange interface in association with the host plant (Hardham 2006; Whisson et al. 2007; Bozkurt et al. 2012). A representative amount of oomycteal effectors and their targets *in planta* have already been described to be secreted from haustoria, whereas nutrient exploitation by oomycetes, especially of *Hpa*, is in general still poorly understood (Whisson et al. 2007; Schornack et al. 2010; Stassen and Van den Ackerveken 2011; Bailey et al. 2011; Bozkurt et al. 2012; Asai et al. 2014; McGowan and Fitzpatrick 2017; Pel et al. 2014). Among the oomycetes, nutrient uptake and metabolism of the hemibiotrophic *Phytophthora spec.* has been studied best so far. For example, isotope labelling studies confirmed that sucrose is transferred from plant to the pathogen (Clark and Spencer-Phillips 1993). Also, genome and transcriptome studies of *Phytophthora*

identified sugar and amino acid transporters expressed in the biotrophic stage (Chen et al. 2007; Abrahamian et al. 2016). Further, the expression of α-amylase for starch utilization as well as the expression of an adenylyl-sulfate kinase (PAPS) for incorporation of sulfate was identified for *P. infestans* on potato tubers (Ah-Fong et al. 2017). Additionally, *Phytophthora* spec. are sterol and thiamine auxtrophs, which implies, that both compounds need to be scavenged from the host (Rodenburg et al. 2018).

Similar to *Phytophthora* spec., *Hpa* is also characterized by a streamlined metabolism, which reflects its major reliance on its host *Arabidopsis* (Baxter et al. 2010; Judelson 2017). For example, downy mildew genomes do not harbor core genes for nitrite, nitrate and sulfate assimilation, which indicates the requirement of host scavenging for these nutrients (Baxter et al. 2010; Judelson 2017). Apparently, also obligate oomycetes are not able to synthesizes unsaturated fatty acids (Judelson 2017).

5. The Trojan Horse tactic – Learning from the Good

Interestingly, colonization procedures of phylogenetically distant filamentous microbes on plant tissues seem to have distinct similarities, at least on a morphological level (Parniske 2000). Even if *Hpa* colonizes the leaf mesophyll and AMF are restricted to the root, alike arbuscular mycorrhiza colonization, *Hpa* spreads inside the plant leaf via an intraradical hyphal network and introduces interface structures into single plant cells, which provide a large contact area with the host cytosol (Soylu and Soylu 2003; Dodds et al. 2009; Mims et al. 2004). Similar to arbuscule insertion, haustorium insertion does not break the plant cell membrane. The specialized plant-derived EHM can be accounted as analog to the PAM in function and morphology (Soylu and Soylu 2003; Mims et al. 2004; Ried et al. 2018; Lu et al. 2012). Strikingly, not only form and function of accommodation structures between mutualistic and pathogenic filamentous microbes seem to be similar. Several studies already found evidence that the colonization success of mutualistic as well as pathogenic microbes relies on the same host genes. For example, the symbiotic *Medicago* LysM receptor NFP (NFR5 in *Lotus japonicus)* does not only facilitate functional association of *Medicago* with AMF and nitrogen fixing bacteria (Zipfel and Oldroyd 2017; Maillet et al. 2011; Sun et al. 2015; Czaja et al. 2012). Even if the effect is apparently contrary to symbiosis, NFP also intervenes in plant immunity as *nfp* of *Medicago* is more susceptible the root oomycete

Aphanomyces euteiches (Rey et al. 2013). Furthermore, *Medicago* plants, which carry mutations in AM and root-nodule symbiosis genes, exhibited implications for the oomycetal colonization and disease development of *Phytophthora palmivora* (Wang et al. 2012; Rey et al. 2015). Recently, a study by Ried et al. discovered, that in the non AM-competent *Brassicacea, Arabidopsis thaliana,* mutations in homologs of the common symbiosis genes *POLLUX*, *SYMRK* and *NUP107-160* (see chapter 2.3), perturb the reproduction and the development of *H. arabidopsidis* (Ried et al. 2018). These findings support the idea, that pathogens like oomycetes exploit plant symbiosis signaling pathways for their own parasitic success (Delaux et al. 2013).

All in all, this suggests that beneficial as well as pathogenic filamentous microbes might have evolved similar strategies for colonization and intercellular accommodation by adopting common core components from evolutionary older plant-microbe interactions like AMS (Rey and Schornack 2013; Evangelisti et al. 2014; Ried et al. 2018; Parniske 2000).

VII. Aims of the thesis

Reciprocal nutrient transfer between AMF and the host plant is the key feature of the arbuscular mycorrhiza symbiosis. This transport is facilitated via the arbuscule, which is indicated by existence of exclusively PAM-harbored nutrient transporters. As studies on the *pt4* mutant suggest, nutrient delivery of the symbiotic fungus determines arbuscule lifetime and the maintenance of the association (Javot et al. 2011). In turn, RNAi-based knock-out of a fungal monosaccharide transporter and undersupply of carbon in colonized plant roots due to defective phloem loading or reduced invertase activity negatively affect fungal colonization and development inside the root. These findings imply that reciprocal nutrient exchange is decisive for establishment and maintenance of AMS (Schaarschmidt et al. 2007; Helber et al. 2011; Breuillin-Sessoms et al. 2015). This nutrient trade does not only emphasize the true mutualistic association, which is based on contribution from both sides, but also highlights the importance to understand nutrient fluxes in order to use the potential of AMS most efficiently for applied agriculture and sustainable food production.

The hypothesis that photosynthetically fixed carbohydrates are the exclusive cargo sent to the fungus in reward for fungal delivered mineral nutrients was still prominent at the beginning of my doctoral work. However, accumulating knowledge about AM-induced lipid biosynthesis genes and most importantly the fact that AMF do not possess a *de novo* fatty acid synthase machinery weakened this hypothesis deeply and put plant lipid biosynthesis in the spotlight of arbuscular mycorrhiza research (Wang et al. 2012; Bravo et al. 2016; Wewer et al. 2014; Ropars et al. 2016; Salvioli et al. 2016; Tang et al. 2016). Two *L. japonicus* mutants perturbed in arbuscular mycorrhiza accommodation have been identified (Groth et al. 2013), and their respective causative mutations have been identified already prior to my work (Bucerius and Parniske; Pimprikar and Gutjahr). Both mutants, *dis (disorganized arbuscule)* and *ram2 (reduced arbuscular mycorrhiza 2)* contain point mutations in genes encoding AM-specific lipid biosynthesis genes, which are specifically induced in roots upon AMF colonization. Therefore, the main goal of my work was to understand the role of these genes and of plant derived lipids in AMS. I found evidence that AM-induced lipid biosynthesis is severely impaired in *Ljdis, Ljram2* and the ABCG half-transporter mutant *Ljstr.* Therefore, the next goal was to understand the role of the missing AM-induced lipids and to examine whether lipids are transported from plant to fungus.

I further contributed to the research of Prof. Dörmann, to characterize the thioesterase FatM as another component of the AM-specific lipid biosynthesis pathway in *Lotus japonicus.*

In addition, this thesis intended to go beyond the boundaries AM research and aimed to investigate if plant lipid biosynthesis plays a predominant role not only for AMS but also for other plant-microbe interactions. *Hyaloperonospora arabidopsidis* is a filamentous obligate biotrophic pathogen, which belongs to the linage of oomycetes. As members of the kingdom *Straminipila,* oomycetes are phylogenetically greatly distinct from AMF. However, *Hpa* seems to share common principles of host colonization with AMF. Therefore, by using reverse genetics with *Arabidopsis* mutants of *DIS* and *RAM2* homologs I aimed at understanding if host fatty acid and lipid biosynthesis impact also the interaction of *Hpa* in *Arabidopsis thaliana* leaves.

VIII. Results

Paper I: Lipid transport from plants to arbuscular mycorrhiza fungi

Reference: Keymer A#, Pimprikar P#, Wewer V, Huber C, Brands M, Bucerius SL, Delaux PM, Klingl V, von Roepenack-Lahaye E, Wang TL, Eisenreich W, Dörmann P, Parniske M, Gutjahr C (2017). Lipid transfer from plants to arbuscular mycorrhiza fungi. eLife 6. pii: e29107.
# These authors contributed equally to the work

eLIFE elifesciences.org

RESEARCH ARTICLE

Lipid transfer from plants to arbuscular mycorrhiza fungi

Andreas Keymer[1†], Priya Pimprikar[1†], Vera Wewer[2‡], Claudia Huber[3], Mathias Brands[2], Simone L Bucerius[1], Pierre-Marc Delaux[4], Verena Klingl[1], Edda von Röpenack-Lahaye[5§], Trevor L Wang[6], Wolfgang Eisenreich[3], Peter Dörmann[2], Martin Parniske[1], Caroline Gutjahr[1*]

[1]Faculty of Biology, Genetics, LMU Munich, Biocenter Martinsried, Munich, Germany; [2]Institute of Molecular Physiology and Biotechnology of Plants, University of Bonn, Bonn, Germany; [3]Biochemistry, Technical University Munich, Garching, Germany; [4]Laboratoire de Recherche en Sciences Végétale, Centre National de la Recherche Scientifique, Toulouse, France; [5]Faculty of Biology, Plant Sciences, LMU Munich, Biocenter Martinsried, Munich, Germany; [6]John Innes Centre, Norwich Research Park, Norwich, United Kingdom

***For correspondence:** caroline.gutjahr@lmu.de

[†]These authors contributed equally to this work

Present address: [‡]Mass Spectrometry Metabolomics Facility, Cluster of Excellence on Plant Sciences, University of Cologne Biocenter, Cologne, Germany; [§]Analytics Facility, Center for Plant Molecular Biology, University of Tübingen, Tübingen, Germany

Competing interests: The authors declare that no competing interests exist.

Funding: See page 28

Received: 31 May 2017
Accepted: 13 July 2017
Published: 20 July 2017

Reviewing editor: Gary Stacey, University of Missouri, United States

Abstract Arbuscular mycorrhiza (AM) symbioses contribute to global carbon cycles as plant hosts divert up to 20% of photosynthate to the obligate biotrophic fungi. Previous studies suggested carbohydrates as the only form of carbon transferred to the fungi. However, *de novo* fatty acid (FA) synthesis has not been observed in AM fungi in absence of the plant. In a forward genetic approach, we identified two *Lotus japonicus* mutants defective in AM-specific paralogs of lipid biosynthesis genes (*KASI* and *GPAT6*). These mutants perturb fungal development and accumulation of emblematic fungal 16:1ω5 FAs. Using isotopolog profiling we demonstrate that ^{13}C patterns of fungal FAs recapitulate those of wild-type hosts, indicating cross-kingdom lipid transfer from plants to fungi. This transfer of labelled FAs was not observed for the AM-specific lipid biosynthesis mutants. Thus, growth and development of beneficial AM fungi is not only fueled by sugars but depends on lipid transfer from plant hosts.
DOI: 10.7554/eLife.29107.001

Introduction

Arbuscular mycorrhiza (AM) is a widespread symbiosis between most land plants and fungi of the Glomeromycota (***Smith and Read, 2008***). The fungi provide mineral nutrients to the plant. These nutrients are taken up from the soil and released inside root cortex cells at highly branched hyphal structures, the arbuscules (***Javot et al., 2007***). For efficient soil exploration, arbuscular mycorrhiza fungi (AMF) develop extended extraradical hyphal networks. Their growth requires a large amount of energy and carbon building blocks, which are transported mostly as lipid droplets and glycogen to the growing hyphal tips (***Bago et al., 2002***, ***2003***). AMF are obligate biotrophs, as they depend on carbon supply by their host (***Smith and Read, 2008***). In the past, detailed ^{13}C-labeled tracer-based NMR studies demonstrated that hexose sugars are a major vehicle for carbon transfer from plants to fungi (***Shachar-Hill et al., 1995***). In addition, a fungal hexose transporter, with high transport activity for glucose is required for arbuscule development and quantitative root colonization as shown by host induced gene silencing (***Helber et al., 2011***), indicating the importance of hexose transfer for intra-radical fungal development.

AMF store carbon mainly in the form of lipids (***Trépanier et al., 2005***). The predominant storage form is triacylglycerol (TAG) and the major proportion of FAs found in AMF is composed of 16:0 (palmitic acid), and of 16:1ω5 (palmitvaccenic acid). The latter is specific to AM fungi and certain

eLife digest Most land plants are able to form partnerships with certain fungi – known as arbuscular mycorrhiza fungi – that live in the soil. These fungi supply the plant with mineral nutrients, especially phosphate and nitrogen, in return for receiving carbon-based food from the plant. To exchange nutrients, the fungi grow into the roots of the plant and form highly branched structures known as arbuscules inside plant cells.

Due to the difficulties of studying this partnership, it has long been believed that plants only provide sugars to the fungus. However, it has recently been discovered that these fungi lack important genes required to make molecules known as fatty acids. Fatty acids are needed to make larger fat molecules that, among other things, store energy for the organism and form the membranes that surround each of its cells. Therefore, these results raise the possibility that the plant may provide the fungus with some of the fatty acids the fungus needs to grow.

Keymer, Pimprikar et al. studied how arbuscules form in a plant known as *Lotus japonicus*, a close relative of peas and beans. The experiments identified a set of mutant *L. japonicus* plants that had problems forming arbuscules. These plants had mutations in several genes involved in fat production that are only active in plant cells containing arbuscules.

Further experiments revealed that certain fat molecules that are found in fungi, but not plants, were present at much lower levels in samples from mutant plants colonized with the fungus, compared to samples from normal plants colonized with the fungus. This suggests that the fungi colonizing the mutant plants may be starved of fat molecules. Using a technique called stable isotope labelling it was possible to show that fatty acids made in normal plants can move into the colonizing fungus.

The findings of Keymer, Pimprikar et al. provide evidence that the plant feeds the fungus not only with sugars but also with fat molecules. The next challenge will be to find out exactly how the fat molecules are transferred from the plant cell to the fungus. Many crop plants are able to form partnerships with arbuscular mycorrhizal fungi. Therefore, a better understanding of the role of fat molecules in these relationships may help to breed crop plants that, by providing more support to their fungal partner, may grow better in the field.

DOI: 10.7554/eLife.29107.002

bacteria and is frequently used as marker for the detection of AM fungi in soil (**Graham et al., 1995**; **Bentivenga and Morton, 1996**; **Madan et al., 2002**; **Trépanier et al., 2005**). Fungus-specific 16:1ω5 FAs are not exclusive to glycerolipids but also incorporated into membrane phospholipids (**van Aarle and Olsson, 2003**). Furthermore, 18:1ω7 and 20:1∂11 are considered specific for AMF but do not occur in all AMF species (**Madan et al., 2002**; **Stumpe et al., 2005**).

It has long been assumed that AMF use sugars as precursors for lipid biosynthesis (**Pfeffer et al., 1999**). However, *de novo* biosynthesis of fungal fatty acids (FAs) was only observed inside colonized roots and not in extraradical mycelia or spores (**Pfeffer et al., 1999**; **Trépanier et al., 2005**). The authors concluded that AM fungi can produce FAs only inside the host. The hypothesis that plants directly provide lipids to the fungus could not be supported at that time (**Trépanier et al., 2005**), due to experimental limitations and the lack of appropriate plant mutants. However, recently available whole genome sequences of AMF have revealed that genes encoding multi-domain cytosolic FA synthase subunits, typically responsible for most of the *de novo* 16:0 FA synthesis in animals and fungi, are absent from the genomes of the model fungi *Rhizophagus irregularis*, *Gigaspora margarita* and *Gigaspora rosea* (**Wewer et al., 2014**; **Ropars et al., 2016**; **Salvioli et al., 2016**; **Tang et al., 2016**). Hence, AMF appear to be unable to synthesize sufficient amounts of 16:0 FAs, but their genomes do encode the enzymatic machinery for 16:0 FA elongation to higher chain length and for FA desaturation (**Trépanier et al., 2005**; **Wewer et al., 2014**).

Development of fungal arbuscules is accompanied by activation of a cohort of lipid biosynthesis genes in arbuscocytes (arbuscule-containing plant cells) (**Gaude et al., 2012a**, **2012b**). Furthermore, lipid producing plastids increase in numbers and together with other organelles such as the endoplasmic reticulum change their position and gather in the vicinity of the arbuscule (**Lohse et al., 2005**; **Ivanov and Harrison, 2014**), symptomatic of high metabolic activity to satisfy the high

demands of arbscocytes for metabolites including lipids. The importance of plant lipid biosynthesis for arbuscule development has been demonstrated by *Medicago truncatula* mutants in AM-specific paralogs of two lipid biosynthesis genes *FatM* and *REDUCED ARBUSCULAR MYCORRHIZA2* (*RAM2*) (**Wang et al., 2012**; **Bravo et al., 2017**). *FatM* encodes an ACP-thioesterase, which terminates fatty acid chain elongation in the plastid by cleaving the ACP off the acyl group releasing free FAs and soluble ACP (**Jones et al., 1995**). *RAM2* encodes a glycerol 3-phosphate acyl transferase (GPAT) and is most similar to *Arabidopsis* GPAT6. In *Arabidopsis*, GPAT6 acetylates the *sn*-2 position of glycerol-3-phosphate with an FA and cleaves the phosphate from lysophosphatidic acid, thereby producing *sn*-2-monoacylglycerol (ßMAG, **Yang et al., 2010**). Mutations in both *FatM* and *RAM2* impair arbuscule branching (**Wang et al., 2012**; **Bravo et al., 2017**). In addition, arbuscule branching requires a complex of two half ABC transporters STR and STR2 (**Zhang et al., 2010**; **Gutjahr et al., 2012**). The substrate of STR/STR2 is unknown but other members of the ABCG transporter family are implicated in lipid transport (**Wittenburg and Carey, 2002**; **Wang et al., 2011**; **Fabre et al., 2016**; **Hwang et al., 2016**; **Lee et al., 2016**). Therefore, and due to its localization in the peri-arbuscular membrane (**Zhang et al., 2010**) it was speculated that the STR/STR2 complex may transport lipids towards arbuscules (**Gutjahr et al., 2012**; **Bravo et al., 2017**). Transcriptional activation of *RAM2* and *STR* is controlled by the GRAS transcription factor *REDUCED ARBUSCULAR MYCORRHIZA1* (*RAM1*) (**Gobbato et al., 2012**; **Park et al., 2015**; **Pimprikar et al., 2016**) and also in *ram1* mutants, arbuscule branching is impaired (**Park et al., 2015**; **Xue et al., 2015**; **Pimprikar et al., 2016**). Thus, *RAM1*, *FatM*, *RAM2* and *STR/STR2* appear to form an AM-specific operational unit for lipid biosynthesis and transport in arbuscocytes. Consistently, they were found to be absent from genomes of plants that have lost the ability to form AM (**Delaux et al., 2014**; **Favre et al., 2014**; **Bravo et al., 2016**).

Here, we analyzed two *Lotus japonicus* mutants identified in a forward genetic screen, which are impaired in arbuscule branching (**Groth et al., 2013**). Positional cloning combined with genome resequencing revealed mutations in a novel AM-specific *β-keto-acyl ACP synthase I* (*KASI*) gene and in the *L. japonicus* ortholog of *M. truncatula RAM2*. KASI likely acts upstream of RAM2 in producing 16:0 FAs. The identity of the genes and the phenotypes led us to hypothesize that AMF may depend on delivery of 16:0 FAs from the plant host. Using a combination of microscopic mutant characterization, lipidomics and isotopolog profiling of 16:0 and 16:1ω5 FAs in roots and extraradical fungal mycelium, we provide strong evidence for requirement of both genes for AM-specific lipid biosynthesis and cross-kingdom lipid transfer from plants to AMF.

Results

Two *L. japonicus* arbuscule-branching mutants are defective in lipid-biosynthesis genes

We previously identified two *L. japonicus* mutants *disorganized arbuscules* (*dis-1*, SL0154-N) and SL0181-N (*red*) deficient in arbuscule branching (**Groth et al., 2013**) (**Figure 1A–B**). Both mutants also suffered from a reduction in root length colonization and blocked the formation of lipid-containing vesicles of the fungus *Rhizophagus irregularis* (**Figure 1C–D**). We identified the causative mutations with a combination of classical mapping and next generation sequencing (see Materials and methods). *DIS* encodes a *β*-keto-acyl ACP synthase I (KASI, **Figure 1—figure supplements 1A–C** and **2**). KASI enzymes catalyze successive condensation reactions during fatty acyl chain elongation from C4:0-ACP to C16:0-ACP (**Li-Beisson et al., 2010**). SL0181-N carries one mutation (*ram2-1*) in the *L. japonicus* orthologue of the previously identified *Medicago truncatula REDUCED ARBUSCULAR MYCORRHIZA2* (*RAM2*, **Figure 1—figure supplements 3** and **4**). Arabidopsis GPAT6 has been shown to produce ß-MAG with a preference for 16:0 FAs (**Yang et al., 2012**). Therefore, we hypothesized that DIS and RAM2 act in the same biosynthetic pathway.

We identified additional allelic *dis* mutants by TILLING (**Figure 1—figure supplement 1E**, **Supplementary file 1**) (**Perry et al., 2003**) and a *ram2* mutant caused by a LORE1 insertion in the *RAM2* gene (**Figure 1—figure supplement 3B**) (**Małolepszy et al., 2016**). Among the allelic *dis* mutants we chose *dis-4* for further investigation because it suffers from a glycine replacement at the border of a conserved ß-sheet (**Figure 1—figure supplement 2**), which likely affects protein folding (**Perry et al., 2009**). Both allelic mutants *dis-4* and *ram2-2* phenocopied *dis-1* and *ram2-1*,

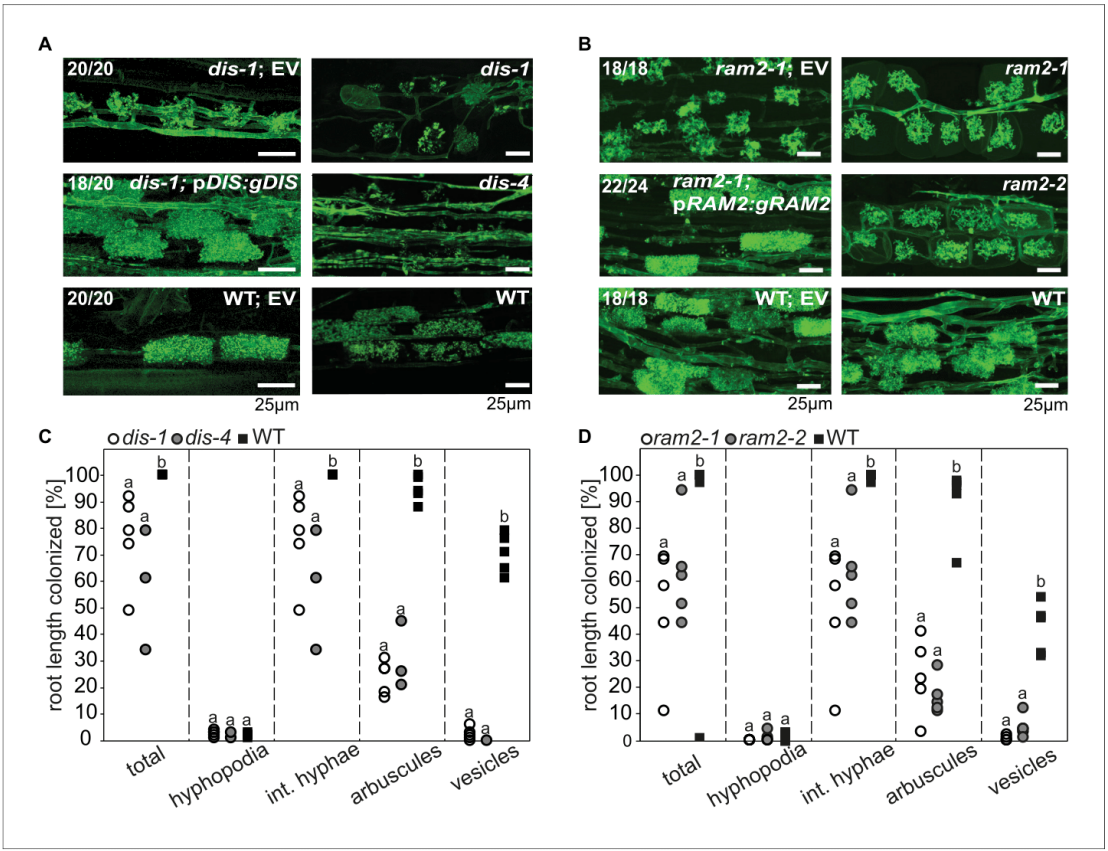

Figure 1. *DIS* and *RAM2* are required for arbuscule branching and vesicle formation. Arbuscule phenotype and complementation of *dis* (**A**) and *ram2* (**B**) mutants. The fungus was stained with wheat-germ agglutinin (WGA)-AlexaFluor488. (**C-D**) Percent root length colonization of *dis* (**C**) and *ram2* (**D**) mutants as compared to wild-type. Different letters indicate significant differences among treatments (ANOVA; posthoc Tukey). (**C**): n = 13; $p \leq 0.1$, $F_{2,10} = 8.068$ (total & int. hyphae); $p \leq 0.001$ $F_{2,10} = 124.5$ (arbuscules); $p \leq 0.001$, $F_{2,10} = 299.1$ (vesicles) (**D**): n = 15; $p \leq 0.1$, $F_{2,12} = 10.18$ (total & int. hyphae); $p \leq 0.001$ $F_{2,12} = 57.86$ (arbuscules); $p \leq 0.001$, $F_{2,12} = 72.37$ (vesicles). (**A-D**) Plants were inoculated with *R. irregularis* and harvested at 5 weeks post inoculation (wpi).

DOI: 10.7554/eLife.29107.003

The following figure supplements are available for figure 1:

Figure supplement 1. Identification of the *dis* mutation.

DOI: 10.7554/eLife.29107.004

Figure supplement 2. Protein sequence alignment of *L. japonicus* DIS with other KASI proteins.

DOI: 10.7554/eLife.29107.005

Figure supplement 3. Identification of mutation in the *RAM2* gene.

DOI: 10.7554/eLife.29107.006

Figure supplement 4. Protein sequence alignment of *L.*

DOI: 10.7554/eLife.29107.007

respectively. Furthermore, transgenic complementation of both *dis-1* and *ram2-1* with the wild-type versions of the mutated genes restored arbuscule-branching and wild-type-like levels of root length colonization and vesicle formation (***Figure 1A-B***). Taken together this confirmed identification of both causal mutations.

DIS and *RAM2* expression in arbuscocytes is sufficient for arbuscule development

Transcript levels of both *DIS* and *RAM2* increased in colonized roots (***Figure 3—figure supplement 1***A). To analyze the spatial activity pattern of the *DIS* and *RAM2* promoters during colonization we fused 1.5 kb for *DIS* and 2.275 kb for *RAM2* upstream of the translational start site to the *uidA* gene. Consistent with a role of both genes in arbuscule development GUS activity was predominantly detected in arbuscocytes (arbuscule-containing cells) in both wild-type and the corresponding mutant roots (***Figure 2—figure supplement 1A–B***).

To correlate promoter activity with the precise stage of arbuscule development we used nuclear localized YFP as a reporter. To visualize the fungus, the promoter:reporter cassette was co-transformed with a second expression cassette containing secreted *mCherry* fused to the *SbtM1* promoter. This promoter drives expression in colonized cells, in cells neighboring apoplastically growing hyphae and in cells forming pre-penetration *apparatuus* (PPAs, cytoplasmic aggregations that assemble in cortex cells *prior* to arbuscule development) (***Genre et al., 2008***; ***Takeda et al., 2009***, ***2012***). When expressed under the control of the *SbtM1* promoter, secreted mCherry accumulates in the apoplast surrounding fungal structures and PPAs, thereby revealing the silhouette of these structures (***Figure 2A–B***, ***Videos 1–2***). Nuclear localized YFP fluorescence indicated activity of both promoters in cells containing PPAs (c, ***Videos 1–2***) and containing sparsely branched (d) or mature (e) arbuscules. Furthermore, we rarely detected YFP fluorescence in non-colonized cells in direct neighborhood of arbuscocytes, which were possibly preparing for PPA formation (a). However, YFP signal was absent from cells containing collapsed arbuscules (f), indicating that the promoters were active during arbuscule development and growth but inactive during arbuscule degeneration (***Figure 2A–B***). *RAM2* promoter activity was strictly correlated with arbuscocytes, while the *DIS* promoter showed additional activity in cortical cells of non-colonized root segments (***Figure 2A–B***, ***Figure 2—figure supplement 1C–D***, ***Videos 3–6***).

To examine, whether arbuscocyte-specific expression of *DIS* and *RAM2* is sufficient for fungal development we complemented the *dis-1* and *ram2-1* mutants with the corresponding wild-type genes fused to the arbuscocyte-specific *PT4* promoter (***Volpe et al., 2013***). This restored arbuscule-branching, vesicle formation as well as root length colonization in the mutants (***Figure 2C–F***), showing that arbuscocyte-specific expression of *DIS* and *RAM2* suffices to support AM development. Thus, expression of lipid biosynthesis genes in arbuscocytes is not only important for arbuscule branching but also for vesicle formation and quantitative colonization.

The *KASI* family comprises three members in *L. japonicus*

Growth and development of *dis* and *ram2* mutants are not visibly affected (***Figure 3—figure supplement 2***), although they carry defects in important lipid biosynthesis genes. *RAM2* is specific to AM-competent plants (***Wang et al., 2012***; ***Delaux et al., 2014***; ***Favre et al., 2014***; ***Bravo et al., 2016***) and activated in an AM-dependent manner (***Figure 2***, ***Figure 3—figure supplement 1A***) (***Gobbato et al., 2012***, ***2013***). Plants contain an additional *GPAT6* paralog, which likely fulfills the housekeeping function (***Figure 1—figure supplement 4***, ***Yang et al., 2012***; ***Delaux et al., 2015***). To understand whether the same applies to *DIS* we searched the *L. japonicus* genome for additional *KASI* genes. We detected three paralogs *KASI*, *DIS* and *DIS-LIKE* (***Figure 1—figure supplement 1D–E*** and ***Figure 1—figure supplement 2***), of which only *DIS* was transcriptionally activated in AM roots (***Figure 3—figure supplement 1A***). Phylogenetic analysis revealed a split of seed plant KASI proteins into two different clades, called KASI and DIS (***Figure 3***). Members of the KASI clade, are presumably involved in housekeeping functions as this clade contains the product of the *KASI* single copy gene in *Arabidopsis* (***Wu and Xue, 2010***). Members of the *DIS* clade are found specifically in AM-host dicotyledons and in a gymnosperm (***Figure 3***). As confirmed by synteny analysis (***Figure 3—figure supplement 3***), *DIS* is absent from all eight analyzed non-host dicotyledon genomes, a phylogenetic pattern similar to other symbiosis genes (***Delaux et al., 2014***; ***Favre et al., 2014***; ***Bravo et al., 2016***). The occurrence of *DIS* in *Lupinus* species, which lost AM competence but still form root nodule symbiosis, may be a relic from the AM competent ancestor. An apparently, *Lotus*-specific, and thus recent duplication of the *DIS* gene resulted in an 87% identical copy (*DIS-LIKE*) located directly adjacent to *DIS* in a tail-to-tail orientation (***Figure 1—figure supplements 1B–C***, ***2***). *DIS-LIKE* was expressed at very low levels and not induced upon AM (***Figure 3—figure***

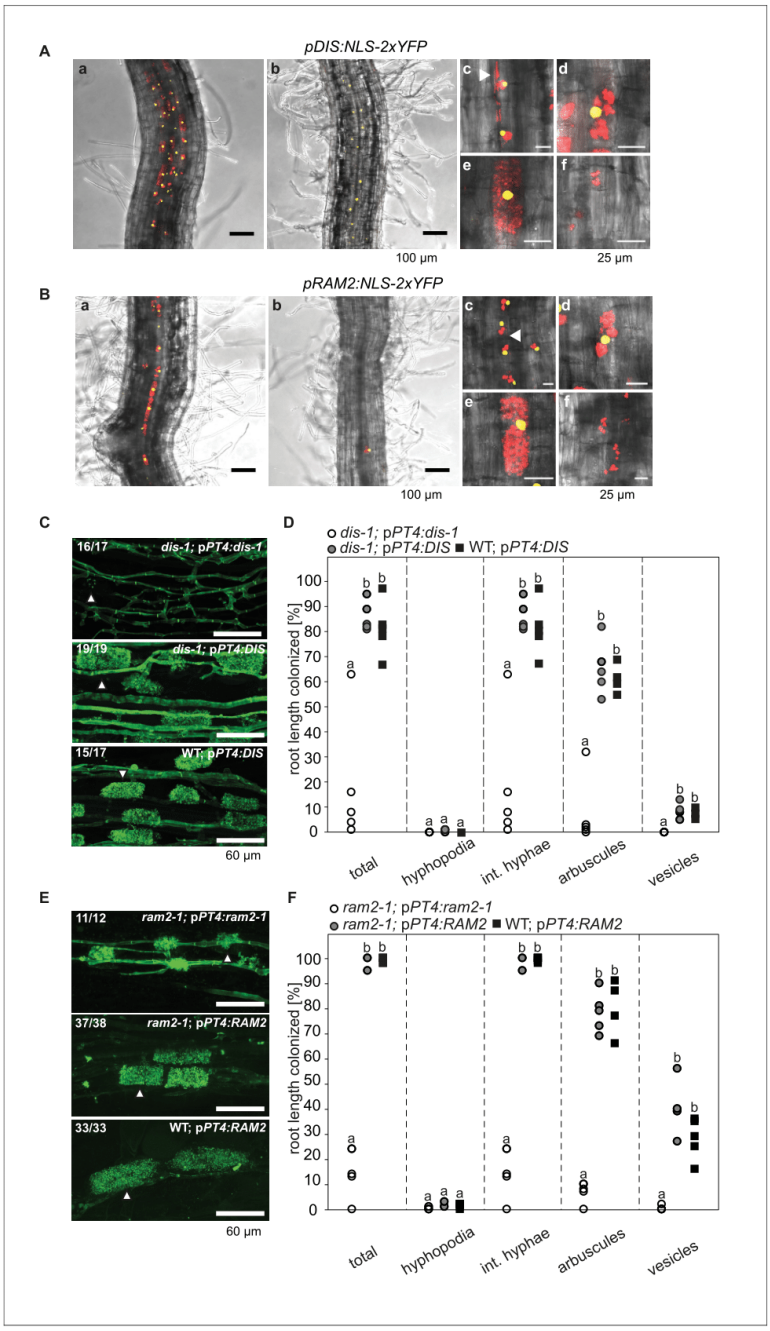

Figure 2. Arbuscocyte-specific expression of *DIS* and *RAM2* is sufficient for arbuscule branching. Promoter activity indicated by nuclear localized yellow fluorescence in colonized transgenic *L. japonicus* wild-type roots transformed with constructs containing a 1.5 kb promoter fragment of *DIS* (**A**) or a 2.275 kb promoter fragment of *RAM2* (**B**) fused to *NLS-YFP*. (**A-B**) Red fluorescence resulting from expression of *pSbtM1:SP-mCherry* labels the apoplastic space surrounding pre-penetration *apparatuus* (PPAs) and fungal structures, thereby evidencing the silhouette of these structures. a

Figure 2 continued on next page

Figure 2 continued

Colonized root, b non-colonized part of colonized root, c PPAs, (white arrow heads indicate the silhouette of fungal intraradical hyphae) d small arbuscules, e fully developed arbuscules f collapsed arbuscules. Merged confocal and bright field images of whole mount roots are shown. (**C-D**) Transgenic complementation of *dis-1* (C) and *ram2-1* (D) hairy roots with the respective wild-type gene driven by the *PT4* promoter. The mutant gene was used as negative control. White arrowheads indicate arbuscules. (**E-F**) Quantification of AM colonization in transgenic roots shown in (**C-D**). Different letters indicate significant differences (ANOVA; posthoc Tukey; n = 15; $p \leq 0.001$) among genotypes for each fungal structure separately. Int. hyphae, intraradical hyphae. (**E**): $F_{2,12} = 26.53$ (total), $F_{2,12} = 46.97$ (arbuscules), $F_{2,12} = 27.42$ (vesicles). (**F**) $F_{2,12} = 341.5$ (total), $F_{2,12} = 146.3$ (arbuscules), $F_{2,12} = 35.86$ (vesicles).

DOI: 10.7554/eLife.29107.008

The following figure supplement is available for figure 2:

Figure supplement 1. *DIS* and *RAM2* promoter activity in wild type and *dis* and *ram2* mutants.

DOI: 10.7554/eLife.29107.009

supplement 1A). Nevertheless, because of its sequence similarity to *DIS*, we examined whether *DIS-LIKE* is also required for arbuscule formation using the *dis-like-5* mutant, which suffers from a glycine replacement at position 180 at the border of a highly conserved β-sheet that likely affects protein function (***Perry et al., 2009***) (***Supplementary file 1***, ***Figure 1—figure supplement 2***). However, in roots of *dis-like-5* AM and arbuscule development was indistinguishable from wild type (***Figure 3—figure supplement 1B***). Therefore, *DIS-LIKE* might have lost its major role in arbuscule development after the duplication.

DIS functions like a canonical KASI *in planta*

We examined whether DIS can substitute the phylogenetically related housekeeping KASI. To this end we transgenically complemented an *Arabidopsis kasI* mutant (***Wu and Xue, 2010***) with *Lotus DIS* driven by the *Arabidopsis KASI* promoter. Ar*abidopsis kasI* exhibits an altered FA profile and reduced rosette growth (***Wu and Xue, 2010***). Complementation with *DIS* restored both wild-type-like rosette growth and FA accumulation. The *kasI* phenotypes persisted when the *dis-1* mutant allele was transformed as a negative control (***Figure 4C–E***). In the reverse cross-species complementation *AtKASI* driven by the *DIS* promoter restored colonization, arbuscule branching and vesicle

Video 1. 3D animation of ***Figure 2Ac*** illustrating that the silhouette of the fungal intraradical hyphae (red fluorescent vertical line) aligns with the silhouette of pre-penetration *apparatuus* (red fluorescent bag-like structure). Yellow fluorescence in nuclei indicates activation of p*DIS:YFP*.

DOI: 10.7554/eLife.29107.010

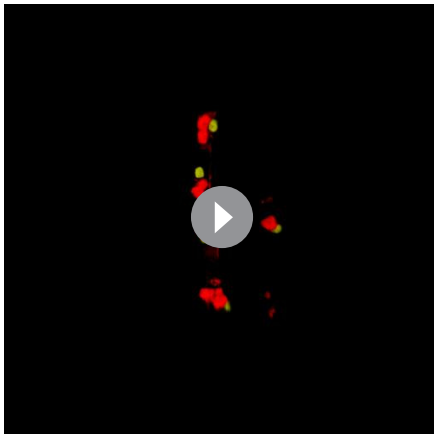

Video 2. 3D animation of ***Figure 2Bc*** illustrating that the silhouette of the fungal intraradical hyphae (red fluorescent vertical line) aligns with the silhouette of pre-penetration *apparatuus* (red fluorescent bag-like structure). Yellow fluorescence in nuclei indicates activation of p*RAM2:YFP*.

DOI: 10.7554/eLife.29107.011

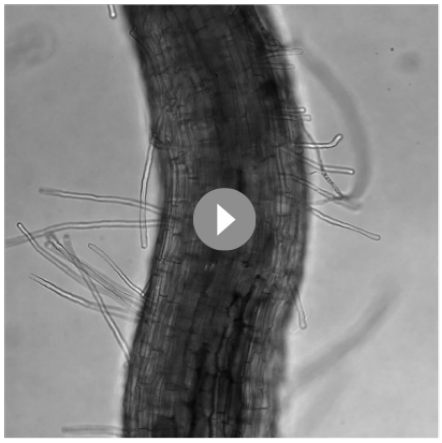

Video 3. Scan through confocal z-stack of ***Figure 2Aa*** illustrating correlation of *DIS* promoter activity with arbuscocytes.
DOI: 10.7554/eLife.29107.012

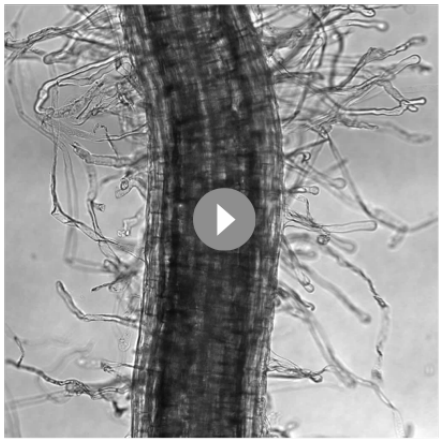

Video 4. Scan through confocal z-stack of ***Figure 2Ab*** illustrating *DIS* promoter activity exclusively in the cortex.
DOI: 10.7554/eLife.29107.013

formation in *dis-1* roots (***Figure 4A–B***). Furthermore, DIS contains a KASI-typical plastid transit peptide and - as predicted - localizes to plastids in *Nicotiana benthamiana* leaves and *L. japonicus* roots (***Figure 1—figure supplement 1F*** ***Figure 4F–G***). Thus, the enzymatic function of DIS is equivalent to the housekeeping KASI of *Arabidopsis* and the AM-specific function must result from its AM-dependent expression pattern.

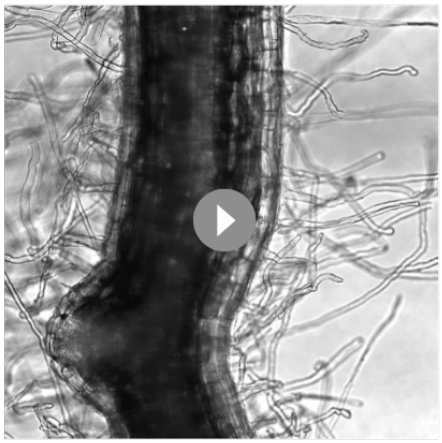

Video 5. Scan through confocal z-stack of ***Figure 2Ba*** illustrating correlation of *RAM2* promoter activity with arbuscocytes.
DOI: 10.7554/eLife.29107.014

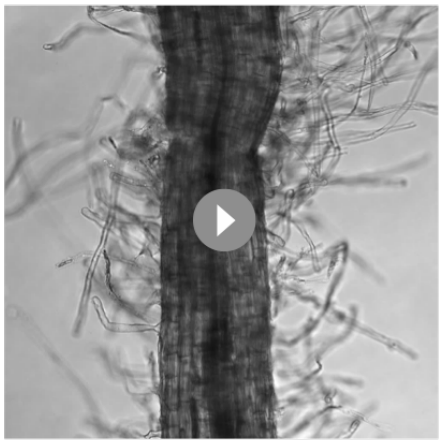

Video 6. Scan through confocal z-stack of ***Figure 2Bb*** illustrating absence of *RAM2* promoter activity from non-colonized cells.
DOI: 10.7554/eLife.29107.015

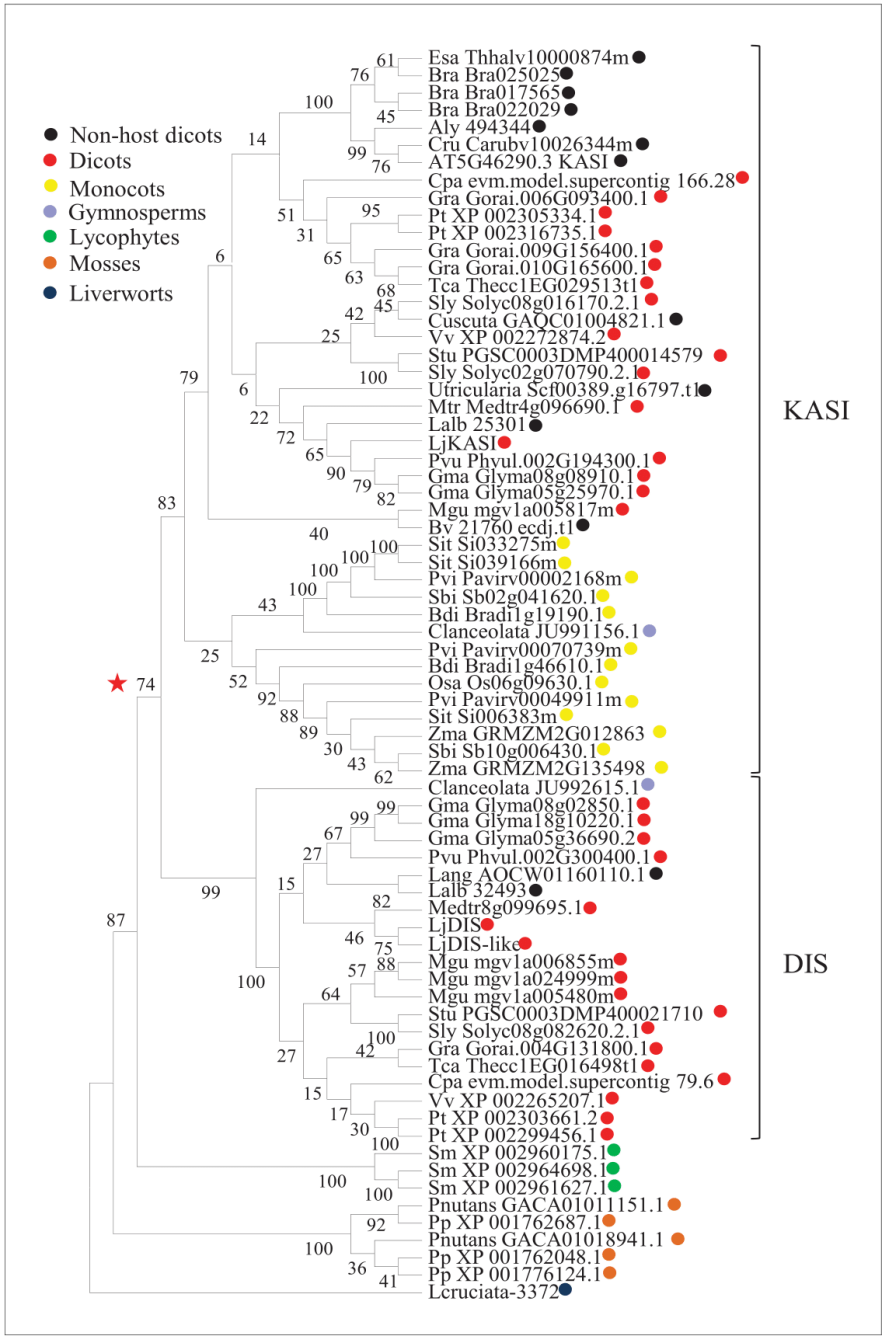

Figure 3. Phylogenetic tree of KASI proteins in land plants. Protein sequences were aligned using MAFFT. Phylogenetic trees were generated by neighbor-joining implemented in MEGA5 (***Tamura et al., 2011***). Partial gap

Figure 3 continued on next page

Figure 3 continued

deletion (95%) was used together with the JTT substitution model. Bootstrap values were calculated using 500 replicates. DIS likely originated before the angiosperm divergence (red star).

DOI: 10.7554/eLife.29107.016

The following source data and figure supplements are available for figure 3:

Source data 1. Accession numbers for protein sequences used in the phyologenic tree.

DOI: 10.7554/eLife.29107.017

Figure supplement 1. Transcript accumulation of *KASI* and *RAM2* genes.

DOI: 10.7554/eLife.29107.018

Figure supplement 2. Shoot phenotypes of *dis* and *ram2* mutants.

DOI: 10.7554/eLife.29107.019

Figure supplement 3. Genomic comparison of the *DIS* locus in host and non-host species.

DOI: 10.7554/eLife.29107.020

The AM-specific increase in 16:0 and 16:1ω5 FA containing lipids is abolished in the *dis* mutant

To characterize the role of DIS in determining the lipid composition of non-colonized and colonized roots we quantified triacylglycerols (TAGs), diacylglycerols (DAGs), galactolipids and phospholipids in wild-type and *dis-1*. The lipid profile of colonized roots contains both plant and fungal lipids, however using the fungal marker FA 16:1ω5 and previous data on fungus-specific lipids (***Wewer et al., 2014***), many fungal lipids can be clearly distinguished from plant lipids. The lipid profile of non-colonized roots was not affected by the *dis-1* mutation. However, the strong and significant increase of 16:0 and 16:1 (most probably fungus-specific 16:1ω5) containing TAGs, which is characteristic for colonization of wild-type roots (***Wewer et al., 2014***) was abolished in *dis-1* (***Figure 5A–D***, ***Figure 5—figure supplement 1B***). Also, AM- and fungus-specific DAG and phospholipid molecular species were enhanced in colonized wild-type roots but not in colonized *dis-1* roots (***Figure 5—figure supplements 1A*** and ***2***). In contrast, galactolipids were not affected by root colonization or genotype (***Figure 5—figure supplement 3***). In summary, DIS affects the glycerolipid and phospholipid profile of colonized *L. japonicus* roots and does not interfere with lipid accumulation in the non-colonized state. Most lipids affected by the *DIS* mutation are fungus-specific and therefore reflect the amount of root colonization and of fungal lipid-containing vesicles. However, since the root lipid profile is hardly affected, absence of FA elongation by DIS was the cause of reduced lipid accumulation and root colonization.

RAM1, *DIS*, *RAM2* and *STR* are required for accumulation of AM signature lipids

Similar to *dis* and *ram2 L. japonicus* mutants in the ABCG half-transporter STR and the GRAS protein RAM1 are affected in arbuscule branching (***Kojima et al., 2014***; ***Pimprikar et al., 2016***; ***Xue et al., 2015***), quantitative root colonization and formation of lipid-containing fungal vesicles (***Figure 5—figure supplement 4***). Moreover, the AM-dependent transcriptional activation of *DIS* and *KASIII*, the latter of which is a single copy gene in *L. japonicus* and produces precursors for DIS-activity by catalyzing FA chain elongation from C2 to C4, was absent from *ram1* mutants (***Figure 6***). In contrast, induction of the single copy gene *KASII*, which elongates fatty acyl chains from C16 to C18 was not hampered by *RAM1* deficiency. Thus, *RAM1* may play an important role in the regulation of lipid biosynthesis in arbuscocytes, since it also mediates expression of *RAM2* and *STR* (***Gobbato et al., 2012***; ***Park et al., 2015***; ***Pimprikar et al., 2016***; ***Luginbuehl et al., 2017***).

We hypothesized that RAM1, DIS, RAM2 and STR form a specific operational unit for lipid biosynthesis and transport in arbuscocytes. Therefore, we directly compared their impact on the AM-specific root lipid profile and measured galactolipids, phospholipids, TAGs and also total and free fatty acids in colonized roots of *ram1*, *dis*, *ram2*, *str* mutants and wild-type in parallel. Consistent with our previous observation in *dis-1*, galactolipid accumulation was similar in colonized roots of wild-type and all mutants (***Figure 5—figure supplement 3C–D***). In contrast, total 16:0 FAs (FAMEs) as well as 16:1 and 18:1 (likely 18:1ω7 FA of fungal origin) FAs were strongly reduced in all colonized mutants compared to the corresponding wild-type. Free FAs showed a similar pattern except for 18:1 FAs

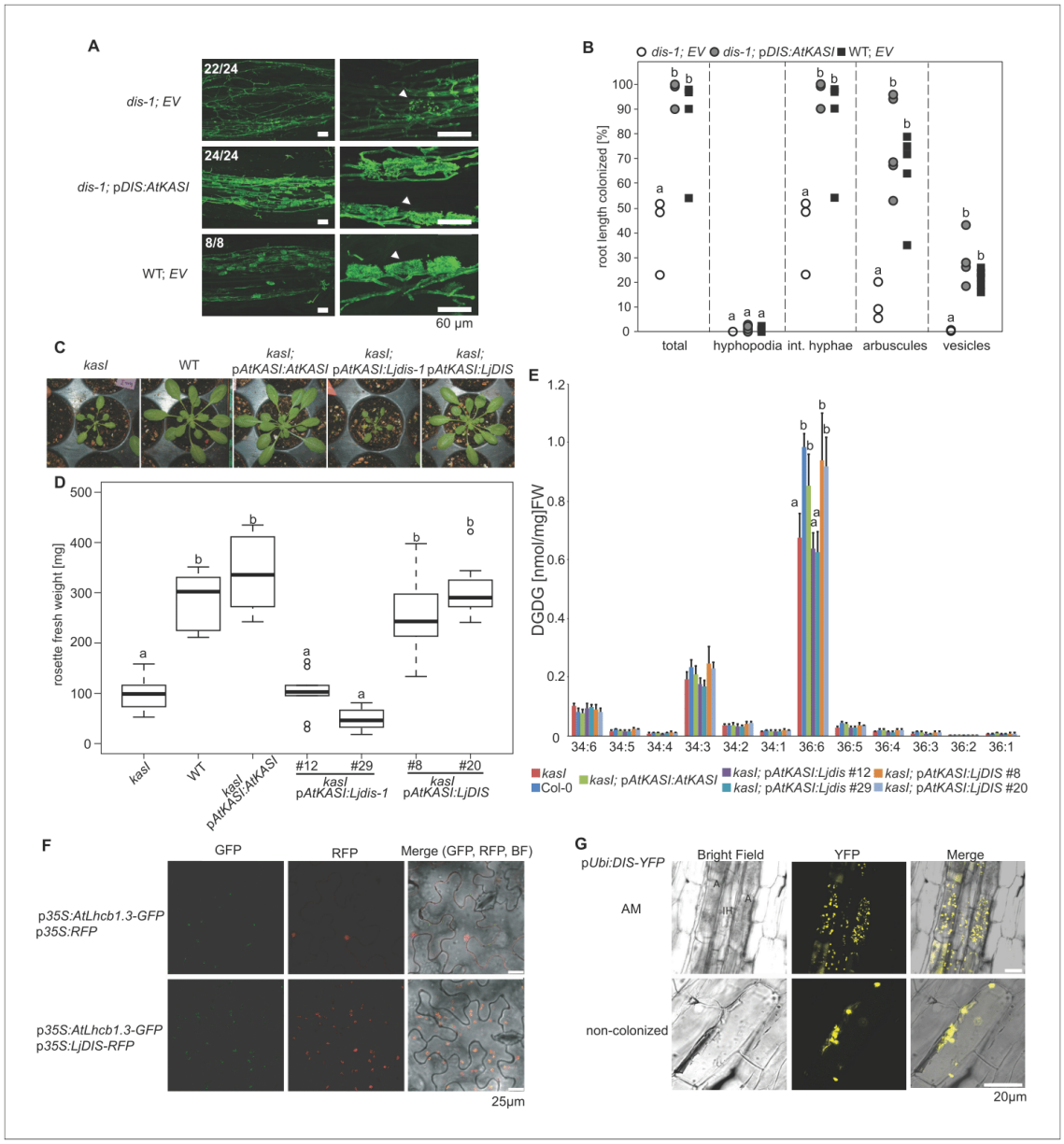

Figure 4. DIS function is equivalent to a canonical KASI. (**A**) Microscopic AM phenotype of transgenic *dis-1* mutant and wild-type hairy roots transformed with either an empty vector (EV) or the *Arabidopsis KASI* gene fused to the *L. japonicus DIS* promoter. White arrowheads indicate arbuscules. (**B**) Quantification of AM colonization in transgenic roots of *dis-1* transformed with EV (open circles), *dis-1* transformed with p*DIS-AtKASI* (grey circles) and wild-type transformed with EV (black squares). int. hyphae, intraradical hyphae. Different letters indicate significant differences (ANOVA; posthoc Tukey; n = 15; $p \leq 0.001$) among genotypes for each fungal structure separately. $F_{2,12} = 0.809$ (total and intraradical hyphae), $F_{2,12} = 43.65$ (arbuscules), $F_{2,12} = 0.0568$ (vesicles). (**C**) Rosettes of *Arabidopsis*, *kasI* mutant, Col-0 wild-type plants and *kasI* mutant plants transformed either

Figure 4 continued on next page

Figure 4 continued

with the native *AtKASI* gene, the *dis-1* mutant or the *DIS* wild-type gene driven by the *Arabidopsis KASI* promoter at 31 days post planting. (**D**) Rosette fresh weight of *kasI* mutant, Col-0 wild-type plants, one transgenic *pAtKASI:AtKASI* complementation line (***Wu and Xue, 2010***) and two independent transgenic lines each of *kasI* mutant plants transformed either with the *dis-1* mutant or the *DIS* wild-type gene driven by the *Arabidopsis KASI* promoter at 31 days post planting. Different letters indicate significant differences (ANOVA; posthoc Tukey; n = 70; $p \leq 0.001$; $F_{6,63} = 34.06$) among genotypes. (**E**) Q-TOF MS/MS analysis of absolute amount of digalactosyldiacylglycerols (DGDG) containing acyl chains of 16:x + 18:x(34:x DGDG) or di18:x(36:x DGDG) derived from total leaf lipids of the different *Arabidopsis* lines. Different letters indicate significant differences (ANOVA; posthoc Tukey; n = 32; ($p \leq 0.05$, $F_{6,25} = 14.48$ (36:6)). (**F**) Subcellular localization of DIS in transiently transformed *Nicotiana benthamiana* leaves. Free RFP localizes to the nucleus and cytoplasm (upper panel). RFP fused to DIS co-localizes with the *Arabidopsis* light harvesting complex protein AtLHCB1.3-GFP in chloroplasts (lower panel). (**G**) Subcellular localization in plastids of DIS-YFP expressed under the control of the *L. japonicus Ubiquitin* promoter in *R. irregularis* colonized (upper panel) and non-colonized (lower panel) *L. japonicus* root cortex cells. BF, bright field; IH, intercellular hypha; A, arbuscule.
DOI: 10.7554/eLife.29107.021

(***Figure 5—figure supplement 5***). Also for TAGs and phospholipids, AMF-specific molecular species and 16:0 FA containing molecular species were strongly reduced in all mutants (***Figure 5E–H***, ***Figure 5—figure supplements 6–11***). However, the two allelic *ram2* mutants formed an exception. They specifically over-accumulated 16:0-16:0 FA-containing phospholipids in particular 32:0 PA and 32:0-PC but also to a smaller extend 32:0-PE and 32:0-PI (***Figure 5—figure supplements 6–10***). A similar pattern was observed for tri-16:0 TAGs (***Figure 5F***). This suggests that RAM2 acts downstream of DIS in a biosynthetic pathway and uses the 16:0 FAs synthesized by DIS in arbuscocytes as substrates. In the absence of functional RAM2 the FA products of DIS, are probably redirected into phospholipid biosynthesis and storage lipid biosynthesis *via* PA and PC (***Li-Beisson et al., 2010***) leading to the observed higher accumulation of 16:0 FA containing lipid species in *ram2* mutants. This higher accumulation of specific lipids did not correlate with colonization levels in *ram2* mutants (***Figure 5—figure supplement 4***) confirming that reduced colonization levels are not the primary cause for altered lipid profiles in the colonized mutant roots. Instead, defective AM-specific lipid biosynthesis in the mutants more likely impairs fungal development.

The abundance of 16:0 ß-monoacyl-glycerol is reduced in all mutants

The first step in TAG and phospholipid production after FA biosynthesis is the esterification of FAs with glycerol by GPATs in the plastid or endoplasmic reticulum to produce α-MAGs (sn1/3-MAGs, ***Li-Beisson et al., 2010***). RAM2 is predicted to produce a different type of glycerolipid ß-MAG (sn2-MAG) with a preference towards 16:0 and 18:1 FAs (***Yang et al., 2010***; ***Wang et al., 2012***; ***Yang et al., 2012***). To examine the role of RAM2 in MAG biosynthesis, we quantified α-MAG and ß-MAG species in colonized roots of wild-type and all mutants. The abundance of ß-MAGs was generally lower than that of α-MAGs (***Figure 7***). The amount of most α-MAG species did not differ among the genotypes. Only the fungus-specific 16:1 and 18:1ω7 α-MAGs were reduced in all mutants reflecting the lower fungal biomass (***Figure 7A***). Fungus-specific ß-MAGs with 16:1 and 18:1ω7 acyl groups were not detected and most ß-MAG molecular species accumulated to similar levels in all genotypes. Exclusively the levels of 16:0 ß-MAGs were significantly lower in all mutants as compared to the corresponding wild-type roots (***Figure 7B***). This supports a role of RAM2 in 16:0 ß-MAG synthesis during AM and a role of DIS in providing 16:0 FA precursors for RAM2 activity. A low accumulation, of 16:0 ß-MAGs in *ram1* mutants is consistent with RAM1's role in regulating the FA and lipid biosynthesis genes (***Figure 6***) (***Gobbato et al., 2012***; ***Pimprikar et al., 2016***). In *str* 16:0 ß-MAGs likely did not accumulate because of reduced *RAM2* expression in *str* roots due to low root length colonization and/or a regulatory feedback loop (***Bravo et al., 2017***).

DIS, *RAM2* and *STR* are required for transfer of ^{13}C label from plant to fungus

In plants, ß-MAGs serve as precursors for cutin polymers at the surface of aerial organs (***Yang et al., 2012***; ***Yeats et al., 2012***). For their use in membrane or storage lipid biosynthesis they first need to be isomerized to α-MAGs (***Li-Beisson et al., 2010***). The recruitment of a GPAT6 (RAM2) instead of a α-MAG-producing GPAT for AM-specific lipid synthesis supports the idea that RAM2-products are destined for something else than membrane biosynthesis of the host cell. Since AM fungal genomes lack genes encoding cytosolic FA synthase subunits (***Wewer et al., 2014***; ***Ropars et al., 2016***;

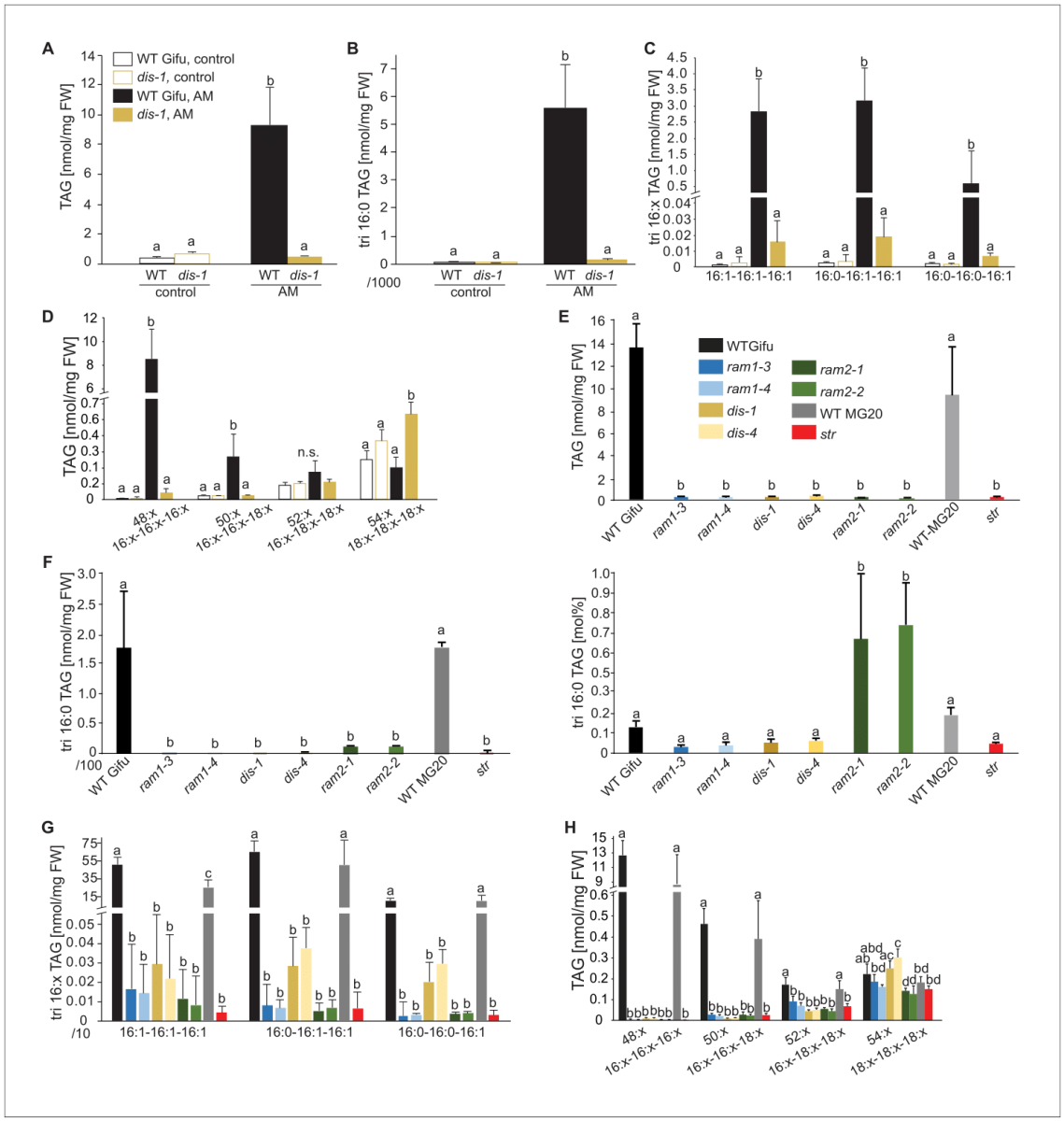

Figure 5. Lack of characteristic accumulation of triacylglycerols in AM-defective mutants. (**A-D**) Quantitative accumulation of (**A**) total triacylglycerols, (**B**) tri16:0-triacylglycerol (**C**) tri16:x-triacylglycerols and (**D**) of triacylglycerols harbouring 16:x and 18:x FA-chains in non-colonized and *R. irregularis* colonized wild-type and *dis-1* roots. Different letters indicate significant differences (ANOVA; posthoc Tukey) (**A**): n = 18; $p \leq 0.001$; $F_{3,14} = 68.16$. (**B**): n = 18; $p \leq 0.001$; $F_{3,14} = 68.48$. (**C**): n = 19; $p \leq 0.01$, $F_{3,15} = 7.851$ (16:1-16:1-16:1); $p \leq 0.001$, $F_{3,15} = 14.52$ (16:0-16:1-16:1); $p \leq 0.001$, $F_{3,15} = 39.22$ (16:0-16:0-16:1). (**D**): n = 19; $p \leq 0.001$, $F_{3,15} = 12.15$ (48:x), $F_{3,15} = 15.56$ (50:x); $p \leq 0.01$, $F_{3,15} = 22.93$ (54:x). (**E-G**) Quantitative accumulation of (**E**) total triacylglycerols, (**F**) tri16:0-triacylglycerols, (**G**) tri16:x-triacylglycerols and (**H**) of triacylglycerols harbouring 16:x and 18:x FA-chains in colonized roots of *L. japonicus* wild-type Gifu, wild-type MG-20 and arbuscule-defective mutants. Different letters indicate significant differences (ANOVA; posthoc Tukey).

Figure 5 continued on next page

Figure 5 continued

(**E**): n = 40; $p \leq 0.001$; $F_{8,31} = 38.42$. (**F**) Left: absolute tri16:0 TAG content: n = 40; $p \leq 0.001$; $F_{8,31} = 19.05$. Right: tri16:0 TAG proportion among all TAGs, n = 40; $p \leq 0.001$; $F_{8,31} = 14.21$. (**G**): $p \leq 0.001$; n = 41, $F_{8,32} = 86.16$ (16:1-16:1-16:1); n = 39, $F_{8,30} = 24.16$ (16:0-16:1-16:1); n = 40, $F_{8,31} = 17.67$ (16:0-16:0-16:1). (**H**): n = 40; $p \leq 0.001$, $F_{8,31} = 39.26$ (48:x), $F_{8,31} = 28.93$ (50:x); $p \leq 0.01$, $F_{8,31} = 19.78$ (52:x); $p \leq 0.05$, $F_{8,31} = 13.77$ (54:x). (**A-H**) Bars represent means ±standard deviation (SD) of 3–5 biological replicates.

DOI: 10.7554/eLife.29107.022

The following source data and figure supplements are available for figure 5:

Source data 1. Raw data for lipid profiles in ***Figure 5*** and ***Figure 5—figure supplements 1–3*** and ***5–11***.

DOI: 10.7554/eLife.29107.023

Figure supplement 1. Diacylglycerol (DAG) and triacylglycerol (TAG) profiles of *L. japonicus* WT and *dis-1* control and AM roots.

DOI: 10.7554/eLife.29107.024

Figure supplement 2. Profiles of phospholipids in non-colonized and colonized *L. japonicus* WT Gifu and *dis-1* roots.

DOI: 10.7554/eLife.29107.025

Figure supplement 3. MGDG and DGDG profiles do not differ among *L. japonicus* wild-type and mutant roots.

DOI: 10.7554/eLife.29107.026

Figure supplement 4. All arbuscule-deficient mutants show reduced root length colonization.

DOI: 10.7554/eLife.29107.027

Figure supplement 5. Total fatty acid and free fatty acid profiles of colonized *L. japonicus* WT and AM-defective mutant roots.

DOI: 10.7554/eLife.29107.028

Figure supplement 6. Triacylglycerol (TAG) profiles of colonized *L. japonicus* WT and AM-defective mutant roots.

DOI: 10.7554/eLife.29107.029

Figure supplement 7. Phosphatidic acid (PA) profiles in *L. japonicus* WT and AM-defective mutants.

DOI: 10.7554/eLife.29107.030

Figure supplement 8. Profile of phosphatidylcholines (PC) in *L. japonicus* WT and AM-defective mutants.

DOI: 10.7554/eLife.29107.031

Figure supplement 9. Phosphatidylethanolamine (PE) profile in *L. japonicus* WT and AM-defective mutants.

DOI: 10.7554/eLife.29107.032

Figure supplement 10. Phosphatidylinositol (PI) profile in *L. japonicus* WT and AM-defective mutants.

DOI: 10.7554/eLife.29107.033

Figure supplement 11. Phosphatidylserine (PS) profile in *L. japonicus* WT and AM-defective mutants.

DOI: 10.7554/eLife.29107.034

Tang et al., 2016) we hypothesized that 16:0 ß-MAGs synthesized by DIS- and RAM2 are predominantly delivered to the fungus. To test this hypothesis, we examined lipid transfer by FA isotopolog profiling. Isotopologs are molecules that differ only in their isotopic composition. For isotopolog profiling an organism is fed with a heavy isotope labelled precursor metabolite. Subsequently the labelled isotopolog composition of metabolic products is analyzed. The resulting characteristic isotopolog pattern yields information about metabolic pathways and fluxes (***Ahmed et al., 2014***).

We could not detect fungus-specific 16:1ω5 ß-MAGs in colonized roots (***Figure 7B***). Therefore, we reasoned that either a downstream metabolite of ß-MAG is transported to the fungus, or alternatively, ß-MAG is rapidly metabolized in the fungus prior to desaturation of the 16:0 acyl residue. Since the transported FA groups can be used by the fungus for synthesizing a number of different lipids, we focused on total 16:0 FA methyl esters (FAMEs, subsequently called FAs for simplicity) and 16:1ω1 FAMEs as markers for lipid transfer. We fed *L. japonicus* wild-type, *dis-1*, *ram2-1* and *str* with [U-$^{13}C_6$]glucose and then measured the isotopolog composition of 16:0 FAs and 16:1ω5 FAs in *L. japonicus* roots and in associated extraradical fungal mycelium with spores. To generate sufficient hyphal material for our measurements the fungus was pre-grown on split Petri dishes in presence of a carrot hairy root system as nurse plant (***Figure 8—figure supplement 1***). Once the fungal mycelium had covered the plate, *L. japonicus* seedlings were added to the plate on the side opposing the carrot root. During the whole experiment, the fungus was simultaneously supported by the carrot hairy root and the *L. japonicus* seedling. Once the *L. japonicus* roots had been colonized, labelled glucose was added to the side containing *L. japonicus*. After an additional week, FAs were esterified and extracted from colonized *L. japonicus* roots and from the associated extraradical mycelium and the total amount of ^{13}C labelled 16:0 and 16:1ω5 FAs as well as their isotopolog composition was determined. In *L. japonicus* wild-type ^{13}C-labeled 16:0 and 16:1ω5 FAs were detected in colonized

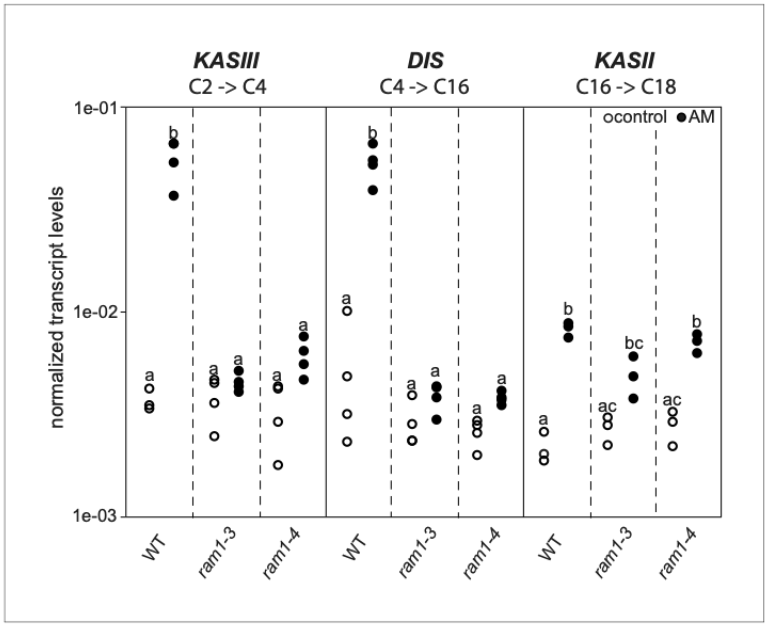

Figure 6. Loss of *RAM1* affects AM-dependent induction of *KASIII* and *DIS*. (**A**) *RAM1* effects on AM-dependent induction of *KASIII* and *DIS*, which catalyze 16:0 FA biosynthesis, and absence of effects on KASII. According to BLAST analysis via Kazusa (http://www.kazusa.or.jp/lotus/) and NCBI (http://www.ncbi.nlm.nih.gov/) *KASIII* and *KASII* are single copy genes in *L.japonicus*. Transcript accumulation of *KASIII, DIS* and *KASII* in non-colonized (open circles) and colonized (black circles) roots of Gifu WT, *ram1-3* and *ram1-4*. Different letters indicate different statistical groups (ANOVA; posthoc Tukey; $p \leq 0.001$; n = 23 $F_{5,12}$ = 65.04(*KASIII*); n = 24 $F_{5,18}$ = 54.42 (*DIS*); n = 18 $F_{5,12}$ = 33.11 (*KASII*)). Transcript accumulation was determined by qRT-PCR and the housekeeping gene *Ubiquitin10* was used for normalization. AM plants were inoculated with *R. irregularis* and harvested 5 wpi.
DOI: 10.7554/eLife.29107.035

roots as well as in the extraradical fungal mycelium (***Figure 8A–B***, ***Figure 8—figure supplement 2A–B***), indicating that ^{13}C-labelled organic compounds were transferred from the root to the fungus. No labelled FAs were detected in the fungal mycelium when the fungus was supplied with [U-$^{13}C_6$] glucose in absence of a plant host (***Figure 8A–B***, ***Figure 8—figure supplements 2A–B,3***), indicating that the fungus itself could not metabolize labelled glucose to synthesize FAs. The three mutants incorporated ^{13}C into 16:0 FAs at similar amounts as the wild-type but hardly any ^{13}C was transferred to the fungus (***Figure 8A–B***, ***Figure 8—figure supplement 2A–B***).

Host plants determine the isotopolog pattern of fungal FAs

Remarkably, the isotopolog profile of 16:0 FAs was close to identical between colonized *L. japonicus* roots and the connected extraradical mycelium, for 11 independent samples of wild-type Gifu (***Figure 8C–D***, ***Figure 8—figure supplement 4***) and for 5 independent samples of wild-type MG20 (***Figure 8—figure supplement 2C–D***). Moreover, the isotopolog profile of fungus-specific 16:1ω5 FAs mirrored the profile of 16:0 FAs (***Figure 8C***, ***Figure 8—figure supplements 2,4***). Pattern conservation between root and associated extraradical mycelium occurred independently of pattern variation among individual samples. Since the fungus does not incorporate ^{13}C into the analyzed FAs in the absence of the plant (***Figure 8A–B***, ***Figure 8—figure supplement 2A–B***) this conserved pattern demonstrates transfer of 16:0 FA-containing lipids from the host plant to the fungus because the plant determines the isotopolog pattern of fungal 16:0 and 16:1ω5 FAs. The 16:0 FA isotopolog pattern of colonized *dis-1*, *ram2* and *str* mutant roots resembled the wild-type profile, indicating intact uptake and metabolism of labelled glucose. However, the 16:0 FA isotopolog pattern of the

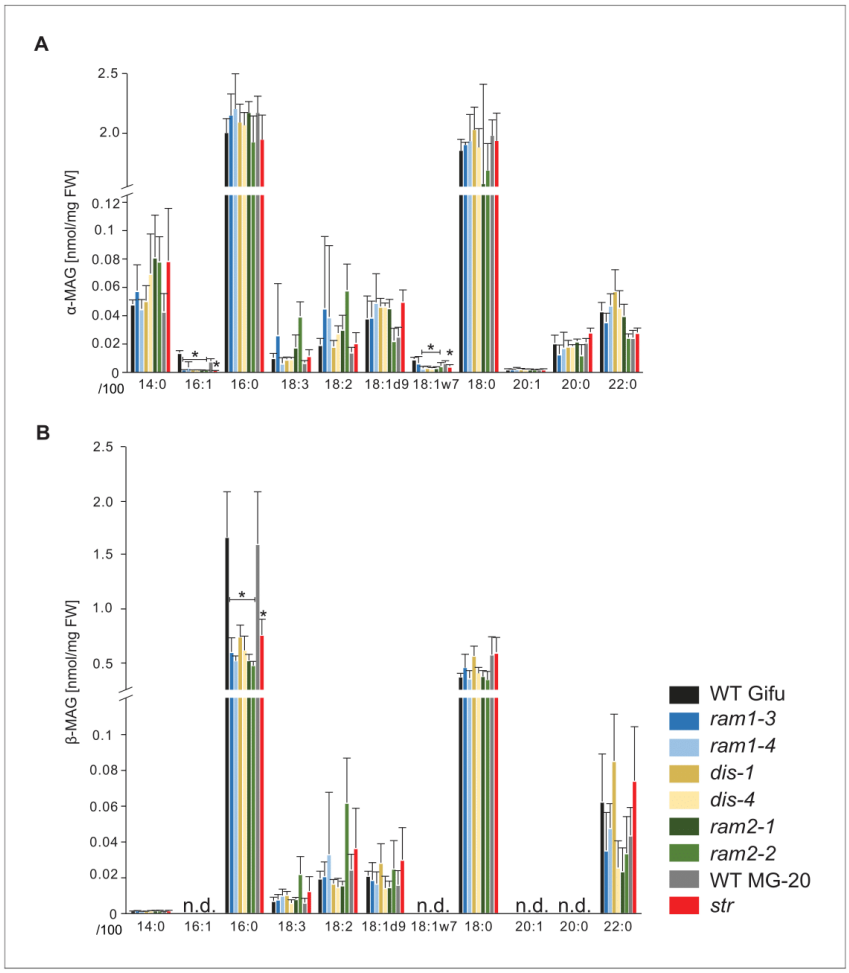

Figure 7. *sn-1* monoacylglycerol (α-MAG) and *sn-2* monoacylglycerol (β-MAG) profiles of colonized *L. japonicus* wild-type and AM-defective mutant roots. (**A**) Total amounts of α-MAG molecular species in the different genotypes. (**B**) Total amounts of β-MAG molecular species in the different genotypes. 16:0 β-MAG levels are significantly reduced in all mutant lines compared to the respective wild-type. (**A–B**) Bars represent means ±standard deviation (SD) of 3–5 biological replicates. Black asterisk indicates significant difference of mutants vs. wild-type according to Student's t-test, $p<0.05$.
DOI: 10.7554/eLife.29107.036

extraradical mycelium associated with mutant roots and the fungal 16:1ω5 FA profile inside and outside the roots differed strongly from the 16:0 FA profile of the mutant host roots (***Figure 8C***, ***Figure 8—figure supplements 2C,4***), consistent with very low FA transfer from the mutant plants to the fungus. The losses in isotopolog profile conservation between plant and fungal FAs in the mutants likely result from dilution of labelled FAs by unlabeled FAs from the carrot hairy root (***Figure 8D***, ***Figure 8—figure supplements 1*** and ***2D***) and/or from biases due to quantification of FAs at the detection limit.

To confirm that the plant determines the fungal FA isotopolog pattern we switched plant system and profiled isotopologs after labelling carrot root organ culture (ROC) in the absence of *L.*

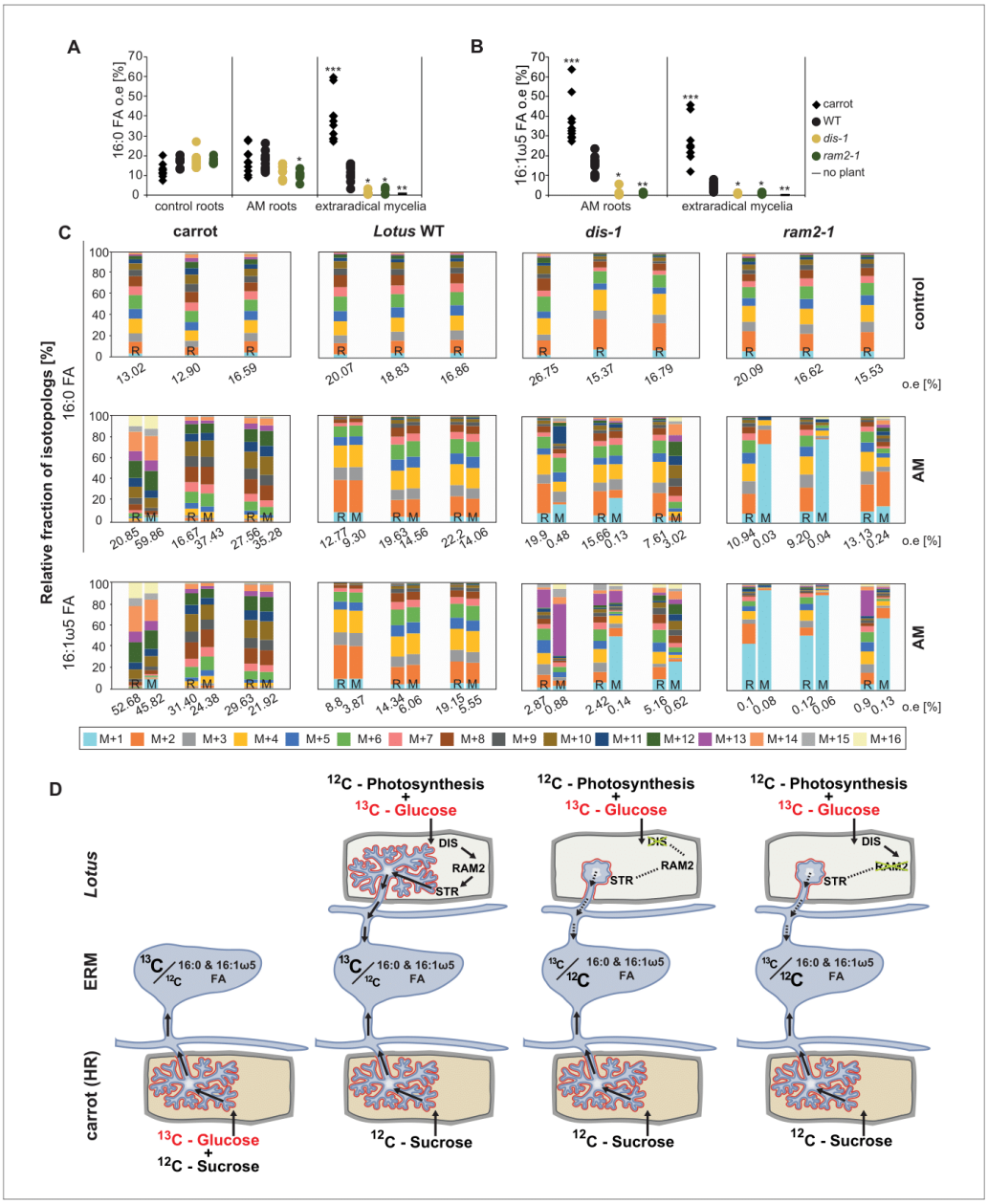

Figure 8. Isotopolog profiling indicates lipid transfer from plant to fungus. (**A–B**) Overall excess (o.e.) ^{13}C over air concentration in 16:0 FAs (**A**) and in 16:1ω5 FAs (**B**) detected in non-colonized (only 16:0 FAs) and colonized carrot, *L. japonicus* wild-type, *dis-1*, *ram2-1* roots and in the extraradical mycelium of *R. irregularis*. P values were generated by ANOVA using the Dunnett Test for multiple comparisons to *L. japonicus* wild-type (n = 29 (16:0 control roots); n = 33 (16:0 root AM); n = 39 (16:0 extraradical mycelium); n = 33 (16:1ω5 root AM); n = 39 (16:1ω5 extraradical mycelium), ***p<0.001,

Figure 8 continued on next page

Figure 8 continued

p<0.01, *p<0.05). (C**) Relative fraction of ^{13}C isotopologs for 16:0 FAs of three replicates of carrot, *L. japonicus* WT Gifu, *dis-1, ram2-1* in control roots (upper panel) and AM roots and each of the associated *R. irregularis* extraradical mycelia with spores (middle panel) and 16:1ω5 FAs in AM roots and extraradical mycelia with spores (lower panel). Individual bars and double bars indicate individual samples. Values from roots are indicated by 'R' and from fungal extraradical mycelia with spores by 'M'. For carrot and *L. japonicus* WT the ^{13}C labelling pattern of 16:0 and 16:1ω5 FAs in the plant is recapitulated in the fungal extraradical mycelium. Extraradical mycelium associated with *dis-1* and *ram2-1* does not mirror these patterns. Compare bars for AM roots and extraradical mycelium side by side. Black numbers indicate ^{13}C o. e. for individual samples. Colors indicate ^{13}C-isotopologs carrying one, two, three, etc. ^{13}C-atoms (M + 1, M + 2, M + 3, etc.). (**D**) Schematic and simplified illustration of carbon flow and ^{12}C vs.^{13}C-carbon contribution to plant lipid metabolism and transport to the fungus in the two-compartment cultivation setup used for isotope labelling. Carbohydrate metabolism and transport is omitted for simplicity. ERM, extraradical mycelium.

DOI: 10.7554/eLife.29107.037

The following source data and figure supplements are available for figure 8:

Source data 1. Raw data for isotopolog profiles in ***Figure 8*** and ***Figure 8—figure supplements 2,4***.

DOI: 10.7554/eLife.29107.038

Figure supplement 1. Two-compartment cultivation setup used for labelling experiments.

DOI: 10.7554/eLife.29107.039

Figure supplement 2. Isotopolog profiles of wild-type MG20 and *str*.

DOI: 10.7554/eLife.29107.040

Figure supplement 3. Proportion of 16:0 and 16:1ω5 FA containing only non-labelled ^{12}C in plant and fungal tissue.

DOI: 10.7554/eLife.29107.041

Figure supplement 4. Isotopolog profiles of additional samples.

DOI: 10.7554/eLife.29107.042

japonicus seedlings (***Figure 8D***, ***Figure 8—figure supplement 1***). In these root organ cultures, sugar uptake from the medium does not compete with photosynthesis, as in whole seedlings. Additionally, the carrot roots explore a larger surface of the Petri dish, increasing access to substances in the nutrient medium. Consequently, and likely because of increased uptake of labelled glucose from the medium, the isotopolog pattern of carrot ROCs differed from *Lotus* and was shifted towards more highly labeled 16:0 FA isotopologs. This fingerprint was again recapitulated in the extraradical fungal mycelium as well as in fungus-specific 16:1ω5 FAs inside and outside the root for 10 independent samples (***Figure 8C***, ***Figure 8—figure supplement 4***). These data provide strong support for direct transfer of a 16:0 FA containing lipid from plants to AMF (***Figure 9***).

Discussion

Here we identified *DIS* and *RAM2*, two AM-specific paralogs of the lipid biosynthesis genes *KASI* and *GPAT6* using forward genetics in *Lotus japonicus*. The *dis* and *ram2* mutants enabled us to demonstrate lipid transfer from plants to AMF using isotopolog profiling.

During AM symbiosis, an array of lipid biosynthesis genes is induced in arbuscocytes (***Gaude et al., 2012a***, ***2012b***), indicating a large demand for lipids in these cells. Indeed, two genes encoding lipid biosynthesis enzymes, the thioesterase FatM and the GPAT6 RAM2, have previously been shown to be required for arbuscule branching in *M. truncatula* (***Wang et al., 2012***; ***Bravo et al., 2017***; ***Jiang et al., 2017***). Both enzymes have a substrate preference for 16:0 FAs (***Salas and Ohlrogge, 2002***; ***Yang et al., 2012***; ***Bravo et al., 2017***) and, consistent with this, we and others observed that colonized *ram2* mutant roots over-accumulate 16:0 FA containing phospholipids and TAGs (***Figure 7***, [***Bravo et al., 2017***]), indicating re-channeling of superfluous 16:0 FAs in the absence of RAM2 function and placing RAM2 downstream of FatM (***Figure 9***).

Our discovery of *DIS*, a novel and AM-specific *KASI* gene, now provides evidence for the enzyme which synthesizes these 16:0 FAs in arbuscocytes. The arbuscule phenotype, as well as the lipid profile of colonized *dis* mutants is very similar to *fatm* and *ram2* mutants except for the accumulation of 16:0 FA-containing lipids in *ram2* (***Figure 1***, ***Figure 5*** and all figure supplements), consistent with the predicted function. Together, this strongly suggests that DIS, FatM and RAM2 act in the same lipid biosynthesis pathway, which is specifically and cell-autonomously induced when a resting root cortex cell differentiates into an arbuscocyte (***Figure 2A–B***, ***Figure 9***, [***Bravo et al., 2017***]). Interestingly, *DIS* was exclusively found in genomes of AM-competent dicotyledons and a gymnosperm (***Figure 3***). This implies that *DIS* has been lost at the split of the mono- from dicotyledons. Despite the

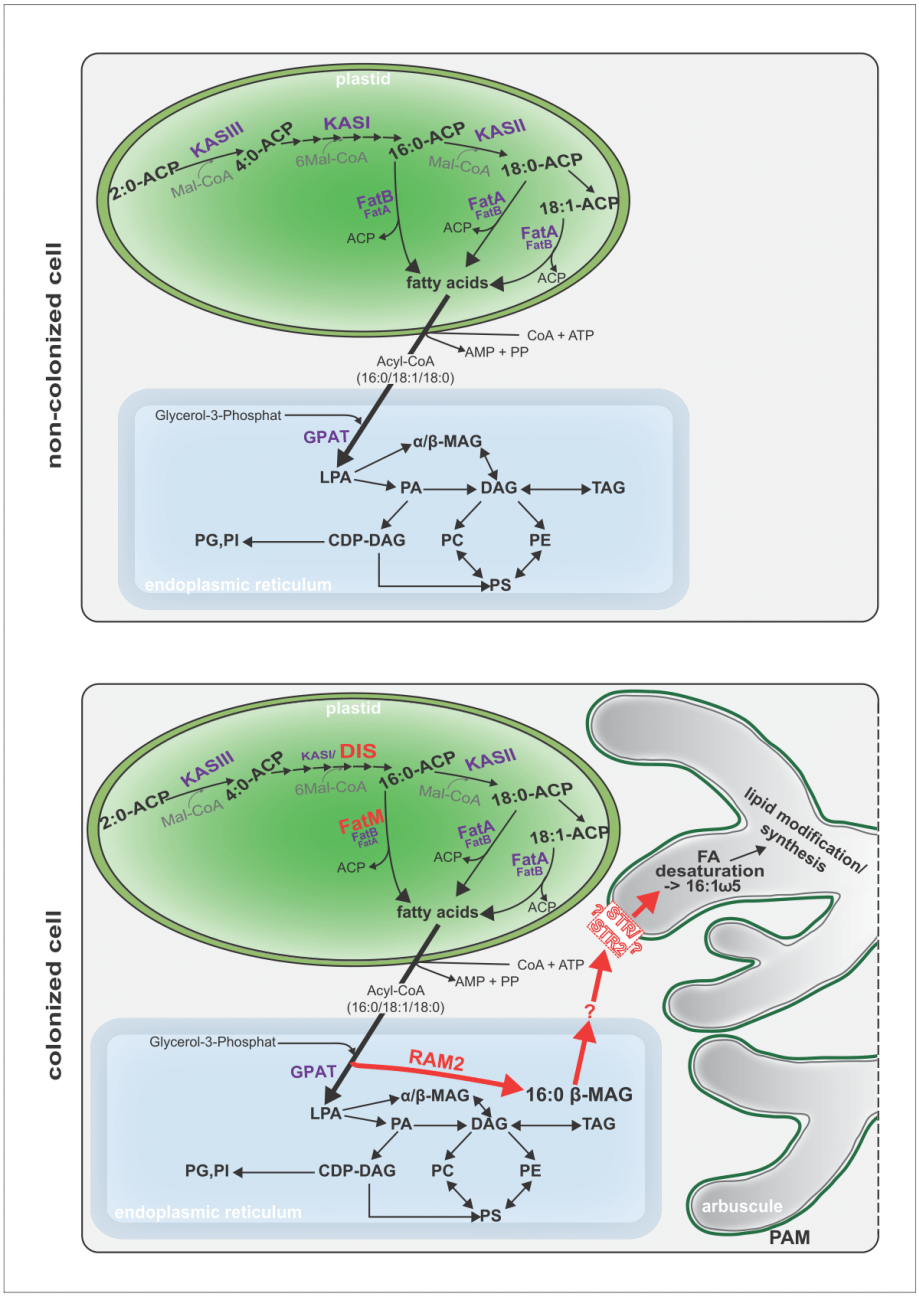

Figure 9. Schematic representation of plant fatty acid and lipid biosynthesis in a non-colonized root cell and a root cell colonized by an arbuscule. In non-colonized cells FAs are synthesized in the plastid, bound via esterification to glycerol to produce LPA in the ER, where further lipid synthesis and modification take place. Upon arbuscule formation AM-specific FA and lipid biosynthesis genes encoding DIS, FatM and RAM2 are activated to synthesize specifically high amounts of 16:0 FAs and 16:0-ß-MAGs or further modified lipids (this work and ***Bravo et al., 2017***). These are transported

Figure 9 continued on next page

Figure 9 continued

from the plant cell to the fungus. The PAM-localized ABCG transporter STR/STR2 is a hypothetical candidate for lipid transport across the PAM. Desaturation of 16:0 FAs by fungal enzymes (**Wewer et al., 2014**) leads to accumulation of lipids containing specific 16:1ω5 FAs. Mal-CoA, Malonyl-Coenzyme A; FA, fatty acid; KAS, β-keto-acyl ACP synthase; GPAT, Glycerol-3-phosphate acyl transferase; PAM, periarbuscular membrane; LPA, lysophosphatic acid; MAG, monoacylglycerol; DAG, diacylglycerol; TAG, triacylglycerol; PA, phosphatidic acid; PC, phosphatidylcholine; PE, phosphatidylethanolamine; PS, phosphatidylserine; CDP-DAG, cytidine diphosphate diacylglycerol; PG, phosphatidylglycerol; PI, phosphatidylinositol.
DOI: 10.7554/eLife.29107.043

phylogenetic divergence, *DIS* and the single copy housekeeping *KASI* gene of *Arabidopsis* are interchangeable (**Figure 5**). Therefore, the specificity of *DIS* to function in AM symbiosis is probably encoded in its promoter (**Figure 2**). In monocotyledons, the promoter of the housekeeping *KASI* gene may have acquired additional regulatory elements, sufficient for arbuscocyte-specific activation, thus making *DIS* dispensable.

We provide several pieces of complementary evidence that lipids synthesized by DIS and RAM2 in the arbuscocyte are transferred from plants to AMF and are required for fungal development. We fed host plants with [U-$^{13}C_6$]glucose and subsequently determined the isotopolog profile of freshly synthetized 16:0 and 16:1ω5 FAs in roots and associated fungal extraradical mycelia (**Figure 8**). This showed that: (1) AMF were unable to incorporate ^{13}C into FAs when fed with [U-$^{13}C_6$]glucose in absence of the host plant. (2) When associated with a wild-type host, the fungal extraradical mycelium accumulated ^{13}C labelled 16:0 FAs and the isotopolog profile of these 16:0 FAs was almost identical with the host profile. (3) The 16:0 FA isotopolog fingerprint differed strongly between two different wild-type plant systems (*Lotus* seedling and carrot hairy root) but for each of them the fungal mycelium recapitulated the isotopolog profile. Therefore clearly, the plant dominates the profile of the fungus, because it is impossible that the fungus by itself generates the same FA isotopolog pattern as the plant – especially in the absence of cytosolic FA synthase. Therefore, this result provides compelling evidence for interkingdom transfer of 16:0 FAs from plants to AMF. (4) In agreement, the isotopolog profile of fungus-specific 16:1 ω5 FAs inside and outside the root also resembled the plant 16:0 FA profile. (5) Colonized *dis* and *ram2* mutant roots resembled the 16:0 FA isotopolog profile of *L. japonicus* wild-type roots. However, the 16:0 FA profile of the fungal extraradical mycelium and the 16:1ω5 FA profile inside the roots showed a very different pattern, consistent with very low transport of labelled FAs to the fungus when associated with the mutants. (6) DIS and RAM2 are specifically required for the synthesis of 16:0 ß-MAG (**Figure 7**) and the predominant FA chain length found in AM fungi is precisely 16. (7) *dis* and *ram2* roots do not allow the formation of lipid-containing fungal vesicles and accumulate very low levels of fungal signature lipids (**Figure 5** and figure supplements). Together this strongly supports the idea that DIS and RAM2 are required to provide lipids for transfer to the fungus. Consequently, in the mutants, the fungus is deprived of lipids.

The *L. japonicus* mutants were originally identified due to their defective arbuscule branching (**Groth et al., 2013**). The promoters of *DIS* and *RAM2* are active in arbusocytes and already during PPA formation, the earliest visible stage of arbuscocyte development. Together with the stunted arbuscule phenotype of *dis*, *ram2* and *fatm* mutants (**Figure 1** [**Bravo et al., 2017**]) this suggests that plant lipids are needed for arbuscule growth, probably to provide material for the extensive plasma-membrane of the highly branched fungal structure. It also indicates that the arbuscule dictates development of the AMF as a whole, since lipid uptake at the arbuscule is required for vesicle formation, full exploration of the root and development of extraradical mycelia and spores. Defective arbuscule development was also observed for the different and phylogenetically distantly related AMF *Gigaspora rosea* (**Groth et al., 2013**), which similar to *R. irregularis* lacks genes encoding cytosolic FA synthase from their genomes (**Wewer et al., 2014**; **Tang et al., 2016**). Hence the dependence on plant lipids delivered at the arbuscule is likely a common phenomenon among AMF and a hallmark of AMF obligate biotrophy.

Despite the obvious central importance of lipid uptake by the arbuscule, the fungus can initially colonize the mutant roots with a low amount of intraradical hyphae and stunted arbuscules (**Figure 1**, **Figure 5—figure supplement 4**). The construction of membranes for this initial colonization may be supported by the large amounts of lipids stored in AMF spores. This would be consistent with the frequent observation that in wild-type roots, at initial stages of root colonization, AMF form

arbuscules immediately after reaching the inner cortex and before colonizing longer distances, possibly as a strategy to accquire lipids quickly after the reserves in the spore have been depleted. Alternatively, it is possible that plant housekeeping enzymes provide lipids to intraradical hyphae before arbuscule formation. Activity of the housekeeping KASI may also be responsible for slightly higher colonization levels observed for *dis* in some experiments as compared to other mutants.

It has recently been reported that photosynthetic wild-type nurse plants can restore arbuscule-branching in *Medicago ram2* and *str* mutants (**Jiang et al., 2017**; **Luginbuehl et al., 2017**), suggesting that lipids can be supplied to arbuscules via the extraradical hyphal network and intraradical hyphae through this route support arbuscule fine-branching. Based on four observations, we favor an alternative szenario, in which lipids need to be provided cell-autonomously by the arbuscocyte to support arbuscule fine-branching. However, we cannot exclude that our observations differ from the reported observations due to growth conditions or plant species. (1) Presence of nurse carrot hairy roots did not restore arbuscule branching in *dis*, *ram2* and *str* (**Figure 8—figure supplement 1C–F**). (2) *dis* and *ram2* were found in a forward genetics screen based on their stunted arbuscule phenotype. In this screen, the fungal inoculum was provided *via* chive nurse plants (**Groth et al., 2013**). (3) Map-based cloning of *Lotus dis*, *ram2* and *str* (**Kojima et al., 2014**) was performed with segregating mutant populations grown in the same pot, in which the wild-type and heterozygeous siblings acted as nurse plants on the homozygeous mutants. In this system, the stunted arbuscule phenotype was easily observable. (4) Arbuscule branching in a rice *str* mutant was not restored by wild type nurse plants (**Gutjahr et al., 2012**).

It still remains to be shown, which types of lipids are transported from the plant arbuscocyte to the fungal arbuscule and how. RAM2 is the most downstream acting enzyme in arbuscocyte-specific lipid biosynthesis known to date (**Figure 9**). It is predicted to synthesize ß-MAG and we and others have shown that 16:0 ß-MAGs are indeed reduced in colonized roots of *dis*, *fatm* and *ram2* mutants, providing evidence that this is likely the case (**Figure 7**, [**Bravo et al., 2017**]). Although, we cannot exclude that a downstream metabolite of 16:0 ß-MAG is transported to the fungus, 16:0 ß-MAG as transport vehicle for 16:0 FAs to the fungus is a good candidate because conceptually this molecule may bear certain advantages. It has been shown in *Arabidopsis* that ß-MAGs are not used for plant storage or membrane lipid biosynthesis but rather as pre-cursors for cuticle formation (**Li et al., 2007**). The production of ß-MAGs could therefore, be a way, to withdraw FAs from the plants own metabolism to make them available to the fungus. In addition, ß-MAGs are small and amphiphilic and could diffuse across the short distance of the hydrophilic apoplastic space between plant and fungal membrane. At the newly growing arbuscule branches the distance between the plant and fungal membrane is indeed very small and has been measured to be 80–100 nm on TEM images of high-pressure freeze-substituted samples (**Bonfante, 2001**). However, we could not detect fungus-specific 16:1ω5 ß-MAGs in colonized roots. This could mean that the fungus metabolizes them before desaturation of the 16:0 FAs to synthesize membrane and storage lipids. Alternatively, ß-MAGs may not be taken up by the fungus. ß-MAGs are known to isomerize to α-MAGs in acid or basic conditions (**Iqbal and Hussain, 2009**). It is therefore, possible that they isomerize in the acidic periarbuscular space (**Guttenberger, 2000**) before being taken up by the arbuscule.

How are MAGs transported across the peri-arbuscular membrane? Good candidates for MAG transporters are the ABCG half transporters STR and STR2. Similar ABCG transporters have been implicated genetically in cuticle formation, which also requires ß-MAGs (**Pighin et al., 2004**; **Panikashvili et al., 2011**; **Yeats et al., 2012**). The half ABCG transporters STR and STR2 are both independently required for arbuscule branching and they need to interact to form a full transporter (**Zhang et al., 2010**). We found that colonized roots of a *L. japonicus str* mutant, did not allow the formation of fungal vesicles and had the same lipid profile as *dis* and *ram2* (**Figure 5** and figure supplements). Furthermore, our ^{13}C labelling experiment demonstrated that *str* mutants do not transfer lipids to the fungus (**Figure 8—figure supplement 2**). Although these are encouraging indications, strong evidence for the role of STR in lipid transport across the periarbuscular membrane is still lacking and the substrate of STR remains to be determined. Therefore, currently, it cannot be excluded that mutation of *str* has an indirect effect on lipid transport and alternative mechanisms for example lipid translocation *via* vesicle fission and fusion are possible. Nevertheless, also in AMF, several ABC transporter genes are expressed *in planta* (**Tisserant et al., 2012**; **Tang et al., 2016**). They are not characterized, but if lipid transport via ABC transporters instead of other mechanisms would play a role, some of them could be involved in uptake of lipids into the fungal cytoplasm.

We found that mutants in the GRAS gene *RAM1* are impaired in AM-specific lipid accumulation in colonized roots and in AM-mediated activation of *DIS* and the single copy gene *KASIII* (**Figure 6**), in addition to *FatM*, *RAM2* and *STR* (**Wang et al., 2012**; **Park et al., 2015**; **Pimprikar et al., 2016**; **Luginbuehl et al., 2017**). This suggests that plants have evolved an AM-specific regulatory module for lipid production in arbuscocytes and delivery to the fungus. It remains to be shown, whether RAM1 regulates lipid biosynthesis genes directly and how this occurs mechanistically.

Our finding that plants transfer lipids to AMF completely changes the previous view that the fungus receives only sugars from the plant (**Pfeffer et al., 1999**; **Trépanier et al., 2005**). It will now be interesting to determine the relative contributions of sugar and lipid transfer to AMF, and whether this may be a determinant of variation in root length colonization and extraradical mycelium formation depending on the plant-fungal genotype combination (**Sawers et al., 2017**). An interesting question refers to why AMF have lost the genes encoding cytosolic FA synthase to depend on the lipid biosynthesis machinery of the host. FA biosynthesis consumes more energy than biosynthesis of carbohydrates and organic carbon provided by the plant needs to be transported in fungal hyphae over long distances from the inside of the root to the extremities of the extraradical mycelium. Therefore, it is conceivable that supply of plant lipids to the fungus plus fungal lipid transport is more energy efficient for the symbiosis as a whole than fungal carbohydrate transport plus fungal lipid biosynthesis. Hence, inter-organismic lipid transfer followed by loss of fungal FA biosynthesis genes may have been selected for during evolution because it likely optimized the symbiosis for most rapid proliferation of extraradical mycelium, thus ensuring efficient mineral nutrient acquisition from the soil for supporting the plant host. Lipid transfer across kingdoms has also been observed in human parasites or symbiotic bacteria of insects (**Caffaro and Boothroyd, 2011**; **Elwell et al., 2011**; **Herren et al., 2014**). It will be interesting to learn whether this is a more widespread phenomenon among biotrophic inter-organismic interactions.

Materials and methods

Plant growth and inoculation with AM fungi

Lotus japonicus ecotype Gifu wild-type, *ram1-3, ram1-4, dis-1, dis-4, dis-like-5, ram2-1, ram2-2* and ecotype MG-20 wild-type and *str* mutant (kindly provided by Tomoko Kojima (NARO, Tochigi, Japan) seeds were scarified and surface sterilized with 1% NaClO. Imbibed seeds were germinated on 0.8% Bacto Agar (Difco) at 24°C for 10–14 days. Seedlings were cultivated in pots containing sand/vermiculite (2/1 vol.) as substrate. For colonization with *Rhizophagus irregularis* roots were inoculated with 500 spores (SYMPLANTA, Munich, Germany or Agronutrition, Toulouse, France) per plant. Plants were harvested 5 weeks post inoculation (wpi); except for *dis-1* complementation in **Figure 1A**, which was harvested at 4 wpi. *Arabidopsis thaliana* seeds of Col-0 wild-type, *kasI* mutant in the Col-0 background and the transgenically complemented *kasI* mutant were surface sterilized with 70% EtOH +0.05% Tween 20% and 100% EtOH, germinated on MS-Medium for 48 hr at 4°C in the dark followed by 5–6 days at 22°C (8 hr light/dark).

Identification of *DIS* by map-based cloning and next generation sequencing

The *L. japonicus dis* mutant (line SL0154, [**Groth et al., 2013**]) resulting from an EMS mutagenesis program (**Perry et al., 2003**, **2009**) was backcrossed to ecotype Gifu wild-type and outcrossed to the polymorphic mapping parent ecotype MG-20. The *dis* locus segregated as a recessive monogenic trait and was previously found to be linked to marker TM2249 on chromosome 4 (**Groth et al., 2013**). We confirmed the monogenic segregation as 26 of 110 individuals originating from the cross to MG-20 (χ^2: P(3:1)=0.74) and 32 of 119 individuals originating from the cross to Gifu (χ^2: P(3:1) =0.63) exhibited the mutant phenotype. To identify SL0154-specific mutations linked to the *dis* locus, we employed a genome re-sequencing strategy. Nuclear DNA of Gifu wild-type and the SL0154 mutant was subjected to paired end sequencing (2 × 100 bp) of a 300–500 bp insert library, on an Illumina Hi-Seq 2000 instrument resulting in between 16.7 and 19.5 Gigabases per sample, equivalent to roughly 35–41 fold coverage assuming a genome size of 470 Megabases. Reads were mapped to the reference genome of MG-20 v2.5 (**Sato et al., 2008**) and single nucleotide polymorphisms identified using CLC genomics workbench (CLC bio, Aarhus, Denmark). SL0154-specific

SNPs were identified by subtracting Gifu/MG-20 from SL0154/MG-20 polymorphisms. 19 potentially EMS induced (11x G->A, 8x C->T) SNPs called consistently in all mapped reads from SL0514 but not in Gifu were identified between the markers TM0046/TM1545, the initial *dis* target region (***Figure 1—figure supplement 1A***. In a screen for recombination events flanking the *dis* locus, 63 mutants out of 254 total F2 individuals of a cross MG-20 x SL0154 were genotyped with markers flanking the *dis* locus (***Figure 1—figure supplement 1B***). Interrogating recombinant individuals with additional markers in the region narrowed down the target interval between TM2249 and BM2170 (2 cM according to markers; ca. 650 kb). In this interval, 3 SL0154-specific SNPs with typical EMS signature (G to A transition) remained, of which one was predicted to be located in exon 3 of CM0004.1640.r2 (reference position 40381558 in *L. japonicus* genome version 2.5; http://www.kazusa.or.jp/lotus/), a gene annotated as ketoacyl-(acyl carrier protein) synthase. This co-segregation together with phenotyping of one additional mutant allele obtained through TILLING (***Supplementary file 1***, [***Perry et al., 2003***, ***2009***]) as well as transgenic complementation (***Figure 1A***)) confirmed the identification of the mutation causing the *dis* phenotype of the SL0514 line. The two remaining mutations in the target region were located in a predicted intron of chr4. CM0004.1570.r2.a, a cyclin-like F-box protein (reference position: 40356684) and in a predicted intergenic region (reference position: 40364479). Untranslated regions of *DIS* and *DIS-LIKE* were determined using the Ambion FirstChoice RLM RACE kit according to manufacturer's instructions (http://www.ambion.de/). *DIS* sequence information can be found under the NCBI accession number KX880396.

Identification of *RAM2* by map-based cloning and Sanger sequencing

The *L. japonicus* Gifu mutant *reduced and degenerate arbuscules* (*red*, line SL0181-N) resulting from an EMS mutagenesis (***Perry et al., 2003***, ***2009***) was outcrossed to the ecotype MG-20 and previously reported to segregate for two mutations, one on chromosome 1 and one on chromosome 6 (***Groth et al., 2013***). They were separated by segregation and the mutation on chromosome 1 was previously found in the GRAS transcription factor gene *REDUCED ARBUSCULAR MYCORRHIZA 1* (*RAM1*) (***Pimprikar et al., 2016***). A plant from the F2 population, which showed wild-type phenotype but was heterozygous for the candidate interval on chromosome 6 and homozygous Gifu for the candidate interval on chromosome 1 was selfed for producing an F3. The F3 generation segregated for only one mutation as 38 out of 132 individuals exhibited the mutant phenotype (χ^2: P(3:1)=0.68). A plant from the F3 population, which displayed wild-type phenotype but was heterozygous for the candidate interval on chromosome 6 was selfed for producing an F4. The F4 generation also segregated for only one mutation as 17 out of 87 individuals exhibited the mutant phenotype (χ^2: P(3:1) =0.76). To identify the mutation on chromosome 6 linked to the previously identified interval (***Groth et al., 2013***), we employed additional markers for fine mapping in F3 segregating and F4 mutant populations. This positioned the causative mutation between TM0082 and TM0302 (***Figure 1—figure supplement 3A***). Due to a suppression of recombination in this interval we could not get closer to the mutation and also next generation sequencing (see [***Pimprikar et al., 2016***] for the methodology) failed to identify a causative mutation. The *Medicago truncatula ram2* mutant displays stunted arbuscules similar to our mutant (***Wang et al., 2012***). *L. japonicus RAM2* had not been linked to any chromosome but was placed on chromosome 0, which prevented identification of a *RAM2* mutation in the target interval on chromosome 6. Therefore, we sequenced the *RAM2* gene by Sanger sequencing. Indeed, mutants with stunted arbuscule phenotype in the F3 and F4 generation carried an EMS mutation at base 1663 from G to A leading to amino acid change from Glycine to Glutamic acid, which co-segregated with the mutant phenotype (***Figure 1—figure supplement 3B-C***). An additional allelic mutant *ram2-2* (***Figure 1—figure supplement 3B***) caused by a LORE1 retrotransposon insertion (***Małolepszy et al., 2016***) and transgenic complementation with the wild-type *RAM2* gene confirmed that the causative mutation affects *RAM2* (***Figure 1B***). Untranslated regions of *RAM2* were determined using the Ambion FirstChoice(R) RLM RACE kit according to manufacturer's instructions (http://www.ambion.de/). A 1345 bp long sequence upstream of ATG was available from the http://www.kazusa.or.jp/lotus/blast.html. To enable cloning a 2275 bp promoter fragment upstream of ATG of *RAM2* the remaining upstream sequence of 1047 bp was determined by primer walking on TAC Lj T46c08. *L. japonicus RAM2* sequence information can be found under the NCBI accession number KX823334 and the promoter sequence under the number KX823335.

Plasmid generation

Genes and promoter regions were amplified using Phusion PCR according to standard protocols and using primers indicated in **Supplementary file 2**. Plasmids were constructed as indicated in **Supplementary file 3**. For localization of DIS in *L. japonicus* hairy roots the LIII tricolor plasmid (**Binder et al., 2014**) was used. The plasmid containing *35S:RFP* for localization of free RFP in *Nicotiana benthamiana* leaves was taken from **Yano et al. (2008)**.

Induction of transgenic hairy roots in *L. japonicus*

Hypocotyls of *L. japonicus* were transformed with plasmids shown in **Supplementary file 3** for hairy root induction using transgenic *Agrobacterium rhizogenes* AR1193 as described (**Takeda et al., 2009**).

Floral dipping and rosette growth assay of *Arabidopsis thaliana*

Five plants per pot were sown. One week before transformation the primary bolt was cut off to induce growth of secondary floral bolts. 5 ml LB culture of *A. tumefaciens* transformed with a binary vector was incubated at 28°C, 300 rpm over night. 500 µl of the preculture was added to 250 µl LB medium with appropriate antibiotics. This culture was incubated again at 28°C, 300 rpm over night until an OD600 of 1.5 was reached. Plants were watered and covered by plastic bags the day before the dipping to ensure high humidity. The cells were harvested by centrifugation (10 min, 5000 rpm) and resuspended in infiltration medium (0.5 x MS medium, 5% sucrose). The resuspended cell culture was transferred to a box and Silwet L-77 was added (75 µl to 250 ml medium). The floral bolts of the plants were dipped into the medium for 5 s and put back into plastic bags and left in horizontal position for one night. After that, plants were turned upright, bags were opened and mature siliques were harvested. For rosette growth assays T3 plants were used. 31 days post sowing the rosettes were photographed and then cut and dried in an oven at 65°C for the determination of rosette dry weight.

Spatial analysis of promoter activity

For promoter:GUS analysis *L. japonicus* hairy roots transformed with plasmids containing the *DIS* and *RAM2* promoter fused to the *uidA* gene and colonized by *R. irregularis* were subjected to GUS staining as described (**Takeda et al., 2009**). To correlate *DIS* and *RAM2* promoter activity precisely with the stage of arbuscule development two expression cassettes were combined in the same golden gate plasmid for simultaneous visualization of arbuscule stages and promoter activity. The fungal silhouette including all stages of arbuscule development and pre-penetration *apparatuus* were made visible by expressing secretion peptide coupled *mCherry* under the control of the *SbtM1* promoter region comprising 704 bp upstream of the *SbtM1* gene (**Takeda et al., 2009**). Promoter activity was visualized using a YFP reporter fused to a nuclear localization signal (NLS).

Transient transformation of *N. benthamiana* leaves

N. benthamiana leaves were transiently transformed by infiltration of transgenic *A. tumefaciens* AGL1 as described (**Yano et al., 2008**).

Real time qRT-PCR

For analysis of transcript levels, plant tissues were rapidly shock frozen in liquid nitrogen. RNA was extracted using the Spectrum Plant Total RNA Kit (www.sigmaaldrich.com). The RNA was treated with Invitrogen DNAse I amp. grade (www.invitrogen.com) and tested for purity by PCR. cDNA synthesis was performed with 500 ng RNA using the Superscript III kit (www.invitrogen.com). qRT-PCR was performed with GoTaq G2 DNA polymerase (Promega), 5 x colorless GoTaq Buffer (Promega) and SYBR Green I (Invitrogen S7563, 10.000x concentrated, 500 µl) - diluted to 100x in DMSO. Primers (**Supplementary file 2**) were designed with primer3 (58). The qPCR reaction was run on an iCycler (Biorad, www.bio-rad.com/) according to manufacturer's instructions. Thermal cycler conditions were: 95°C 2 min, 45 cycles of 95°C 30 s, 60°C/62°C 30 s and 72°C 20 s followed by dissociation curve analysis. Expression levels were calculated according to the $\Delta\Delta$Ct method (**Rozen and Skaletsky, 2000**). For each genotype and treatment three to four biological replicates were tested and each sample was represented by two to three technical replicates.

Sequence alignement and phylogeny

L. japonicus KASI, DIS, DIS-LIKE, RAM2, Lj1g3v2301880.1 (GPAT6) protein sequences were retrieved from Lotus genome V2.5 and V3.0 respectively (http://www.kazusa.or.jp/lotus/) and *A. thaliana* KASI, *E. coli* KASI, *E. coli* KASII, *M. truncatula* RAM2 and Medtr7g067380 (GPAT6) were obtained from NCBI (http://www.ncbi.nlm.nih.gov). The sequences from *L. japonicus* were confirmed with a genome generated by next generation sequencing in house. Protein alignment for DIS was performed by CLC Main Workbench (CLC bio, Aarhus, Denmark). The Target Peptide was predicted using TargetP 1.0 Server (www.cbs.dtu.dk/services/TargetP-1.0/). RAM2 Protein alignment was performed by MEGA7 using ClustalW. The percentage identity matrix was obtained by Clustal Omega (http://www.ebi.ac.uk/Tools/msa/clustalo/).

To collect sequences for phylogeny construction corresponding to potential DIS orthologs, *Lotus* DIS and KASI (outgroup) protein sequences were searched in genome and transcriptome datasets using BLASTp and tBLASTn respectively. The list of species and the databases used are indicated in ***Figure 3—source data 1***. Hits with an e-value $>10^{-50}$ were selected for the phylogenetic analysis. Collected sequences were aligned using MAFFT (http://mafft.cbrc.jp/alignment/server/) and the alignment manually checked with Bioedit. Phylogenetic trees were generated by Neighbor-joining implemented in MEGA5 (***Tamura et al., 2011***). Partial gap deletion (95%) was used together with the JTT substitution model. Bootstrap values were calculated using 500 replicates.

Synteny analysis

A ~200 kb sized region in the *L. japonicus* genome containing the *DIS* locus (CM00041640.r2.a) was compared to the syntenic region in *A. thaliana* (Col-0) using CoGe Gevo (https://genomevolution.org/CoGe/GEvo.pl - (***Lyons et al., 2008***) as described in ***Delaux et al. (2014)***. Loci encompassing *DIS* orthologs from *Medicago truncatula*, *Populus trichocarpa*, *Carica papaya, Phaseolus vulgaris* and *Solanum lycopersicum* were added as controls.

AM staining and quantification

Rhizophagus irregularis in colonized *L. japonicus* roots was stained with acid ink (***Vierheilig et al., 1998***). Root length colonization was quantified using a modified gridline intersect method (***McGonigle et al., 1990***). For confocal laser scanning microscopy (CLSM) fungal structures were stained with 1 µg WGA Alexa Fluor 488 (Molecular Probes, http://www.lifetechnologies.com/) (***Panchuk-Voloshina et al., 1999***).

Microscopy

For quantification of AM colonization in *L. japonicus* roots a light microscope (Leica) with a 20x magnification was used. For observation of GUS-staining in *L. japonicus* hairy roots an inverted microscope (Leica DMI6000 B) was used with 10x and 20x magnification. Transformed roots were screened by stereomicroscope (Leica MZ16 FA) using an mCherry fluorescent transformation marker or the p*SbtM1:mCherry* marker for fungal colonization (for ***Figure 2A and B***). Confocal microscopy (Leica SP5) for WGA-AlexaFluor488 detection using 20x and 63x magnification was performed as described (***Groth et al., 2010***). Transgenic roots showing mCherry fluorescence signal due to *SbtM1* promoter activity linked with fungal colonization were cut into pieces immediately after harvesting. The living root pieces were placed on a glass slide with a drop of water, covered by a cover slip and immediately subjected to imaging. Sequential scanning for the YFP and RFP signal was carried out simultaneously with bright field image acquisition. YFP was excited with the argon ion laser 514 nm and the emitted fluorescence was detected from 525 to 575 nm; RFP was excited with the Diode-Pumped Solid State laser at 561 nm and the emitted fluorescence was detected from 580 to 623 nm. Images were acquired using LAS AF software. Several z-optical sections were made per area of interest and assembled to a z-stack using Fiji. The z-stack movies and 3D projections were produced using the 3D viewer function in Fiji (***Schindelin et al., 2012***).

Extraction and purification of phospho- and glycoglycerolipids and triacylglycerols

Approximately 50–100 mg of root or leaf material was harvested, weighed and immediately frozen in liquid nitrogen to avoid lipid degradation. The frozen samples were ground to a fine powder

before extraction with organic solvents. Total lipids were extracted as described previously (**Wewer et al., 2011**, **2014**). Briefly, 1 mL chloroform/methanol/formic acid (1:1:0.1, v/v/v) was added and the sample was shaken vigorously. At this point the internal standards for TAG and fatty acid analysis were added. Phase separation was achieved after addition of 0.5 mL 1M KCl/0.2 M H_3PO_4 and subsequent centrifugation at 4000 rpm for 5 min. The lipid-containing chloroform phase was transferred to a fresh glass tube and the sample was re-extracted twice with chloroform. The combined chloroform phases were dried under a stream of air and lipids were re-dissolved in 1 mL chloroform to yield the total lipid extract.

For phospho- and glycerolipid analysis 20 µl of the total lipid extract were mixed with 20 µl of the internal standard mix and 160 µl of methanol/chloroform/300 mM ammonium acetate (665:300:35, v/v/v) (**Welti et al., 2002**). For triacylglycerol analysis 500 µl of the total lipid extract were purified by solid phase extraction on Strata silica columns (1 ml bed volume; Phenomenex) as described (**Wewer et al., 2011**). TAGs were eluted from the silica material with chloroform, dried under a stream of air and re-dissolved in 1 mL methanol/chloroform/300 mM ammonium acetate (665:300:35, v/v/v).

Extraction and purification of free fatty acids and monoacylglycerol (MAG)

Total lipids were extracted into chloroform and dried as described above. 15–0 FA and a mixture of 15–0 α-MAG and β-MAG were added as internal standard before the extraction. Dried extracts were resuspended in 1 ml n-hexane and applied to silica columns for solid-phase extraction with a n-hexane:diethylether gradient. Free fatty acids were eluted with a mixture of 92:8 (v/v) n-hexane: diethylether as described bevore (**Gasulla et al., 2013**) and pure diethylether were used for elution of MAG.

Analysis of total fatty acids and free fatty acids by GC-FID

For measurement of total fatty acids, 100 µl of the total lipid extract were used. For measurement of free fatty acids, the SPE-fraction containing free fatty acids was used. Fatty acid methyl esters (FAMEs) were generated from acyl groups of total lipids and free fatty acids by addition of 1 mL 1N methanolic HCL (Sigma) to dried extracts and incubation at 80˚C for 30 min (**Browse et al., 1986**). Subsequently, FAMEs were extracted by addition of 1 mL n-hexane and 1 mL of 0.9% (w/v) NaCl and analyzed on a gas chromatograph with flame-ionization detector (GC-FID, Agilent 7890A PlusGC). FAMEs were separated on an SP 2380 fused silica GC column (Supelco, 30 mx 0.53 mm, 0.20 µm film) as described (**Wewer et al., 2013**), with a temperature -gradient starting at 100˚C, increased to 160˚C with 25˚C/min, then to 220˚C with10˚C/min and reduced to 100˚C with 25 ˚C/min. FAMEs were quantified in relation to the internal standard pentadecanoic acid (15:0).

For MAG measurement, dried diethylether fractions were resuspended in 4:1 (v/v %) pyridine:*N*-Methyl-*N*-(trimethylsilyl)trifluoroacetamide (MSTFA), incubated at 80˚C for 30 min, dried and re-suspended in hexane prior to application on an Agilent 7890A Plus gas chromatography-mass spectrometer. MAGs were quantified by extracted ion monitoring, using [M+ - 103] for α-MAGs and [M+ - 161] for β-MAGs as previously reported for 16:0 MAG (**Destaillats et al., 2010**) and 24:0 MAG (**Li et al., 2007**).

Quantification of glycerolipids by Q-TOF MS/MS

Phosphoglycerolipids (PC, PE, PG, PI, PS), glycoglycerolipids (MGDG, DGDG, SQDG) and triacylglycerol (TAG) were analyzed in positive mode by direct infusion nanospray Q-TOF MS/MS on an Agilent 6530 Q-TOF instrument as described previously (**Lippold et al., 2012**; **Gasulla et al., 2013**). A continuous flow of 1 µl/min methanol/chloroform/300 mM ammonium acetate (665:300:35, v/v/v) (**Welti et al., 2002**) was achieved using a nanospray infusion ion source (HPLC/chip MS 1200 with infusion chip). Data are displayed as X:Y, where X gives the number of C atoms of the fatty acid chain and Y the amount of desaturated carbo-carbon bonds inside that fatty acid chain.

Internal standards

Internal standards for phospho- and glycoglycerolipid analysis were prepared as described previously (**Gasulla et al., 2013**; **Wewer et al., 2014**). The following standards were dissolved in 20 µl of

chloroform/methanol (2:1, v/v): 0.2 nmol of each di14:0-PC, di20:0-PC, di14:0-PE, di20:0-PE, di14:0 PG, di20:0 PG, di14:0 PA and di20:0 PA; 0.03 nmol of di14:0-PS and di20:0-PS; 0.3 nmol of 34:0-PI; 0.15 nmol of 34:0-MGDG, 0.10 nmol of 36:0-MGDG; 0.2 nmol of 34:0-DGDG, 0.39 nmol of 36:0 DGDG and 0.4 nmol of 34:0 SQDG. 1 nmol each of tridecanoin (tri-10:0) and triundecenoin (tri-11:1), and 2 nmol each of triarachidin (tri-20:0) and trierucin (tri22:1) were used as internal standards for TAG quantification (***Lippold et al., 2012***). For quantification of total fatty acids and free fatty acids 5 µg of pentadecanoic acid (FA 15:0) was added to the samples (***Wewer et al., 2013***).

Cultivation and ^{13}C-Labeling of *L. japonicus* and *Daucus carota* hairy roots

The method for cultivation and stable isotope labelling of *Lotus japonicus* and *Daucus carota* hairy roots as well as for isotopolog profiling are described in more detail at Bio-protocol (***Keymer et al., 2018***). To determine lipid transfer from *L. japonicus* to the fungus we used the carrot root organ culture system (***Bécard et al., 1988***) to obtain sufficient amounts of fungal material for isotopolog profiling. (On petri dishes this was not possible with *L. japonicus* and in particular the lipid mutants alone). One compartment (carrot compartment) of the 2- compartmented petri dish system (***Trépanier et al., 2005***) was filled with MSR-medium (3% gelrite) containing 10% sucrose to support the shoot-less carrot root, and the other compartment (*Lotus* compartment) was filled with MSR-medium (3% gelrite) without sucrose. *Ri T-DNA* transformed *Daucus carota* hairy roots were placed in the carrot compartment. 1 week later, roots were inoculated with *R. irregularis*. Petri dishes were incubated at constant darkness and 30°C. Within 5 weeks *R. irregularis* colonized the carrot roots and its extraradical mycelium spread over both compartments of the petri dish and formed spores. At this stage two 2 week old *L. japonicus* seedlings (WT, *dis-1, ram2-1)* were placed into the *Lotus* compartment (***Figure 8—figure supplement 1***).

The plates were incubated at 24°C (16 hr light/8 hr dark). To keep the fungus and root in the dark the petri dishes were covered with black paper. 3 weeks after *Lotus* seedlings were placed into the petri dish [U-$^{13}C_6$]glucose (100 mg diluted in 2 ml MSR-medium) (Sigma-Aldrich) was added to the *Lotus* compartment. Therefore, only *Lotus* roots but not the carrot roots took up label. For transfer experiments with carrot roots no *Lotus* plant was placed into the *Lotus* compartment and the [U-$^{13}C_6$]glucose was added to the carrot compartment. 1 week after addition of [U-$^{13}C_6$]glucose the roots were harvested. The extraradical mycelium was extracted from the agar using citrate buffer pH 6 and subsequent filtration, after which it was immediately shock-frozen in liquid nitrogen.

Isotopolog profiling of ^{13}C-labelled 16:0 and 16:1ϖ5 fatty acids

Root and fungal samples were freeze dried and subsequently derivatised with 500 µl MeOH containing 3 M HCl (Sigma-Aldrich) at 80°C for 20 hr. MeOH/HCL was removed under a gentle stream of nitrogen and the methyl esters of the fatty acids were solved in 100 µl dry hexane.

Gas chromatography mass spectrometry was performed on a GC-QP 2010 plus (Shimadzu, Duisburg, Germany) equipped with a fused silica capillary column (equity TM-5; 30 m by 0.25 mm,0.25-µm film thickness; Supelco, Bellafonte, PA). The mass detector worked in electron ionization (EI) mode at 70 eV. An aliquot of the solution was injected in split mode (1:5) at an injector and interface temperature of 260°C. The column was held at 170°C for 3 min and then developed with a temperature gradient of 2 °C/min to a temperature of 192°C followed by a temperature gradient of 30°C/min to a final temperature of 300°C. Samples were analyzed in SIM mode (m/z values 267 to 288) at least three times. Retention times for fatty acids 16:1ω5 (unlabeled m/z 268) and 16:0 (unlabeled m/z 270) are 12.87 min and 13.20 min, respectively. Data were collected with LabSolution software (Shimadzu, Duisburg, Germany). The overall ^{13}C enrichment and the isotopolog compositions were calculated according to (***Lee et al., 1991***) and (***Ahmed et al., 2014***). The software package is open source and can be downloaded by the following link: http://www.tr34.uni-wuerzburg.de/software_developments/isotopo/.

Four independent labeling experiments were performed. Overall excess (o.e.) is an average value of ^{13}C atoms incorporated into 16:0/16:1ω5 fatty acids.

Data availability

Lunularia cruciata: For this species, the raw RNAseq reads have been previously deposited to NCBI under the accession number SRR1027885. It is annotated with *Rhizophagus irregularis* (10% of sequences) as the transcriptome was partly prepared from *Lunularia* plant tissue colonized by the fungus *Rhizophagus irregularis*. The corresponding *Lunularia* transcriptomic assembly is available at www.polebio.lrsv.ups-tlse.fr/Luc_v1/

Statistics

All statistical analyses (***Source code 1***) were performed and all boxplots were generated in R (www.r-project.org).

Acknowledgements

We are grateful to Tomoko Kojima (NARO, Tochigi, Japan) for providing *Lotus japonicus str* mutant seeds and to LotusBase for providing LORE1 insertion lines. We thank Julia Mayer for help with setting up carrot hairy root systems, Samy Carbonnel, David Chiasson, Michael Paries and José Antonio Villaécija-Aguilar for contributing a golden gate module.

Additional information

Funding

Funder	Grant reference number	Author
Deutsche Forschungsgemeinschaft	SFB924 B03 Function of the GRAS protein RAM1 in arbuscule development	Caroline Gutjahr
Deutsche Forschungsgemeinschaft	Emmy Noether program GU1423/1-1	Caroline Gutjahr
Deutsche Forschungsgemeinschaft	PA493/7-1 Plant genes required for arbuscular mycorrhiza symbiosis	Martin Parniske
Deutsche Forschungsgemeinschaft	SFB924 B03 Genetic dissection of arbuscular mycorrhiza development	Martin Parniske
Deutsche Forschungsgemeinschaft	SPP1212	Peter Dörmann
Deutsche Forschungsgemeinschaft	Research Training Group GRK 2064 Do520/15-1	Peter Dörmann
Hans Fischer Gesellschaft e. V.		Wolfgang Eisenreich
Biotechnology and Biological Sciences Research Council		Trevor L Wang

The funders had no role in study design, data collection and interpretation, or the decision to submit the work for publication.

Author contributions

AK, Conceptualization, Data curation, Formal analysis, Investigation, Visualization, Writing - contributed method description and figure legends; PP, Conceptualization, Data curation, Formal analysis, Investigation, Visualization; VW, Conceptualization, Investigation, Methodology; CH, Data curation, Investigation, Writing - contributed method description; MB, Data curation, Investigation, Methodology, Writing - contributed method description; SLB, VK, Investigation; P-MD, Formal analysis, Investigation; EvR-L, Investigation, generation of important preliminary data; TLW, Resources, Funding acquisition, Methodology; WE, Resources, Supervision, Funding acquisition; PD, Conceptualization, Supervision, Funding acquisition; MP, Conceptualization, Supervision, Funding acquisition, Investigation, Project administration, Writing—review and editing; CG, Conceptualization, Formal analysis,

Supervision, Funding acquisition, Investigation, Writing—original draft, Project administration, Writing—review and editing

Author ORCIDs
Andreas Keymer, http://orcid.org/0000-0001-9933-3662
Mathias Brands, http://orcid.org/0000-0001-6548-1448
Pierre-Marc Delaux, http://orcid.org/0000-0002-6211-157X
Peter Dörmann, http://orcid.org/0000-0002-5845-9370
Martin Parniske, http://orcid.org/0000-0001-8561-747X
Caroline Gutjahr, http://orcid.org/0000-0001-6163-745X

Additional files

Supplementary files

• Source code 1. Source code for ANOVA statistical test in R
DOI: 10.7554/eLife.29107.044

• Supplementary file 1. Mutations in *DIS* and *DIS-LIKE* identified by TILLING or in a LORE1 insertion collection.
DOI: 10.7554/eLife.29107.045

• Supplementary file 2. Primers used in this study.
DOI: 10.7554/eLife.29107.046

• Supplementary file 3. Plasmids used in this study were produced by classical cloning, Gateway cloning (Entry plasmids and Destination plasmids) and Golden Gate cloning (Level I, II and III). The Golden Gate toolbox is described in ***Binder et al. (2014)***. EV, empty vector; HR, hairy root; trafo, transformation.
DOI: 10.7554/eLife.29107.047

• Supplementary file 4. Accession numbers for protein sequences used in the phyologenic tree (***Figure 3***).
DOI: 10.7554/eLife.29107.048

References

Ahmed Z, Zeeshan S, Huber C, Hensel M, Schomburg D, Münch R, Eylert E, Eisenreich W, Dandekar T. 2014. 'Isotopo' a database application for facile analysis and management of mass isotopomer data. *Database* **2014**: bau077. doi: 10.1093/database/bau077, PMID: 25204646

Bago B, Pfeffer PE, Abubaker J, Jun J, Allen JW, Brouillette J, Douds DD, Lammers PJ, Shachar-Hill Y. 2003. Carbon export from arbuscular mycorrhizal roots involves the translocation of carbohydrate as well as lipid. *Plant Physiology* **131**:1496–1507. doi: 10.1104/pp.102.007765, PMID: 12644699

Bago B, Zipfel W, Williams RM, Jun J, Arreola R, Lammers PJ, Pfeffer PE, Shachar-Hill Y. 2002. Translocation and utilization of fungal storage lipid in the arbuscular mycorrhizal symbiosis. *Plant Physiology* **128**:108–124. doi: 10.1104/pp.010466, PMID: 11788757

Bentivenga SP, Morton JB. 1996. Congruence of fatty acid methyl ester profiles and morphological characters of arbuscular mycorrhizal fungi in *Gigasporaceae*. *PNAS* **93**:5659–5662. doi: 10.1073/pnas.93.11.5659, PMID: 11607684

Binder A, Lambert J, Morbitzer R, Popp C, Ott T, Lahaye T, Parniske M. 2014. A modular plasmid assembly kit for multigene expression, gene silencing and silencing rescue in plants. *PLoS One* **9**:e88218. doi: 10.1371/journal.pone.0088218, PMID: 24551083

Bonfante P. 2001. At the interface between mycorrhizal fungi and plants: the structural organization of cell wall, plasma membrane and cytoskeleton. In: Hock B (Ed). *The Mycota IX*. Heidelberg: Springer Verlag. doi: 10.1007/978-3-662-07334-6_4

Bravo A, Brands M, Wewer V, Dörmann P, Harrison MJ. 2017. Arbuscular mycorrhiza-specific enzymes FatM and RAM2 fine-tune lipid biosynthesis to promote development of arbuscular mycorrhiza. *New Phytologist* **214**: 1631–1645. doi: 10.1111/nph.14533, PMID: 28380681

Bravo A, York T, Pumplin N, Mueller LA, Harrison MJ. 2016. Genes conserved for arbuscular mycorrhizal symbiosis identified through phylogenomics. *Nature Plants* **2**:15208. doi: 10.1038/nplants.2015.208, PMID: 27249190

Browse J, McCourt PJ, Somerville CR. 1986. Fatty acid composition of leaf lipids determined after combined digestion and fatty acid methyl ester formation from fresh tissue. *Analytical Biochemistry* **152**:141–145. doi: 10.1016/0003-2697(86)90132-6, PMID: 3954036

Bécard G, Fortin JA, Ja F. 1988. Early events of vesicular-arbuscular mycorrhiza formation on Ri T-DNA transformed roots. *New Phytologist* **108**:211–218. doi: 10.1111/j.1469-8137.1988.tb03698.x

Caffaro CE, Boothroyd JC. 2011. Evidence for host cells as the Major contributor of lipids in the intravacuolar network of Toxoplasma-infected cells. *Eukaryotic Cell* **10**:1095–1099. doi: 10.1128/EC.00002-11, PMID: 21685319

Delaux PM, Radhakrishnan GV, Jayaraman D, Cheema J, Malbreil M, Volkening JD, Sekimoto H, Nishiyama T, Melkonian M, Pokorny L, Rothfels CJ, Sederoff HW, Stevenson DW, Surek B, Zhang Y, Sussman MR, Dunand C, Morris RJ, Roux C, Wong GK, et al. 2015. Algal ancestor of land plants was preadapted for symbiosis. *PNAS* **112**:13390–13395. doi: 10.1073/pnas.1515426112, PMID: 26438870

Delaux PM, Varala K, Edger PP, Coruzzi GM, Pires JC, Ané JM. 2014. Comparative phylogenomics uncovers the impact of symbiotic associations on host genome evolution. *PLoS Genetics* **10**:e1004487. doi: 10.1371/journal.pgen.1004487, PMID: 25032823

Destaillats F, Cruz-Hernandez C, Nagy K, Dionisi F. 2010. Identification of monoacylglycerol regio-isomers by gas chromatography-mass spectrometry. *Journal of Chromatography A* **1217**:1543–1548. doi: 10.1016/j.chroma.2010.01.016, PMID: 20097347

Elwell CA, Jiang S, Kim JH, Lee A, Wittmann T, Hanada K, Melancon P, Engel JN. 2011. *Chlamydia trachomatis* co-opts GBF1 and CERT to acquire host sphingomyelin for distinct roles during intracellular development. *PLoS Pathogens* **7**:e1002198. doi: 10.1371/journal.ppat.1002198, PMID: 21909260

Fabre G, Garroum I, Mazurek S, Daraspe J, Mucciolo A, Sankar M, Humbel BM, Nawrath C. 2016. The ABCG transporter PEC1/ABCG32 is required for the formation of the developing leaf cuticle in Arabidopsis. *New Phytologist* **209**:192–201. doi: 10.1111/nph.13608, PMID: 26406899

Favre P, Bapaume L, Bossolini E, Delorenzi M, Falquet L, Reinhardt D. 2014. A novel bioinformatics pipeline to discover genes related to arbuscular mycorrhizal symbiosis based on their evolutionary conservation pattern among higher plants. *BMC Plant Biology* **14**:333. doi: 10.1186/s12870-014-0333-0, PMID: 25465219

Gasulla F, Vom Dorp K, Dombrink I, Zähringer U, Gisch N, Dörmann P, Bartels D. 2013. The role of lipid metabolism in the acquisition of desiccation tolerance in Craterostigma plantagineum: a comparative approach. *The Plant Journal* **75**:726–741. doi: 10.1111/tpj.12241, PMID: 23672245

Gaude N, Bortfeld S, Duensing N, Lohse M, Krajinski F. 2012a. Arbuscule-containing and non-colonized cortical cells of mycorrhizal roots undergo extensive and specific reprogramming during arbuscular mycorrhizal development. *The Plant Journal* **69**:510–528. doi: 10.1111/j.1365-313X.2011.04810.x, PMID: 21978245

Gaude N, Schulze WX, Franken P, Krajinski F. 2012b. Cell type-specific protein and transcription profiles implicate periarbuscular membrane synthesis as an important carbon sink in the mycorrhizal symbiosis. *Plant Signaling & Behavior* **7**:461–464. doi: 10.4161/psb.19650, PMID: 22499167

Genre A, Chabaud M, Faccio A, Barker DG, Bonfante P. 2008. Prepenetration apparatus assembly precedes and predicts the colonization patterns of arbuscular mycorrhizal fungi within the root cortex of both *Medicago truncatula* and *Daucus carota*. *The Plant Cell Online* **20**:1407–1420. doi: 10.1105/tpc.108.059014, PMID: 18515499

Gobbato E, Marsh JF, Vernié T, Wang E, Maillet F, Kim J, Miller JB, Sun J, Bano SA, Ratet P, Mysore KS, Dénarié J, Schultze M, Oldroyd GE. 2012. A GRAS-type transcription factor with a specific function in mycorrhizal signaling. *Current Biology* **22**:2236–2241. doi: 10.1016/j.cub.2012.09.044, PMID: 23122845

Gobbato E, Wang E, Higgins G, Bano SA, Henry C, Schultze M, Oldroyd GE. 2013. *RAM1* and *RAM2* function and expression during arbuscular mycorrhizal symbiosis and *Aphanomyces euteiches* colonization. *Plant Signaling & Behavior* **8**:e26049. doi: 10.4161/psb.26049, PMID: 24270627

Graham JH, Hodge NC, Morton JB. 1995. Fatty Acid methyl ester profiles for characterization of glomalean fungi and their endomycorrhizae. *Applied and Environmental Microbiology* **61**:58–64. PMID: 16534923

Groth M, Kosuta S, Gutjahr C, Haage K, Hardel SL, Schaub M, Brachmann A, Sato S, Tabata S, Findlay K, Wang TL, Parniske M. 2013. Two *Lotus japonicus* symbiosis mutants impaired at distinct steps of arbuscule development. *The Plant Journal* **75**:117–129. doi: 10.1111/tpj.12220, PMID: 23627596

Groth M, Takeda N, Perry J, Uchida H, Dräxl S, Brachmann A, Sato S, Tabata S, Kawaguchi M, Wang TL, Parniske M. 2010. NENA, a *Lotus japonicus* homolog of Sec13, is required for rhizodermal infection by arbuscular mycorrhiza fungi and rhizobia but dispensable for cortical endosymbiotic development. *The Plant Cell Online* **22**:2509–2526. doi: 10.1105/tpc.109.069807, PMID: 20675572

Gutjahr C, Radovanovic D, Geoffroy J, Zhang Q, Siegler H, Chiapello M, Casieri L, An K, An G, Guiderdoni E, Kumar CS, Sundaresan V, Harrison MJ, Paszkowski U. 2012. The half-size ABC transporters STR1 and STR2 are indispensable for mycorrhizal arbuscule formation in rice. *The Plant Journal* **69**:906–920. doi: 10.1111/j.1365-313X.2011.04842.x, PMID: 22077667

Guttenberger M. 2000. Arbuscules of vesicular-arbuscular mycorrhizal fungi inhabit an acidic compartment within plant roots. *Planta* **211**:299–304. doi: 10.1007/s004250000324, PMID: 10987547

Helber N, Wippel K, Sauer N, Schaarschmidt S, Hause B, Requena N. 2011. A versatile monosaccharide transporter that operates in the arbuscular mycorrhizal fungus *Glomus* sp is crucial for the symbiotic relationship with plants. *The Plant Cell* **23**:3812–3823. doi: 10.1105/tpc.111.089813, PMID: 21972259

Herren JK, Paredes JC, Schüpfer F, Arafah K, Bulet P, Lemaitre B. 2014. Insect endosymbiont proliferation is limited by lipid availability. *eLife* **3**:e02964. doi: 10.7554/eLife.02964, PMID: 25027439

Hwang JU, Song WY, Hong D, Ko D, Yamaoka Y, Jang S, Yim S, Lee E, Khare D, Kim K, Palmgren M, Yoon HS, Martinoia E, Lee Y. 2016. Plant ABC transporters enable many unique aspects of a terrestrial plant's lifestyle. *Molecular Plant* **9**:338–355. doi: 10.1016/j.molp.2016.02.003, PMID: 26902186

Iqbal J, Hussain MM. 2009. Intestinal lipid absorption. *AJP: Endocrinology and Metabolism* **296**:E1183–E1194. doi: 10.1152/ajpendo.90899.2008, PMID: 19158321

Ivanov S, Harrison MJ. 2014. A set of fluorescent protein-based markers expressed from constitutive and arbuscular mycorrhiza-inducible promoters to label organelles, membranes and cytoskeletal elements in Medicago truncatula. *The Plant Journal* **80**:1151–1163. doi: 10.1111/tpj.12706, PMID: 25329881

Javot H, Penmetsa RV, Terzaghi N, Cook DR, Harrison MJ. 2007. A *Medicago truncatula* phosphate transporter indispensable for the arbuscular mycorrhizal symbiosis. *PNAS* **104**:1720–1725. doi: 10.1073/pnas.0608136104, PMID: 17242358

Jiang Y, Wang W, Xie Q, Liu N, Liu L, Wang D, Zhang X, Yang C, Chen X, Tang D, Wang E. 2017. Plants transfer lipids to sustain colonization by mutualistic mycorrhizal and parasitic fungi. *Science* **356**:1172–1175. doi: 10.1126/science.aam9970, PMID: 28596307

Jones A, Davies HM, Voelker TA. 1995. Palmitoyl-acyl carrier protein (ACP) thioesterase and the evolutionary origin of plant acyl-ACP thioesterases. *The Plant Cell Online* **7**:359–371. doi: 10.1105/tpc.7.3.359, PMID: 7734968

Keymer A, Huber C, Eisenreich W, Gutjahr C. 2018. Tracking Lipid Transfer by Fatty Acid Isotopolog Profiling from Host Plants to Arbuscular Mycorrhiza Fungi. *BIO-PROTOCOL* **8**:e2786. doi: 10.21769/BioProtoc.2786

Kojima T, Saito K, Oba H, Yoshida Y, Terasawa J, Umehara Y, Suganuma N, Kawaguchi M, Ohtomo R. 2014. Isolation and phenotypic characterization of *Lotus japonicus* mutants specifically defective in arbuscular mycorrhizal formation. *Plant and Cell Physiology* **55**:928–941. doi: 10.1093/pcp/pcu024, PMID: 24492255

Lee JY, Kinch LN, Borek DM, Wang J, Wang J, Urbatsch IL, Xie XS, Grishin NV, Cohen JC, Otwinowski Z, Hobbs HH, Rosenbaum DM. 2016. Crystal structure of the human sterol transporter ABCG5/ABCG8. *Nature* **533**:561–564. doi: 10.1038/nature17666, PMID: 27144356

Lee WN, Byerley LO, Bergner EA, Edmond J. 1991. Mass isotopomer analysis: theoretical and practical considerations. *Biological Mass Spectrometry* **20**:451–458. doi: 10.1002/bms.1200200804, PMID: 1768701

Li Y, Beisson F, Ohlrogge J, Pollard M. 2007. Monoacylglycerols are components of root waxes and can be produced in the aerial cuticle by ectopic expression of a suberin-associated acyltransferase. *Plant Physiology* **144**:1267–1277. doi: 10.1104/pp.107.099432, PMID: 17496107

Li-Beisson Y, Shorrosh B, Beisson F, Andersson MX, Arondel V, Bates PD, Baud S, Bird D, Debono A, Durrett TP, Franke RB, Graham IA, Katayama K, Kelly AA, Larson T, Markham JE, Miquel M, Molina I, Nishida I, Rowland O, et al. 2010. Acyl-lipid metabolism. *The Arabidopsis Book* **8**:e0133. doi: 10.1199/tab.0133, PMID: 22303259

Lippold F, vom Dorp K, Abraham M, Hölzl G, Wewer V, Yilmaz JL, Lager I, Montandon C, Besagni C, Kessler F, Stymne S, Dörmann P. 2012. Fatty acid phytyl ester synthesis in chloroplasts of *Arabidopsis*. *The Plant Cell* **24**:2001–2014. doi: 10.1105/tpc.112.095588, PMID: 22623494

Lohse S, Schliemann W, Ammer C, Kopka J, Strack D, Fester T. 2005. Organization and metabolism of plastids and mitochondria in arbuscular mycorrhizal roots of *Medicago truncatula*. *Plant Physiology* **139**:329–340. doi: 10.1104/pp.105.061457, PMID: 16126866

Luginbuehl LH, Menard GN, Kurup S, Van Erp H, Radhakrishnan GV, Breakspear A, Oldroyd GED, Eastmond PJ. 2017. Fatty acids in arbuscular mycorrhizal fungi are synthesized by the host plant. *Science* **356**:1175–1178. doi: 10.1126/science.aan0081, PMID: 28596311

Lyons E, Pedersen B, Kane J, Alam M, Ming R, Tang H, Wang X, Bowers J, Paterson A, Lisch D, Freeling M. 2008. Finding and comparing syntenic regions among *Arabidopsis* and the outgroups papaya, poplar, and grape: coge with rosids. *Plant Physiology* **148**:1772–1781. doi: 10.1104/pp.108.124867, PMID: 18952863

Madan R, Pankhurst C, Hawke B, Smith S. 2002. Use of fatty acids for identification of AM fungi and estimation of the biomass of AM spores in soil. *Soil Biology and Biochemistry* **34**:125–128. doi: 10.1016/S0038-0717(01)00151-1

Małolepszy A, Mun T, Sandal N, Gupta V, Dubin M, Urbański D, Shah N, Bachmann A, Fukai E, Hirakawa H, Tabata S, Nadzieja M, Markmann K, Su J, Umehara Y, Soyano T, Miyahara A, Sato S, Hayashi M, Stougaard J, et al. 2016. The LORE1 insertion mutant resource. *The Plant Journal* **88**:306–317. doi: 10.1111/tpj.13243, PMID: 27322352

McGonigle TP, Miller MH, Evans DG, Fairchild GL, Swan JA. 1990. A new method which gives an objective measure of colonization of roots by vesicular-arbuscular mycorrhizal fungi. *New Phytologist* **115**:495–501. doi: 10.1111/j.1469-8137.1990.tb00476.x

Panchuk-Voloshina N, Haugland RP, Bishop-Stewart J, Bhalgat MK, Millard PJ, Mao F, Leung WY, Haugland RP. 1999. Alexa dyes, a series of new fluorescent dyes that yield exceptionally bright, photostable conjugates. *Journal of Histochemistry & Cytochemistry* **47**:1179–1188. doi: 10.1177/002215549904700910, PMID: 10449539

Panikashvili D, Shi JX, Schreiber L, Aharoni A. 2011. The Arabidopsis ABCG13 transporter is required for flower cuticle secretion and patterning of the petal epidermis. *New Phytologist* **190**:113–124. doi: 10.1111/j.1469-8137.2010.03608.x, PMID: 21232060

Park HJ, Floss DS, Levesque-Tremblay V, Bravo A, Harrison MJ. 2015. Hyphal Branching during Arbuscule Development Requires Reduced Arbuscular Mycorrhiza1. *Plant Physiology* **169**:2774–2788. doi: 10.1104/pp.15.01155, PMID: 26511916

Perry J, Brachmann A, Welham T, Binder A, Charpentier M, Groth M, Haage K, Markmann K, Wang TL, Parniske M. 2009. TILLING in *Lotus japonicus* identified large allelic series for symbiosis genes and revealed a Bias in functionally defective ethyl methanesulfonate alleles toward glycine replacements. *Plant Physiology* **151**:1281–1291. doi: 10.1104/pp.109.142190, PMID: 19641028

Perry JA, Wang TL, Welham TJ, Gardner S, Pike JM, Yoshida S, Parniske M. 2003. A TILLING reverse genetics tool and a web-accessible collection of mutants of the legume *Lotus japonicus*. *Plant Physiology* **131**:866–871. doi: 10.1104/pp.102.017384, PMID: 12644638

Pfeffer PE, Douds DD, Becard G, Shachar-Hill Y. 1999. Carbon uptake and the metabolism and transport of lipids in an arbuscular mycorrhiza. *Plant Physiology* **120**:587–598. doi: 10.1104/pp.120.2.587, PMID: 10364411

Pighin JA, Zheng H, Balakshin LJ, Goodman IP, Western TL, Jetter R, Kunst L, Samuels AL. 2004. Plant cuticular lipid export requires an ABC transporter. *Science* **306**:702–704. doi: 10.1126/science.1102331, PMID: 15499022

Pimprikar P, Carbonnel S, Paries M, Katzer K, Klingl V, Bohmer MJ, Karl L, Floss DS, Harrison MJ, Parniske M, Gutjahr C. 2016. A CCaMK-CYCLOPS-DELLA complex activates transcription of RAM1 to regulate Arbuscule branching. *Current Biology* **26**:987–998. doi: 10.1016/j.cub.2016.01.069, PMID: 27020747

Ropars J, Toro KS, Noel J, Pelin A, Charron P, Farinelli L, Marton T, Krüger M, Fuchs J, Brachmann A, Corradi N. 2016. Evidence for the sexual origin of heterokaryosis in arbuscular mycorrhizal fungi. *Nature Microbiology* **1**: 16033. doi: 10.1038/nmicrobiol.2016.33, PMID: 27572831

Rozen S, Skaletsky H. 2000. Primer3 on the WWW for general users and for biologist programmers. In: Krawets S, Misener S (Eds). *Bioinformatics Methods and Protocols: Methods in Molecular Biology*. Totwana: Humana Press. p. 365–386.

Salas JJ, Ohlrogge JB. 2002. Characterization of substrate specificity of plant FatA and FatB acyl-ACP thioesterases. *Archives of Biochemistry and Biophysics* **403**:25–34. doi: 10.1016/S0003-9861(02)00017-6, PMID: 12061798

Salvioli A, Ghignone S, Novero M, Navazio L, Venice F, Bagnaresi P, Bonfante P. 2016. Symbiosis with an endobacterium increases the fitness of a mycorrhizal fungus, raising its bioenergetic potential. *The ISME Journal* **10**:130–144. doi: 10.1038/ismej.2015.91, PMID: 26046255

Sato S, Nakamura Y, Kaneko T, Asamizu E, Kato T, Nakao M, Sasamoto S, Watanabe A, Ono A, Kawashima K, Fujishiro T, Katoh M, Kohara M, Kishida Y, Minami C, Nakayama S, Nakazaki N, Shimizu Y, Shinpo S, Takahashi C, et al. 2008. Genome structure of the legume, *Lotus japonicus*. *DNA Research* **15**:227–239. doi: 10.1093/dnares/dsn008, PMID: 18511435

Sawers RJ, Svane SF, Quan C, Grønlund M, Wozniak B, Gebreselassie MN, González-Muñoz E, Chávez Montes RA, Baxter I, Goudet J, Jakobsen I, Paszkowski U. 2017. Phosphorus acquisition efficiency in arbuscular mycorrhizal maize is correlated with the abundance of root-external hyphae and the accumulation of transcripts encoding PHT1 phosphate transporters. *New Phytologist* **214**:632–643. doi: 10.1111/nph.14403, PMID: 28098948

Schindelin J, Arganda-Carreras I, Frise E, Kaynig V, Longair M, Pietzsch T, Preibisch S, Rueden C, Saalfeld S, Schmid B, Tinevez JY, White DJ, Hartenstein V, Eliceiri K, Tomancak P, Cardona A. 2012. Fiji: an open-source platform for biological-image analysis. *Nature Methods* **9**:676–682. doi: 10.1038/nmeth.2019, PMID: 22743772

Shachar-Hill Y, Pfeffer PE, Douds D, Osman SF, Doner LW, Ratcliffe RG. 1995. Partitioning of intermediary carbon metabolism in vesicular-arbuscular mycorrhizal leek. *Plant Physiology* **108**:7–15. doi: 10.1104/pp.108.1.7, PMID: 12228450

Smith S, Read D. 2008. *Mycorrhizal Symbiosis*. Academic Press London.

Stumpe M, Carsjens JG, Stenzel I, Göbel C, Lang I, Pawlowski K, Hause B, Feussner I. 2005. Lipid metabolism in arbuscular mycorrhizal roots of *Medicago truncatula*. *Phytochemistry* **66**:781–791 https://doi.org/. doi: 10.1016/j.phytochem.2005.01.020, PMID: 15797604

Takeda N, Maekawa T, Hayashi M. 2012. Nuclear-localized and deregulated calcium- and calmodulin-dependent protein kinase activates rhizobial and mycorrhizal responses in *Lotus japonicus*. *The Plant Cell Online* **24**:810–822. doi: 10.1105/tpc.111.091827, PMID: 22337918

Takeda N, Sato S, Asamizu E, Tabata S, Parniske M. 2009. Apoplastic plant subtilases support arbuscular mycorrhiza development in *Lotus japonicus*. *The Plant Journal* **58**:766–777. doi: 10.1111/j.1365-313X.2009.03824.x, PMID: 19220794

Tamura K, Peterson D, Peterson N, Stecher G, Nei M, Kumar S. 2011. MEGA5: molecular evolutionary genetics analysis using maximum likelihood, evolutionary distance, and maximum parsimony methods. *Molecular Biology and Evolution* **28**:2731–2739. doi: 10.1093/molbev/msr121, PMID: 21546353

Tang N, San Clemente H, Roy S, Bécard G, Zhao B, Roux C. 2016. A survey of the Gene repertoire of *Gigaspora rosea* unravels conserved features among Glomeromycota for Obligate Biotrophy. *Frontiers in Microbiology* **7**: 233. doi: 10.3389/fmicb.2016.00233, PMID: 26973612

Tisserant E, Kohler A, Dozolme-Seddas P, Balestrini R, Benabdellah K, Colard A, Croll D, Da Silva C, Gomez SK, Koul R, Ferrol N, Fiorilli V, Formey D, Franken P, Helber N, Hijri M, Lanfranco L, Lindquist E, Liu Y, Malbreil M, et al. 2012. The transcriptome of the arbuscular mycorrhizal fungus *Glomus intraradices* (DAOM 197198) reveals functional tradeoffs in an obligate symbiont. *New Phytologist* **193**:755–769. doi: 10.1111/j.1469-8137.2011.03948.x, PMID: 22092242

Trépanier M, Bécard G, Moutoglis P, Willemot C, Gagné S, Avis TJ, Rioux JA. 2005. Dependence of arbuscular-mycorrhizal fungi on their plant host for palmitic acid synthesis. *Applied and Environmental Microbiology* **71**: 5341–5347. doi: 10.1128/AEM.71.9.5341-5347.2005, PMID: 16151123

van Aarle IM, Olsson PA. 2003. Fungal lipid accumulation and development of mycelial structures by two arbuscular mycorrhizal fungi. *Applied and Environmental Microbiology* **69**:6762–6767. doi: 10.1128/AEM.69.11.6762-6767.2003, PMID: 14602638

Vierheilig H, Coughlan AP, Wyss U, Piche Y. 1998. Ink and vinegar, a simple staining technique for arbuscular-mycorrhizal fungi. *Applied and Environmental Microbiology* **64**:5004–5007. PMID: 9835596

Volpe V, Dell'Aglio E, Giovannetti M, Ruberti C, Costa A, Genre A, Guether M, Bonfante P. 2013. An AM-induced, MYB-family gene of *Lotus japonicus* (*LjMAMI*) affects root growth in an AM-independent manner. *The Plant Journal* **73**:442–455. doi: 10.1111/tpj.12045, PMID: 23051146

Wang E, Schornack S, Marsh JF, Gobbato E, Schwessinger B, Eastmond P, Schultze M, Kamoun S, Oldroyd GE. 2012. A common signaling process that promotes mycorrhizal and oomycete colonization of plants. *Current Biology* **22**:2242–2246. doi: 10.1016/j.cub.2012.09.043, PMID: 23122843

Wang J, Grishin N, Kinch L, Cohen JC, Hobbs HH, Xie XS. 2011. Sequences in the nonconsensus nucleotide-binding domain of ABCG5/ABCG8 required for sterol transport. *Journal of Biological Chemistry* **286**:7308–7314. doi: 10.1074/jbc.M110.210880, PMID: 21209088

Welti R, Li W, Li M, Sang Y, Biesiada H, Zhou HE, Rajashekar CB, Williams TD, Wang X. 2002. Profiling membrane lipids in plant stress responses. role of phospholipase D alpha in freezing-induced lipid changes in Arabidopsis. *The Journal of Biological Chemistry* **277**:31994–32002. doi: 10.1074/jbc.M205375200, PMID: 12077151

Wewer V, Brands M, Dörmann P. 2014. Fatty acid synthesis and lipid metabolism in the obligate biotrophic fungus *rhizophagus irregularis* during mycorrhization of *Lotus japonicus*. *The Plant Journal* **79**:398–412. doi: 10.1111/tpj.12566, PMID: 24888347

Wewer V, Dombrink I, vom Dorp K, Dörmann P. 2011. Quantification of sterol lipids in plants by quadrupole time-of-flight mass spectrometry. *Journal of Lipid Research* **52**:1039–1054. doi: 10.1194/jlr.D013987, PMID: 21382968

Wewer V, Dörmann P, Hölzl G. 2013. Analysis and quantification of plant membrane lipids by thin-layer chromatography and gas chromatography. In: Munnik T, Heilmann I (Eds). *Plant Lipid Signaling Protocols*. Totowa: Humana Press. p. 69–78. doi: 10.1007/978-1-62703-401-2_8

Wittenburg H, Carey MC. 2002. Biliary cholesterol secretion by the twinned sterol half-transporters ABCG5 and ABCG8. *Journal of Clinical Investigation* **110**:605–609. doi: 10.1172/JCI0216548, PMID: 12208859

Wu GZ, Xue HW. 2010. *Arabidopsis β*-ketoacyl-[acyl carrier protein] synthase i is crucial for fatty acid synthesis and plays a role in chloroplast division and embryo development. *The Plant Cell* **22**:3726–3744. doi: 10.1105/tpc.110.075564, PMID: 21081696

Xue L, Cui H, Buer B, Vijayakumar V, Delaux PM, Junkermann S, Bucher M. 2015. Network of GRAS transcription factors involved in the control of arbuscule development in *Lotus japonicus*. *Plant Physiology* **167**:854–871. doi: 10.1104/pp.114.255430, PMID: 25560877

Yang W, Pollard M, Li-Beisson Y, Beisson F, Feig M, Ohlrogge J. 2010. A distinct type of glycerol-3-phosphate acyltransferase with *sn*-2 preference and phosphatase activity producing 2-monoacylglycerol. *PNAS*USA **107**:12040–12045. doi: 10.1073/pnas.0914149107, PMID: 20551224

Yang W, Simpson JP, Li-Beisson Y, Beisson F, Pollard M, Ohlrogge JB. 2012. A land-plant-specific glycerol-3-phosphate acyltransferase family in Arabidopsis: substrate specificity, sn-2 preference, and evolution. *Plant Physiology* **160**:638–652. doi: 10.1104/pp.112.201996, PMID: 22864585

Yano K, Yoshida S, Müller J, Singh S, Banba M, Vickers K, Markmann K, White C, Schuller B, Sato S, Asamizu E, Tabata S, Murooka Y, Perry J, Wang TL, Kawaguchi M, Imaizumi-Anraku H, Hayashi M, Parniske M. 2008. CYCLOPS, a mediator of symbiotic intracellular accommodation. *PNAS* **105**:20540–20545. doi: 10.1073/pnas.0806858105, PMID: 19074278

Yeats TH, Martin LB, Viart HM, Isaacson T, He Y, Zhao L, Matas AJ, Buda GJ, Domozych DS, Clausen MH, Rose JK. 2012. The identification of cutin synthase: formation of the plant polyester cutin. *Nature Chemical Biology* **8**:609–611. doi: 10.1038/nchembio.960, PMID: 22610035

Zhang Q, Blaylock LA, Harrison MJ. 2010. Two *Medicago truncatula* half-ABC transporters are essential for arbuscule development in arbuscular mycorrhizal symbiosis. *The Plant Cell Online* **22**:1483–1497. doi: 10.1105/tpc.110.074955, PMID: 20453115

Figures and figure supplements

Lipid transfer from plants to arbuscular mycorrhiza fungi

Andreas Keymer *et al*

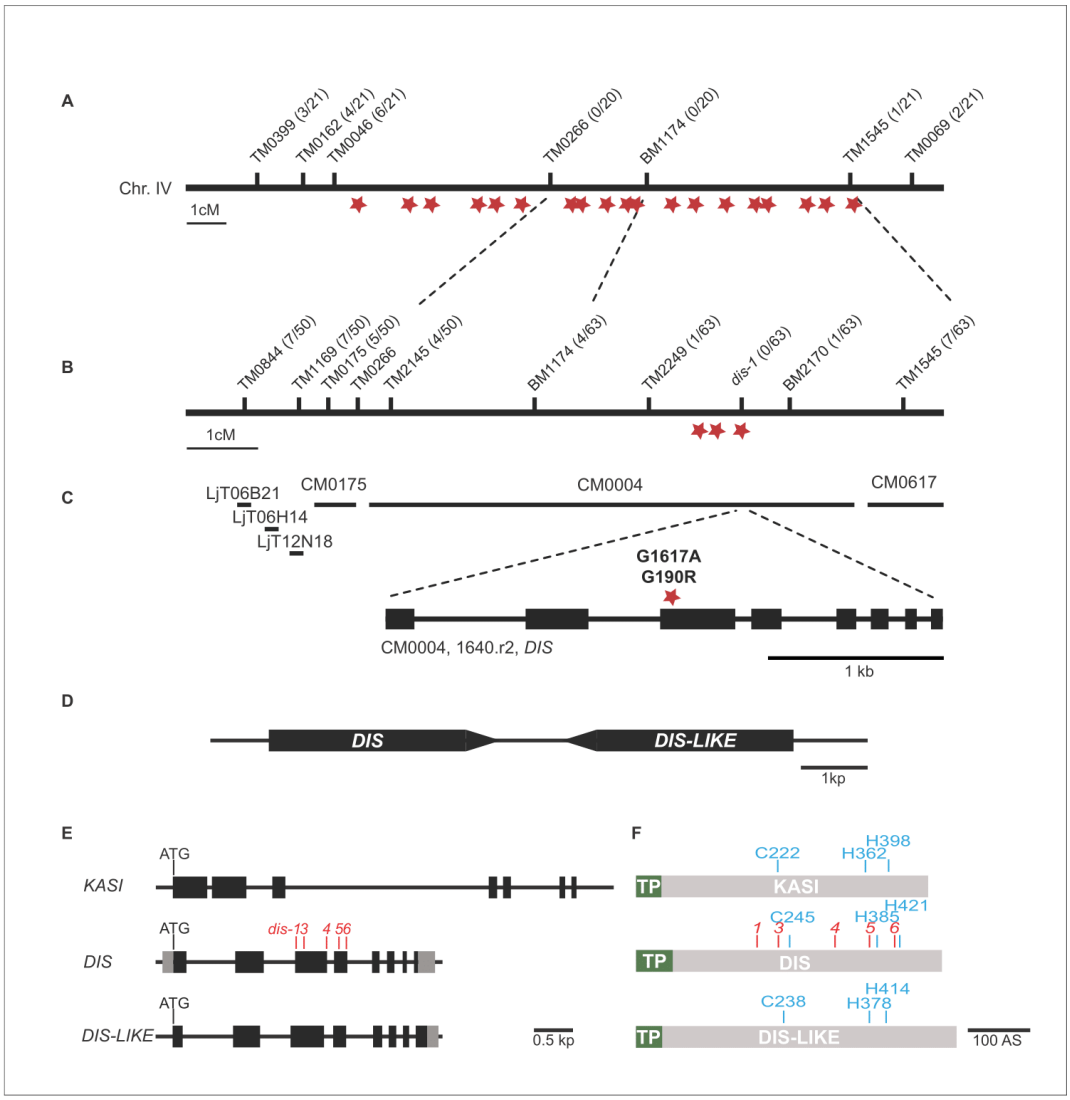

Figure 1—figure supplement 1. Identification of the *dis* mutation. (**A–B**) Genetic map of the *DIS* locus on chromosome 4. Numbers next to marker positions refer to the proportion of recombinant individuals among the number of analyzed F2 mutant plants. Rough mapping had previously identified the position of the *dis* mutation on the south arm of chromosome 4 (***Groth et al., 2013***). (**A**) In the first fine-mapping round, the interval narrowed down by recombinants comprised 19 EMS-induced SNPs (red stars), that could be confirmed by re-sequencing the mutant genome using next generation sequencing. (**B**) Further fine mapping resulted in an interval with 3 of these confirmed SNPs. (**C**) Physical map of the *DIS* locus. LjT followed by a number refers to TAC clones. CM followed by a number refers to contigs. One of the three SNPs causes a G to A transition in exon 3 of chr.4. CM004.1640.r2.a resulting in an amino acid change from glycine to arginine at position 190 of the protein product, which shares 79% sequence identity with a β-keto-acyl ACP synthase I (KASI) from *Arabidopsis thaliana*. Black boxes indicate exons separated by introns. (**D**) The *DIS* gene is duplicated in

Figure 1—figure supplement 1 continued on next page

Figure 1—figure supplement 1 continued

tandem. (**E**) Gene structure of *DIS*, *DIS-LIKE* and *KASI*. Black boxes display exons separated by introns (black lines). Grey boxes indicate determined untranslated regions. (**F**) DIS, DIS-LIKE and KASI are predicted to contain a plastid transit peptide (green). The catalytic triad is shown in blue and the location of mutations identified by TILLING in the *DIS* gene are shown in red. We chose the *dis-4* mutant for further analysis because the mutation resulted in a glycine replacement, which likely affects the functionality of the protein.

DOI: 10.7554/eLife.29107.004

	LjDIS	LjDIS-LIKE	LjKASI	AtKASI
LjDIS	100	87	79	78
LjDIS-LIKE	87	100	75	72
LjKASI	79	75	100	83
AtKASI	78	72	83	100

Figure 1—figure supplement 2. Protein sequence alignment of *L. japonicus* DIS with other KASI proteins. (**A**) Sequence alignment of LjDIS, LjDIS-LIKE, LjKASI, AtKASI and *E. coli* KASI and KASII. (**B**) Identity matrix of LjDIS, LjDIS-LIKE, LjKASI and AtKASI.

Figure 1—figure supplement 2 continued on next page

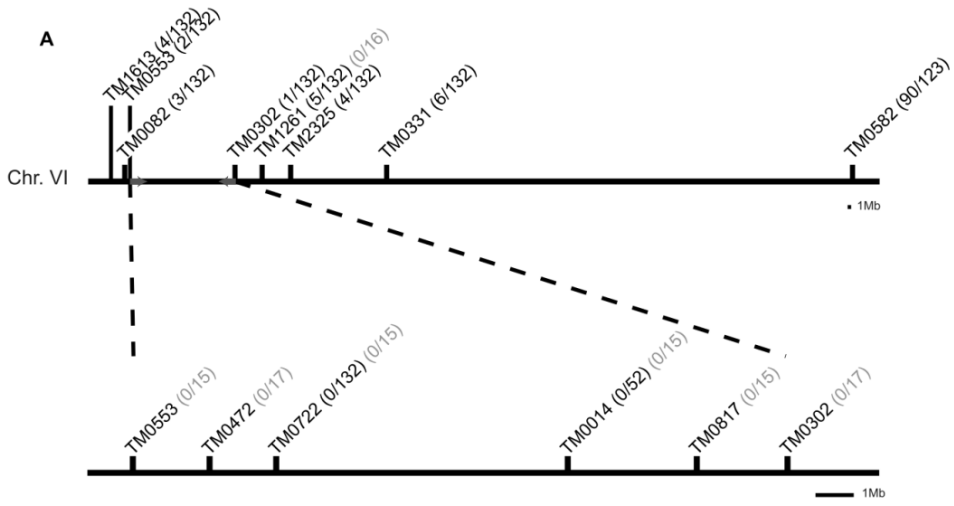

C

Generation	Phenotype	TM0553	TM0302	Nucleotide	No. of plants
F3	wild type	MG20	MG20	G	3
F3	wild type	Het	Het	R	8
F3	mutant	Gifu	Gifu	A	10
F4	wild type	Het	Het	R	4
F4	mutant	Gifu	Gifu	A	4

Figure 1—figure supplement 3. Identification of mutation in the *RAM2* gene. (**A**) Genetic map of the *red* locus on chromosome 6. Numbers next to the marker position refer to the proportion of recombinant individuals among the number of analysed F3 (black) and F4 (grey) segregating and mutant plants respectively. Fine mapping narrowed down the interval between TM0553 and TM0302. Red arrows indicate the genomic interval that contains the causative mutation. (**B**) Gene structure of *L. japonicus RAM2* with locations of the identified EMS-induced mutation at position 1663 (star, *ram2-1*) leading to an amino acid exchange from glycine to glutamic acid at position 555 of the RAM2 protein and LORE1 insertion (triangle, *ram2-2*). Black boxes indicate exons separated by intron (thin black line). Grey boxes indicate untranslated regions (UTRs) comprising 77 bp (5'UTR) and 151 bp (3'UTR). (**C**) Co-segregation analysis of arbuscule phenotype and mutation in the *RAM2* gene in a number of F3 and F4 plants from segregating populations containing only the mutation on chromosome 6. The number of plants analysed per generation, arbuscule phenotype, genotype at markers TM0053 and TM0302 and the nucleotide observed at position 1663 in the *RAM2* gene are indicated. The *ram2* mutation at position 1663 clearly co-segregates with the stunted arbuscule phenotype.

DOI: 10.7554/eLife.29107.006

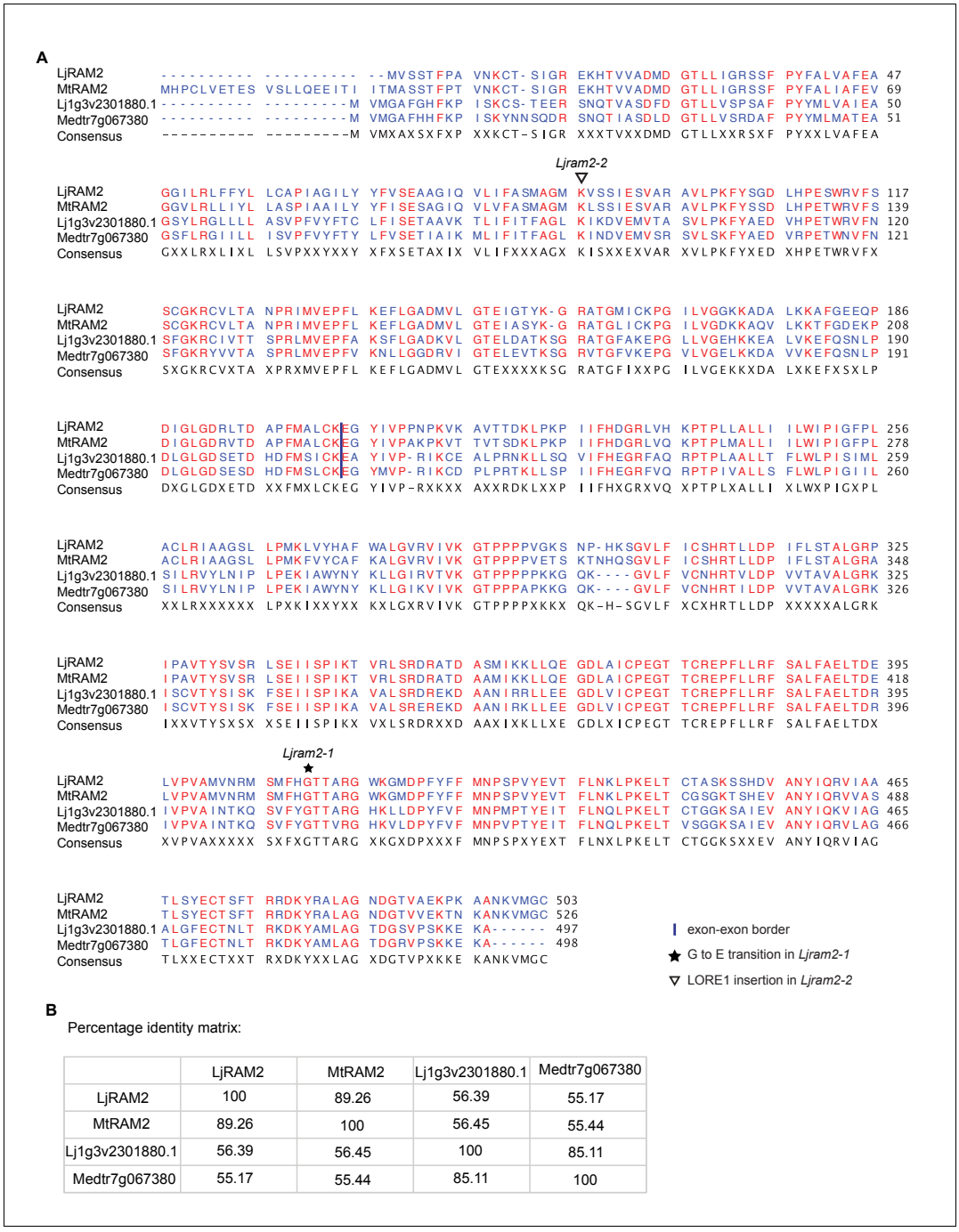

	LjRAM2	MtRAM2	Lj1g3v2301880.1	Medtr7g067380
LjRAM2	100	89.26	56.39	55.17
MtRAM2	89.26	100	56.45	55.44
Lj1g3v2301880.1	56.39	56.45	100	85.11
Medtr7g067380	55.17	55.44	85.11	100

Figure 1—figure supplement 4. Protein sequence alignment of *L. japonicus* RAM2 with *M. truncatula* RAM2. Sequence alignment (**A**) and identity matrix (**B**) of LjRAM2, Lj1g3v2301880.1, MtRAM2 and Medtr7g067380.

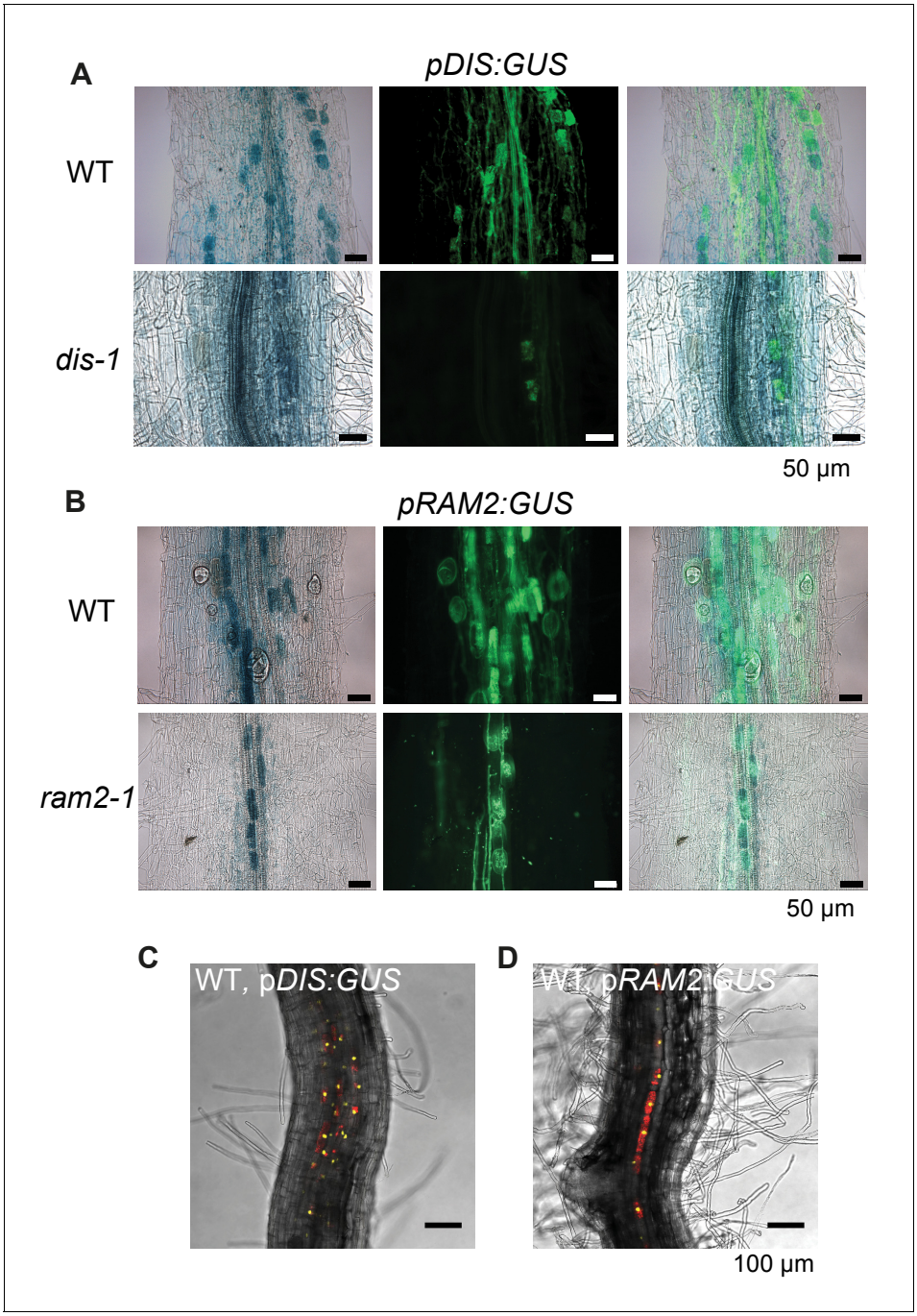

Figure 2—figure supplement 1. *DIS* and *RAM2* promoter activity in wild type and *dis* and *ram2* mutants. GUS activity in colonized transgenic *L. japonicus* wild-type and mutant roots transformed with constructs containing a 1.5 kb promoter fragment of *DIS* (**A**) or a 2.275 kb promoter fragment of

Figure 2—figure supplement 1 continued on next page

Figure 2—figure supplement 1 continued

RAM2 (**B**) fused to the *uidA* gene. Left micrographs: bright field channel to detect GUS-staining, middle micrographs: GFP-channel to detect (WGA)-AlexaFluor488 stained fungal structures. Right micrographs: Merge. (C-D) Single optical section of z-stack shown in ***Figure 2Aa*** (C) and ***Figure 2Ba*** (D) showing that *DIS* and *RAM2* promoter activity is detected exclusively in the cortex.

DOI: 10.7554/eLife.29107.009

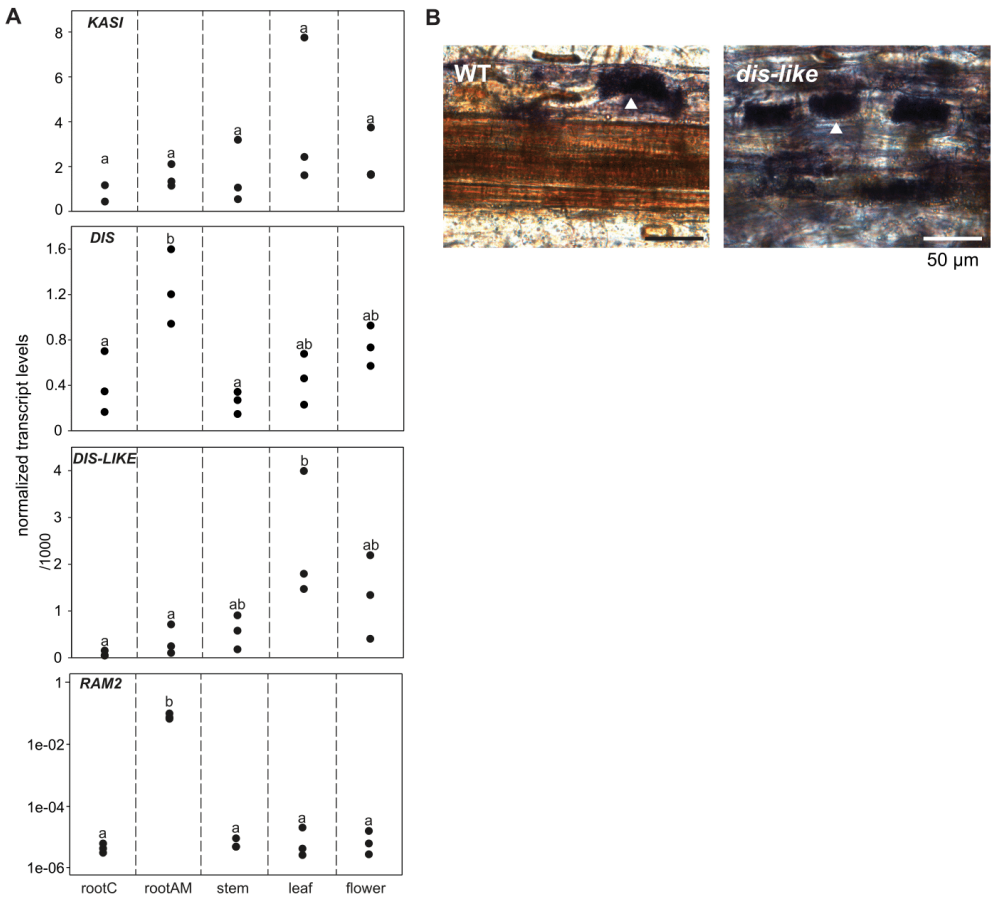

Figure 3—figure supplement 1. Transcript accumulation of *KASI* and *RAM2* genes. (**A**) Transcript accumulation of *DIS, DIS-LIKE, KASI* and *RAM2* in control (mock) and *R. irregularis* colonized (AM) roots and in different organs of *L. japonicus* assessed by qRT-PCR. Expression values were normalized to those of the constitutively expressed gene *EF1α* (*DIS, DIS-LIKE, KASI*) and *Ubiquitin10* (*RAM2*). Black circles represent three biological replicates. Different letters indicate significant differences (ANOVA; posthoc Tukey; n = 15; $p \leq 0.05$, $F_{4,14}$(*KASI*) = 1.191, $F_{4,14}$(*DIS*) = 8.412, $F_{4,14}$(*DIS-LIKE*) = 4.563; $p \leq 0.001$, $F_{4,14}$ = 67.41 (*RAM2*)). AM plants were inoculated with *R. irregularis*. Control and AM plants were harvested 5 wpi. (**B**) Arbuscule phenotype in wild type and *dis-like-5* mutant roots after 5 wpi with *R. irregularis* as indicated by acid ink staining. White arrow heads indicate arbuscules.
DOI: 10.7554/eLife.29107.018

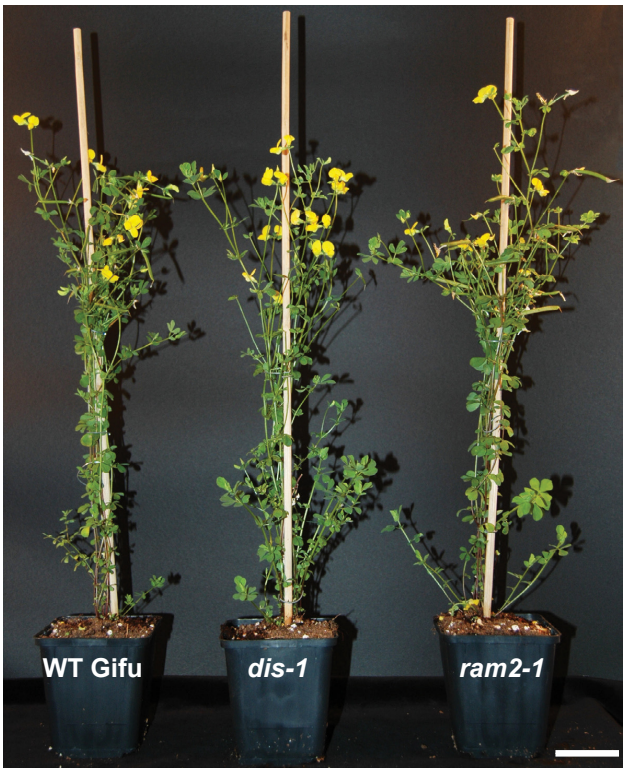

Figure 3—figure supplement 2. Shoot phenotypes of *dis* and *ram2* mutants. *dis* and *ram2* mutants do not show growth differences in shoot growth as compared to Gifu wild-type. The image has been taken 17 weeks post planting (size bar, 5 cm).
DOI: 10.7554/eLife.29107.019

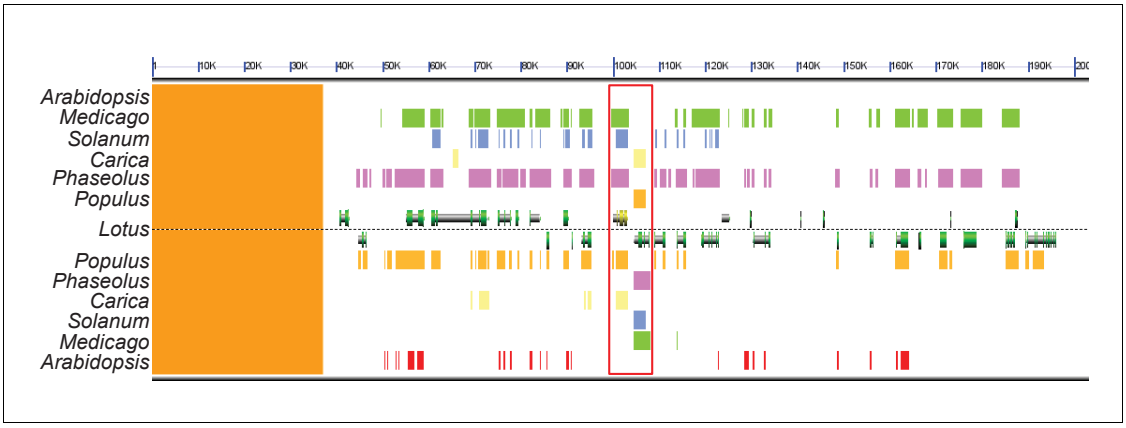

Figure 3—figure supplement 3. Genomic comparison of the *DIS* locus in host and non-host species. Synteny analysis of a ~ 200 kb sized region in the *Lotus japonicus*, *Medicago truncatula* (green), *Populus trichocarpa* (orange), *Phaseolus vulgaris* (pink), *Solanum lycopersicum* (blue) and *Carica papaya* (yellow) genomes containing the *DIS* locus. The genomic block is well conserved in these host species. By contrast, no *DIS* homolog was detected in the corresponding genomic block of *Arabidopsis thaliana* (red). The red rectangle indicates the *DIS* and *DIS-LIKE* locus, *DIS* is indicated in yellow. The sequences above *Lotus* correspond to the forward strand and those below *Lotus* to the reverse strand. The orange strip on the left side corresponds to a non-assembled region of the *L. japonicus* genome.
DOI: 10.7554/eLife.29107.020

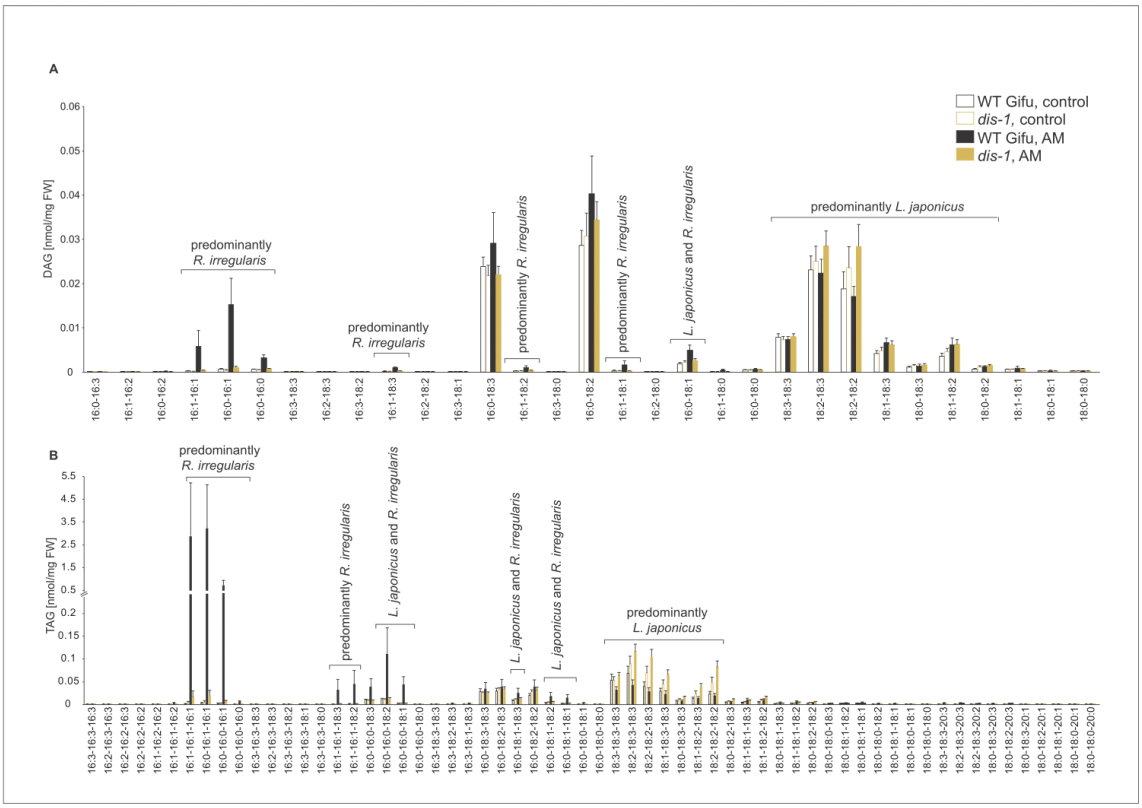

Figure 5—figure supplement 1. Diacylglycerol (DAG) and triacylglycerol (TAG) profiles of *L. japonicus* WT and *dis-1* control and AM roots. (**A**) Profile of diacylglycerols in control and AM-colonized *L. japonicus* WT and *dis-1* roots. (**B**) Profile of triacylglycerols in control and AM-colonized *L. japonicus* WT and *dis-1* roots. (**A–B**) Bars represent means ±standard deviation (SD) of 3–5 biological replicates. '*L. japonicus* and *R. irregularis*' marks lipids which are found in both organisms according to (***Wewer et al., 2014***) .

DOI: 10.7554/eLife.29107.024

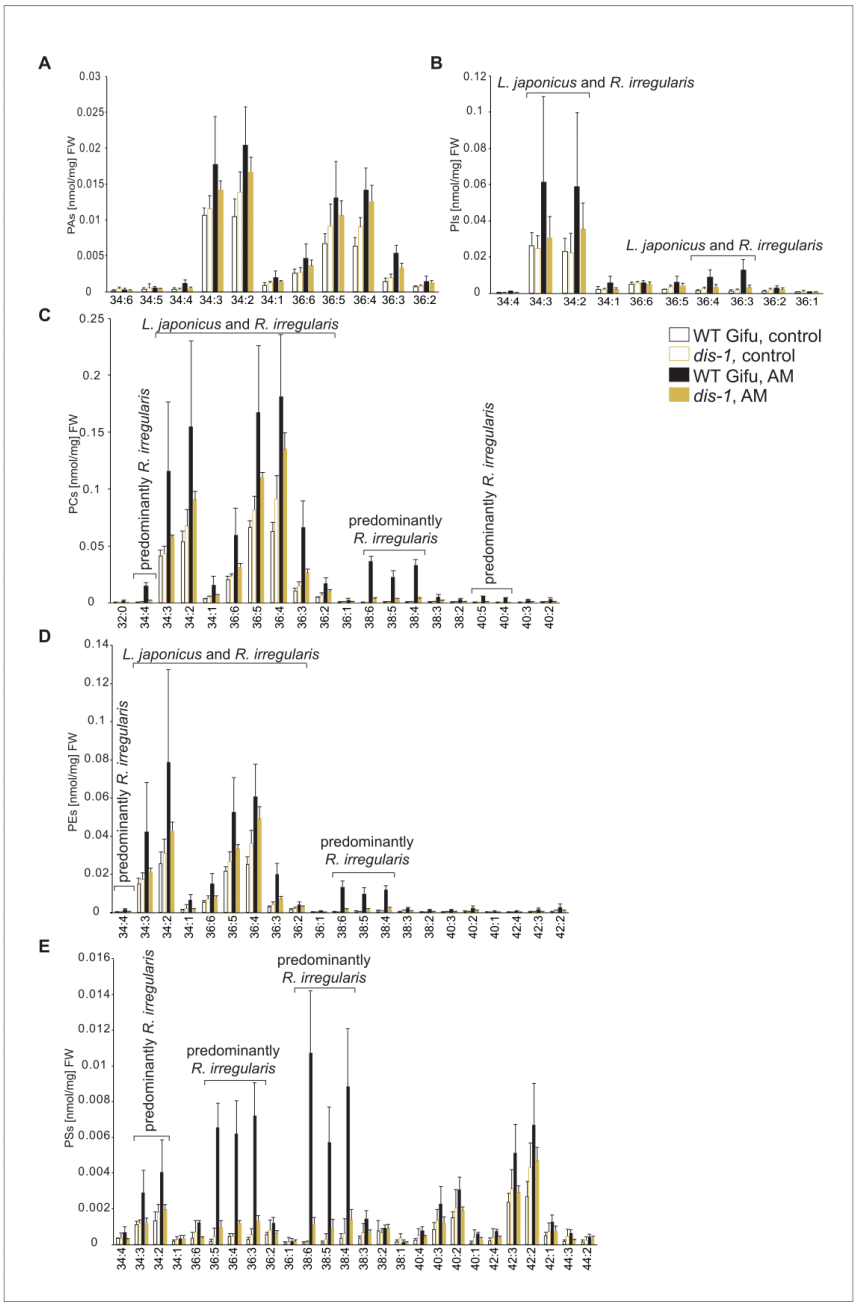

Figure 5—figure supplement 2. Profiles of phospholipids in non-colonized and colonized *L. japonicus* WT Gifu and *dis-1* roots. (**A**) Absolute amounts of phosphatidic acid (PA) species. (**B**) Absolute amounts of phosphatidylinositol (PI) species. (**C**) Absolute amounts of phosphatidylcholine (PC) species.
Figure 5—figure supplement 2 continued on next page

Figure 5—figure supplement 2 continued

(**D**) Absolute amounts of phosphatidylethanolamine (PE) species. (**E**) Absolute amounts of phosphatidylserine (PS) species. (**A–D**) Bars represent means ±standard deviation (SD) of 3–5 biological replicates. '*L. japonicus* and *R. irregularis*' marks lipids which are found in both organisms according to ***Wewer et al. (2014)***.
DOI: 10.7554/eLife.29107.025

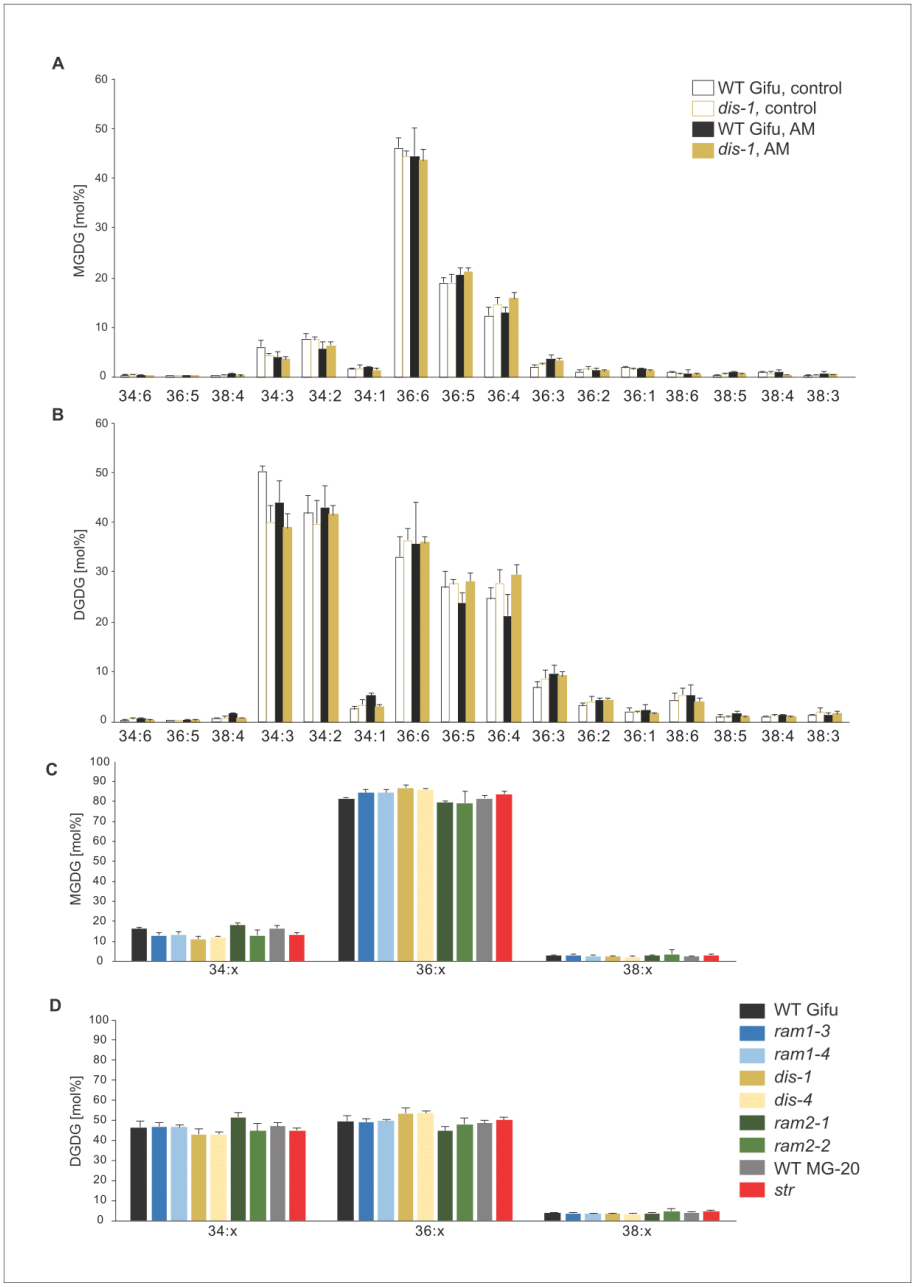

Figure 5—figure supplement 3. MGDG and DGDG profiles do not differ among *L. japonicus* wild-type and mutant roots. (**A**) Relative amounts of monogalactosyldiacylglycerol (MGDG) in control and colonized roots of Gifu WT and *dis-1*. (**B**) Relative amount of digalactosyldiacylglycerol (DGDG) in

Figure 5—figure supplement 3 continued on next page

Figure 5—figure supplement 3 continued

control and colonized roots of Gifu WT and *dis-1*. (**C**) Relative amounts of monogalactosyldiacylglycerols (MGDG) containing acyl chains of 16:x + 18:x (34:x MGDG), di18:x(36:x MGDG) or 18:x + 20:x(38:x MGDG) in the different colonized genotypes. (**D**) Relative amount of digalactosyldiacylglycerols (DGDG) containing acyl chains of 16:x + 18:x(34:x DGDG), di18:x(36:x DGDG) or 18:x + 20:x(38:x DGDG) of the different colonized genotypes. (**A–D**) Bars represent means ±standard deviation (SD) of 3–5 biological replicates.

DOI: 10.7554/eLife.29107.026

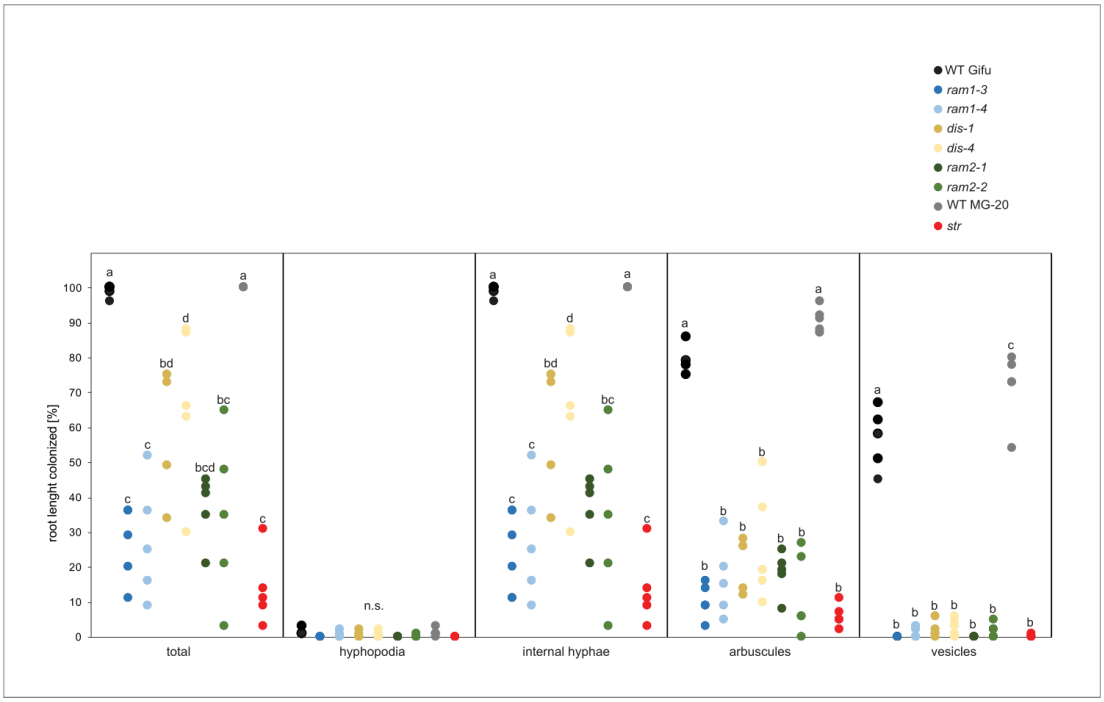

Figure 5—figure supplement 4. All arbuscule-deficient mutants show reduced root length colonization. Quantitative AM colonization in root samples employed for lipidomics (***Figure 3D–F***, ***Figure 5E–H***, ***Figure 7***, ***Figure 5—figure supplements 1–3*** and ***5–11***) as determined by modified grid-line intersect methods after acid-ink staining. WT Gifu, WT MG-20 and all AM-deficient mutants in the Gifu background (*ram1-3, ram1-4, dis-1, dis-4, ram2-1* and *ram2-2)* and the *str* mutant in the MG-20 background. Different letters indicate significant differences (ANOVA; posthoc Tukey; n = 45) among genotypes for each fungal structure separately. $p \leq 0.05$, $F_{8,36} = 21.69$ (total and intraradical hyphae); $p \leq 0.001$, $F_{8,36} = 62.1$ (arbuscules), $F_{8,36} = 176.5$ (vesicles).

DOI: 10.7554/eLife.29107.027

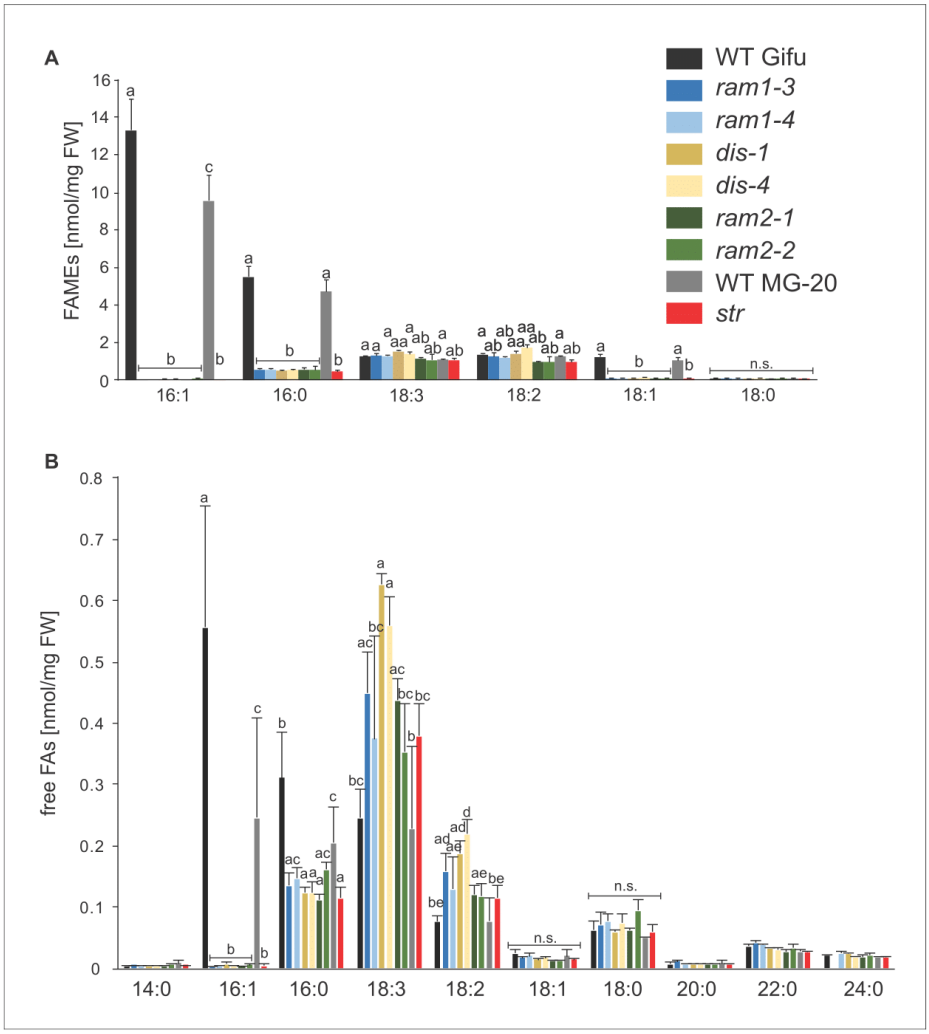

Figure 5—figure supplement 5. Total fatty acid and free fatty acid profiles of colonized *L. japonicus* WT and AM-defective mutant roots. (**A**) Total amounts of fatty acids (FAME) in colonized *L. japonicus* roots of the different genotypes. Fatty acid methyl esters (FAME) were prepared from total root lipids and analysed by GC. Different letters indicate significant differences (ANOVA; posthoc Tukey; $p \leq 0.01$; (n = 42, $F_{8,33}$ = 29.91 (16:1); n = 43, $F_{8,34}$ = 20.25 (16:0); n = 43, $F_{8,34}$ = 11.34 (18:3); $F_{8,34}$ = 13.14 (18:2)). (**B**) Free fatty acid composition in colonized *L. japonicus* roots from Gifu WT, MG-20 WT, *ram1-3, ram1-4, dis-1, dis-4, ram2-1, ram2-2* and *str*. Free fatty acids were isolated from total root lipids and converted into fatty acid methyl esters for quantification by GC Different letters indicate significant differences (ANOVA; posthoc Tukey; n = 44; ($p \leq 0.001$, $F_{8,35}$ = 230.6 (16:0); $p \leq 0.001$, $F_{8,35}$ = 257.7 (16:1); $F_{8,35}$ = 222.5 (18:1); $F_{8,35}$ = 15.48 (18:2); $F_{8,35}$ = 8.225 (18:3)). (**A–B**) Bars represent means ±standard deviation (SD) of 3–5 biological replicates.

DOI: 10.7554/eLife.29107.028

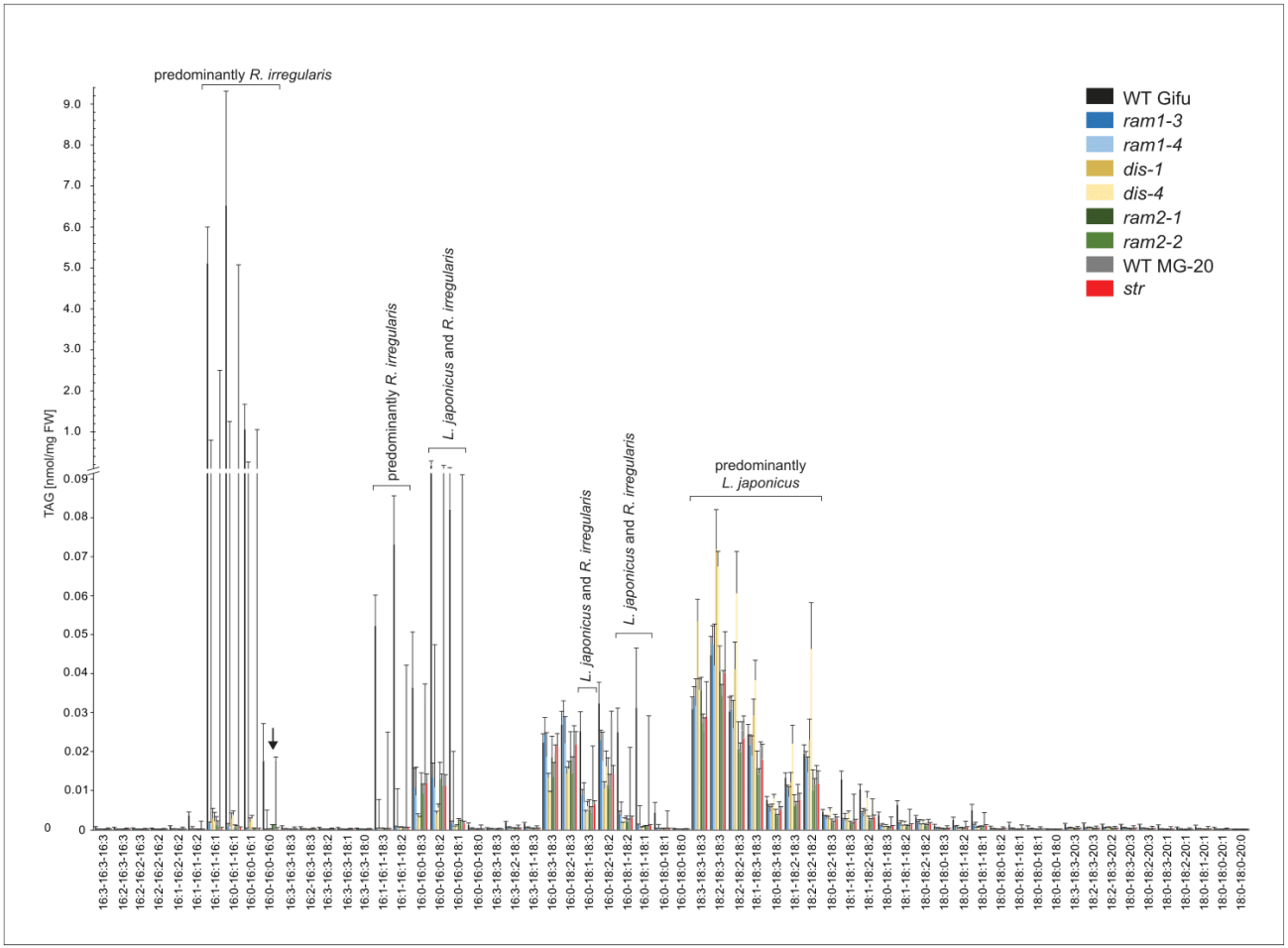

Figure 5—figure supplement 6. Triacylglycerol (TAG) profiles of colonized *L. japonicus* WT and AM-defective mutant roots. Absolute amounts of triacylglycerol molecular species in colonized *L. japonicus* roots of WT Gifu, WT MG-20 *ram1-3, ram1-4, dis-1, dis-4, ram2-1, ram2-2* and *str*. Black arrow indicates accumulation of tri 16:0 TAG in *ram2-1* and *ram2-2*. Bars represent means ±standard deviation (SD) of 3–5 biological replicates.

DOI: 10.7554/eLife.29107.029

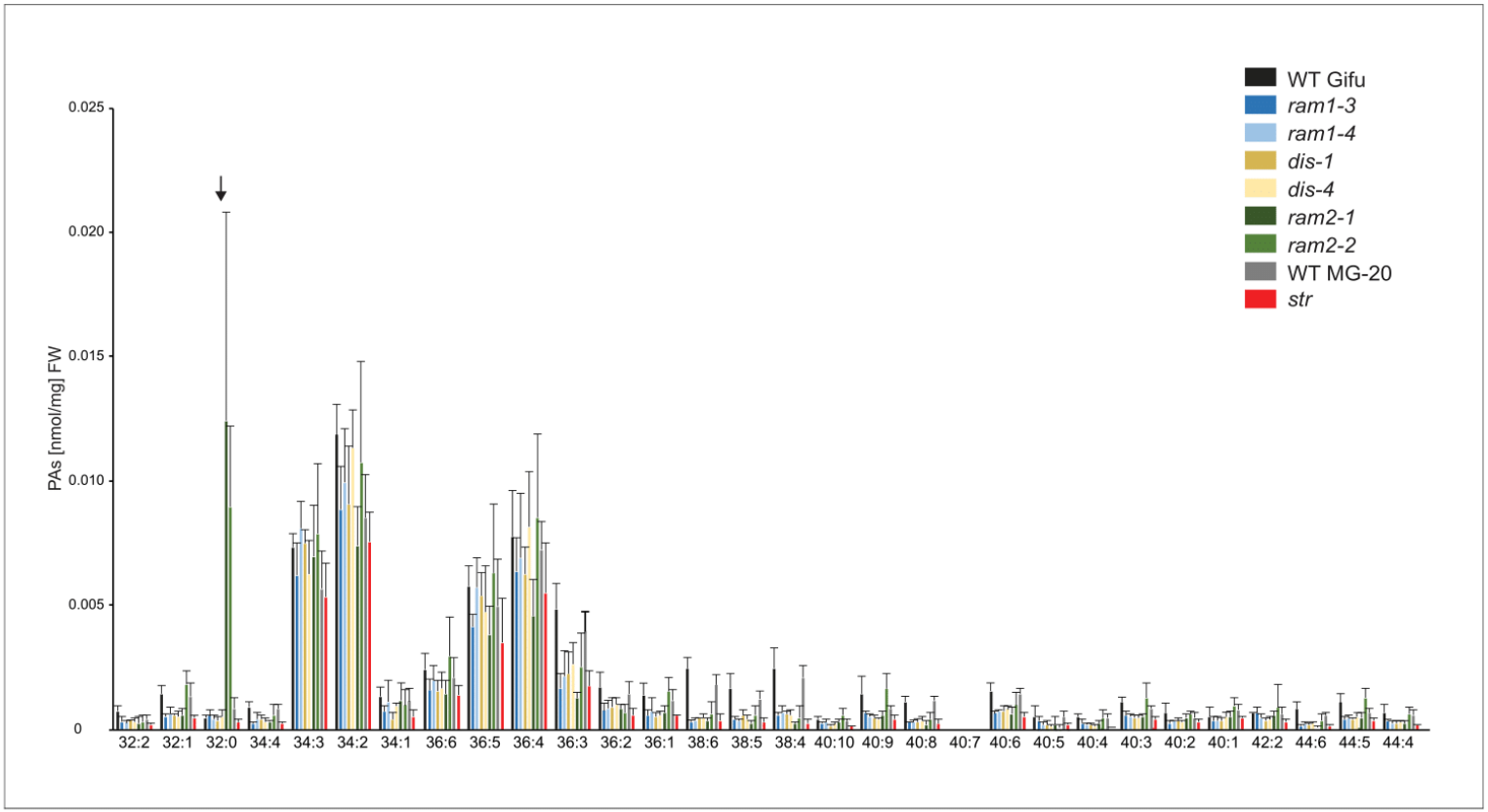

Figure 5—figure supplement 7. Phosphatidic acid (PA) profiles in *L. japonicus* WT and AM-defective mutants. Absolute amounts of phosphatidic acid molecular species in colonized *L. japonicus* roots of WT Gifu, WT MG-20 *ram1-3, ram1-4, dis-1, dis-4, ram2-1, ram2-2* and *str*. Black arrow indicates accumulation of 32:0 (di16:0) PA in *ram2-1* and *ram2-2*. Bars represent means ±standard deviation (SD) of 3–5 biological replicates.

DOI: 10.7554/eLife.29107.030

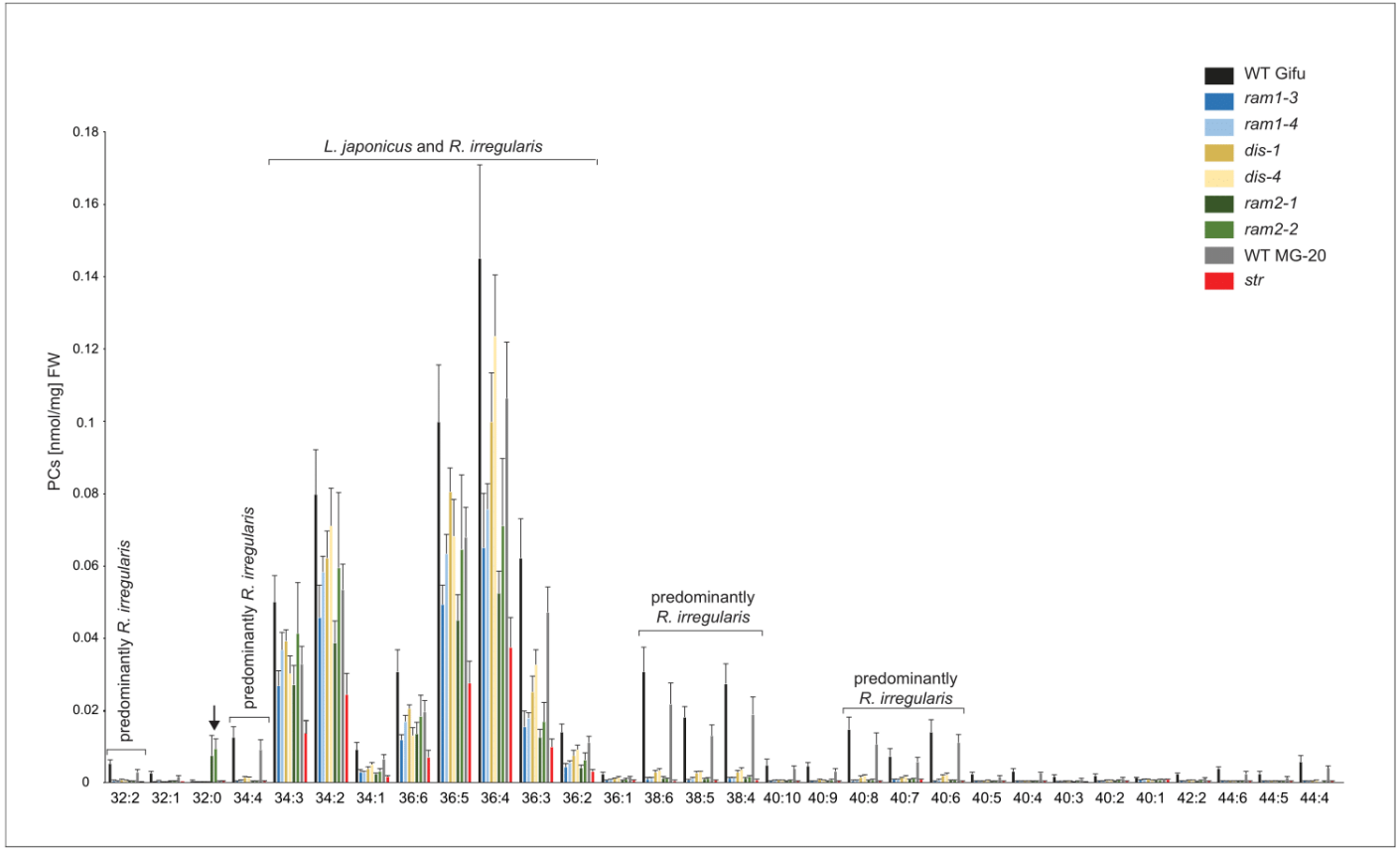

Figure 5—figure supplement 8. Profile of phosphatidylcholines (PC) in *L. japonicus* WT and AM-defective mutants. Absolute amounts of phosphatidylcholine molecular species in colonized *L. japonicus* roots of WT Gifu, WT MG-20, *ram1-3, ram1-4, dis-1, dis-4, ram2-1, ram2-2* and *str*. Bars represent means ±standard deviation (SD) of 3–5 biological replicates. '*L. japonicus* and *R. irregularis*' marks lipids which are found in both organisms according to ***Wewer et al. (2014)***. Arrow highlights the exclusive accumulation of unusual 32:0 (di16:0) PC in *ram2-1* and *ram2-2*.

DOI: 10.7554/eLife.29107.031

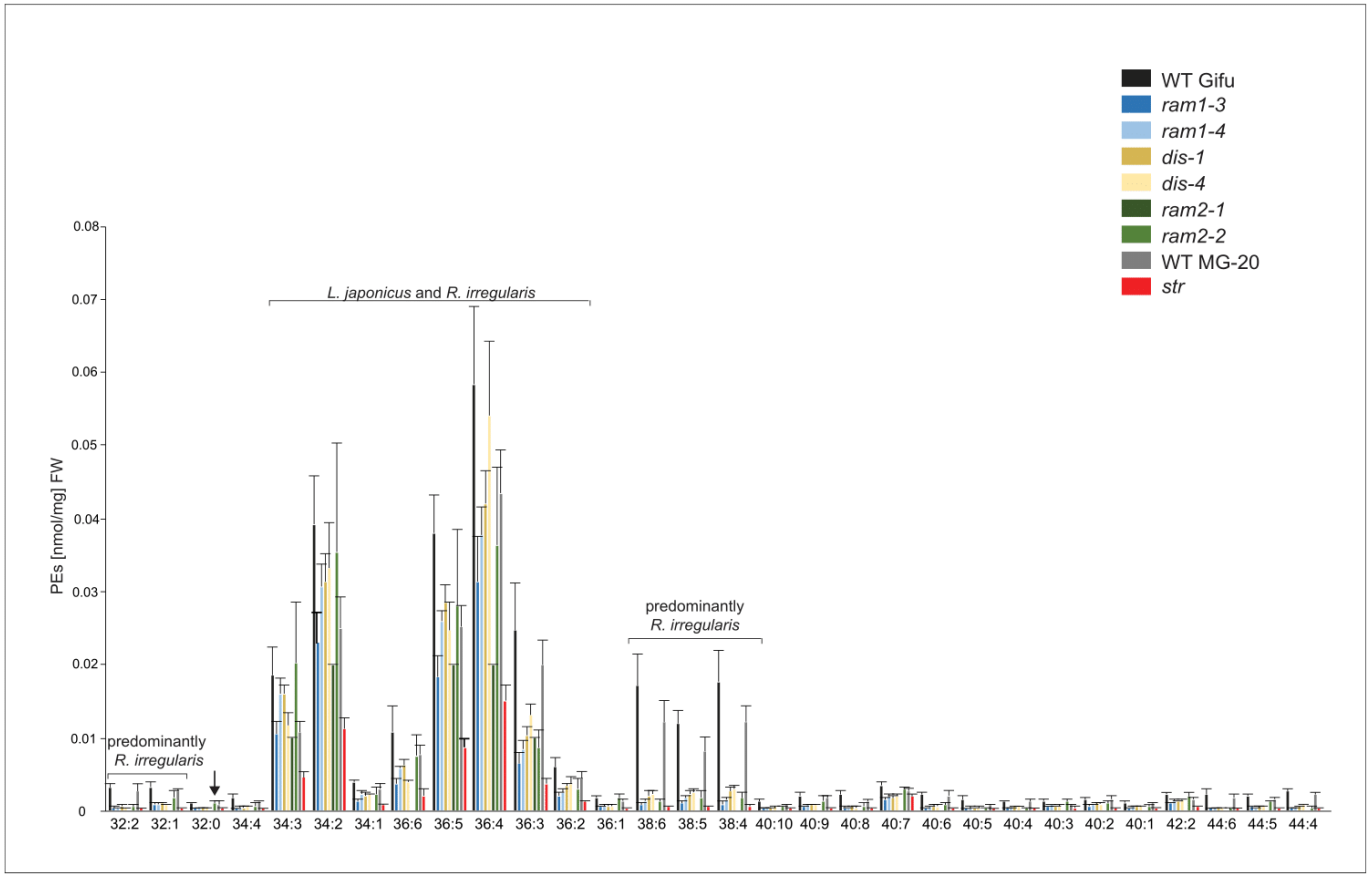

Figure 5—figure supplement 9. Phosphatidylethanolamine (PE) profile in *L. japonicus* WT and AM-defective mutants. Absolute amounts of phosphatidylethanolamine molecular species in colonized *L. japonicus* roots of WT Gifu, WT MG-20, *ram1-3, ram1-4, dis-1, dis-4, ram2-1, ram2-2* and *str*. Bars represent means ±standard deviation (SD) of 3–5 biological replicates. '*L. japonicus* and *R. irregularis*' marks lipids which are found in both organisms according to ***Wewer et al. (2014)***. Arrow highlights the exclusive accumulation of unusual 32:0 (di16:0) PE in *ram2-1* and *ram2-2*.
DOI: 10.7554/eLife.29107.032

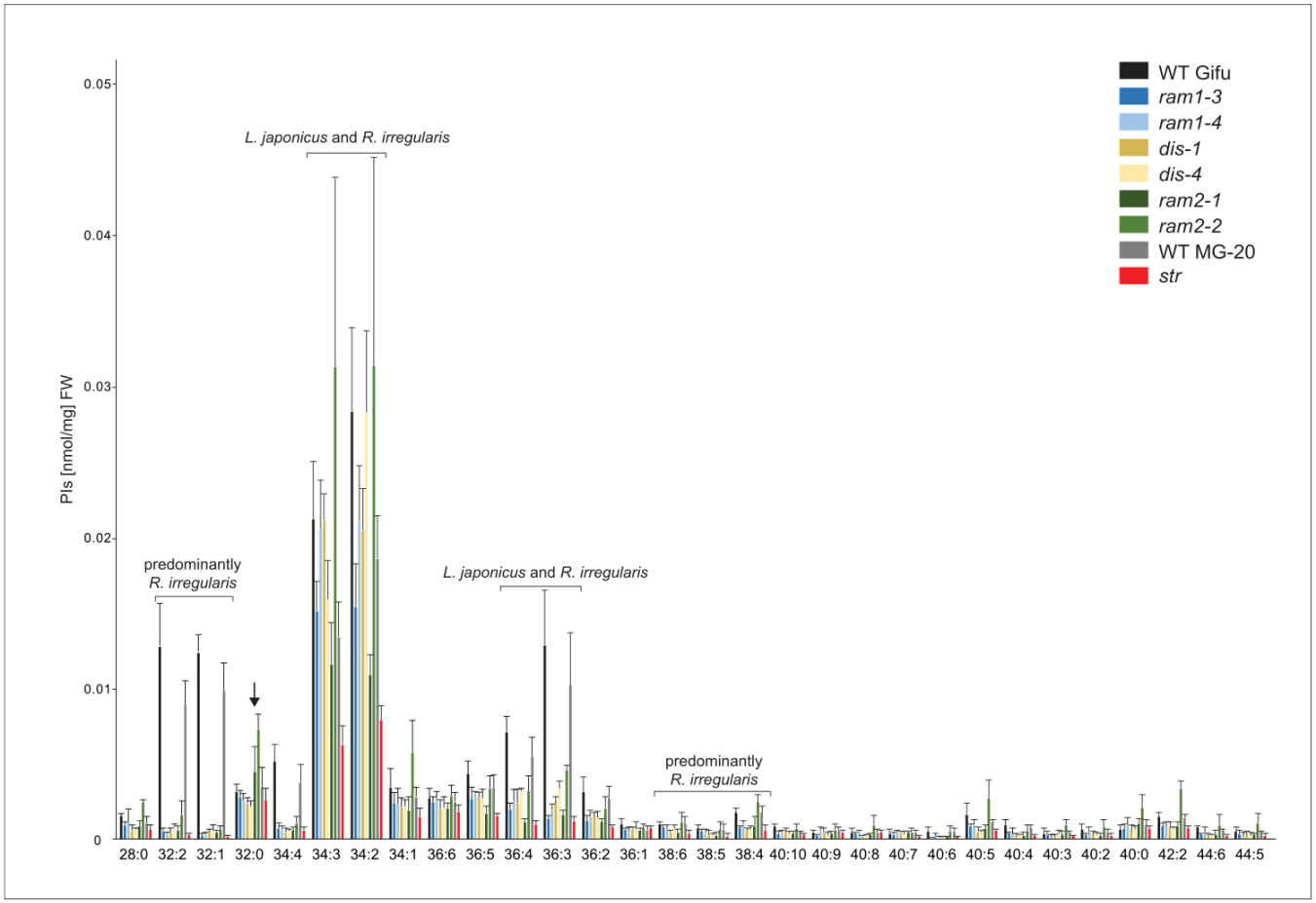

Figure 5—figure supplement 10. Phosphatidylinositol (PI) profile in *L. japonicus* WT and AM-defective mutants. Absolute amounts of phosphatidylinositol molecular species in colonized *L. japonicus* roots of WT Gifu, WT MG-20, *ram1-3, ram1-4, dis-1, dis-4, ram2-1, ram2-2* and *str*. Bars represent means ± standard deviation (SD) of 3–5 biological replicates. '*L. japonicus* and *R. irregularis*' marks lipids which are found in in both organisms according to ***Wewer et al. (2014)***. Arrow highlights the exclusive accumulation of unusual 32:0 PI in *ram2-1* and *ram2-2*.

DOI: 10.7554/eLife.29107.033

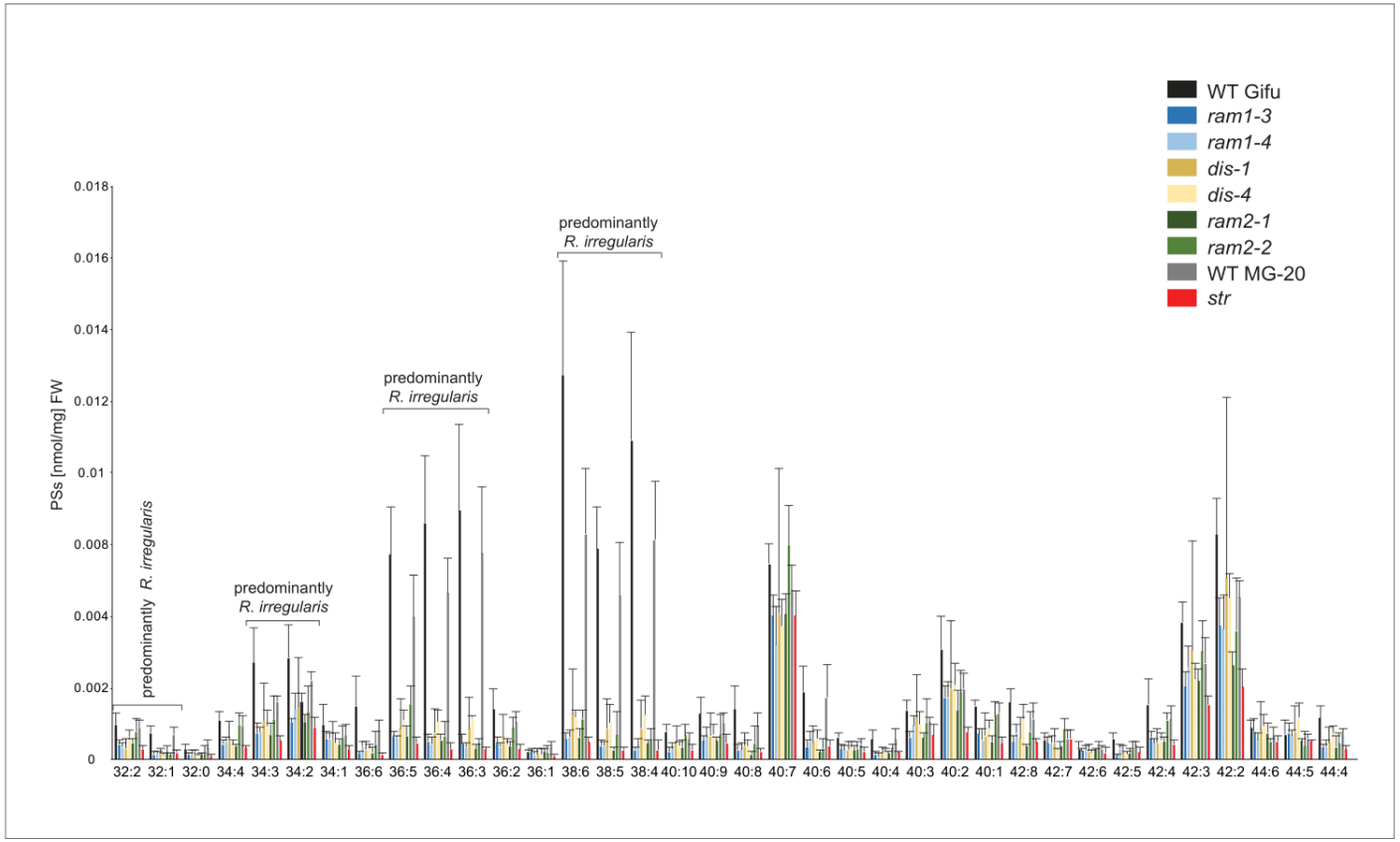

Figure 5—figure supplement 11. Phosphatidylserine (PS) profile in *L. japonicus* WT and AM-defective mutants. Absolute amounts of phosphatidylserine molecular species in colonized *L. japonicus* roots of WT Gifu WT, WT MG-20, *ram1-3, ram1-4, dis-1, dis-4, ram2-1, ram2-2* and *str*. Bars represent means ± standard deviation (SD) of 3–5 biological replicates.

DOI: 10.7554/eLife.29107.034

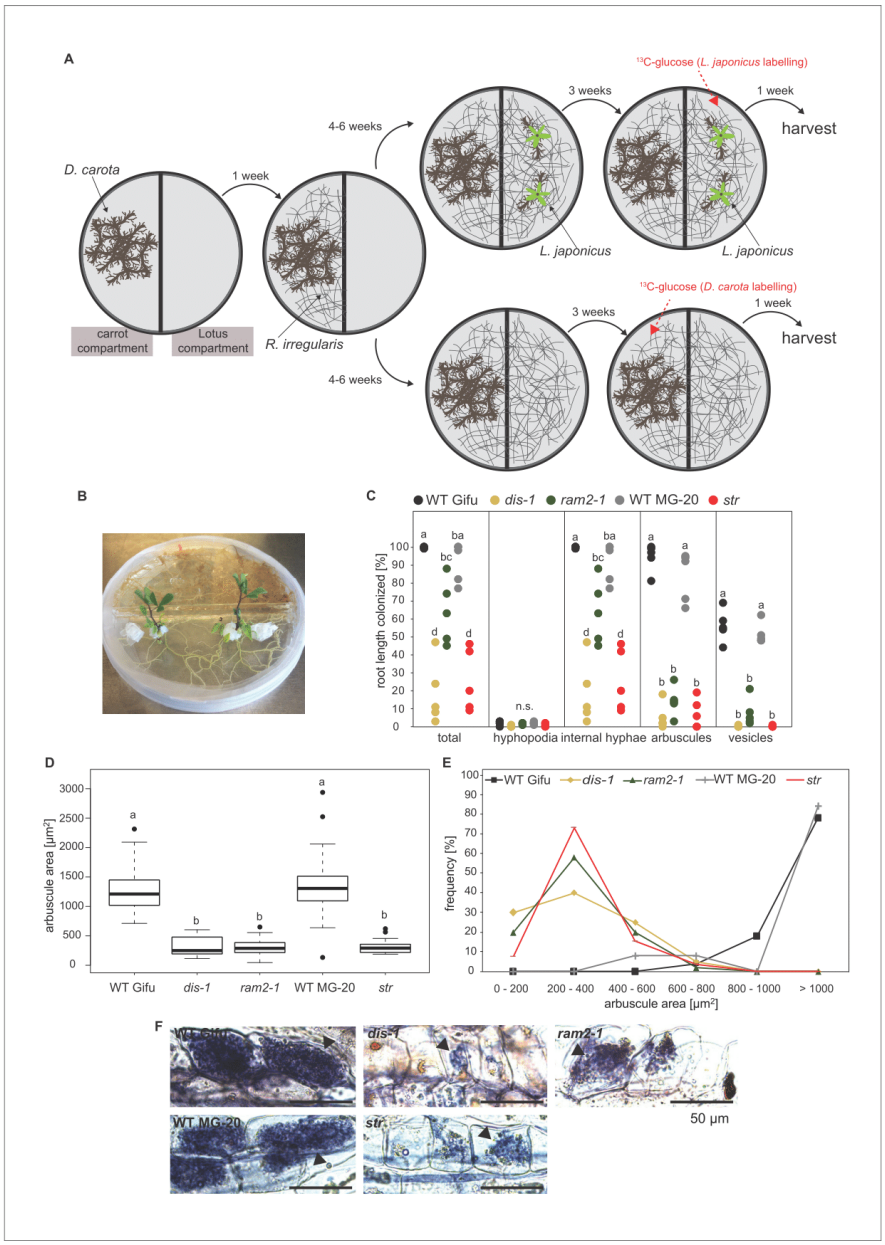

Figure 8—figure supplement 1. Two-compartment cultivation setup used for labelling experiments. (**A**) Schematic representation of cultivation setup which was used for ^{13}C-glucose labelling experiments (***Figure 8***, ***Figure 8—figure supplement 2–4***). [U-$^{13}C_6$]Glucose as substrate was either applied

Figure 8—figure supplement 1 continued on next page

Figure 8—figure supplement 1 continued

to the carrot compartment or the *Lotus* compartment. Colonized roots and extraradical mycelia populating the plate were harvested separately. (**B**) Photo of the 2-compartment setup. 2 week old *Lotus* seedlings were cultivated for 4 weeks on this setup. 100 mg of [U-$^{13}C_6$]Glucose was applied one week before harvest. (**C**) Quantitative AM colonization as determined by the modified grid-line intersect method after acid-ink staining in roots of genotypes indicated in the figure from plants grown in the Petri dish system (**A and B**) in parallel with the plants used for isotopolog profiling. Different letters indicate significant differences (ANOVA; posthoc Tukey; n = 25) among genotypes for each fungal structure separately. $p \leq 0.01$, $F_{4,20} = 32.49$ (total and intraradical hyphae); $F_{4,20} = 110.1$ (arbuscules), $F_{4,20} = 112.6$ (vesicles). (**D**) Arbuscule area and (**E**) frequency distribution of arbuscule area in the root samples used in (**C**). 10 arbuscules were analysed per root system. For wild-type Gifu, MG20 and *ram2-1* five, for *str* three and for *dis-1* two root systems were available. Different letters in (**D**) indicate significant differences (ANOVA; posthoc Tukey; n = 196) in arbuscule area among genotypes. $p \leq 0.001$, $F_{4,191} = 127.4$. (**E**) Representative bright-field images of arbuscules in roots of the samples analyzed in C-D.

DOI: 10.7554/eLife.29107.039

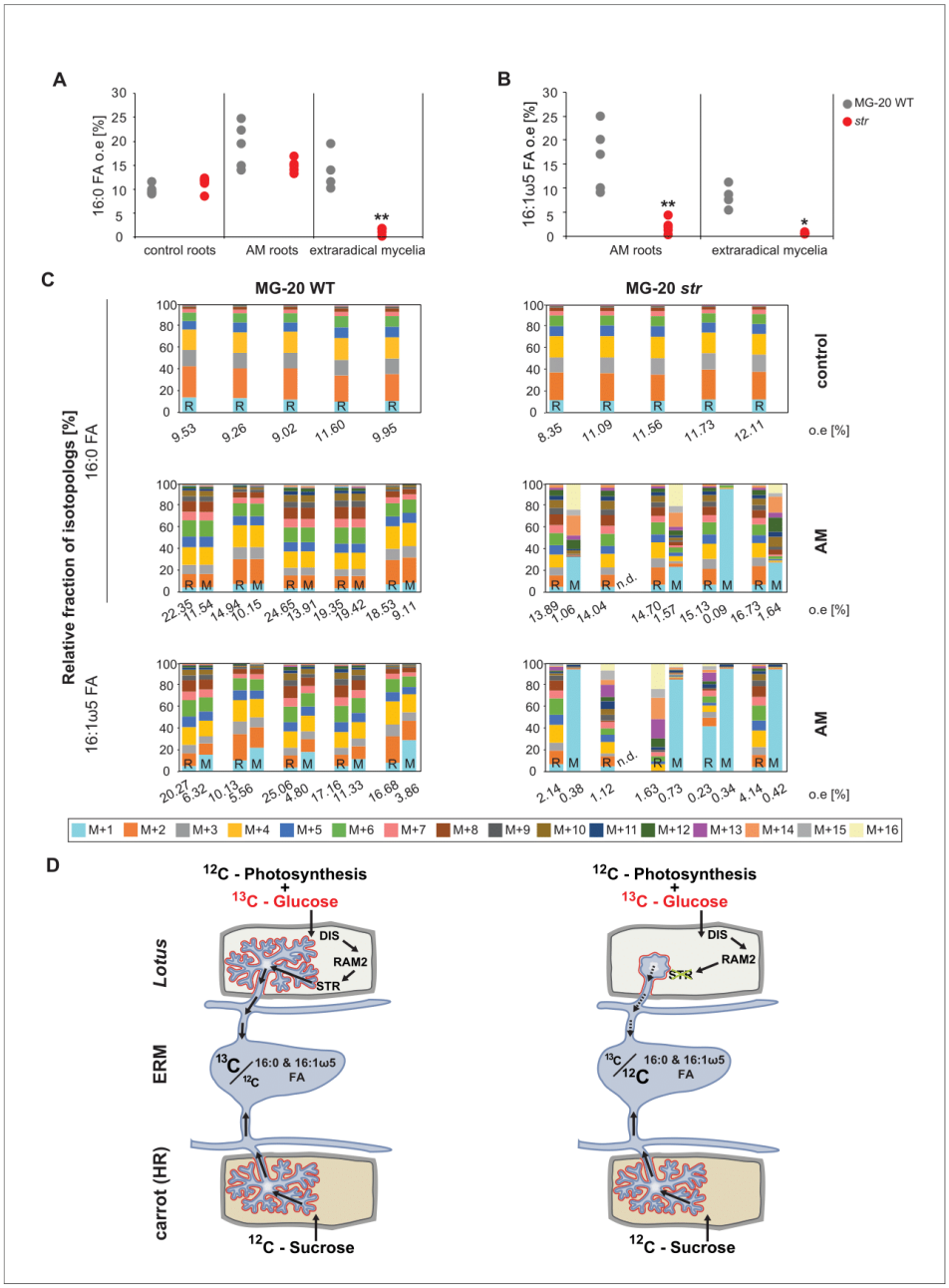

Figure 8—figure supplement 2. Isotopolog profiles of wild-type MG20 and *str*. (**A–B**) Overall excess (o.e.) of ^{13}C over air concentration in 16:0 FAs (**A**) and in AMF specific 16:1ω5 FAs (**B**) detected in non-colonized (only 16:0 FAs) and colonized, *L. japonicus* wild-type and *str* roots and in the extraradical

Figure 8—figure supplement 2 continued on next page

Figure 8—figure supplement 2 continued

mycelium of *R. irregularis*. Five biological replicates of each genotype and treatment are shown. Black asterisks indicate statistically significant differences between mutant lines and wild-type according to Student's t-test *p<0.05; **p<0.01. (**C**) Relative fraction of ^{13}C isotopologs for 16:0 fatty acids of five replicates (individual bars and double bars) of *L. japonicus* WT MG-20 and *str* in control roots (upper panel) and AM roots and each of the associated *R. irregularis* extraradical mycelia (middle panel). The same is shown for fungus-specific 16:1ω5 FAs in AM roots and extraradical mycelia (lower panel). Values from roots are indicated by 'R' and from fungal extraradical mycelia by 'M'. For *L. japonicus* wild-type the ^{13}C labelling pattern of 16:0 and 16:1ω5 FAs in the plant is recapitulated in the fungal extraradical mycelium. Extraradical hyphae associated with *str* do not mirror these patterns. Compare bars for AM roots and extraradical hyphae side by side. Black numbers indicate ^{13}C overall excess for individual samples. Colors indicate ^{13}C-isotopologues carrying one, two, three, etc. ^{13}C-atoms (M + 1, M + 2, M + 3, etc.). (n. d. = not detected). (**D**) Schematic and simplified illustration of carbon flow and ^{12}C vs.^{13}C contribution to plant lipid metabolism and transport to the fungus in the two-compartment cultivation setup used for isotope labelling. Carbohydrate metabolism and transport is omitted for simplicity. ERM, extraradical mycelium.

DOI: 10.7554/eLife.29107.040

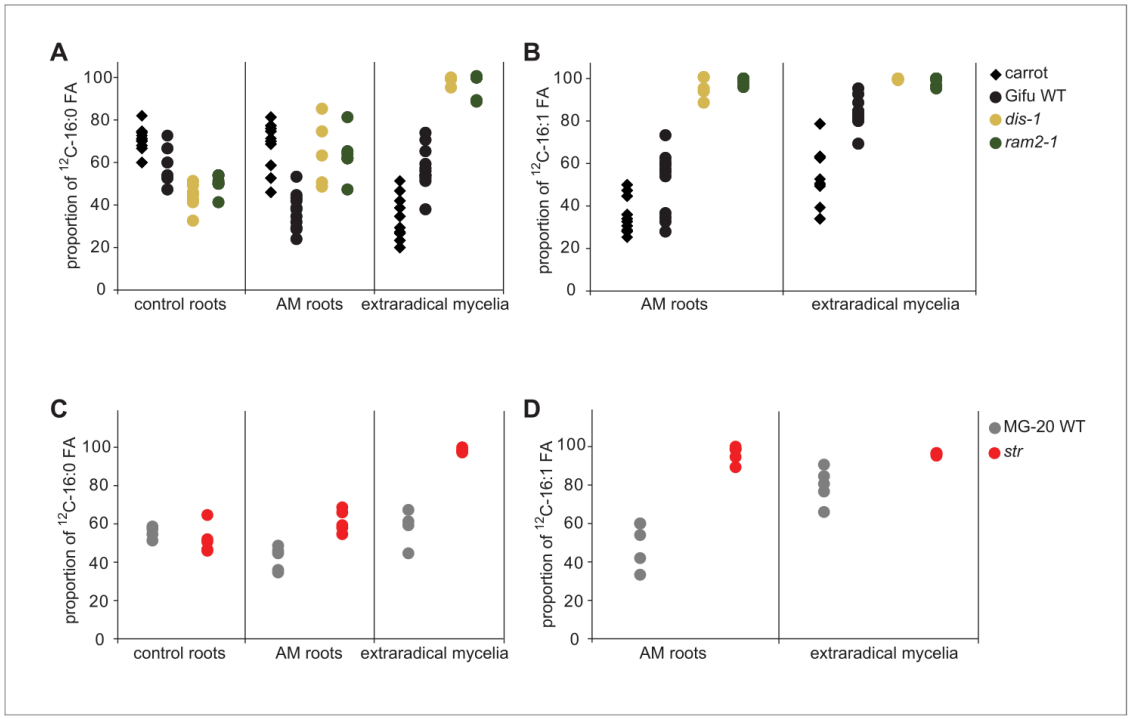

Figure 8—figure supplement 3. Proportion of 16:0 and 16:1ω5 FA containing only non-labelled ^{12}C in plant and fungal tissue. Proportion of ^{12}C 16:0 fatty acids (M + 0) in non-colonized and colonized carrot, *L. japonicus* Gifu wild-type, *dis-1*, *ram2-1* roots and in the extraradical mycelium of *R. irregularis* (**A**) as well as in *L. japonicus* MG-20 wild-type, *str* roots and in the extraradical mycelium of *R.irregularis* (**C**). Proportion of non-labeled ^{12}C AMF specific 16:1ω5 fatty acids (M + 0) in colonized carrot, *L. japonicus* Gifu wild-type, *dis-1*, *ram2-1* roots and in the extraradical mycelium of *R. irregularis* (**B**) as well as in *L. japonicus* MG-20 wild-type, *str* and in the extraradical mycelium of *R. irregularis* (**D**).

DOI: 10.7554/eLife.29107.041

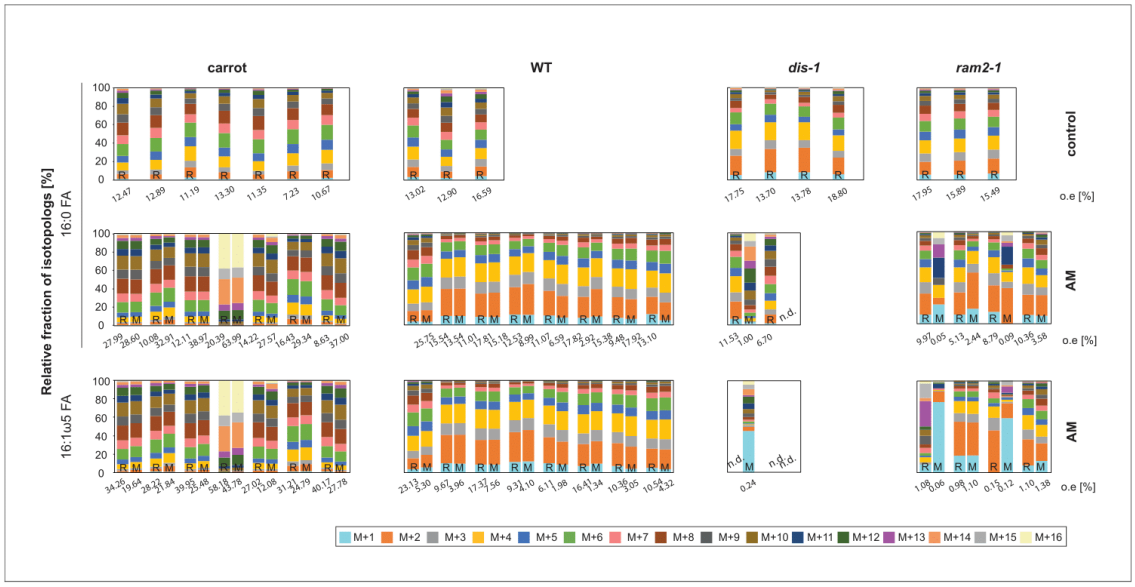

Figure 8—figure supplement 4. Isotopolog profiles of additional samples. Relative fraction of ^{13}C isotopologs for 16:0 fatty acids (individual bars and double bars) of *D. carota*, *L. japonicus* WT Gifu, *dis-1*, *ram2-1* in control roots (upper panel) and AM roots and each of the associated *R. irregularis* extraradical mycelia (middle panel) and 16:1ω5 FAs in AM roots and extraradical mycelia (lower panel). Values from roots are indicated by 'R' and from fungal extraradical mycelia by 'M'. Compare bars for AM roots and extraradical hyphae side by side. Isotopolog profiles shown here and in ***Figure 8C*** were generated from 3 independent experiments for *L. japonicus* wild-type and, 2 independent experiments for *L. japonicus* mutants and carrot roots. Transfer of ^{13}C-label from plant to fungus is higher for carrot than for *L. japonicus* wild-type. This is possibly caused by the fungus being exclusively dependent on carrot when carrot is labelled, while lipid transfer from *L. japonicus* competes with un-labeled transfer from carrot from the other side of the petri dish. Whatever the isotopolog pattern of wild-type roots, it is mirrored in the extrarical fungal mycelium, indicating lipid transfer. However, the isotopolog pattern is for most cases not mirrored in extraradical mycelium associated with lipid biosynthesis mutants. (n.d. = not detected).

DOI: 10.7554/eLife.29107.042

Table S1. Mutations in *DIS* and *DIS-LIKE* identified by TILLING or in a LORE1 insertion collection.

Allele	Line ID	aa change / insertion	Source
dis-1	SL0154-N	G190R	(Groth et al., 2013)
dis-2	30035849	LORE1 intron 2 insertion	(Małolepszy et al., 2016)
dis-3	SL4113-1	T221I	RevGen, UK
dis-4	SL0614-1	G314D	RevGen, UK
dis-5	SL5510-1	E338K	RevGen, UK
dis-6	SL0494-1	P376L	RevGen, UK
disl-1	SL3509-1	P61S	RevGen, UK
disl-2	30034395	LORE1 exon 2 insertion	(Małolepszy et al., 2016)
disl-3	SL1481-1	D109N	RevGen, UK
disl-4	SL5555-1	G176E	RevGen, UK
disl-5	SL1474-1	G180E	RevGen, UK
disl-6	SL4156-1	V193M	RevGen, UK

Groth M, Kosuta S, Gutjahr C, Haage K, Hardel SL, Schaub M, Brachmann A, Sato S, Tabata S, Findlay K, et al. 2013. Two *Lotus japonicus* symbiosis mutants impaired at distinct steps of arbuscule development. *Plant J,* **75**: 117-129. 10.1111/tpj.12220.

Małolepszy A, Mun T, Sandal N, Gupta V, Dubin M, Urbański D, Shah N, Bachmann A, Fukai E, Hirakawa H, et al. 2016. The LORE1 insertion mutant resource. *Plant J*: DOI: 10.1111/tpj.13243. 10.1111/tpj.13243.

Table S2. Primers used in this study.

Purpose	Name	Sequence
g*DIS* cloning for p*DIS:gDIS*	SH71 SH72	CACCGGAACGGGACAAAAGACTCC TTAGGGCCTGAATGGAGCAAAGACAA
p*DIS* cloning for p*DIS:GUS*	SH94 SH104	ATTTAAGCTTGGAACGGGACAAAAGACTCC AATCAGGATCCTGTTCAATGTGTCTGTGGCA
DIS cloning for *DIS-RFP* localization in *N. benthamiana*	SH93 SH92	CACCATGGCAAGCATTGCTGGTTC GGGCCTGAATGGAGCAAAGACAAC
p*LjPT4* cloning for p*PT4:DIS*	CG466 CG467	TTTGGTCTCTGCGGGGACTCAAGAAACCATGCTATC TTTGGTCTCTCAGACTTGAACGATGTCGATTTAGTTTG
DIS/dis-1 frag.1 cloning for p*PT4:DIS/dis-1*	SH124 SH125	ATGAAGACTTTACGGGTCTCACACCATGGCAAGCATTGC TGGTTC TTGAAGACTTTTCGATTTCAGGGCTCTCTTTGTTACCTGA TGACAACAAGCACCCTTTTGG
DIS/dis-1 frag.1 cloning for p*PT4:DIS/dis-1*	SH126 SH127	TTGAAGACTTCGAAACCCTGATGATTATT ATGAAGACTTCAGAGGTCTCACCTTGGGCCTGAATGGA GCAA
p*DIS* cloning for p*DIS:AtKASI*	SH122 SH123	ATGAAGACTTTACGGGTCTCAGCGGGGAACGGGACAAA AGACTCC ATGAAGACTTCAGAGGTCTCAGGTGTGTTCAATGTGTCT GTGG
p*AtKASI* cloning for p*AtKASI:LjDIS*	SH113 SH109	TTGGTCTCACACCGAGTCACAAAGATGCTATCG GGTCTCACCATGGTGGATCCAGAAATTGAGAG
3'UTR AtKASI cloning for p*AtKASI:LjDIS*	SH118 SH119	TGAGGTCTCGTTTCTTCATACCTTTTAGATTC TGAGGTCTCGCCTTCAGTATAAATCTAATTTCTTC
g*DIS* frag.1 cloning for p*AtKASI:LjDIS*	SH110 SH114	TGAGGTCTCTATGGCAAGCATTGCTGGTTCATG TGAGGTCTCTTTCGATTTCAGGGCTCTCT
g*DIS* frag.2 cloning for p*AtKASI:LjDIS*	SH115 SH117	TTGGTCTCACGAAACCCTGATGATTATTAG TGAGGTCTCGGAAATTAGGGCCTGAATGGAGC
AtKASI frag.1 cloning for p*DIS:AtKASI*	CG455 CG456	ATGAAGACTTTACGGGTCTCACACCATGCAAGCTCTTCA ATCTTCATCTCT ATGAAGACTTGTCGCAAAGGTCGCGCATTG
AtKASI frag.2 cloning for p*DIS:AtKASI*	CG457 CG458	ATGAAGACTTCGACGACAACAACGTTCCTTCA ATGAAGACTTGAGTCCCATACCAGTAATGACAAC
AtKASI frag.3 cloning for p*DIS:AtKASI*	CG459 CG460	ATGAAGACTTACTCGTCTCTGTGTTTGGTAACG ATGAAGACTTTGGCTCTCTCCAAAACAAAATGTCA

AtKASI frag.4 cloning for p*DIS:AtKASI*	CG461 CG462	ATGAAGACTTGCCACTAATTGTTGTATGCCCTAATAG ATGAAGACTTCAGAGGTCTCACCTTTCAGGGTTTGAAGG CAGAGAAGGC
qPCR of *LjEF1alpha*	EF1alpha_F EF1alpha_R	GCAGGTCTTTGTGTCAAGTCTT CGATCCAGAACCCAGTTCT
qPCR of *LjKASI*	LjKASI_qPCR_F LjKASI_qPCR_R	TCCCAACGCTAACTTCAAGC CCCTGCATCATTGAGGCTAT
qPCR of *LjKASII*	AK42 AK43	CGAGAAAGACTTGATCTCCCCAG CGTGGTTACATCACTTGGTCATG
qPCR of *LjKASIII*	AK44 AK45	GATTTGCATAGTAATGGTGATGG GCATGAATATGAGGACTGCTTGG
qPCR of *LjDIS*	qPCR_DIS4_F qPCR_DIS4_R	CATTCATTGATTTCGGGACA CCAAACACAGAAGCAGATCAGA
qPCR of *LjDIS-like*	qPCR_DISL4_F qPCR_DISL4_R	CATGTTATCGATTTGTGTTTGGA TGACTACTACCCATTTGCTGAAAG
qPCR of *LjUbiquitin*	qPCR_F_LjUbi qPCR_R_LjUbi	ATGCAGATCTTCGTCAAGACCTT ACCTCCCCTCAGACGAAG
qPCR of *LjRAM2*	PP101 PP102	ATCCTATGAGTGCACTAGCTTTACTAGAAG AACGAGCAAATTAAAACTGAAAGAGAGTAC
qPCR for *LjSbtM1*		CACGTTGTTAGGACCCCAAT TTGAGCAGCACCCTCTCTATC
qPCR for *LjBCP1*		TCATCTGTCCTTGGGGTCAT CAGCTGCAGAAGTTGCATTT
qPCR for *LjPT4*		GAATAAAGGGGCCAAAATCG GCTGTATCCTATCCCCATGC
qPCR for *LjAMT2.2*		TGGTTCAACTTTTCGTTCCA CTTATCACCCTGACCCCAGA
qPCR for *LjSTR*		CTATATTGGTGACGAGGGAAGG GTCCTGAGGTAGGTTCATCCAG
p*RAM2_1a* cloning for p*RAM2:*g*RAM2* and p*RAM2:GUS*	PP103 PP104	ATGAAGACTTTACGGGTCTCAGCGGGATTGAAAGCTTCC CCATAG TAGAAGACAAATCTTCTCCTAGTATTTTTTTTTTAAAG

p*RAM2_1b* cloning for p*RAM2:*g*RAM2* and p*RAM2:GUS*	PP105 PP106	ATGAAGACTTAGATCATTCCACGGAGGAG ATGAAGACTTCAGAGGTCTCACAGAGGTGAATGCACTTG TTGTTACTC
g*RAM2* cloning for p*PT4:*g*RAM2/ram2-1*	AK20 AK21	ATGAAGACTTTACGGGTCTCACACCATGGTGTCATCAAC G ATGAAGACTTCAGAGGTCTCACCTTGCAACCCATGACTT TGTTTG
p*RAM2* primer walking using TAC Lj T46c08	PP132	GTCGTTTTAGAAGAATTTTTTG
p*RAM2* primer walking using TAC Lj T46c08	PP133	AGGATAGGCTCAATACTTTGA
p*RAM2* primer walking using TAC Lj T46c08	PP134	ATGGGTGAAAGTGGTAAGATGG
p*RAM2* primer walking using TAC Lj T46c08	PP135	GCGTGACAAACATGGAAGG
p*RAM2* primer walking using TAC Lj T46c08	PP136	AGCAAAGTTGGGGGAGAAAT
p*RAM2* primer walking using TAC Lj T46c08	PP137	AGGTGGGTATTGGAGGTGGA
p*RAM2* primer walking using TAC Lj T46c08	PP138	ACACTTAAAAAAGAACGGAG
p*RAM2* primer walking using TAC Lj T46c08	PP139	CTCTAACAATCCACTATCTTG
p*RAM2* primer walking using TAC Lj T46c08	PP140	CACACAAGAACTTCATGCAC
p*RAM2* primer walking using TAC Lj T46c08	PP141	GAGCTTGATCACCTACTAATTAT
p*RAM2* primer walking using TAC Lj T46c08	PP142	CTTGTATGCCAGCAGCCTCAGAG
p*SbtM1 frag.1* cloning for pSbtM1:SPP-mCherry	JAVA-23 JAVA-24	ATGAAGACTTTACGGGTCTCAGCGGAACATTGAGGACA GATTAAGG TAGAAGACAATTGCCTTCATTTGTGCCAAA

p*SbtM1 frag.2* cloning for pSbtM1:SPP-mCherry	JAVA-25 JAVA-26	TAGAAGACAAGCAAATAAACCGTCCAAGGC ATGAAGACTTCAGAGGTCTCTCAGAGCTCCATCTTTAAT TGGAATTTGATG
SbtM1 secretion signal peptide cloning for pSbtM1:SPP-mCherry	SC278 SC279	TATGGTCTCATCTGATGGAGCAAACCAAGTATAGGA TATGGTCTCAGGTGTCATGCTCTTGGCCTTCCT

Table S3: Plasmids used in this study

Produced by classical cloning, Gateway cloning (Entry plasmids and Destination plasmids) and Golden Gate cloning (Level I, II and III). The Golden Gate toolbox is described in (48). EV, empty vector; HR, hairy root; trafo, transformation

Purpose	**Name**	**Description**
dis-1 transgenic complementation (Fig. 1A)	Entry: pENTR-p*DIS*:g*DIS*	PCR amplification of *DIS* promoter and gene with primers SH71 + SH72 and subcloning into pENTR/D-TOPO.
	HR Trafo: p*DIS*:g*DIS*	LR clonase (Invitrogen) recombination of ENTR-p*DIS*:g*DIS* with pK7RWG2.0 w/o 35S promoter *(56)*.
	HR Trafo: EV	Removal of Gateway casette from pK7RWG2.0 w/o 35S promoter (Antolín-Llovera et al., 2014) by EcoRV digest and religation.
Localization of *DIS* promoter activity (Fig. 2_S1)	p*DIS-GUS*	PCR amplification of 1.5 kb *DIS* promoter region with primers SH94 + SH104 and insertion into the HindIII and BamHI restriction sites of pBI101(Jefferson et al., 1987).
Cross species complementation *of Arabidopsis kasI* mutant with *LjDIS* (Fig. 4C)	Entry: pENTR-*pAtKASI:DIS:3' UTR AtKASI* (pCG92)	Assembled from L0 p*AtKASI*, L0 *DIS*, L0 *3' UTR KASI* and pENTR-BsaI (BB04) by BsaI cut ligation
	Entry: pENTR-p*AtKASI*:*DIS*:3' UTR *AtKASI* (pCG93)	Assembled from L0 p*AtKASI*, L0 *dis-1*, L0 *3' UTR KASI* and pENTR-BsaI (BB04) by BsaI cut ligation
	Arabidopsis Trafo: p*KASI*:*DIS* (pCG94)	LR clonase (Invitrogen) recombination of pCG92 with pMDC99 *(Curtis & Grossniklaus, 2003)*.
	Arabidopsis Trafo: p*KASI*:*dis-1* (pCG95)	LR clonase (Invitrogen) recombination of pCG93 with pMDC99 (Curtis & Grossniklaus, 2003).
Localization of DIS in *N. benthamiana* leaves (Fig. 4F)	Entry: pENTR-*DIS* w/o stop	PCR amplification of *DIS* gene with primers SH93 + SH92 and subcloning into pENTR/D-TOPO.
	N. benthamiana Trafo: p*35S:DIS:RFP*	LR clonase (Invitrogen) recombination of ENTR-pENTR-*DIS* w/o stop with pK7RWG2.0 (Karimi et al., 2002).
	N. benthamiana Trafo: p*35S:AtLhcb1.3:YFP*	LR clonase (Invitrogen) recombination of pENTR/D-TOPO-*AtLhcb1.3* w/o stop (kind gift from Jürgen Soll) with pB7FWG2.0 (Karimi et al., 2002).
Golden Gate level 0 and I (L0, LI) elements		

	L0 p*AtKASI*	PCR amplification of *AtKASI* 1.3 kb promoter fragment with SH113 + SH109 and assembly by StuI cut ligation into L0 pUC57 plasmid (BB01).
	L0 *DIS* and L0 *dis-1*	Assembled by StuI cut ligation into L0 pUC57 plasmid (BB01) from 2 PCR fragments amplified from genomic DNA of *L. japonicus* Gifu wild type (*DIS*) and *dis-1* mutant (*dis-1*). Primers: Fragment 1: SH110 + SH 114 Fragment 2: SH115 + SH117
	L0 3' UTR *AtKASI*	3' UTR of *AtKASI* (343 bp) was PCR amplified with primers SH118 + SH119 and assembled by StuI cut ligation into L0 pUC57 plasmid (BB01).
	L0 p*RAM2A*	PCR amplification of 906 bp fragment *L. japonicus* Gifu genomic DNA with primers PP103+PP104. Assembly by SmaI cut ligation into LI-Amp (BB01)
	L0 p*RAM2B*	PCR amplification of 1434 bp fragment *L. japonicus* Gifu genomic DNA with primers PP105+PP106. Assembly by SmaI cut ligation into LI-Amp (BB01)
	LI A-C p*DIS* (pCG124)	PCR amplification of 1.5 kb *DIS* promoter from *L. japonicus* Gifu genomic DNA with primers SH122 + SH123 and BpiI cut ligation into LI-BpiI (BB03) plasmid.
	LI C-D *AtKASI* (pCG125)	Assembled 4 PCR fragments amplified from *A. thaliana* Col-0 gDNA by BpiI cut ligation into LI-BpiI plasmid (BB03). Primers: Fragment 1: CG455 + CG456 Fragment 2: CG457 + CG458 Fragment 3: CG459 + CG460 Fragment 4: CG461 + CG462
	LI A-B p*PT4*	PCR amplification of 2.2 kb *PT4* promoter region from *L. japonicus* Gifu genomic DNA with primers CG466 + CG467 and assembly by BpiI cut ligation into LI-BpiI plasmid (BB03).
	LI C-D *DIS* LI C-D *dis-1*	Assembled from two PCR amplified fragments from genomic DNA of *L. japonicus* Gifu wild type (*DIS*) and *dis-1* mutant (*dis-1*). Assembly by BpiI cut ligation into LI-BpiI plasmid (BB03). Primers: Fragment 1: SH124 + SH138 Fragment 2: SH126 + SH127
	LI A-B *pRAM2*	Assembled by BpiI cut ligation from: L0 p*RAM2A* + L0 p*RAM2B* + LI-BpiI (BB03)
	LI C-D *RAM2* LI C-D *ram2-1*	PCR amplification of 1998 bp fragment *L. japonicus* Gifu genomic DNA with primers AK20 + AK21. Assembled by SmaI blunt end cut ligation: pUC57 (BB02) + Fragment: AK20 + AK21
	LI C-D *GUS*	(Pimprikar et al., 2016)

	LI A-B p*SbtM1*	*PCR amplification of 559 bp fragment with primers JAVA-23 + JAVA-24 and of 211 bp fragment with primers JAVA-25 + JAVA-26 from pENTR D-TOPO pSbtM1. Assembled by BpiI cut ligation from 559 bp fragment + 211 bp fragment + LI-BpiI (BB03)*
	LI B-C SSP (SbtM1 secretion signal peptide)	*PCR amplification of 135 bp fragment L. japonicus Gifu genomic DNA with primers SC278 + SC279. Assembly by SmaI cut ligation into LI-pUC57 (BB02)*
Golden Gate level II (LII) plasmids		
	LII R 3-4 p*35S:mCherry* (selection marker for HR)	Assembled by BsaI cut ligation from: LI A-C p*35S* (G009) + LI C-D mCherry (G057) + LI dy D-E (B008) + LI E-F 35S-T (G059) + LI dy F-G (BB09) + LII R 3-4
	LII F 1-2 p*DIS*:*AtKASI* (pCG126)	Assembled by BsaI cut ligation from: LI A-C p*DIS* + LI C-D *AtKASI* + LI dy D-E (BB08) + LI E-F nos-T(G006) + LI dy F-G (BB09) + LIIc F 1-2 (BB30)
	LII F 1-2 p*DIS*:*EV* (pCG127)	Assembled by BsaI cut ligation from: LI A-C p*DIS* + LI dy C-D (BB07) + LI dy D-E (BB08) + LI E-F nos-T(G006) + LI dy F-G (BB09) + LIIc F 1-2 (BB30)
	LII F 1-2 p*PT4*:*DIS* (pCG130)	Assembled by BsaI cut ligation from: LI A-B p*PT4* + LI dy B-C (BB06) + LI C-D *DIS* + LI E-F nos-T(G006) + LI dy F-G (BB09) + LIIc F 1-2 (BB30)
	LII F 1-2 p*PT4*:*dis-1* (pCG131)	Assembled by BsaI cut ligation from: LI A-B p*PT4* + LI dy B-C (BB06) + LI C-D *dis-1*+ LI E-F nos-T(G006) + LI dy F-G (BB09) + LIIc F 1-2 (BB30)
	LIIc F 1-2 p*RAM2:gRAM2* pPP106	Assembled by BsaI cut ligation from: LI A-B p*RAM2* + LI B-C dy (BB06) + LI C-D *RAM2* + LI D-E dy (BB08) + LI E-F nos-T (G006) + LI F-G dy (BB09) + LIIc F 1-2 (BB30)
	LII F 3-4 *pPT4:gRAM2* (pAK12)	Assembled by BsaI cut ligation from: LI A-B p*PT4* + LI dy B-C (BB06) + LI C-D *RAM2* + LI E-F nos-T(G006) + LI dy F-G (BB09) + LIIc F 3-4 (BB34)
	LII F 3-4 *pPT4:gram2-1* (pAK13)	Assembled by BsaI cut ligation from: LI A-B p*PT4* + LI dy B-C (BB06) + LI C-D *ram2* + LI E-F nos-T(G006) + LI dy F-G (BB09) + LIIc F 3-4 (BB34)
	LIIc F 1-2 p*RAM2:GUS* pPP107	Assembled by BsaI cut ligation from: LI A-B p*RAM2* + LI B-C dy (BB06) + LI C-D GUS + LI D-E dy (BB08) + LI E-F nos-T (G006) + LI F-G dy (BB09) + LIIc F 1-2 (BB30)

	LIIc R 3-4 p*Ubi:mCherry* (pPP101)	*(Pimprikar et al., 2016)*
	LIIβ F 5-6 p*POI:NLS-2XYFP:NosT* (pGC134)	Assembled by BsaI cut ligation from: LI A-B Esp3I-*lacZ* dy (G082) + LI B-C NLS (G60) + LI C-D YFP (G54) + LI D-E YFP (G12) + LI E-F Nos-T (G006) + LI F-G dy (BB09) + LIIβ F 5-6 (BB28)
	LIIc F 1-2 p*SbtM1:SPP-mCherry: HspT* (pPP137)	Assembled by BsaI cut ligation from: LI A-B p*SbtM1* + LI B-C SPP + LI C-D *mCherry* + LI D-E dy (BB08) + LI E-F Hsp-T (G045) + LI F-G dy (BB09) + LIIc F 1-2 (BB30)
Golden Gate level III (LIII) plasmids for plant transformation		
ram2-1 transgenic complementation (Fig. 1A)	LIIIβ F A-B p*RAM2:RAM2* (pPP162)	Assembled by BpiI cut ligation from: LIIc F 1-2 p*RAM2:RAM2* + LII 2-3 ins (BB43) + LIIc R 3-4 p*Ubi:mCherry* + LII 4-6 dy (BB41) + LIIIβ F A-B (BB53)
Localization of *DIS* promoter activity (Fig 2_S1)	LIIIβ F A-B p*DIS:GUS* (pMP2)	Assembeled by Esp3I Cut-Ligation. PCR product of p*DIS* + pPP170 [LIIc F 1-2 p*RAM1:GUS* + LII 2-3 ins (BB43) + LIIc R 3-4 p*Ubi:mCherry* + LII 4-6 dy (BB41) + LIIIβ F A-B (BB53)] (Pimprikar et al., 2016).
Localization of *RAM2* promoter activity (Fig 2_S1)	LIIIβ F A-B pRAM2*:GUS* (pPP163)	Assembled by BpiI cut ligation from: LIIc F 1-2 p*RAM2:GUS* + LII 2-3 ins (BB43) + LIIc R 3-4 p*Ubi:mCherry* + LII 4-6 dy (BB41) + LIIIβ F A-B (BB53)
Cross species complementation *of dis-1* mutant with *Arabidopsis KASI* (Fig. 2C)	LIIIβ F A-B p*DIS:AtKASI* (pCG128) LIIIβ F A-B p*DIS:EV* (pCG129)	Assembled by BpiI cut ligation from: LII F 1-2 p*DIS:AtKASI* + LII ins 2-3 (BB43) + LII R 3-4 p35S:mCherry + L II dy 4-6 (BB41) + LIIIβ F A-B Assembled by BpiI cut ligation from: LII F 1-2 p*DIS:EV* + LII ins 2-3 (BB43) + LII R 3-4 p35S:mCherry + L II dy 4-6 (BB41) + LIIIβ F A-B
dis-1 transgenic complementation with p*PT4:DIS* (Fig. 2C)	LIIIβ F A-B p*PT4:DIS* (pCG132) LIIIβ F A-B p*PT4:dis-1* (pCG133)	Assembled by BpiI cut ligation from: LII F 1-2 p*PT4:DIS* + LII ins 2-3 (BB43) + LII R 3-4 p35S:mCherry + L II dy 4-6 (BB41) + LIIIβ F A-B Assembled by BpiI cut ligation from: LII F 1-2 p*PT4:dis-1* + LII ins 2-3 (BB43) + LII R 3-4 p35S:mCherry + L II dy 4-6 (BB41) + LIIIβ F A-B
ram2-1 transgenic complementation with p*PT4*:RAM2 (Fig. 2C)	LIIIβ F A-B p*PT4:RAM2* (pAK14) LIIIβ F A-B p*PT4:ram2-1* (pAK15)	Assembled by BpiI cut ligation from: LII F 1-2 p*Ubi:mCherry* + LII ins 2-3 (BB43) + LII F 3-4 p*PT4:gRAM2* + L II dy 4-6 (BB41) + LIIIβ F A-B Assembled by BpiI cut ligation from: LII F 1-2 *pUbi:mCherry* + LII ins 2-3 (BB43) + LII F 3-4 p*PT4:ram2-1* + L II dy 4-6 (BB41) + LIIIβ F A-B
Esp3I compatible destination backbone for Localization of promoter activity	Esp3I cut ligation compatible backbone: LIIIβ F A-B p*SbtM1:SP-mCherry_pPOI:NLS-2XYFP* (pPP217)	Assembled by BpiI cut ligation from: LIIc F 1-2 *pSbtM1:SP-mCherry*: HspT + LII 2-3 ins (BB43) + LII 3-4 dy (BB64) + LII 4-5 ins (BB44) + LIIβ F 5-6 *pPOI:NLS-2XYFP:NosT* + LIIIβ F A-B (BB53)

BsaI compatible destination backbone for Localization of promoter activity	BsaI cut ligation compatible backbone: LIIIβ F A-B p*SbtM1:SP-mCherry*_p*POI:NLS-2XYFP* (pPP218)	Assembled by Esp3I cut ligation from: LIIIβ F A-B *pSbtM1:SP-mCherry_pPOI:NLS-2XYFP* + LI A-B Esp3I-ccdB dy (G084)
Localization of promoter activity of *pDIS* (Fig 2A)	LIIIβ F A-B p*SbtM1:SSP:mCherry+pDIS:NLS-2xYFP* (pPP241)	Assembled by BsaI cut ligation from: LI A-B pDIS + LIIIβ F A-B p*SbtM1:SP-mCherry*_p*POI:NLS-2XYFP* (pPP218)
Localization of promoter activity of *pRAM2* (Fig 2B)	LIIIβ F A-B p*SbtM1:SSP:mCherry+pRAM2:NLS-2xYFP* (pPP238)	Assembled by BsaI cut ligation from: LI A-B pRAM2 + LIIIβ F A-B p*SbtM1:SP-mCherry*_p*POI:NLS-2XYFP* (pPP218)

References

Antolín-Llovera M, Ried Martina K, Parniske M. 2014. Cleavage of the SYMBIOSIS RECEPTOR-LIKE KINASE ectodomain promotes complex formation with Nod Factor Receptor 5. *Current Biology* **24**(4): 422-427. 10.1016/j.cub.2013.12.053.

Curtis MD, Grossniklaus U. 2003. A gateway cloning vector set for high-throughput functional analysis of genes *in planta*. *Plant Physiology* **133**(2): 462-469. 10.1104/pp.103.027979.

Jefferson RA, Kavanagh TA, Bevan MW. 1987. GUS fusions: beta-glucuronidase as a sensitive and versatile gene fusion marker in higher plants. *EMBO J* **6**: 3901-3907.

Karimi M, Inzé D, Depicker A. 2002. GATEWAY™ vectors for *Agrobacterium*-mediated plant transformation. *Trends in Plant Science* **7**(5): 193-195. 10.1016/S1360-1385(02)02251-3.

Pimprikar P, Carbonnel S, Paries M, Katzer K, Klingl V, Bohmer M, Karl L, Floss D, Harrison M, Parniske M, et al. 2016. A CCaMK-CYCLOPS-DELLA complex regulates transcription of RAM1, a central regulator of arbuscule branching. *Current Biology* **26**: 987-998. 10.1016/j.cub.2016.01.069.

Paper II: The *Lotus japonicus* acyl-acyl carrier protein thioesterase FatM is required for mycorrhiza formation and lipid accumulation of *Rhizophagus irregularis*

Reference: Brands M, Wewer V, **Keymer A**, Gutjahr C, Dörmann P (2018). The *Lotus japonicus* acyl-acyl carrier protein thioesterase FatM is required for mycorrhiza formation and lipid accumulation of *Rhizophagus irrgeularis.* **Plant Journal,** DOI: 10.1111/tüj.13943.

the plant journal

SEB Society for Experimental Biology

The Plant Journal (2018) **95,** 219–232 doi: 10.1111/tpj.13943

The *Lotus japonicus* acyl-acyl carrier protein thioesterase FatM is required for mycorrhiza formation and lipid accumulation of *Rhizophagus irregularis*

Mathias Brands[1], Vera Wewer[1,2], Andreas Keymer[3], Caroline Gutjahr[3,4] and Peter Dörmann[1,*]

[1]*Institute for Molecular Biotechnology and Physiology of Plants (IMBIO), University of Bonn, Karlrobert-Kreiten-Straße 13, 53115, Bonn, Germany,*

[2]*Center of Excellence in Plant Sciences (CEPLAS), Mass Spectrometry Platform, University of Cologne, Zülpicher Straße 47b, 50674, Cologne, Germany,*

[3]*Faculty of Biology, Genetics, Biocenter, Martinsried, LMU Munich, Großhaderner Straße 2-4, 82152, Martinsried, Germany, and*

[4]*Plant Genetics, School of Life Sciences Weihenstephan, Technical University of Munich, Emil Ramann Straße 4, 85354, Freising, Germany*

Received 23 January 2017; revised 26 March 2018; accepted 5 April 2018; published online 23 April 2018.
*For correspondence (e-mail doermann@uni-bonn.de).

SUMMARY

Arbuscular mycorrhiza (AM) fungi establish symbiotic interactions with plants, providing the host plant with minerals, i.e. phosphate, in exchange for organic carbon. Arbuscular mycorrhiza fungi of the order Glomerales produce vesicles which store lipids as an energy and carbon source. Acyl-acyl carrier protein (ACP) thioesterases (Fat) are essential components of the plant plastid-localized fatty acid synthase and determine the chain length of *de novo* synthesized fatty acids. In addition to the ubiquitous FatA and FatB thioesterases, AM-competent plants contain an additional, AM-specific, *FatM* gene. Here, we characterize FatM from *Lotus japonicus* by phenotypically analyzing *fatm* mutant lines and by studying the biochemical function of the recombinant FatM protein. Reduced shoot phosphate content in *fatm* indicates compromised symbiotic phosphate uptake due to reduced arbuscule branching, and the fungus shows reduced lipid accumulation accompanied by the occurrence of smaller and less frequent vesicles. Lipid profiling reveals a decrease in mycorrhiza-specific phospholipid forms, AM fungal signature fatty acids (e.g. 16:1ω5, 18:1ω7 and 20:3) and storage lipids. Recombinant FatM shows preference for palmitoyl (16:0)-ACP, indicating that large amounts of 16:0 fatty acid are exported from the plastids of arbuscule-containing cells. Stable isotope labeling with [$^{13}C_2$]acetate showed reduced incorporation into mycorrhiza-specific fatty acids in the *fatm* mutant. Therefore, colonized cells reprogram plastidial *de novo* fatty acid synthesis towards the production of extra amounts of 16:0, which is in agreement with previous results that fatty acid-containing lipids are transported from the plant to the fungus.

Keywords: acyl-ACP thioesterase, arbuscular mycorrhiza, carbon transfer, lipid, plastid, symbiosis, fatty acid, stable isotope labeling.

INTRODUCTION

Arbuscular mycorrhiza (AM) symbiosis is an ancient association established by the majority of land plants with obligate biotrophic fungi of the Glomeromycota (Corradi and Bonfante, 2012). Arbuscular mycorrhiza symbiosis enhances the nutrient supply of plants because AM fungi have access to extrarhizospheric minerals due to exploration of the soil by their extraradical mycelium. In exchange, plants deliver photosynthetic assimilates to the fungus (Smith and Smith, 2011; Roth and Paszkowski, 2017). Upon contact with the host root, AM fungi form hyphopodia that allow penetration of the host's epidermal barrier. After entering the root, intraradical hyphae colonize the root cortex, where they form intracellular structures, tree-shaped arbuscules that enter cortex cells but remain surrounded by host membranes, the so-called periarbuscular membrane (PAM) (Gutjahr and Parniske, 2013). Arbuscular mycorrhiza fungi of the suborder Glominea additionally form vesicles at terminal ends of the intraradical hyphae that serve as propagules for hyphal outgrowth

(Smith and Read, 2008). In AM fungi, lipid droplets are transported throughout the mycelium (Bago *et al.*, 2002). These lipids account for more than 50% of the vesicle dry mass, and consist of glycolipids, sphingolipids, phospholipids, sterols and, in particular, triacylglycerol (TAG) as a storage lipid, with palmitvaccenic acid (16:1ω5; number of carbons:number of double bonds, position of double bond) representing the most abundant fatty acid (Jabaji-Hare *et al.*, 1984).

Labeling experiments with ^{14}C have shown that extraradical hyphae cannot synthesize fatty acids, and it was concluded that the fungus is either deficient in *de novo* fatty acid synthesis or only intraradical hyphae are capable of fatty acid synthesis (Trepanier *et al.*, 2005). Recent analysis of genomic and transcriptomic data revealed that AM fungi lack cytosolic type-I fatty acid synthase (FAS) (Tisserant *et al.*, 2013; Wewer *et al.*, 2014; Ropars *et al.*, 2016; Sedzielewska Toro and Brachmann, 2016; Tang *et al.*, 2016). Therefore, the obligate biotrophy of AM fungi might in part be a consequence of the lack of *de novo* fatty acid synthesis (Wewer *et al.*, 2014), and it was shown that, in addition to carbohydrates, fatty acids are supplied by the plant to the fungus (Jiang *et al.*, 2017; Keymer *et al.*, 2017; Luginbuehl *et al.*, 2017). In line with this scenario, genes encoding enzymes of lipid biosynthesis were identified by mutant screening and phylogenetic clustering approaches. These genes are specifically expressed during AM formation, are conserved in plants undergoing AM symbiosis and appear to be involved in the production of lipids, which are transported to the fungus (Gaude *et al.*, 2012; Wang *et al.*, 2012; Delaux *et al.*, 2014; Favre *et al.*, 2014; Bravo *et al.*, 2016; Keymer *et al.*, 2017).

The *RAM2* (reduced arbuscular mycorrhiza2) gene encodes an enzyme with high sequence similarity to Arabidopsis glycerol-3-phosphate acyltransferase 6 (GPAT6). The GPAT enzymes catalyze the transfer of an acyl chain from acyl-CoA to glycerol-3-phosphate, resulting in the production of lyso-phosphatidic acid (LPA). Some GPAT enzymes, including Arabidopsis GPAT6, harbor an additional phosphatase domain which produces monoacylglycerol (MAG) from LPA. GPAT6 reveals a preference for the sn-2 position of glycerol, thus producing sn-2 MAG as a precursor for surface polyester (suberin) synthesis (Beisson *et al.*, 2012). Similar to GPAT6, RAM2 from *Medicago truncatula* contains a phosphatase domain and it produces sn-2 MAGs with a preference for 16:0 sn-2 MAG (Wang *et al.*, 2012; Luginbuehl *et al.*, 2017). The corresponding *ram2* mutant of *Medicago* shows a severe arbuscule branching phenotype (Wang *et al.*, 2012). Recent studies on *Medicago* and *Lotus* mutants of *ram2* confirmed that RAM2 is involved in an AM-specific lipid biosynthetic pathway in the plant which is activated upon fungal infection and provides carbon to the fungus in the form of fatty acyl groups (Bravo *et al.*, 2017; Jiang *et al.*, 2017; Keymer *et al.*, 2017; Luginbuehl *et al.*, 2017).

Plants produce about 95% of their fatty acids via the plastidial, canonical type-II FAS enzymes (Ohlrogge and Browse, 1995). One of the key enzymes, β-ketoacyl-acyl carrier protein (ACP) synthase I (KASI) catalyzes the sequential dicarbon chain elongation reactions starting with acetyl-CoA. Arbuscular mycorrhiza competent plants, including *Lotus*, contain two additional *KASI* genes. One of them (*DIS*, disintegrated arbuscules) is induced during AM formation in arbuscocytes. Analysis of the *Lotus dis-1* mutant demonstrated that the *DIS* gene is critical for the production of extra fatty acids in the host and for the accumulation of fatty acid in the fungus (Keymer *et al.*, 2017). The acyl chain specificity of the AM-dependent DIS enzyme was not characterized, but it is probably specific for the production of 16:0-ACP similar to Arabidopsis KASI, because the *DIS* gene complements the developmental and lipid phenotype of the Arabidopsis *kasI* mutant (Keymer *et al.*, 2017).

Acyl-ACP thioesterases (Fat) terminate chain elongation reactions of *de novo* fatty acid synthesis by hydrolyzing the thioester bond of acyl-ACPs. Plant Fat enzymes exhibit preferences for different acyl-ACP substrates. While FatA is highly specific for oleoyl (18:1Δ9)-ACP, FatB thioesterases show substrate specificity mostly for saturated acyl-ACPs (Jones *et al.*, 1995; Moreno-Pérez *et al.*, 2012). The ubiquitous FatB thioesterases present in all plants (e.g. Arabidopsis FatB, *Cuphea hookeriana* FatB1) hydrolyze 16:0-ACP but are also active with 18:0-ACP and 18:1Δ9-ACP (Figure S1 in the online Supporting Information) (Dörmann *et al.*, 1995; Jones *et al.*, 1995). Plants producing medium chain fatty acids in their seeds harbor an additional FatB enzyme with specificity for, for example, 12:0 (FatB1, *Umellularia californica*) or 8:0 and 10:0 (FatB2, *C. hookeriana*) (Figure S1) (Voelker *et al.*, 1992; Dehesh *et al.*, 1996). Through their substrate specificities, Fat enzymes determine which fatty acids are released from the plastid and subsequently converted into acyl-CoAs which are transported to the endoplasmic reticulum (ER) (Li-Beisson *et al.*, 2013). In legumes, expression of a gene with sequence similarity to *FatB* is induced upon AM colonization (Gomez *et al.*, 2009; Wewer *et al.*, 2014). The *FatM* gene (for mycorrhiza specific) from *Medicago* is essential for normal arbuscule development (Bravo *et al.*, 2017). Here, we describe the functional characterization of the *L. japonicus* FatM thioesterase including its role during AM symbiosis, employing lipid measurements and stable isotope labeling experiments of colonized wild-type (WT) and *fatm* roots, as well as assays of the recombinant *Lotus* FatM enzyme.

RESULTS

The *FatM* gene is conserved in plants that form arbuscular mycorrhiza

Expression of the *Lotus* gene *chr5.CM0328.70.r2.d* ('*Lotus FatM*') is highly specific for AM formation (Wewer *et al.*, 2014). The deduced amino acid sequence is orthologous to *Medicago* FatM, and the two FatM sequences are similar to acyl-ACP thioesterases of class B (FatB) from Arabidopsis (Figure S1). Protein BLAST searches in the GenBank database with Arabidopsis FatA1 (At3 g25110), FatA2 (Ag4 g13050) and FatB (At1 g08510) sequences revealed the presence of the orthologous *Lotus* FatA (chr1.TM1516.23_at) and FatB (Ljwgs_022305.1_at) proteins. A fourth Fat sequence from *Lotus*, FatC (Ljwgs_013315.1_at), was retrieved using the orthologous sequence from *Medicago* (Bravo *et al.*, 2016). The FatA, FatB and FatM sequences harbor putative N-terminal chloroplast-targeting sequences (http://www.cbs.dtu.dk/services/ChloroP) (Emanuelsson *et al.*, 1999), suggesting that these thioesterases localize to the plastid. For *Lotus* FatC, only a 5′ truncated sequence is available which lacks the putative transit peptide. A phylogenetic tree was constructed with FatA and FatB sequences from non-AM-competent plants (*Brassica rapa*, *Arabidopsis thaliana*) and with FatA, FatB, FatC and FatM sequences from *L. japonicus*, *M. truncatula*, *Sorghum bicolor* and *Zea mays* (Figures S1). Plants contain at least one ubiquitous FatB protein similar to Arabidopsis FatB, which is specific for 16:0-ACP, 18:0-ACP and 18:1Δ9-ACP. Some plants like *C. hookeriana* or *U. californica* which accumulate medium chain fatty acids, harbor additional FatBs specific for medium chain acyl-ACPs. These latter FatB sequences were included in the phylogenetic tree to study the relation of *Lotus* FatM to the different FatB enzymes. FatA and FatB enzymes were found in all plants, including members of the Brassicaceae, which do not engage in AM symbiosis (Figure S1). Two extra clades of thioesterases, FatC and FatM, can be separated, and these clades are restricted to AM host plants. The FatM clade is more closely related to the FatC and FatB clades than to FatA. On the other hand, FatM sequences are not more similar to the 'ubiquitous' FatB proteins compared with the medium chain-specific FatB enzymes from *C. hookeriana* or *U. californica*.

FatM expression is reduced in *Lotus fatm* mutant lines

Two *Lotus* lines were identified in the *Lotus* LORE1 database (Malolepszy *et al.*, 2016) carrying retrotransposon insertions in the *FatM* locus at positions −218 and −236 upstream of the start codon for *fatm-1* and *fatm-2*, respectively (Figure 1a). The two insertions are presumably localized in the promoter or 5′ untranslated region of the *FatM* gene. The expression of fungal and plant genes in response to AM formation was investigated by RT-PCR at 4 and 7 weeks post-inoculation (wpi) (Figure 1b, c) in *Lotus* WT and the *fatm-1* and *fatm-2* mutants. *FatM* expression was reduced in *fatm-1* and *fatm-2*, to a lesser extent in *fatm-2* at 7 wpi. Therefore, the insertions in the *fatm*-1 and *fatm-2* plants affect *FatM* expression, but the colonized roots still contain low residual transcript levels. In contrast, expression of *FatA* and *FatB* was not affected in the colonized *fatm-1* or *fatm-2* roots. Expression of *FatC* was slightly induced in *fatm-1* or *fatm-2* at both time points. To assess colonization, we examined the *Rhizophagus* α-tubulin gene and the *Lotus* AM marker *PT4* (PHOSPHATE TRANSPORTER 4). Their expression was reduced in the two allelic mutants at 4 wpi and became more similar to the WT at 7 wpi, indicating a decreased colonization rate in *fatm-1* and *fatm-2* at early stages with some recovery at later stages (Figure 1b, c).

Arbuscular mycorrhiza symbiosis is compromised in *fatm* mutant roots

Microscopic examination of AM formation in the *fatm* lines confirmed that the mutants are less colonized than the WT (Figure 3a). However, at 7 wpi root colonization of *fatm-2* reached WT levels, in agreement with the observation that the *FatM* gene was more strongly expressed in colonized *fatm-2* roots compared with *fatm-1*. Therefore, *fatm-2* is a weaker allele. Both allelic mutants contained root areas with stunted arbuscules (Figure 2). As arbuscules are dynamic structures that undergo constant turnover stunted arbuscules were also present in the WT, although these occurred generally in the vicinity of vesicles, indicating a progression in the fungal growth stage. Besides, normal arbuscules were also sporadically formed in *fatm-1* and *fatm-2* roots (Figures 2 and 3b).

To confirm that the increase in stunted arbuscules and the reduced numbers of total hyphae, intraradical hyphae and vesicles in AM colonized *fatm* roots was caused by deficiency in *FatM* gene expression, *fatm-1* hairy roots were transformed with a plasmid containing the *FatM* gene driven by the endogenous promoter (p*FatM*:g*FatM*). Wild-type-like arbuscules developed in the complemented *fatm-1* line, indicating that the increased occurrence of stunted arbuscules in *fatm-1* originated from the deficiency in *FatM* expression. In addition, the transgenic complementation restored quantitative root colonization in *fatm-1* (Figure S2).

In the two allelic mutants, the frequency of vesicles was strongly reduced at 4 and 7 wpi (Figure 3a). In addition, the vesicle surface area was decreased by about one-third in the mutant lines at 4 wpi (Figure 3c). A detailed comparison of the distribution of vesicle surface areas in colonized *fatm-1* and *fatm-2* roots revealed an enrichment of very small vesicles (0–1000 μm^2 and 1000–2000 μm^2 surface area), while medium-sized vesicles (2000–3000 μm^2 and 3000–4000 μm^2) were reduced and large vesicles (4000–

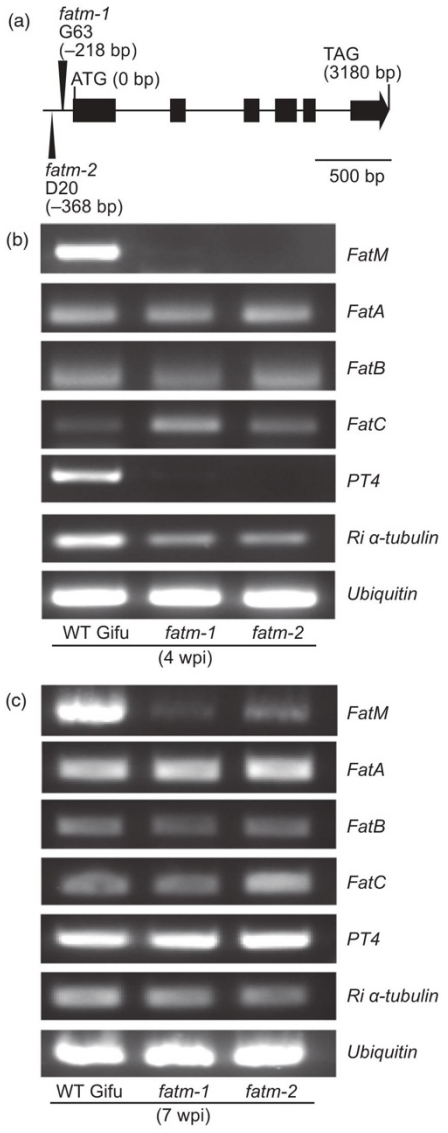

Figure 1. Isolation and expression analysis of *Lotus japonicus* LORE1 insertional mutants for *fatm*.
(a) Positions of the two LORE1 insertions in the *Lotus FatM* locus. Exons and introns are indicated by boxes and lines, respectively. TAG, triacylglycerol. ATG, start codon; TAG, stop codon.
(b), (c) Expression of *Lotus FatM, FatA, FatB, FatC, PT4* and *Rhizophagus* Ri α-tubulin and *Lotus* Ubiquitin (control) in roots by semiquantitative RT-PCR: (b) 4 weeks post-inoculation (wpi); (c) 7 wpi. Reverse transcriptase-PCR was performed using 50 ng of cDNA template with 30 cycles. The same results were obtained using 5 ng of cDNA template. WT, wild type.

5000 μm^2 and >5000 μm^2) were virtually absent (Figure 3d), indicating a reduced ability of the fungus to store lipids when colonizing the mutants. In agreement with decreased arbuscule branching and colonization, *fatm-1* and *fatm-2* did not profit from AM symbiosis at 4 wpi by increasing the inorganic phosphate content in their shoots, and they displayed shoot phosphate levels similar to mock-inoculated plants (Figure 3e). Therefore, the efficiency of AM-mediated phosphate uptake was compromised in *fatm-1* and *fatm-2* roots compared with Gifu WT.

Alterations in lipid composition in *fatm* roots after mycorrhiza colonization

Fatty acids and glycerolipids were measured in colonized and mock-infected roots to address the question of whether the *fatm* mutation causes changes in plant-derived or fungal storage lipids (TAG) or membrane glycerolipids. The distribution of fatty acids in WT, *fatm-1* and *fatm-2* mock-inoculated roots was very similar, in agreement with the exclusive expression of *FatM* in colonized roots (Gomez *et al.*, 2009; Wewer *et al.*, 2014) (Figure S3a). The content of 16:1ω5 increased in the WT with the degree of root colonization (Figure S3a, b). The fungus-specific fatty acids 16:1ω5, 18:1ω7 and 20:3, as well as the common fatty acid 16:0, were decreased in *fatm* mutant roots. As 16:0 and 16:1ω5 are mostly associated with TAG in fungal vesicles (Schliemann *et al.*, 2008; Wewer *et al.*, 2014), their reduction is in agreement with decreased vesicle abundance and size in *fatm* roots (Figure 3a), and this decrease is presumably a general marker for a reduced degree of colonization. Storage lipid (TAG) in the fungus is dominated by the molecular species 48:3 (tri16:1), 48:2 (di16:1-16:0) and 48:1 (16:1-di16:0) (Wewer *et al.*, 2014). In *fatm-1*, the fungal 16:1-containing TAG forms were decreased (Figure S4a), in agreement with the general decrease in 16:1ω5. Furthermore, the amounts of the DAG molecular species di16:1 and 16:1-16:0, precursors for 48:3, 48:2 and 48:1 TAG, were also reduced in colonized *fatm* roots (Figure S4b). Therefore, the *fatm* mutation strongly affects the production of 16:1ω5 for TAG deposition. The molecular species compositions of the membrane glycerolipids in colonized *fatm* and WT roots were very similar (Figures S4 and S5), except that the *Rhizophagus*-specific molecular species of phosphatidylcholine and phosphatidylethanolamine, which are found in colonized WT roots (Wewer *et al.*, 2014), did not accumulate in *fatm* roots (Figure S5).

Taken together, the *fatm* mutation causes a specific decrease in fungal molecular species of storage and membrane lipids, but does not directly affect the composition of plant-derived molecular species. These results indicate that FatM is not involved in the production of lipids, which remain in the plant.

Two MAG regio-isomers, α-MAG (sn-1/3 MAG) and β-MAG (sn-2 MAG), were measured in *Lotus* roots by

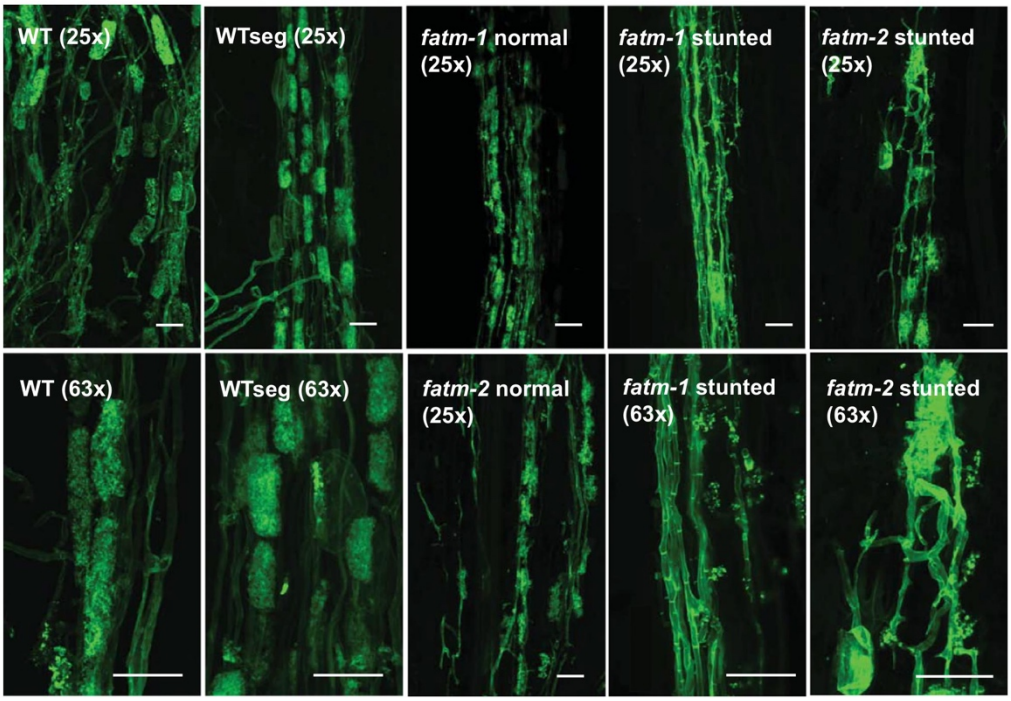

Figure 2. Stunted arbuscules in *fatm-1* and *fatm-2* mutant roots.
Roots of colonized wild type (WT) Gifu, segregating WT from *fatm-1* (WTseg), *fatm-1* and *fatm-2* plants at 4 weeks post-inoculation were stained with Alexa Fluor 488 WGA (wheat germ-agglutinin), and infected cells were observed by confocal laser scanning microscopy at 25 × or 63 × magnification. The *fatm-1* and *fatm-2* mutant roots contain stunted as well as fully developed arbuscules. Bars = 50 μm. [Colour figure can be viewed at wileyonlinelibrary.com].

GC-MS (Figure S6). While α-MAGs are side products of the conventional lipid biosynthesis pathway, β-MAGs are unusual forms of MAG produced by Arabidopsis GPAT6 or by the homologous RAM2 from legumes (Yang *et al.*, 2010; Wang *et al.*, 2012; Luginbuehl *et al.*, 2017). Forms of α-MAG carrying AM-specific fatty acids, 16:1ω5, 18:1ω7, 20:1Δ11, as well as 16:0 which accumulates in fungal TAG, were found in colonized WT roots (Stumpe *et al.*, 2005; Schliemann *et al.*, 2008), and they were decreased in *fatm-1* (Figure S6a). 16:0 β-MAG was the most abundant β-MAG in colonized WT roots, and this form was strongly increased during AM colonization (Figure S6b). In colonized *fatm-1* roots, 16:0 β-MAG was decreased. We also measured α-MAGs and β-MAGs in colonized *Daucus carota* roots growing in one compartment of a split Petri dish, and in extraradical mycelium (ERM; spores, hyphae) harvested from the other compartment. Considerable amounts of 16:0 α-MAG and β-MAGs were found in ERM, and the contents (normalized to mg fresh weight (FW)) were higher than in colonized roots. In addition, α-MAG and β-MAGs carrying 14:0, 18:0 and the AM-specific fatty acid 16:1ω5 were present in ERM. Therefore, the fungus also contained 16:0 β-MAG, as well as other β-MAG forms including fungal-specific 16:1ω5 β-MAG. On the other hand, 16:1ω5 β-MAG was not detected in colonized *Lotus* or *Daucus* roots, suggesting that the accumulation of 16:0 β-MAG in these tissues was part of the plant 16:0 β-MAG pool.

FatM shows thioesterase activity with preference for 16:0-ACP

To study the substrate specificity of the FatM thioesterase, a truncated version of the cDNA, lacking the putative N-terminal plastid targeting signal but containing the complete sequence harboring the thioesterase activity, was expressed in *Escherichia coli*. The construct was introduced into the *E. coli fadD* mutant which is deficient in acyl-CoA synthetase activity and therefore can accumulate free fatty acids after expression of plant thioesterases (Overath *et al.*, 1969; Dörmann *et al.*, 1995). Induction of *FatM* expression in the *E. coli fadD* mutant resulted in the accumulation of free fatty acids, demonstrating that FatM

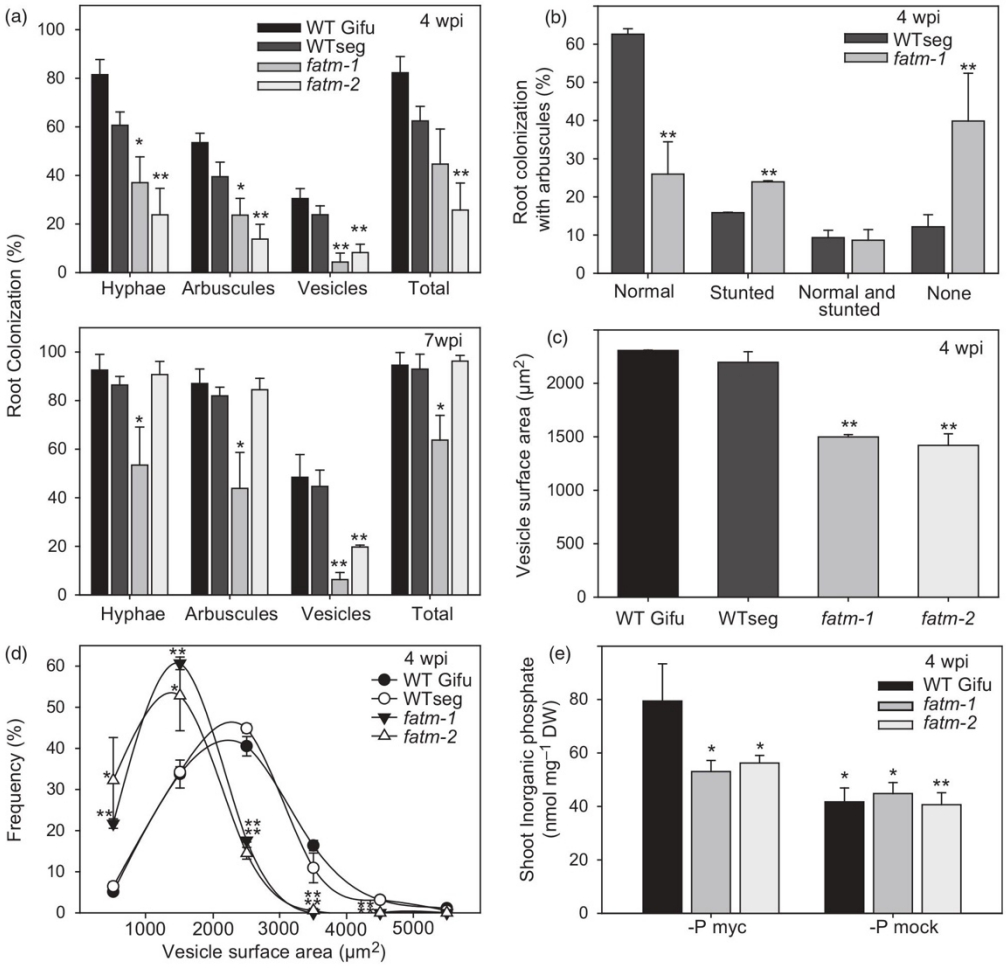

Figure 3. Quantitative arbuscular mycorrhiza phenotypes of *Lotus fatm-1 and fatm-2* mutant lines.
Colonized wild type (WT) Gifu, segregating WT from *fatm-1* (WTseg) and *fatm-1* and *fatm-2* mutant roots were stained with ink–vinegar and fungal structures observed by light microscopy at 4 weeks post-inoculation (wpi) (b–e) or at 4 wpi and 7 wpi (a).
(a) Frequency of root colonization (hyphae, arbuscules, vesicles, total structures) determined by the modified grid-line intersection method ($n = 5$).
(b) Frequency of arbuscule types in colonized WT seg and *fatm-1* determined by the modified grid-line intersection method. Arbuscules were classified as normal, stunted, normal/stunted or no arbuscule (see Figure 2) ($n = 4$).
(c) Total vesicle surface area. The surface area of all vesicles present in the investigated root segments was measured and averaged per root system (n = 5).
(d) Vesicle size population. The vesicle surface areas shown in (c) were sorted into six size categories (0–1000, 1000–2000, 2000–3000, 3000–4000, >5000 µm^2) and the distribution frequency calculated ($n = 5$).
(e) The inorganic phosphate content of the shoots was measured photometrically. Results –P myc are means and SDs for at least eight independent leaf samples from three different pots and –P mock are from at least three individual leaf samples from single pots. –P myc, infected with *R. irregularis*; –P mock, inoculated with carrier material. Student's *t*-test (*$P < 0.05$; **$P < 0.01$).

harbors thioesterase activity (Figure 5a). The most abundant free fatty acids were 14:0, 16:0 and 16:1Δ9. Because the acyl-ACP composition in *E. coli* is presumably different from that in plants and because it is affected by overexpression of FatM we recorded the thioesterase activity of recombinant FatM in an *in vitro* assay with different acyl-ACPs in separate *in vitro* reactions. FatM showed a preference for hydrolyzing 16:0-ACP followed by 18:0-

ACP > 18:1Δ9-ACP > 14:0-ACP (Figure 5b). 10:0-ACP and 12:0-ACP were not hydrolyzed. Therefore, FatM preferably releases 16:0.

FatM is required for the synthesis of fatty acids provided to the fungus

The findings that the *fatm* mutation affects the morphology and abundance of AM structures, particularly of the vesicles (Figures 2 and 3), and that it results in a decrease in AM-specific lipids (Figures S3–S5) suggested that FatM might be involved in the synthesis of lipids in the root cell which are required for normal AM establishment. We studied the impact of FatM deficiency on lipid synthesis in the plant and the fungus using isotopolog profiling. Colonized and mock inoculated roots of WT and *fatm-1* were incubated with [$^{13}C_2$]acetate. Exogenously applied acetate in plants is readily converted into acetyl-CoA and predominantly employed for fatty acid synthesis in the plastid (Lin and Oliver, 2008). Analysis by GC-MS and LC-MS revealed the presence of different ^{13}C isotopologs carrying one, two or more ^{13}C atoms per fatty acid next to the ^{12}C isotopolog peak. The abundance of ^{13}C isotopologs after ^{13}C labeling was increased compared with a non-labeled control due to the incorporation of [$^{13}C_2$]acetate. The ^{13}C overexcess isotopolog abundance was calculated after subtraction of the natural content of ^{13}C from each isotopolog peak, and normalized to the root FW (Bao *et al.*, 2000; Keymer *et al.*, 2017). Figure 5(a) shows that ^{13}C label was incorporated into different fatty acids (16:1ω5, 16:0, 18:2, 18:1, 18:0 and 20:3) while the incorporation into 18:3, 20:1, 20:2 was negligible (not shown). In colonized *fatm* roots, the ^{13}C incorporation into isotopologs of fungal fatty acids (16:1ω5, 20:3) was strongly reduced compared with the wild type, while it was unchanged for 16:0. Interestingly, labeling of fatty acids predominantly found in the plant (18:2, 18:1, 18:0) was significantly increased in colonized *fatm* roots, suggesting that [^{13}C]acetate incorporation in *fatm* mutant roots is redirected from fungal to plant fatty acids. Next, the sums of all ^{13}C isotopologs were calculated (Figure 5b). The amounts of ^{13}C isotopologs in 16:1ω5 and 20:3 of WT myc samples were about 0.127 and 0.016 nmol mg^{-1} FW, equivalent to about 40% and 5% of the sum of the isotopologs of all fatty acids (0.318 nmol mg^{-1} FW) (Figure 5b). Considering that additional ^{13}C label was retrieved in 16:0, which in part has both fungal and plant origin, this result indicates that at least around 45% of the fatty acids synthesized in colonized WT roots are localized to the fungus at 4 wpi.

The finding that the ^{13}C incorporation into fungal fatty acids (16:1ω5, 20:3) was strongly reduced could in principle also be explained by the reduced extent of *fatm* colonization, rather than by a specific effect of the *fatm* mutation on fatty acid synthesis. To address this question, i.e. to take into account the decreased degree of colonization and the reduced amounts of fungal fatty acids in *fatm* roots, the incorporated ^{13}C label was normalized to the total amount of each respective fatty acid. The total amounts of fatty acids were calculated from the sum of all isotopolog peaks (Figure S8a), and this fatty acid composition was comparable to that obtained by GC (Figure S3b). The amounts of ^{13}C labeling of 16:1ω5 and 20:3 normalized to the respective fatty acids were also reduced in *fatm-1* compared with WT, albeit to a lesser extent (Figure S8b). This result is in agreement with the conclusion that the *fatm* mutation not only affects the overall synthesis of fungal fatty acids but also specifically reduces the flux of [^{13}C]acetate into 16:1ω5 and 20:3, suggesting that FatM is involved in a pathway that predominantly provides plant fatty acids to the fungus.

DISCUSSION

The acyl-ACP thioesterase FatM of *L. japonicus* is essential for AM symbiosis because it is required for full arbuscule branching, the establishment of vesicle size and vesicle frequency (Figures 2 and 3). *FatM* is exclusively expressed in roots colonized with AM fungi (Figure S7), and is present only in genomes of AM host plants (Figure S1) (Bravo *et al.*, 2016), suggesting that *FatM* resulted from gene duplication of *FatB* and was maintained during evolution for AM-specific *de novo* synthesis of fatty acids in the plastids of arbuscocytes (Bravo *et al.*, 2017).

FatM is phylogenetically related to FatB and is specific for 16:0-ACP

In addition to FatM, three classes of thioesterases are found in plants, i.e. the ubiquitous FatA and FatB classes, and FatC, which is only found in AM-competent plants (Figure S1) (Bravo *et al.*, 2016). FatA thioesterases are specific for 18:1Δ9-ACP, while the ubiquitous FatB enzymes hydrolyze 16:0-ACP, 18:0-ACP and 18:1Δ9-ACP (Dörmann *et al.*, 1995; Jones *et al.*, 1995). In addition to the ubiquitous FatB enzymes, some plants harbor further FatB thioesterases specific for medium chain acyl-ACPs (e.g. *C. hookeriana*, 8:0, 10:0; *U. californica*, 12:0). FatM sequences are related to the ubiquitous FatB enzymes and to the medium chain-specific FatB proteins (UcFatB1 and ChFatB2) to similar extents, suggesting that the medium chain-specific FatB enzymes evolved later, after the split from FatM (Figure S1). The expression of the FatA and FatB thioesterases from *Lotus* was not affected by the *fatm* mutation, while FatC expression was weakly increased (Figure 1b). Furthermore, FatA, FatB and FatC do not show AM-specific transcript profiles (Figure S7). These three thioesterases probably serve as housekeeping genes, providing the cell with an adequate supply of fatty acids (predominantly 18:1Δ9 and 16:0) for regular AM-independent growth, while

FatM represents a FatB paralog highly expressed during AM colonization.

Expression of *Lotus FatM* in *E. coli fadD* resulted in the release of free fatty acids, mostly 14:0, 16:0 and 16:1Δ9 (Figure 4a). Similarly, expression of the *Sorghum FatM* ortholog in *fadD* resulted in the accumulation of 14:0, 16:0 and 16:1Δ9 (Jing *et al.*, 2011). The finding that the release of free 14:0 fatty acids compared with 16:0 was higher in *Lotus FatM*-expressing *E. coli* (Figure 4a) than the *in vitro* activity of FatM with 14:0-ACP compared with 16:0-ACP (Figure 4b), can be explained by the fact that acyl-ACP concentrations in *E. coli* are not equimolar. During logarithmic growth, the predominant proportion of ACP is not acylated, because acyl-ACPs make up only about 10% of total ACP (Rock and Jackowski, 1982). Most acyl-ACPs have chain lengths of over C16. Furthermore, the hydrolysis of acyl-ACPs by FatM in transformed *fadD* cells results in the depletion of 14:0-ACP and longer chain acyl-ACPs. Thus, the FatM substrate specificity is more accurately determined by *in vitro* assays. Taken together, *in vitro* and *in vivo* measurements of FatM expressed in *E. coli* indicate that FatM acts as a 16:0-ACP thioesterase. Increased expression of *Lotus FatM* during AM formation is thus likely to result in the increase in 16:0-ACP thioesterase activity in arbuscocytes (Bravo *et al.*, 2017). Furthermore, the high similarity in substrate specificities between FatM from *Lotus* and FatB from Arabidopsis support the hypothesis that FatM sequences represent paralogs with a substrate specificity similar to the ubiquitous (16:0-ACP specific) sequences of the FatB class.

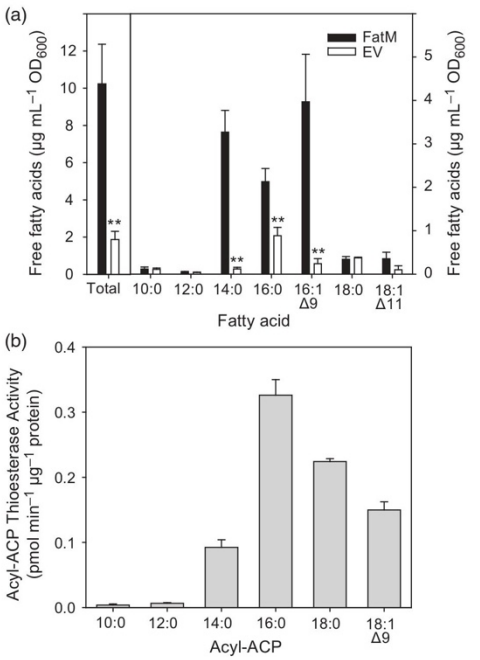

Figure 4. Acyl-acyl carrier protein (ACP) thioesterase activity of the recombinant thioesterase (FatM) enzyme.
(a) Amounts of free fatty acids in *Escherichia coli fadD* cells expressing the *Lotus* FatM cDNA without an N-terminal transit peptide. After induction of FatM expression, free fatty acids were isolated from the *E. coli fadD* culture by solid phase extraction and quantified by GC after conversion into fatty acid methyl esters.
(b) [1-^{14}C]acyl-ACPs were used as substrates for purified recombinant FatM protein in separate reactions. Hydrolyzed free fatty acids were extracted after 30 min and the radioactivity measured by liquid scintillation counting. Values are means and SD (n = 3).

The AM-specific pathway of fatty acid synthesis in the root cortex cell

Expression of different lipid biosynthesis genes is induced in arbuscocytes during colonization. Only few of them, *DIS*, *FatM* and *RAM2*, have been characterized genetically and only for one, RAM2, has the enzymatic specificity been determined (Bravo *et al.*, 2017; Keymer *et al.*, 2017; Luginbuehl *et al.*, 2017). These genes establish an extra AM-specific lipid biosynthesis pathway in root cortex cells which starts with *de novo* fatty acid synthesis in the plastid and proceeds with the assembly of complex lipids at the ER (Figure 6). *Lotus* contains an additional β-ketoacyl-ACP synthase I (KASI) copy, designated DIS, which presumably produces 16:0-ACP in the plastids of colonized roots (Wu and Xue, 2010; Keymer *et al.*, 2017). 16:0-ACP might subsequently be hydrolyzed by FatM, in line with its substrate specificity as determined after expression in *E. coli*. The importance of the fatty acid synthesis pathway in plastids of infected cells is emphasized by the findings that colonized *Medicago* roots show increased plastid proliferation with production of stromules, and the plastids cluster around the arbuscules (Lohse *et al.*, 2005). Furthermore, *Medicago* FatM is localized to these stromulated plastids (Bravo *et al.*, 2017). After export from the plastids, free 16:0 is converted into 16:0-CoA. Next, RAM2 produces 16:0 β-MAG from 16:0-CoA and glycerol-3-phosphate (Luginbuehl *et al.*, 2017). 16:0 β-MAG accumulates during AM formation, representing the most abundant β-MAG form. 16:0 β-MAG is also present in the ERM of *Rhizophagus* when colonizing a carrot hairy root culture (Figure S6). However, in colonized roots, the amount of fungal β-MAG is presumably low, because fungal 16:1ω5 β-MAG was not detected (Bravo *et al.*, 2017; Keymer *et al.*, 2017). The decrease in 16:0 β-MAG in *fatm-1* roots probably indicates a decrease through the AM-specific RAM2 acyltransferase pathway. The mechanism of lipid transfer through the arbuscular and periarbuscular membranes to the fungus, and the identity of the transferred lipid molecule, remain elusive. For example, STR half transporters of the ABC G type, which were shown to be required for AM establishment in *Medicago*, *Lotus* and rice, could be involved in lipid

transfer to the fungus (Zhang *et al.*, 2010; Gutjahr *et al.*, 2012; Bravo *et al.*, 2017; Keymer *et al.*, 2017).

The transfer of lipids to the fungus was recently studied in *Medicago* and *Lotus* roots. Expression of the 12:0-ACP-specific UcFatB thioesterase from *U. californica* in transgenic *Medicago* roots resulted in the accumulation of plant-derived 12:0 in fungal spores, indicating that a 12:0-containing lipid was transferred to the fungus (Jiang *et al.*, 2017; Luginbuehl *et al.*, 2017). incorporation of ^{14}C-sucrose into fatty acids in *Medicago ram2* roots was reduced compared with the WT, although the *ram2* roots were well colonized and contained arbuscules in the presence of a WT nurse plant (Luginbuehl *et al.*, 2017). ^{14}C-acetate was readily incorporated into fatty acids in fungal spores derived from colonized *Medicago* WT roots but not in spores from colonized roots of the *acs* mutant deficient in acetyl-CoA synthetase, indicating that the label was first incorporated into the plant (Lin and Oliver, 2008; Luginbuehl *et al.*, 2017). Finally, ^{13}C-glucose labeling of *Lotus* WT roots resulted in the incorporation of ^{13}C into 16:0 and 16:1ω5 with isotopolog patterns that were very similar in the roots and in the ERM, but when colonized *dis* or *ram2* mutant roots were incubated with ^{13}C-glucose, the isotopolog patterns in the root and in the ERM were very different (Keymer *et al.*, 2017).

We employed ^{13}C-acetate labeling to study the role of FatM during the synthesis of plant and fungal fatty acids (Figures 5, 6 and S8). The incorporation of [$^{13}C_2$]acetate into AM-specific fatty acids (16:1ω5, 20:3) was strongly affected in colonized *fatm-1* roots, while the incorporation into plant-specific or common fatty acids was not changed or even increased (16:0, 18:2, 18:0), suggesting a redirection of the ^{13}C label into plant fatty acids in *fatm*-1 (Figure 5a). The reduced ^{13}C labeling of 16:1ω5 and 20:3 in infected *fatm-1* roots was not due to a general decrease in the abundance of these two fatty acids because ^{13}C labeling of 16:1ω5 and 20:3 was also reduced when normalized to the total amounts of these fatty acids (Figure S8b, c). Therefore, incorporation of [$^{13}C_2$]acetate into fungal lipids depends on FatM, in agreement with the scenario that plant-derived fatty acids are transferred to the fungus. In colonized WT roots, about 45% of the ^{13}C label was found in 16:1ω5 and 20:3, while lower ^{13}C incorporation was detected in the other plant and fungal fatty acids. Because the label accumulating in 16:0 is also in part associated with the fungus, these results indicate that more than about 45% of the fatty acids synthesized in the roots are exported to the fungus.

Taken together, the ^{14}C and ^{13}C labeling experiments presented here and in previous studies demonstrate that the label is first taken up by the plant and employed for *de novo* fatty acid synthesis in the plastids before a fatty acid (presumably 16:0)-containing lipid is transported to the fungus. Thus, carbon flow from the plant to the fungus is based on two compound classes, fatty acids and hexoses, which might allow for a better partitioning of primary metabolic pathways in the fungus. *De novo* fatty acid synthesis represents one of the most expensive biosynthetic pathways, consuming large amounts of ATP and NADPH. Therefore, it is conceivable that AM fungi have lost the capacity for *de novo* fatty acid synthesis during the evolutionary establishment of AM symbiosis because this might have made the association as a whole more energy efficient.

EXPERIMENTAL PROCEDURES

Isolation of *fatm* mutant lines

The FatM transcript sequence (Gene ID, chr5.CM0328.70.r2.d) was retrieved from the *L. japonicus* Gene Expression Atlas (http://ljgea.noble.org/v2/) and used to search for lines carrying LORE1 retrotransposon insertions (Malolepszy *et al.*, 2016). Two mutant lines, designated *fatm-1* (G63) and *fatm-2* (D20), carrying insertions 218 bp and 238 bp upstream of the start codon, respectively, were identified. Homozygous mutant plants were obtained by screening with PCR (for oligonucleotides, see Table S1) (Urbanski *et al.*, 2012). As controls, WT Gifu and a WT segregant of *fatm-1*, designated WT seg, were selected.

Plant growth conditions and inoculation with *Rhizophagus irregularis*

Lotus seeds were scratched using sand paper, surface sterilized with 2% (v/v) sodium hypochlorite and 0.0001% (v/v) Tween 20 for 10 min, washed with sterile water and placed on phytoagar (0.7%, w/v, in tap water). Then, the seeds were incubated in the dark at 4°C for 3 days for stratification and incubated with 16-h light/day at 22°C and 55% relative humidity for 7 days. For inoculation, silica sand (1–2 mm diameter) was washed with tap water and deionized water, mixed 1:1 with vermiculite and autoclaved. Seedlings were placed in pots (7 cm high, 14 cm diameter) containing the sand:vermiculite mixture that was thoroughly mixed with *Rhizophagus* inoculum (Symplanta GmbH, http://www.symplanta.com/) containing approximately 5000 spores per pot. For mock treatments, a carrier material of attapulgite clay powder was added. Plants were watered twice weekly with tap water/deionized water (1:1) and once a week with low-phosphate (–P) nutrient solution containing 50 μM phosphate and grown for 4 or 7 weeks (Wewer *et al.*, 2014).

Colonization frequency and microscopy

For the determination of colonization frequency, roots were stained with ink/vinegar and fungal structures quantified with the modified grid-line intersection method (McGonigle *et al.*, 1990; Vierheilig *et al.*, 1998). Stained colonized root systems were dissected randomly into 1-cm pieces, and 10 1-cm root segments were mounted on a microscope slide. Each of these 1-cm segments was investigated at 10 randomly chosen spots which were scored for the presence of 'normal' (occupying most of the cavity of the cell; see Figure 2) or 'stunted' (strongly reduced structures) 'normal and stunted' or 'no' arbuscules. Per root system two to five microscope slides were employed, and per genotype at least three different root systems were used. Samples were analyzed at 10 × magnification with a bright-field microscope (BH-2, Olympus, https://www.olympus-global.com/). The vesicle surface areas of all vesicles visible in the investigated root segments were measured with the cellSens standard

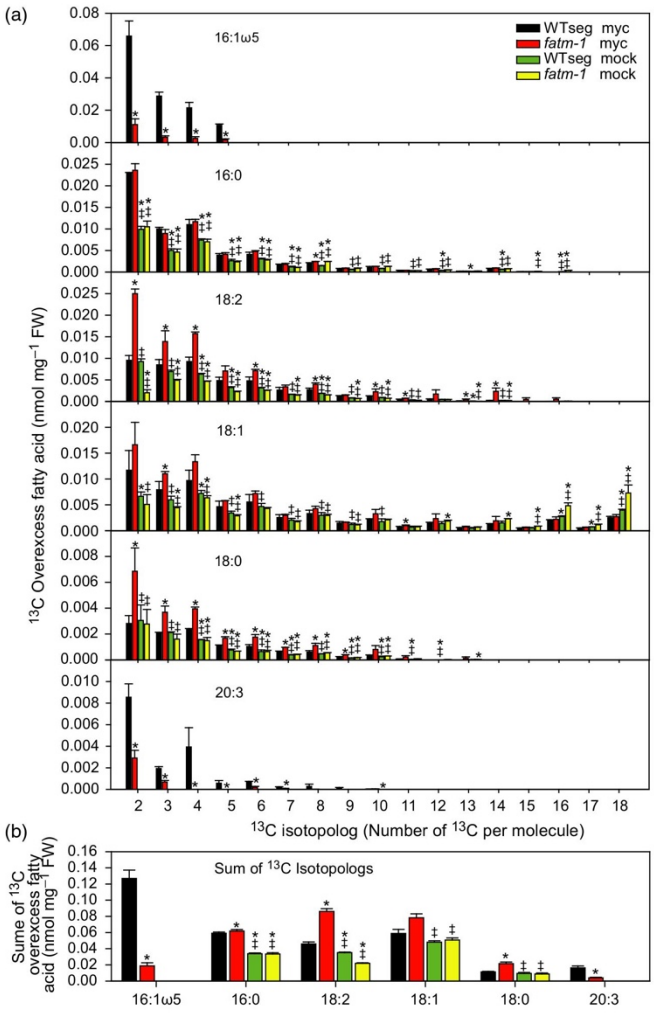

Figure 5. Incorporation of [$^{13}C_2$]acetate into mycorrhiza-specific fatty acids in colonized *fatm-1* mutant roots.
(a) Roots of segregating wild type (WT) from *fatm-1* (WTseg) and *fatm-1* plants infected with *Rhizophagus irregularis* (myc) and control roots (mock) were incubated in the presence of [$^{13}C_2$]acetate. FW, fresh weight.
(b) The sums of all isotopologs of the individual fatty acids shown in (a). Fatty acids were isolated and measured by LC-MS except 16:1ω5 which cannot be separated from plant 16:1Δ9 by LC-MS and was therefore measured by GC-MS. Overexcess ^{13}C isotopolog abundance in each fatty acid peak was calculated by subtracting the amounts of naturally occurring ^{13}C isotopologs. The experiment was repeated twice with similar results. Student's *t*-test (*, significantly different from WTseg myc; ‡, significantly different from *fatm-1* myc; $P < 0.05$). Values are means and SD ($n = 3$). [Colour figure can be viewed at wileyonlinelibrary.com].

software (Olympus). Wheat germ agglutinin (WGA)–Alexa Fluor 488 staining and confocal laser scanning microscopy of colonized roots was done as described (Pimprikar *et al.*, 2016).

Complementation of *fatm*-1 via hairy root transformation

The *FatM* gene and promoter region were amplified with Phusion PCR (NEB, https://www.neb.com/) using the primers indicated in Table S1. Plasmids for complementation were generated using the Golden Gate Assembly (Binder *et al.*, 2014) (Table S2). Hypocotyls of *L. japonicus* were transformed with the vectors as shown in Table S2. Hairy roots were induced using transgenic *Agrobacterium rhizogenes* AR1193 as described (Takeda *et al.*, 2009).

Measurement of shoot inorganic phosphate

The inorganic phosphate content of shoots was determined as described (Itaya and Ui, 1966). Briefly, a 1–3 cm stem segment containing one trifoliate leaf was harvested from each plant and dried at 110°C for 2 h, homogenized and extracted with 1 ml of solution containing 0.33 M sorbitol, 2 mM $MgCl_2$, 1 mM EDTA and 50 mM Tricine. The extract was centrifuged at 4000 ***g*** for 5 min and 20 µl of the supernatant was added to 480 µl of color reagent (one volume 4.2%, w/v, ammonium molybdate in 5 N HCl with three volumes 0.2%, w/v, Malachite Green), 480 µl 1 M HCl and 20 µl 0.1% Tween 20, mixed and absorbance recorded at 660 nm after 30 min. A calibration curve with KH_2PO_4 was established for quantification.

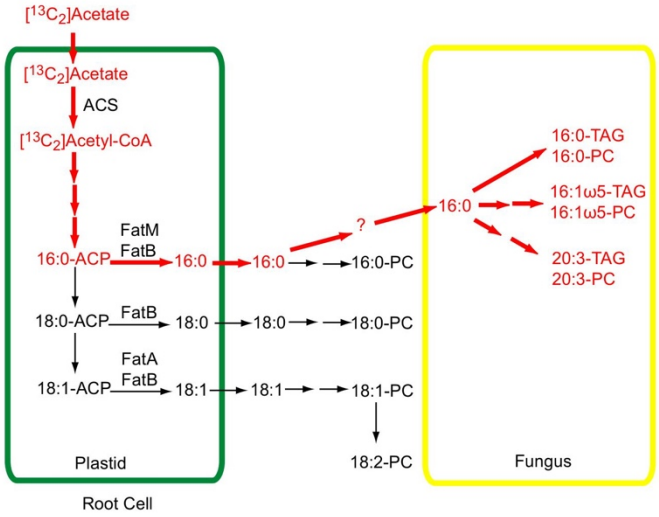

Figure 6. Incorporation of ^{13}C from [$^{13}C_2$]acetate into fatty acids of *Lotus* roots colonized with *Rhizophagus irregularis*.
[$^{13}C_2$]acetate is taken up by root cortex cells and accumulates in the plastids, where it is converted into [$^{13}C_2$]acetyl-CoA by acetyl-CoA synthetase (ACS). ^{13}C-labeled acetyl-CoA is employed for fatty acid synthesis, resulting in the production of 16:0, 18:0 and 18:1, bound to acyl carrier protein (ACP). Acyl-ACPs are hydrolyzed by thioesterases (FatA, FatB, FatM), and the free fatty acids exported from the plastid, where they are used for membrane lipid synthesis (PC, phosphatidylcholine). The presumed pathway of incorporation of ^{13}C into fungal fatty acids includes the *de novo* synthesis of 16:0-ACP in the plastids followed by cleavage by FatM (thick arrows). An unknown 16:0-containing lipid is presumably imported into the arbuscules of the fungus and converted into 16:1ω5, 20:3 or other fungal fatty acids which are incorporated into PC or triacylglycerol (TAG). [Colour figure can be viewed at wileyonlinelibrary.com].

Gene expression analysis

Total RNA was extracted with the plant total RNA Mini Kit (DNA Cloning Service, http://www.dna-cloning.com/) and cDNA synthesized from 1 μg RNA with the cDNA synthesis kit (ThermoFisher Scientific, https://www.thermofisher.com/). Reverse transcriptase-PCR was performed with 30 cycles with 50 ng cDNA as a template. The same results were obtained with RT-PCR reactions using only 5 ng cDNA template. Oligonucleotides and RT-PCR conditions for *Lotus FatA*, *FatB*, *FatM*, *FatC*, *PT4*, *UBI* and *Rhizophagus* α-tubulin are described in Table S1.

Extraction and measurement of lipids and fatty acids

Lipid extraction and measurement of phospholipids, glycolipids, diacylglyerol, triacylglycerol and total fatty acids by quadrupole time of flight mass spectrometry (Q-TOF MS/MS) or gas chromatography–flame ionization detection (GC-FID), respectively, was described previously (Gasulla *et al.*, 2013; Wewer *et al.*, 2014).

Measurement of monoacylglycerol

Roots of *D. carota* colonized with *R. irregularis* were grown in split Petri dishes on MSR medium with the colonized roots in one compartment and ERM (hyphae and spores) in the other (Cranenbrouck *et al.*, 2005). Thirty-five days after inoculation, the medium was dissolved with 10 mM sodium citrate and the ERM and the roots harvested, washed in sterile water and used for lipid extraction. To extract MAGs, total lipid extracts from colonized *D. carota* roots, *R. irregularis* ERM and colonized or mock-treated *Lotus* roots were dried, dissolved in hexane and the MAGs purified by solid-phase extraction on silica columns (vom Dorp *et al.*, 2013). The MAGs were eluted with diethylether then dried by evaporation. Hydroxyl groups were silylated with *N*-methyl-*N*-trimethylsilyl-trifluoroacetamide (MSTFA) (80°C, 30 min) dissolved in pyridine (1:3 v/v). The liquid was evaporated, the lipids dissolved in hexane and injected onto an Agilent 7890A Plus GC-MS instrument (http://www.agilent.com/). The MAGs were identified by retention times and fragmentation patterns and quantified by extracted ion monitoring, using [M^+ 103] for α-MAGs and [M^+ −161] for β-MAGs, as reported for 16:0-MAG (Destaillats *et al.*, 2010) and 24:0-MAG (Li *et al.*, 2007). Fifteen micrograms of a mixture of 15:0 α-MAG/15:0 β-MAG was used as an internal standard.

Stable isotope labeling and ^{13}C fatty acid analysis

Plants were colonized with *R. irregularis* for 4 weeks as described above, removed from pots and washed gently with sterile, deionized water to remove excess substrate and ERM. The roots were submerged in 15 ml of labeling buffer (20 mM MES-KOH, 0.2% (v/v) Tween 20, pH 5.6) containing 4 mM sodium [$^{13}C_2$]acetate (Sigma Aldrich, http://www.sigmaaldrich.com/) in 15-ml Falcon tubes with roots half covered with aluminum foil. In the negative control [$^{13}C_2$]acetate was omitted. The shoots were exposed to continuous light and roots harvested after 12 h of labeling. Total lipids were extracted as described above, after the addition of 5 μg of internal standard (pentadecanoic acid, 15:0). Lipids were dried under N_2 gas and hydrolyzed in 5 ml of 3 M KOH/methanol (1:9 v/v), for 1 h at 80°C. Hydrolysis was stopped by the addition of 500 μl of concentrated HCl and total fatty acids extracted three times with 1 ml of hexane each. The solvent was evaporated and the dried fatty acids dissolved in 200 μl of acetonitrile. Fatty acids were separated on an RP8 column (Knauer Eurospher II,

150 mm × 3 mm; https://www.knauer.net/) and detected by LC-MS with electrospray ionization in the negative mode on an Agilent 6530 Q-TOF mass spectrometer. To separate fatty acid isomers, the acetontrile was evaporated and fatty acids converted into methyl esters for separation by GC-MS in single-ion mode (SIM). For quantification by LC-MS or GC-MS, the abundance of the molecular ion (M^+) of the respective fatty acid isotopolog was used.

The abundance of naturally occurring ^{13}C fatty acid isotopologs was determined in non-labeled roots and subtracted from the isotoplogs measured in ^{13}C-labeled samples giving rise to overexcess amounts of ^{13}C isotopologs (Bao *et al.*, 2000; Keymer *et al.*, 2017). Overexcess isotopologs containing only one ^{13}C were omitted because they could not be quantified due to the large natural ^{13}C isotopolog abundance. The amounts of total fatty acids were derived after addition of all isotopologs (^{12}C and ^{13}C) using the internal standard 15:0. Overexcess isotopologs for a given fatty acid were normalized to the unlabeled total amount of the respective fatty acid (in %) to calculate the relative labeling of individual fatty acids as previously published (Bao *et al.*, 2000).

Heterologous expression of *FatM* in *E. coli* and purification of recombinant protein

A 1041-bp sequence of the FatM cDNA lacking the predicted N-terminal transit sequence of 126 bp was amplified by RT-PCR with *Lotus* WT root RNA using the oligonucleotides bn2340 and bn2355 (Table S1). The purified PCR product was ligated into pJET1.2 (Thermo Fisher Scientific). The *FatM* cDNA was released with *Bam*HI and *Hin*dIII and ligated into pQE-80L (Qiagen, http://www.qiagen.com/).

The FatM-pQE-80L construct was transferred into the *E. coli fadD* 88 mutant (Overath *et al.*, 1969) for the measurement of free fatty acids. *Escherichia coli fadD* 88 cells harboring FatM-pQE-80L were grown at 37°C to an OD_{600} of 0.5. Then they were moved to 16°C and 1 mM isopropyl-β-D-thiogalactopyranoside (IPTG) was added. After 12 h, 2 ml of the culture containing the cells was removed and boiled at 100°C for 10 min. Lipids were extracted from the culture (including cells and medium) with *n*-hexane and the hexane phase was used for purification of free fatty acids by solid-phase extraction (vom Dorp *et al.*, 2013). Free fatty acids were converted into methyl esters with 1 M methanolic HCl and quantified via GC using pentadecanoic acid (15:0) as an internal standard (Browse *et al.*, 1986).

Alternatively, FatM-pQE-80L was transferred into *E. coli* electroSHOX cells (Bioline GmbH, https://www.bioline.com/) for protein purification and measurements of enzyme activity. *Escherichia coli* electroSHOX cells harboring FatM-pQE-80L were grown at 37°C to an OD_{600} of 0.5 and protein expression was induced with 1 mM IPTG for 12 h at 16°C. Then cells were harvested by centrifugation and lyzed. The His-tagged FatM protein was purified by Ni^{2+} affinity chromatography (Qiagen).

Acyl-ACP synthesis and thioesterase assay

Acyl carrier protein was extracted from 500 g of *E. coli* cells (Majerus *et al.*, 1965). The acyl-ACP synthase (Aas) protein from *E. coli* was purified from the *E. coli* overexpression strain C41 (DE3) as reported (Shanklin, 2000). Acylation of ACP was carried out in a reaction containing 17 μg of Aas protein, 1 μCi of [1-^{14}C] fatty acid (10:0, 12:0, 14:0, 16:0, 18:0, 18:1Δ9; Hartmann Analytic, https://www.hartmann-analytic.de/), 5 mM ATP, 2 mM DTT, 100 mM TRIS-HCl pH 8.0, 10 mM $MgCl_2$, 400 mM LiCl and 90 μg of *E. coli* ACP for 4 h at 37°C. Acyl-ACPs were purified by anion-exchange chromatography on 0.15 g of pre-swollen DE52 cellulose (Whatman/GE Healthcare, http://www3.gehealthcare.com/) columns in 1 ml of MES-KOH (10 mM, pH 6.1). After loading the acyl-ACPs, the column was washed with 8 ml of MES-KOH (10 mM, pH 6.1), with 8 ml of isopropanol/10 mM MES-KOH (pH 6.1; 4:1), with 8 ml of MES-KOH (10 mM, pH 6.1) and eluted in two 4-ml fractions with 0.5 M LiCl in MES-KOH (10 mM, pH 6.1). The acyl-ACP fractions were dialyzed against 100 volumes of MES-KOH (10 mM, pH 6.1) using Spectra/Por dialysis membranes with a cutoff of 6000–8000 Da (http://spectrumlabs.com/). Thioesterase assays were performed in 50-μl reactions containing 20 μl of purified FatM protein (2 μg), 5 μl (0.45 μCi μl^{-1}, 1000 decompositions per minute μl^{-1}) of [^{14}C]acyl-ACP and 25 μl of 200 mM Tricine-KOH (pH 8.5). The reaction was incubated at 22°C for 30 min and terminated by adding 50 μl of 1 M acetic acid containing 1 mM non-labeled oleic acid as a carrier. Free fatty acids were extracted three times with 300 μl of *n*-hexane (one volume of *n*-hexane saturated with four volumes of 1:1 isopropanol–water). Hexane was evaporated and the radioactivity determined by liquid scintillation counting.

Lotus japonicus gene identifiers

FatA (chr1.TM1516.23), *FatB* (Ljwgs_013315.1), *FatC* (Ljwgs_022305.1_at), *FatM* (chr5.CM0328.70.r2.d)

ACKNOWLEDGEMENTS

We thank Deborah Ruprecht for help with handling radioactive samples. We are grateful to John Shanklin (Brookhaven National Laboratory, Upton, NY) for the *E. coli* Aas clone. Funding was provided by Deutsche Forschungsgemeinschaft (DFG) for PD (Graduiertenkolleg GRK2064, DO520/15-1 for PD, Sonderforschungsbereich SFB924 and Emmy Noether Programm GU1423/1-1 for CG). The authors declare no conflict of interest.

SUPPORTING INFORMATION

Additional Supporting Information may be found in the online version of this article.

Figure S1. Phylogenetic tree of acyl-ACP thioesterases from arbuscular mycorrhiza host and non-host plants.

Figure S2. Genetic complementation of defective arbuscule morphology in the *fatm-1* mutant.

Figure S3. Quantification of total fatty acids in colonized *fatm* mutant roots.

Figure S4. Relative distribution of triacylglycerol and diacylglycerol molecular species in colonized wild type Gifu and *fatm-1* and *fatm-2* mutant roots at 4 weeks post-inoculation.

Figure S5. Molecular species composition of membrane glycerolipids in colonized WT Gifu and *fatm-1* and *fatm-2* mutant roots at 4 weeks post-inoculation.

Figure S6. Monoacylglycerol in *Lotus japonicus fatm* and *Daucus carota roots.*

Figure S7. Expression patterns of *FatM*, *FatA*, *FatB* and *FatC* from *Lotus japonicus.*

Figure S8. Specific inhibition of 16:1ω5 and 20:3 synthesis in colonized *fatm* mutant roots.

Table S1. Oligonucleotides used for cloning, RT-PCR and genotyping.

Table S2. Generation of constructs for complementation.

REFERENCES

Bago, B., Zipfel, W., Williams, R.M., Jun, J., Arreola, R., Lammers, P.J., Pfeffer, P.E. and Shachar-Hill, Y. (2002) Translocation and utilization of fungal

storage lipid in the arbuscular mycorrhizal symbiosis. *Plant Physiol.* **128**, 108–124.

Bao, X., Focke, M., Pollard, M. and Ohlrogge, J. (2000) Understanding in vivo carbon precursor supply for fatty acid synthesis in leaf tissue. *Plant J.* **22**, 39–50.

Beisson, F., Li-Beisson, Y. and Pollard, M. (2012) Solving the puzzles of cutin and suberin polymer biosynthesis. *Curr. Opin. Plant Biol.* **15**, 329–337.

Binder, A., Lambert, J., Morbitzer, R., Popp, C., Ott, T., Lahaye, T. and Parniske, M. (2014) A modular plasmid assembly kit for multigene expression, gene silencing and silencing rescue in plants. *PLoS ONE*, **9**, e88218.

Bravo, A., York, T., Pumplin, N., Mueller, L.A. and Harrison, M.J. (2016) Genes conserved for arbuscular mycorrhizal symbiosis identified through phylogenomics. *Nat. Plants*, **2**, 15208.

Bravo, A., Brands, M., Wewer, V., Dörmann, P. and Harrison, M.J. (2017) Arbuscular mycorrhiza-specific enzymes FatM and RAM2 fine-tune lipid biosynthesis to promote development of arbuscular mycorrhiza. *New Phytol.* **214**, 1631–1645.

Browse, J., McCourt, P.J. and Somerville, C.R. (1986) Fatty acid composition of leaf lipids determined after combined digestion and fatty acid methyl ester formation from fresh tissue. *Anal. Biochem.* **152**, 141–145.

Corradi, N. and Bonfante, P. (2012) The arbuscular mycorrhizal symbiosis: origin and evolution of a beneficial plant infection. *PLoS Pathog.* **8**, e1002600.

Cranenbrouck, S., Voets, L., Bivort, C., Renard, L., Strullu, D.-G. and Declerck, S. (2005) Methodologies for *in vitro* cultivation of arbuscular mycorrhizal fungi with root organs. In *In Vitro Culture of Mycorrhizas* (Declerck, S., Fortin, J.A. and Strullu, D.-G., eds). Berlin Heidelberg: Springer, pp. 341–375.

Dehesh, K., Jones, A., Knutzon, D.S. and Voelker, T.A. (1996) Production of high levels of 8. 0 and 10:0 fatty acids in transgenic canola by overexpression of *Ch FatB2*, a thioesterase cDNA from *Cuphea hookeriana*. *Plant J.* **9**, 167–172.

Delaux, P.-M., Varala, K., Edger, P.P., Coruzzi, G.M., Pires, J.C. and Ané, J.-M. (2014) Comparative phylogenomics uncovers the impact of symbiotic associations on host genome evolution. *PLoS Genet.* **10**, e1004487.

Destaillats, F., Cruz-Hernandez, C., Nagy, K. and Dionisi, F. (2010) Identification of monoacylglycerol regio-isomers by gas chromatography-mass spectrometry. *J. Chromat. B*, **1217**, 1543–1548.

Dörmann, P., Voelker, T.A. and Ohlrogge, J.B. (1995) Cloning and expression in *Escherichia coli* of a novel thioesterase from *Arabidopsis thaliana* specific for long-chain acyl-acyl carrier proteins. *Arch. Biochem. Biophys.* **316**, 612–618.

vom Dorp, K., Dombrink, I. and Dormann, P. (2013) Quantification of diacylglycerol by mass spectrometry. *Meth. Mol. Biol.* **1009**, 43–54.

Emanuelsson, O., Nielsen, H. and Heijne, G. (1999) ChloroP, a neural network-based method for predicting chloroplast transit peptides and their cleavage sites. *Protein Sci.* **8**, 978–984.

Favre, P., Bapaume, L., Bossolini, E., Delorenzi, M., Falquet, L. and Reinhardt, D. (2014) A novel bioinformatics pipeline to discover genes related to arbuscular mycorrhizal symbiosis based on their evolutionary conservation pattern among higher plants. *BMC Plant Biol.* **14**, 333.

Gasulla, F., vom Dorp, K., Dombrink, I., Zähringer, U., Gisch, N., Dormann, P. and Bartels, D. (2013) The role of lipid metabolism in the acquisition of desiccation tolerance in *Craterostigma plantagineum*: A comparative approach. *Plant J.* **75**, 726–741.

Gaude, N., Bortfeld, S., Duensing, N., Lohse, M. and Krajinski, F. (2012) Arbuscule-containing and non-colonized cortical cells of mycorrhizal roots undergo extensive and specific reprogramming during arbuscular mycorrhizal development. *Plant J.* **69**, 510–528.

Gomez, S.K., Javot, H., Deewatthanawong, P., Torres-Jerez, I., Tang, Y., Blancaflor, E.B., Udvardi, M.K. and Harrison, M.J. (2009) *Medicago truncatula* and *Glomus intraradices* gene expression in cortical cells harboring arbuscules in the arbuscular mycorrhizal symbiosis. *BMC Plant Biol.* **9**, 10.

Gutjahr, C. and Parniske, M. (2013) Cell and developmental biology of arbuscular mycorrhiza symbiosis. *Annu. Rev. Cell Dev. Biol.* **29**, 593–617.

Gutjahr, C., Radovanovic, D., Geoffroy, J. *et al.* (2012) The half-size ABC transporters STR1 and STR2 are indispensable for mycorrhizal arbuscule formation in rice. *Plant J.* **69**, 906–920.

Itaya, K. and Ui, M. (1966) A new micromethod for the colorimetric determination of inorganic phosphate. *Clin. Chim. Acta*, **14**, 361–366.

Jabaji-Hare, S., Deschene, A. and Kendrick, B. (1984) Lipid content and composition of vesicles of a vesicular-arbuscular mycorrhizal fungus. *Mycologia*, **76**, 1024–1030.

Jiang, Y., Wang, W., Xie, Q. *et al.* (2017) Plants transfer lipids to sustain colonization by mutualistic mycorrhizal and parasitic fungi. *Science*, **356**, 1172–1175.

Jing, F., Cantu, D.C., Tvaruzkova, J., Chipman, J.P., Nikolau, B.J., Yandeau-Nelson, M.D. and Reilly, P.J. (2011) Phylogenetic and experimental characterization of an acyl-ACP thioesterase family reveals significant diversity in enzymatic specificity and activity. *BMC Biochem.* **12**, 44.

Jones, A., Davies, H.M. and Voelker, T.A. (1995) Palmitoyl-acyl carrier protein (ACP) thioesterase and the evolutionary origin of plant acyl-ACP thioesterases. *Plant Cell*, **7**, 359–371.

Keymer, A., Pimprikar, P., Wewer, V. *et al.* (2017) Lipid transfer from plants to arbuscular mycorrhiza fungi. *eLife*, **6**, e29107.

Li, Y., Beisson, F., Ohlrogge, J. and Pollard, M. (2007) Monoacylglycerols are components of root waxes and can be produced in the aerial cuticle by ectopic expression of a suberin-associated acyltransferase. *Plant Physiol.* **144**, 1267–1277.

Li-Beisson, Y., Shorrosh, B., Beisson, F. *et al.* (2013) Acyl-lipid metabolism. In *The Arabidopsis Book* (Torii, K., ed). Rockville, MD: The American Society of Plant Biologists, p. e0161.

Lin, M. and Oliver, D.J. (2008) The role of acetyl-coenzyme a synthetase in Arabidopsis. *Plant Physiol.* **147**, 1822–1829.

Lohse, S., Schliemann, W., Ammer, C., Kopka, J., Strack, D. and Fester, T. (2005) Organization and metabolism of plastids and mitochondria in arbuscular mycorrhizal roots of *Medicago truncatula*. *Plant Physiol.* **139**, 329–340.

Luginbuehl, L.H., Menard, G.N., Kurup, S., van Erp, H., Radhakrishnan, G.V., Breakspear, A., Oldroyd, G.E.D. and Eastmond, P.J. (2017) Fatty acids in arbuscular mycorrhizal fungi are synthesized by the host plant. *Science*, **356**, 1175–1178.

Majerus, P.W., Alberts, A.W. and Vagelos, R. (1965) The acyl carrier protein of fatty acid synthesis: Purification, physical properties and substrate binding site. *Proc. Natl Acad. Sci. USA*, **51**, 1231–1238.

Malolepszy, A., Mun, T., Sandal, N. *et al.* (2016) The LORE1 insertion mutant resource. *Plant J.* **88**, 306–317.

McGonigle, T.P., Miller, M.H., Evans, D.G., Fairchild, G.L. and Swan, J.A. (1990) A new method which gives an objective measure of colonization of roots by vesicular-arbuscular mycorrhizal fungi. *New Phytol.* **115**, 495–501.

Moreno-Pérez, A.J., Venegas-Calerón, M., Vaistij, F.E., Salas, J.J., Larson, T.R., Garcés, R., Graham, I.A. and Martinez-Force, E. (2012) Reduced expression of FatA thioesterases in Arabidopsis affects the oil content and fatty acid composition of the seeds. *Planta*, **235**, 629–639.

Ohlrogge, J. and Browse, J. (1995) Lipid biosynthesis. *Plant Cell*, **7**, 957–970.

Overath, P., Pauli, G. and Schairer, H.U. (1969) Fatty acid degradation in *Escherichia coli*. *Eur. J. Biochem.* **7**, 559–574.

Pimprikar, P., Carbonnel, S., Paries, M. *et al.* (2016) A CCaMK-CYCLOPS-DELLA complex activates transcription of RAM1 to regulate arbuscule branching. *Curr. Biol.* **26**, 987–998.

Rock, C.O. and Jackowski, S. (1982) Regulation of phospholipid synthesis in *Escherichia coli*. Composition of the acyl-acyl carrier protein pool *in vivo*. *J. Biol. Chem.* **257**, 10759–10765.

Ropars, J., Toro, K.S., Noel, J. *et al.* (2016) Evidence for the sexual origin of heterokaryosis in arbuscular mycorrhizal fungi. *Nat. Microbiol.* **1**, 16033.

Roth, R. and Paszkowski, U. (2017) Plant carbon nourishment of arbuscular mycorrhizal fungi. *Curr. Opin. Plant Biol.* **39**, 50–56.

Schliemann, W., Ammer, C. and Strack, D. (2008) Metabolite profiling of mycorrhizal roots of *Medicago truncatula*. *Phytochemistry*, **69**, 112–146.

Sedzielewska Toro, K. and Brachmann, A. (2016) The effector candidate repertoire of the arbuscular mycorrhizal fungus *Rhizophagus clarus*. *BMC Genom.* **17**, 101.

Shanklin, J. (2000) Overexpression and purification of the *Escherichia coli* inner membrane enzyme acyl-acyl carrier protein synthase in an active form. *Protein Expr. Purif.* **18**, 355–360.

Smith, S. and Read, D. (2008) Colonization of roots and anatomy of arbuscular mycorrhiza. In *Mycorrhizal Symbiosis* (Smith, S. and Read, D., eds). London: Academic Press, pp. 42–90.

Smith, S.E. and Smith, F.A. (2011) Roles of arbuscular mycorrhizas in plant nutrition and growth. New paradigms from cellular to ecosystem scales. *Annu. Rev. Plant Biol.* **62**, 227–250.

Stumpe, M., Carsjens, J.-G., Stenzel, I., Gobel, C., Lang, I., Pawlowski, K., Hause, B. and Feussner, I. (2005) Lipid metabolism in arbuscular mycorrhizal roots of *Medicago truncatula*. *Phytochemistry*, **66**, 781–791.

Takeda, N., Sato, S., Asamizu, E., Tabata, S. and Parniske, M. (2009) Apoplastic plant subtilases support arbuscular mycorrhiza development in *Lotus japonicus*. *Plant J.* **58**, 766–777.

Tang, N., San Clemente, H., Roy, S., Becard, G., Zhao, B. and Roux, C. (2016) A survey of the gene repertoire of *Gigaspora rosea* unravels conserved features among Glomeromycota for obligate biotrophy. *Front. Microbiol.* **7**, 233.

Tisserant, E., Malbreil, M., Kuo, A. *et al.* (2013) Genome of an arbuscular mycorrhizal fungus provides insight into the oldest plant symbiosis. *Proc. Natl Acad. Sci. USA*, **110**, 20117–20122.

Trepanier, M., Becard, G., Moutoglis, P., Willemot, C., Gagne, S., Avis, T.J. and Rioux, J.-A. (2005) Dependence of arbuscular-mycorrhizal fungi on their plant host for palmitic acid synthesis. *Appl. Environm. Microbiol.* **71**, 5341–5347.

Urbanski, D.F., Malolepszy, A., Stougaard, J. and Andersen, S.U. (2012) Genome-wide LORE1 retrotransposon mutagenesis and high-throughput insertion detection in *Lotus japonicus*. *Plant J.* **69**, 731–741.

Vierheilig, H., Coughlan, A.P., Wyss, U. and Piché, Y. (1998) Ink and vinegar, a simple staining technique for arbuscular-mycorrhizal fungi. *Appl. Environm. Microbiol.* **64**, 5004–5007.

Voelker, T.A., Worrell, A.C., Anderson, L., Bleibaum, J., Fan, C., Hawkins, D.J., Radke, S.E. and Davies, H.M. (1992) Fatty acid biosynthesis redirected to medium chains in transgenic oilseed plants. *Science*, **257**, 72–74.

Wang, E., Schornack, S., Marsh, J.F., Gobbato, E., Schwessinger, B., Eastmond, P., Schultze, M., Kamoun, S. and Oldroyd, G.E.D. (2012) A common signaling process that promotes mycorrhizal and oomycete colonization of plants. *Curr. Biol.* **22**, 2242–2246.

Wewer, V., Brands, M. and Dörmann, P. (2014) Fatty acid synthesis and lipid metabolism in the obligate biotrophic fungus *Rhizophagus irregularis* during mycorrhization of *Lotus japonicus*. *Plant J.* **79**, 398–412.

Wu, G.-Z. and Xue, H.-W. (2010) *Arabidopsis* β-ketoacyl-acyl carrier protein synthase i is crucial for fatty acid synthesis and plays a role in chloroplast division and embryo development. *Plant Cell*, **22**, 3726–3744.

Yang, W., Pollard, M., Li-Beisson, Y., Beisson, F., Feig, M. and Ohlrogge, J. (2010) A distinct type of glycerol-3-phosphate acyltransferase with sn-2 preference and phosphatase activity producing 2-monoacylglycerol. *Proc. Natl Acad. Sci. USA*, **107**, 12040–12045.

Zhang, Q., Blaylock, L.A. and Harrison, M.J. (2010) Two *Medicago truncatula* half-ABC transporters are essential for arbuscule development in arbuscular mycorrhizal symbiosis. *Plant Cell*, **22**, 1483–1497.

Figure S1. Phylogenetic tree of acyl-ACP thioesterases from arbuscular mycorrhiza host and non-host plants.

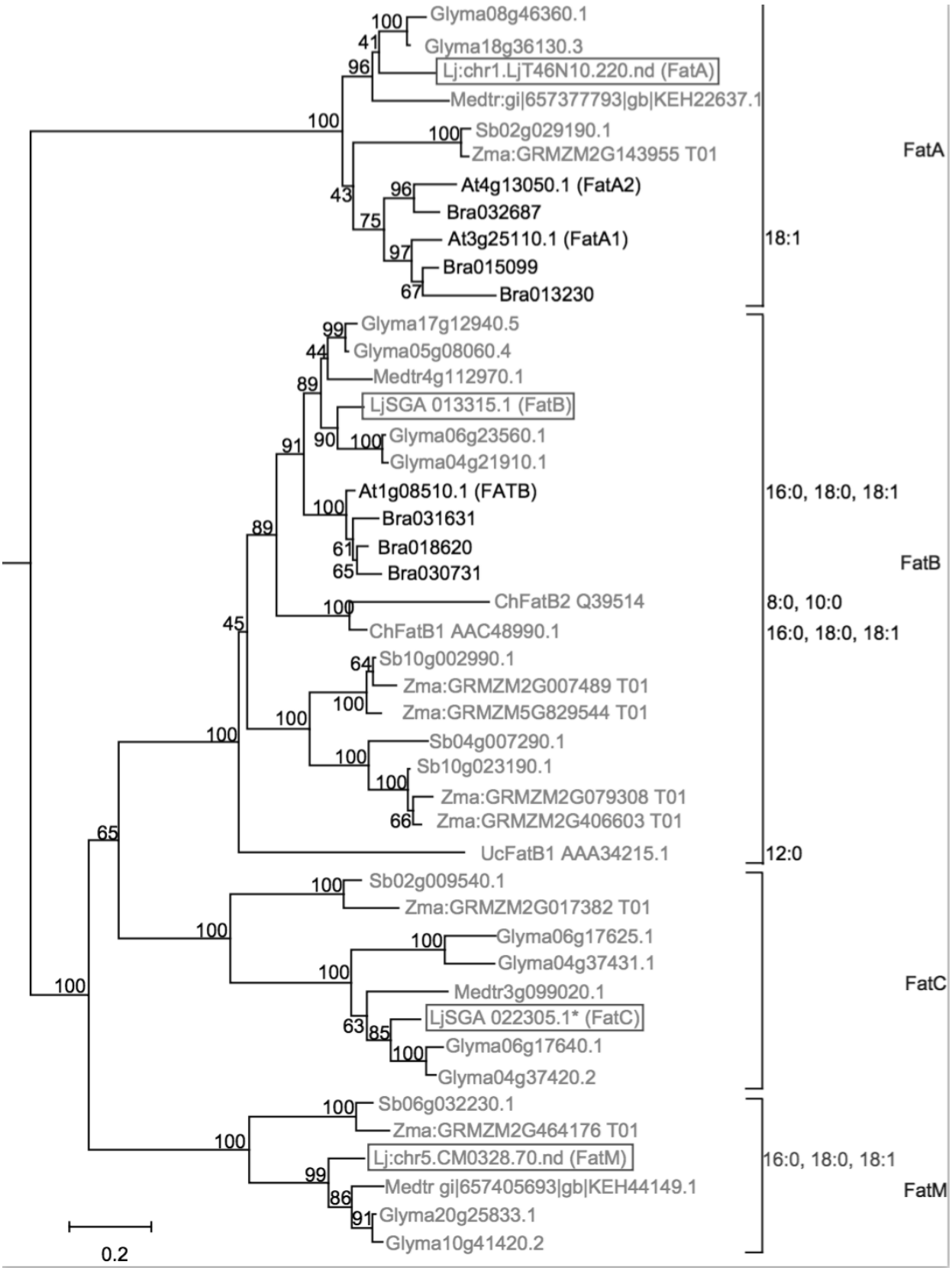

Figure S2. Genetic complementation of defective arbuscule morphology in the *fatm-1* mutant.

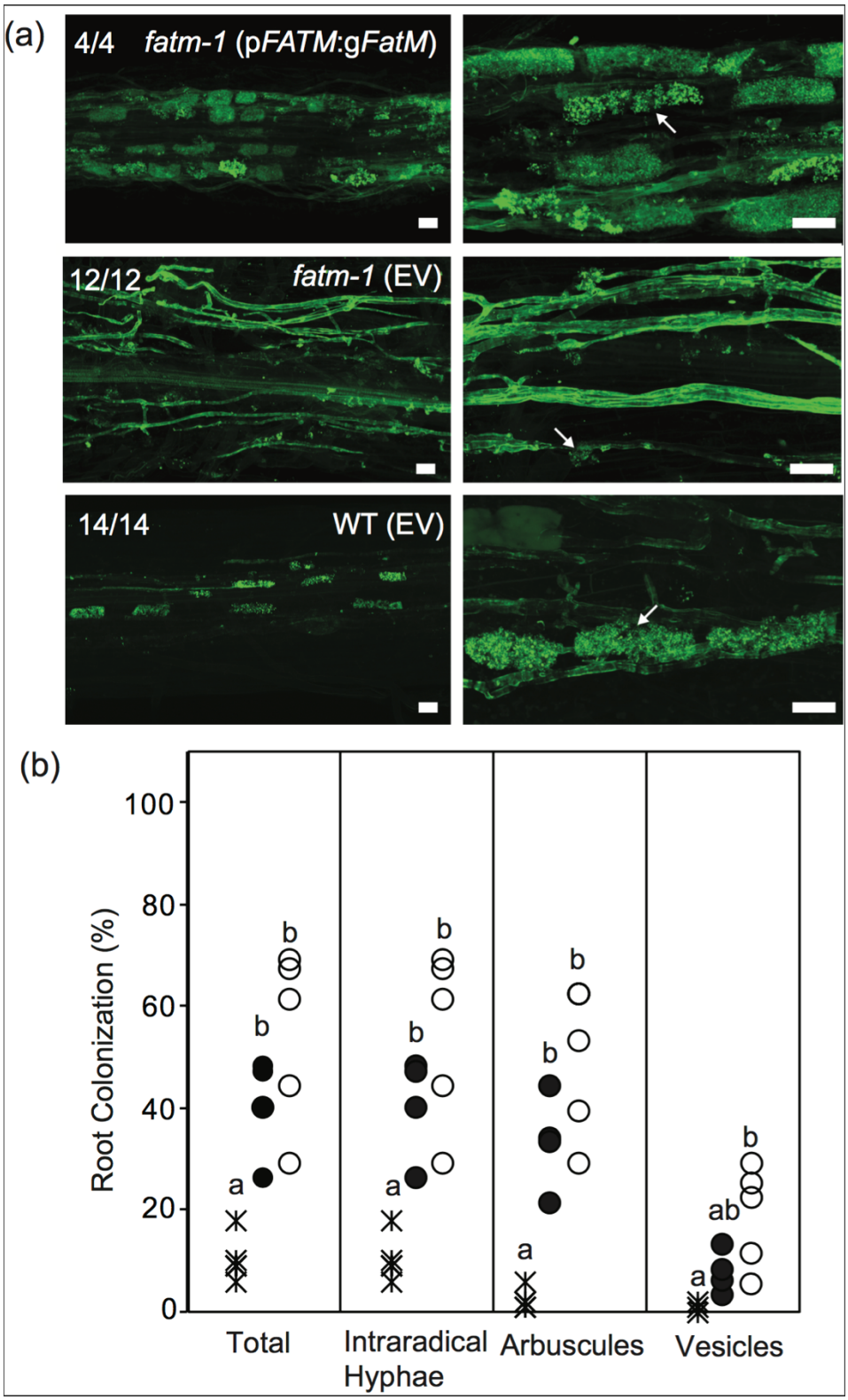

Figure S3. Quantification of total fatty acids in colonized *fatm* mutant roots.

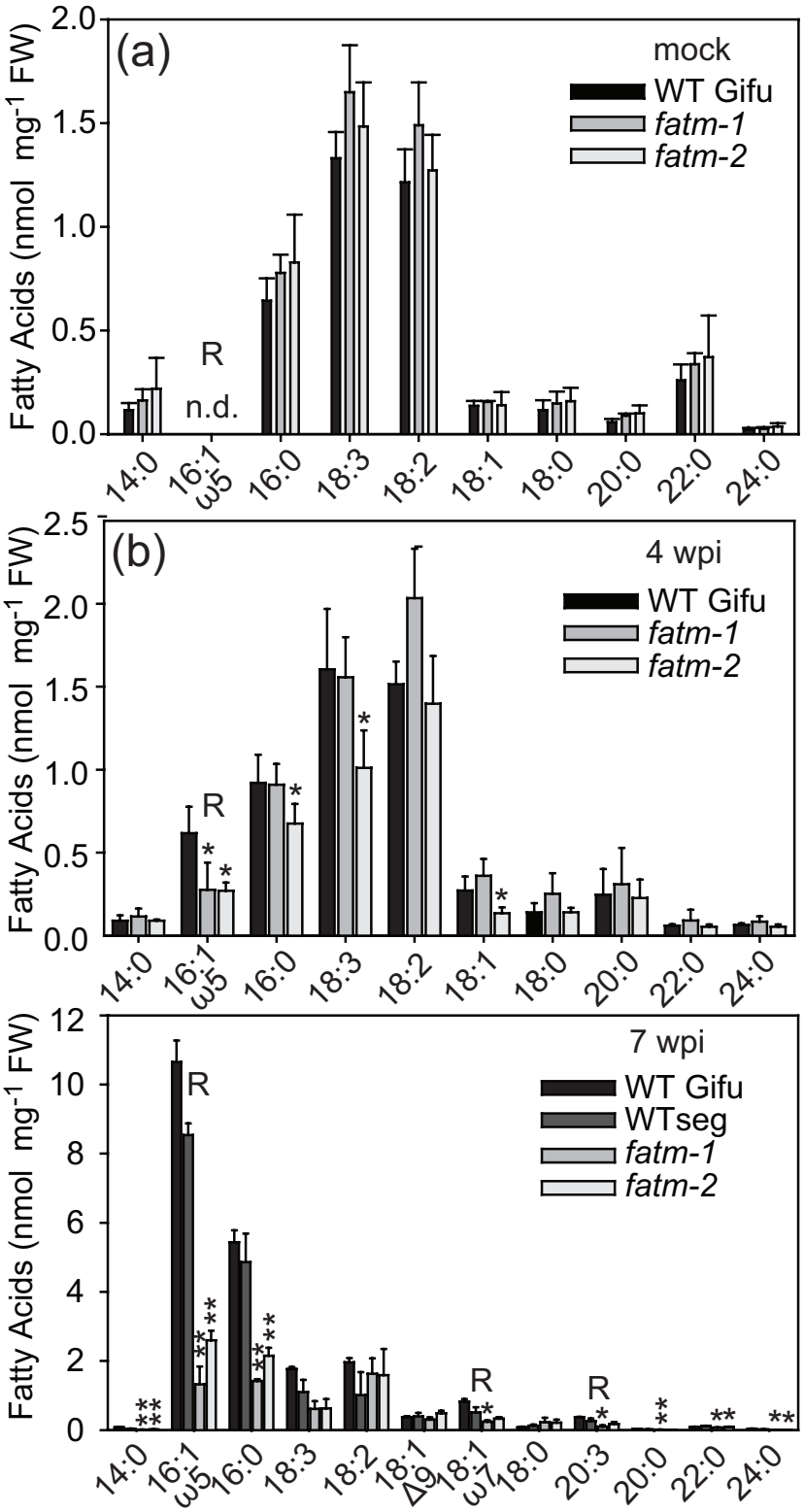

Figure S4. Relative distribution of triacylglycerol and diacylglycerol molecular species in colonized wild type Gifu and *fatm-1* and *fatm-2* mutant roots at 4 weeks post-inoculation.

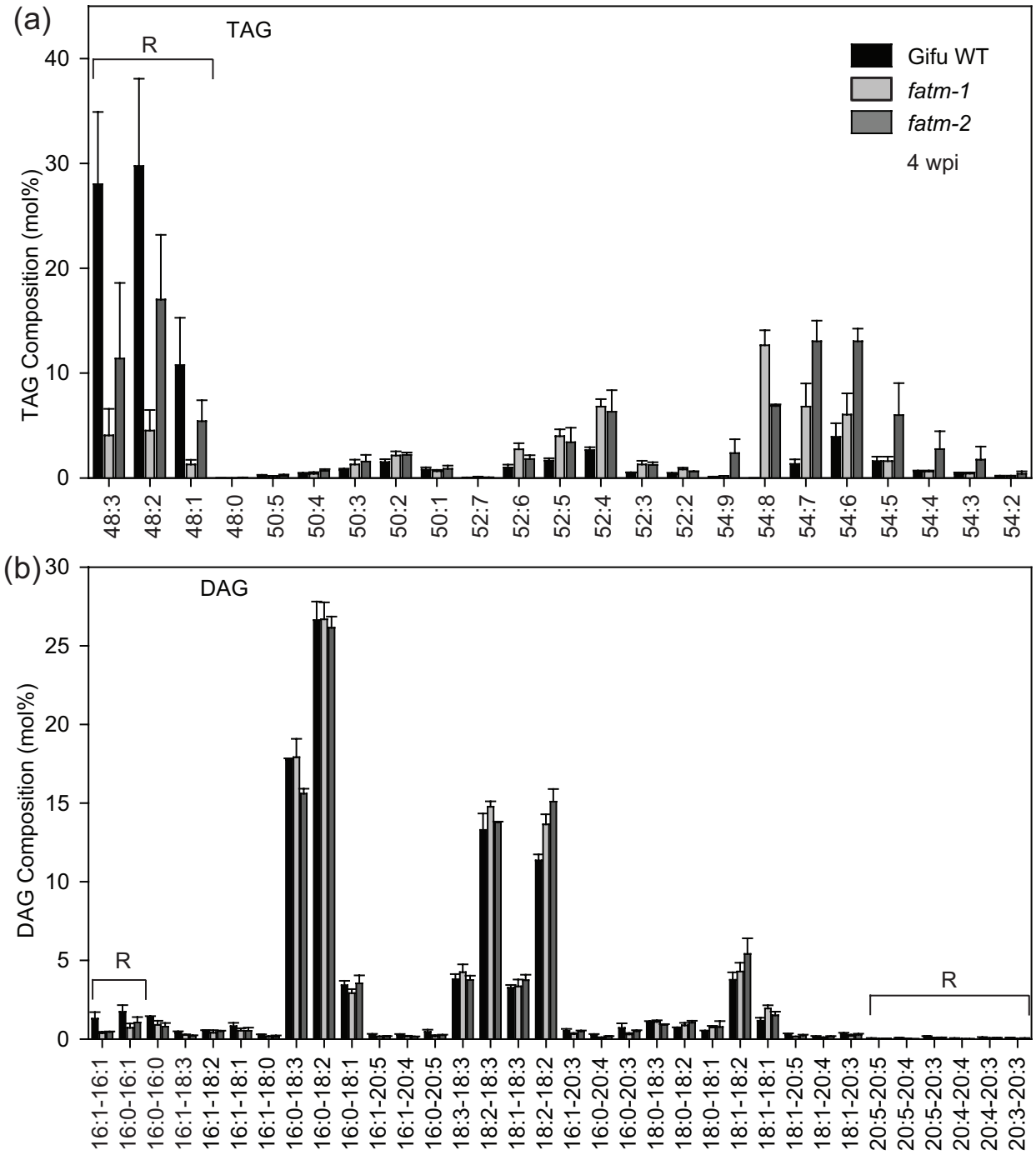

Figure S5. Molecular species composition of membrane glycerolipids in colonized WT Gifu, *fatm-1* and *fatm-2* mutant roots at 4 weeks post-inoculation.

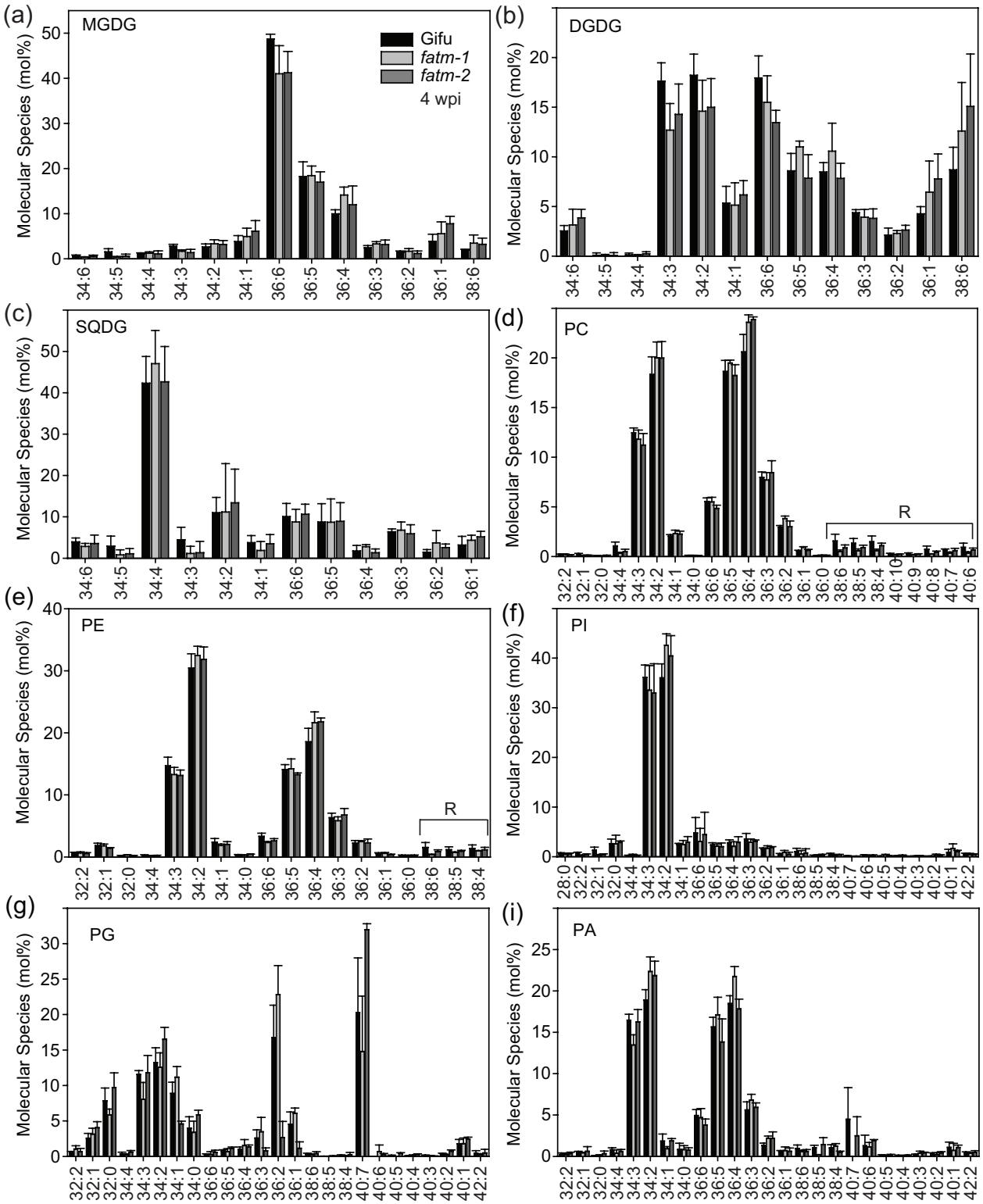

Figure S6. Monoacylglycerol in *Lotus japonicus fatm* and *Daucus carota* roots.

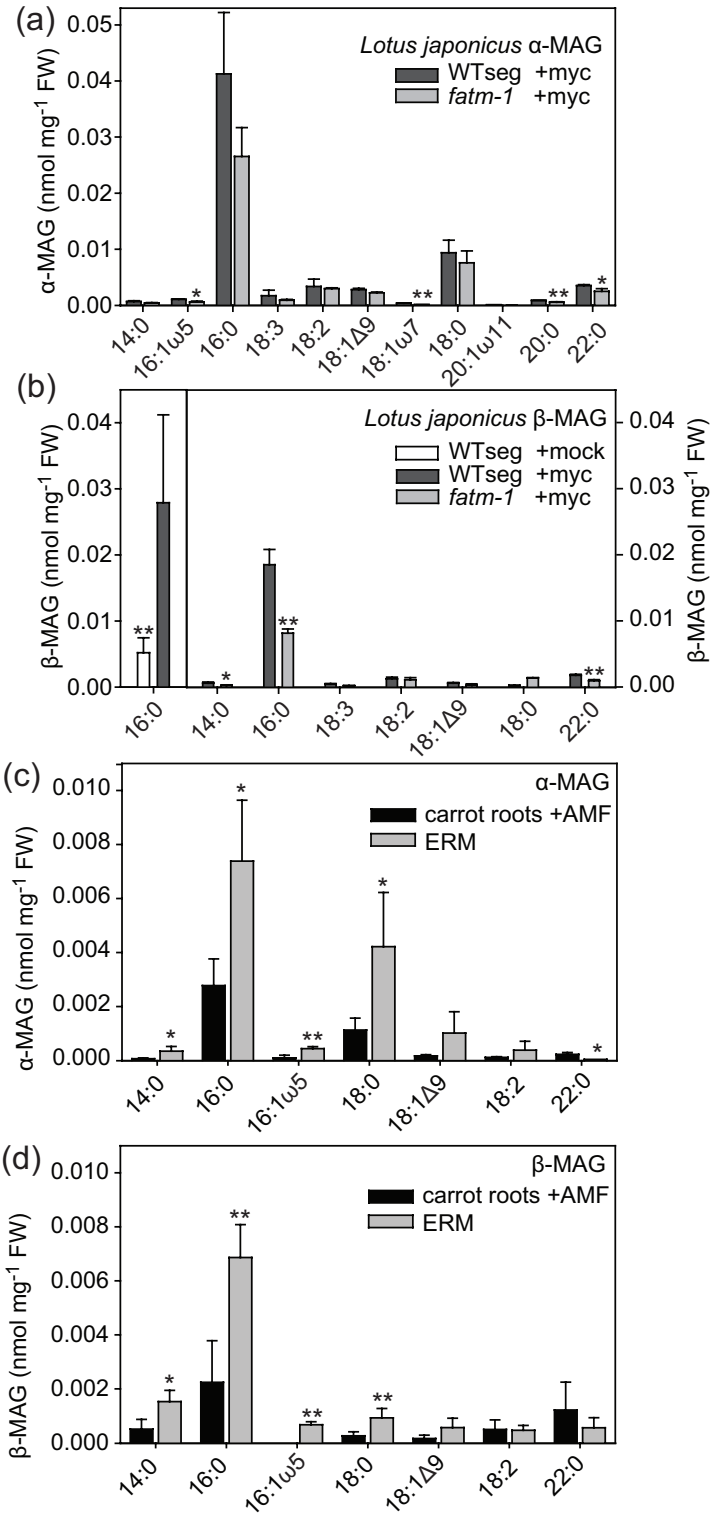

Figure S7. Expression patterns of *FatM, FatA, FatB* and *FatC* from *Lotus japonicus.*

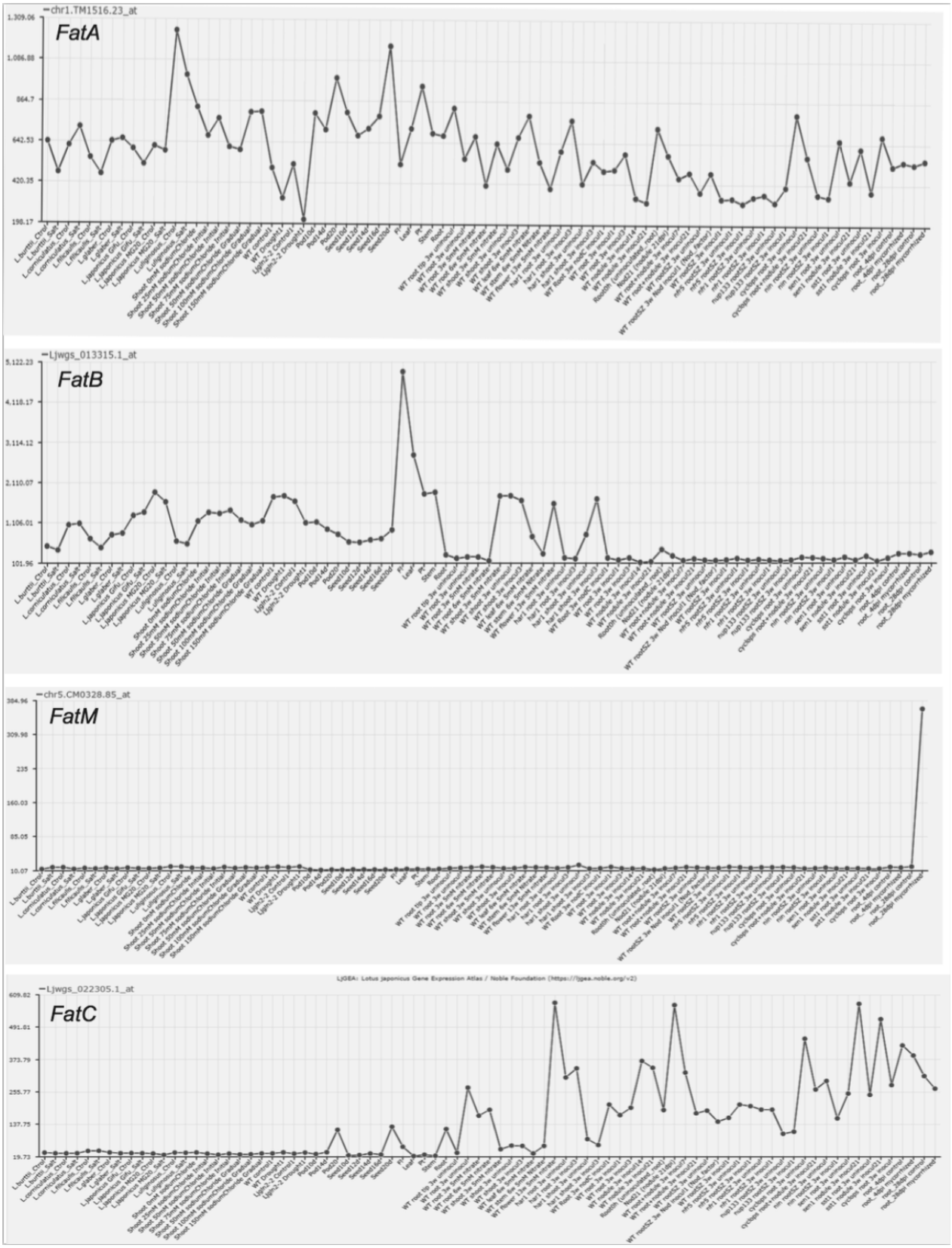

Figure S8. Specific inhibition of 16:1ω5 and 20:3 synthesis in colonized *fatm* mutant roots.

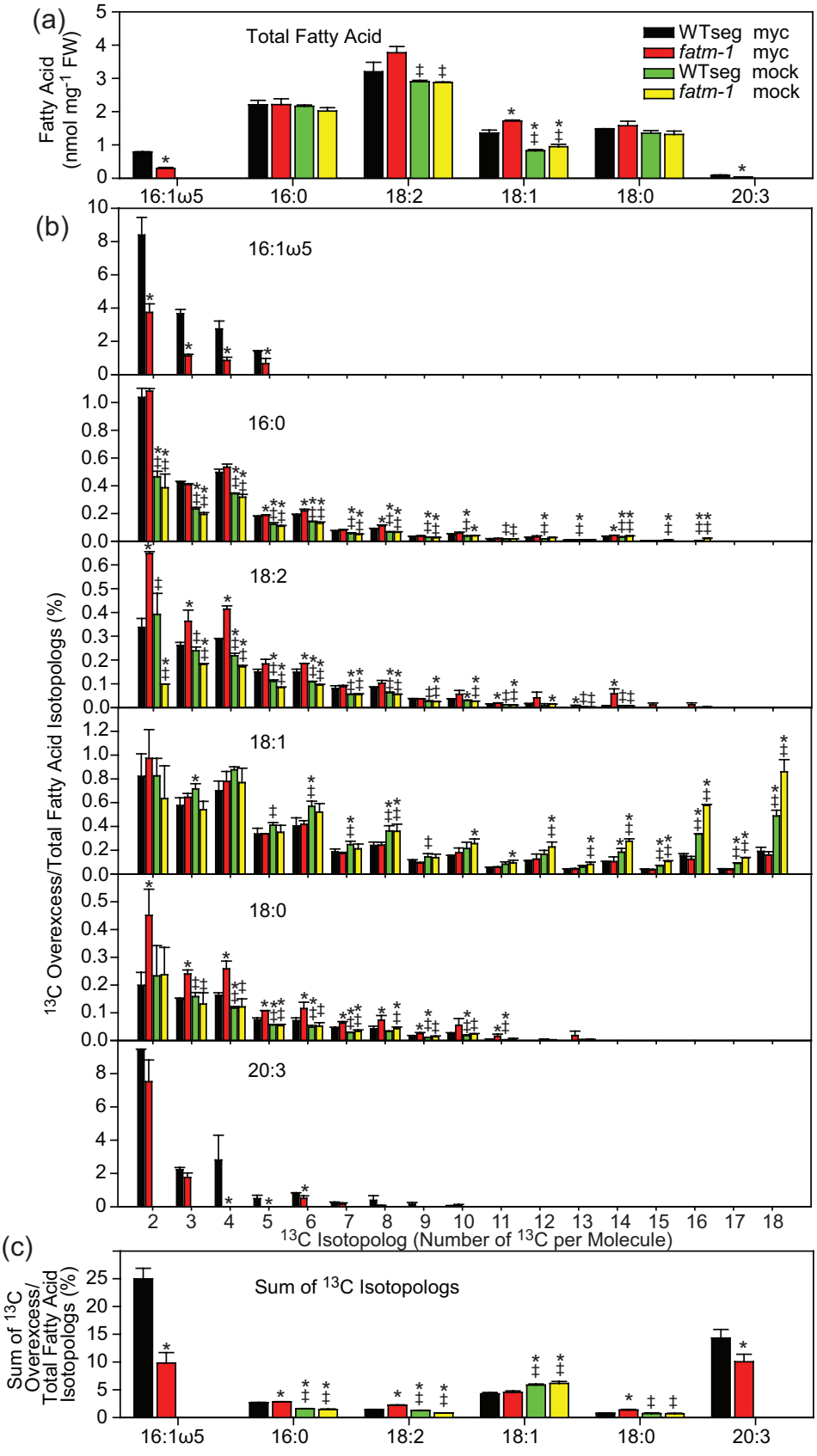

Table S1. Oligonucleotides used for cloning, RT-PCR and genotyping.

Oligonucleotide	Sequence (5'-3')	PCR, Target DNA	Reaction conditions
Expression in	*E. coli*		
FW (bn2340) RW (bn2335)	GCGGGATCCGAGACACTTAGCCACA CGCAAGCTTTAGGTGGAAAATGGAA	Expression of *FatM* in *E. coli*	98°C-30 s, 15 cycles: (98°C-10 s, 57°C-20 s, 7 °C- 35 s), 98°C- 30 s, 20 cycles: (98°C-10 sec, 72°C -25 sec, 72°C- 120 s)
RT-PCR			
FW (bn2221) RW (bn2222)	GAAGGACTCTTGCGGATTAC GAGGCCACAACAAACGATAC	RT-PCR, *Lotus UBI*	95°C-120 s, 30 cycles: (94°C-30 s, 60°C-40 s, 72°C- 40 s), 72°C-10 min
FW (bn2508) RW (bn2509)	GAAGAGCATCCCGTTCTGTT TCTGCTGAAGTGGTAAACGAG	RT-PCR, *Lotus ACT*	95°C-120 s, 30 cycles: (94°C-30 s, 62°C -40 s, 72°C-40 s), 72°C-10 min
FW (bn2027) RW (bn2028)	ACAAGACGCCTCTCCAAAC GTTCCCAATGGCTACTACTTCC	RT-PCR, *Lotus FatM*	95°C-120 s, 30 cycles: (94°C-30 s, 58°C -40 s, 72°C- 40 s), 72°C-10 min
FW (bn2456) RW (bn2457)	GGACTTGTGCCTAGAAGAGCA GCGGTTGATCTCAAGTCCTT	RT-PCR, *Lotus FatA*	95°C-120s , 30 cycles: (94°C-30 s, 60°C-40 s, 72°C-40 s), 72°C-10 min
FW (bn2500) RW (bn2501)	GGGTGGATTCTGGAGAGTGC TGGAACTCGATTCAAAGCATCA	RT-PCR, *Lotus FatB*	95°C-120 s, 30 cycles: (94°C-30 s, 60°C -40 s, 72°C- 40 s), 72°C-10 min
FW (bn2502) RW (bn2503)	ATCTGGGTTGGCTCCAAGG AGTGTGTGTATTGCAGGTCAG	RT-PCR, *Lotus FatC*	95°C-120 s, 30 cycles: (94°C-30 s, 60°C -40 s, 72°C- 40 s), 72°C-10 min
FW (bn2454) RW (bn2455)	CACTCGTCGGAACGTTATCC AGGATGCCTTGAAACCTGCT	RT-PCR, *Lotus PT4*	95°C-120 s, 30 cycles: (94°C-30 s, 58°C -40 s, 72°C-40 s), 72°C-10 min
FW (bn1942) RW (bn1943)	TGTCCAACCGGTTTTAAAGT AAAGCACGTTTGGCGTACAT	RT-PCR, *Rhizophagus α-TUB*	95°C-120 s, 30 cycles: (94°C-30 s, 56°C-40 s, 72°C- 30 s), 72°C-10 min

Genotyping			
FW (bn 2306) RW (bn 2307)	CGGCTCGAACAAGATTGACTCAGTGGA AGCCCTTGGCGATGAGGATCAACC	Genotyping of insertion in *fatm*-1	95°C-180 s, 5 cycles: (95°C-30 s, 72°C-75 s), 10 cycles: (95°C-30 s, 72°C to 68°C with -0.5 °C per cycle, 72°C-45 s), 20 cycles: (95°C-30 s, 68°C-30 s, 72°C-45 s), 72°C-10 min
FW (bn 2300) RW (bn 2301)	CGGCTCGAACAAGATTGACTCAGTGGA AGCCCTTGGCGATGAGGATCAACC	Genotyping of insertion in *fatm*-2	95°C-180 s, 5 cycles: (95°C-30 s, 72°C-75 s), 10 cycles: (95°C-30 s, 72°C to 68°C with -0.5 °C per cycle, 72°C-45 s), 20 cycles: (95°C-30 s, 68°C-30 s, 72°C-45 s), 72°C-10 min
Golden Gate Cloning			
FW (bn 3016) RW (bn 3017)	ATGAAGACTTTACGGGTCTCAGCGGGAATGATCATTATGCCAACA ATGAAGACTTCAGAGGTCTCTCAGATCTTTTTTCTATTTTTTTGG	p*FatM* cloning for p*FatM*:*gFatM*	98°C-30 s, 10 cycles: (98°C-7 s, 52°C-20 s, 72°C- 50 s), 25 cycles: (98°C-7 s, 72°C-20 s, 72°C- 50 s),72°C-2 min
FW (bn 3018) RW (bn 3021)	ATGAAGACTTTACGGGTCTCACACCATGGCTGCTACTTTCACATT TAGAAGACAAAGATCACTTATAAATAGGGTATCC	g*FatM* fragment 1 cloning for p*FatM*:*gFatM*	98°C-30 s, 10 cycles: (98°C-7 s, 55°C-20 s, 72°C- 20 s), 25 cycles: (98°C-7 s, 66°C-20 s, 72°C- 20 s),72°C-2 min
FW (bn 3020) RW (bn 3023)	TAGAAGACAAATCTTCAATGAACGGATCCAGCAT TAGAAGACAAGACTTTCTCATGAAGTAGTTAAAT	g*FatM* fragment 2 cloning for p*FatM*:*gFatM*	98°C-30 s, 10 cycles: (98°C-7 s, 54°C-20 s, 72°C- 17 s), 25 cycles: (98°C-7 s, 66°C-20 s, 72°C- 17 s),72°C-2 min
FW (bn 3022) RW (bn 3019)	TAGAAGACAAAGTCTCATGGGCTTCAGTGTTTTG ATGAAGACTTCAGAGGTCTCTCCTTCTTCCACACTTATTGCTAGG	g*FatM* fragment 3 cloning for p*FatM*:*gFatM*	98°C-30 s, 10 cycles: (98°C-7 s, 62°C-20 s, 72°C- 50 s), 25 cycles: (98°C-7 s, 72°C-20 s, 72°C- 50 s),72°C-2 min

Table S2. Generation of constructs for complementation

Purpose	Construct	Description
Golden Gate level 0 and I (L0, LI) elements		
L0 subcloning of p*FatM* without mutagenesis	L0 pJET1.2 p*LjFatM*	PCR amplification from genomic DNA of *L. japonicus* Gifu wild type. *FatM* 1.8 kb promoter fragment (p*FatM*) with bn 3016 + bn 3017 (1850 bp) and assembly by blunt-end ligation into L0 pJET1.2.
L0 subcloning of *gFatM* with mutagenesis	L0 pJET1.2 *gFatM*-Fragment1 L0 pJET1.2 *gFatM*-Fragment2 L0 pJET1.2 *gFatM*-Fragment3	Assembled by blunt-end ligation of *gFatM* PCR fragment 1, 2 and 3 into L0 pJET1.2 plasmid amplified from genomic DNA of *L. japonicus* Gifu wild type. Primers: Fragment 1: bn 3018 + bn 3021 (643 bp) Fragment 2: bn 3020 + bn2023 (388 bp) Fragment 3: bn 3022 + bn2019 (2244 bp)
LI p*FatM* module generation	LI p*LjFatM*	Assembled 1 fragment from L0 pJET1.2 p*LjFatM* by *BpiI* cut-ligation into LI-pUC57+BpiI plasmid (BB03).
LI *gFatM* module generation	LI *gFatM*	Assembled 3 fragments from L0 pJET1.2 *gFatM* 1,2,3 by BpiI cut ligation into LI-pUC57+BpiI plasmid (BB03).
Golden Gate level II (LII) plasmids		
LII construct generation	LIIc 1_2 p*FatM:gFatM* (pAK44)	Assembled by BsaI cut ligation from: LI A-B p*LjFatM* + LI B-C dy (BB06) + LI *gFatM* + LI D-E dy (BB08) + LI E-F NosT (G006) + LI F-G dy (BB09) + LIIc F 1_2 (BB30)
LII construct generation	LIIc 1_2 p*FatM:EV* (pAK45)	Assembled by BsaI cut ligation from: LI A-B p*LjFatM* + LI B-C dy (BB06) + LI C-D dy (BB07) + LI D-E dy (BB08) + LI E-F NosT (G006) + LI F-G dy (BB09) + LIIc F 1_2 (BB30)
	LIIc 3_4 p35s:*mCherry* (pAK18)	Assembled by BsaI cut ligation from: LI A-B p*35s* (G005) + LI B-C dy (BB06) + LI C-D *mCherry* (G057) + LI D-E dy (BB08) + LI E-F 35sT (G059) + LI F-G dy (BB09) + LIIc R 3_4 (BB34)
Golden Gate level III (LIII) plasmids for plant transformation		
Genetic complementation of *fatm-1*	LIIIβ F A-B p*FatM*:*gFatM* (pAK46)	Assembled by BpiI cut ligation from: LIIc 1_2 p*FatM:gFatM* + LII 2-3 ins (BB43) + LIIc R 3-4 p*35s:mCherry* + LII 4-6 dy (BB41) + LIIIβ F A-B (BB53)
Genetic complementation of *fatm-1*	LIIIβ F A-B p*FatM*:*EV* (pAK47)	Assembled by BpiI cut ligation from: LIIc 1_2 p*FatM:EV* + LII 2-3 ins (BB43) + LIIc R 3-4 p*35s:mCherry* + LII 4-6 dy (BB41) + LIIIβ F A-B (BB53)

Manuscript I: Defective lipid biosynthesis genes of *Arabidopsis thaliana* perturb colonization by the filamentous pathogenic oomycete *Hyaloperonospora arabidopsidis*

Reference: **Keymer A.**, Brands M., Banhara A., Dörmann P, Parniske M., Gutjahr C. (2018). Defective lipid biosynthesis genes of *Arabidopsis thaliana* perturb colonization by the filamentous pathogenic oomycete *Hyaloperonospora arabidopsidis*

Title:

Defective lipid biosynthesis genes of *Arabidopsis thaliana* perturb colonization by the filamentous pathogenic oomycete *Hyaloperonospora arabidopsidis*

Abstract:

The ability of plants to establish close associations with filamentous microbes probably enabled plant colonization of terrestrial environments about 400 million years ago. The mutualistic association of plants with arbuscular mycorrhiza fungi is well known and its reciprocal nutrient transfer is a favorable characteristic. Accumulating data suggest that several developmental and morphological features are shared among beneficial and detrimental microbes, which implies that pathogens might exploit ancestral symbiotic plant pathways to colonize their hosts. Lipid transfer from plants to fungi was recently reported for arbuscular mycorrhiza symbiosis in legume roots and the pathogenic fungus *Erysiphe cichoracearum* on *Arabidopsis* leaves. In this study we discovered an altered development and impaired reproduction of the biotrophic oomycete *Hyaloperonospora arabidopsidis* on *Arabidopsis* fatty acid and lipid biosynthesis mutants. Our results suggest the importance of host lipid biosynthesis not only for the developmental success of fungi but also for plant-colonizing oomycetes such as *Hyaloperonospora arabidopsidis.*

Introduction:

Plants engage in mutualistic and pathogenic endosymbioses with a wide variety of microorganism from bacteria and fungi to oomycetes (Parniske 2000). These diverse plant-microbe interactions affect equally plant and microbial development and performance.

Among these oomycetes represent a lineage of eukaryotic microorganisms that have been early associated with plants. Oomycetes might have been among the first eukaryotes on Earth and many members emerged as endophytes of plants 300-350 million years ago (Krings et al. 2011). Although, being characterized by features resembling fungi, such as hyphal growth and proliferation via spores, oomycetes do not belong to the *Mycota* but to the kingdom of *Straminipila*, which means that they are more related to diatoms and brown algae than to true fungi (Dick 2001). A major discrimination between true fungi and oomycetes is the nature of the cell wall. Whereas

fungal walls are chitin based, oomycete cell walls consist of cellulose (Slusarenko and Schlaich 2003).

Oomycete lifestyles range from biotrophy to necrotrophy and from obligate to facultative pathogenesis (Judelson 2017). The obligate biotrophic oomycete *Hyaloperonospora arabidopsidis* (*Hpa*) belongs to the group of *Peronosporaceae,* which comprises only plant parasites, including severe pathogens like *Phytophthora, Phytium* and *Albugo spec.* (Judelson 2017). *Hpa* is also a prominent pathogen causing downy mildew symptoms on its host plant *Arabidopsis thaliana* (Coates and Beynon 2010; Kamoun et al. 2015).

The *Hpa* life cycle starts with an asexual conidiospore, which germinates on top of a plant leaf and produces an attachment structure, named appressorium. This leads to hyphal penetration into the plant tissue. The hypha inserts a haustorium in at least one epidermal plant cell, which mark the start of hyphal colonization of the mesophyll. Subsequently, *Hpa* starts branching inside the intercellular space of the mesophyll. The colonization is further characterized by embedding of digit-like haustoria into single mesophyll cells. Conidiophores, asexual reproduction organs, develop from hyphal tips in substomatal cavities. Approximately seven days post infection, the mature conidiophores emerge through stomata and form tree-shaped sporangiophores, which carry asexual conidiospores. Sexual reproduction is initiated by interlacing hyphae which form oogonia and paragynous antherida in the leaf/cotyledon. Oogonia subsequently produce sexual oospores. Oospores germinate in favorable conditions to initiate a new life cycle (Koch and Slusarenko 1990; Mauch-Mani and Slusarenko 1993; Slusarenko and Schlaich 2003; Soylu and Soylu 2003).

Strikingly, on a morphological level, plant associated filamentous microbes from different kingdoms seem to share distinct colonization features. No matter if beneficial or pathogenic, filamentous microbes colonize the plant tissue via a dense hyphal network and establish specialized structures, which are inserted into single plant cells to serve as interaction interface between the host and the microbe (Parniske 2000). The form of those structures varies drastically between the different microbes. It includes digit-, knob- or peg-like haustoria of fungal pathogens or oomycetes as well as the structurally highly sophisticated arbuscules of the beneficial arbuscular mycorrhiza fungi (AMF) (Carella et al. 2018; Gutjahr and Parniske 2013; Parniske 2000). However, the function of these different microbial interface structures is believed to be quite similar. Both, haustorium and arbuscule facilitate microbial

colonization by serving as an interface for communication, nutrient exchange and host cell manipulation via the release of effector molecules (Rey and Schornack 2013; Parniske 2000). Interestingly, upon insertion, all interface structures do not break the plant membrane but are enveloped by a newly formed plant-derived peri-microbial membrane, which is highly specialized in composition and function (Parniske 2000).

Considering these developmental commonalities of beneficial and detrimental filamentous microbes, it appears promising to investigate the conservation of developmental and functional processes to gain insights into fundamental mechanisms, which promote plant-microbe interactions.

In order to discover these potential common core components of plant-microbe associations, profound knowledge about the advantages for microbes arising from interaction with the host plant is essential. Especially for biotrophic endosymbionts like AMF and *Hpa* host contribution of nutrients seems to be indispensable, as these microbes are not able to complete their life cycles independently. Accordingly, genomes of both microbes comprise a clear signature for biotrophy, which is characterized by a reduced metabolic complexity and loss of essential pathways. For example, both microbes lost the ability to synthesize thiamine (Tisserant et al. 2013; Judelson 2012). Further, *Hpa* has lost enzymes for assimilation of inorganic sulfur and nitrate and synthesis of arachidonic acid (Baxter et al. 2010; Judelson 2017). AMF genomes do not harbor genes encoding for *de novo* fatty acid synthesis in addition to their thiamine auxotrophy (Tisserant et al. 2013; Wewer et al. 2014). In consequence, lipids are transported from the plant to the fungus, potentially as an energy-rich carbon source and to produce membranes (Jiang et al. 2017; Luginbuehl et al. 2017; Keymer et al. 2017). Subsequently, arbuscular mycorrhiza host plants, harboring causative mutations in AM-specific lipid genes, exhibit severe perturbance of this beneficial association which is phenotypically observable by a reduced fungal colonization, a high proportion of degenerated arbuscules and a drastically reduced number of vesicles in the fungal intraradical mycelium (Bravo et al. 2017; Jiang et al. 2017; Luginbuehl et al. 2017; Keymer et al. 2017; Brands et al. 2018).

Interestingly, dependence on host lipids or lipid parasitism occurs in a range of interorganismic associations with participants from almost all kingdoms (Keymer and Gutjahr 2018). In the present study, we tested the hypothesis if also the hyphal pathogen *Hpa* relies on host fatty acid and lipid biosynthesis genes for a successful completion of its biotrophic life cycle.

A. thaliana is probably the best studied plant species. Hence, considerable research effort has already been taken on fatty acid (FA) and lipid biosynthesis in this organism, and mutants are readily available.

Plant lipid biosynthesis starts with the production of FAs in the plastids (Li-Beisson et al. 2017). Starting from Acetyl-CoA (2C), the respective FA carbon chain is elongated via the consecutive addition of malonyl-ACP, which provides two carbon units in each elongation cycle. This elongation cycle is performed by three different types of β-keto-acyl ACP synthases (KAS). KASIII performs the first condensation reaction to form a C4-ACP, KASI catalyzes elongation from C4 to C16 and KASII subsequently facilitates the production of 18:0-ACP (Li-Beisson et al. 2010). *KASI* is a single-copy gene in *Arabidopsis.* A T-DNA insertion in the 5' UTR results in reduced *KASI* expression and enzyme activity (Wu and Xue 2010). *kasI* plants exhibit smaller and variegated leaves, perturbed chloroplast division in early developmental stages and dramatic change in polar lipid metabolism – especially of 16:x and 18:x FA containing lipids (Wu and Xue 2010; Keymer et al. 2017).

Glycerol-3-phosphate acyltransferases (GPATs) comprise a large group of enzymes which catalyze the esterification of fatty-acyl moieties to glycerol-3-phosphte (G3P) in a regio-specific manner (Chen et al. 2011; Yang et al. 2010). Localizing to different compartments such as plastids, mitochondria or the endoplasmic reticulum (ER), GPATs are involved in diverse metabolic pathways and physiological functions (Chen et al. 2011). Ten *GPAT*-encoding genes are found in the *Arabidopsis* genome (Yang et al. 2010). Eight of these paralogues comprise a phylogenetically distinct group of land-plant specific GPATs (Yang et al. 2010). These plant-specific GPATs fuse acyl-moieties regio-specifically to the *sn2* position of G3P (Yang et al. 2010; Yang et al. 2012). Their products are not used for membrane or storage lipid production but are exported and serve as precursors for cutin and suberin biosynthesis (Li, Beisson, Ohlrogge, et al. 2007).

Localized to the ER, GPAT4, GPAT6 and GPAT8 are members of this land-plant specific clade and are crucial for the production of cutin monomers (Li, Beisson, Ohlrogge, et al. 2007; Li-Beisson et al. 2009; Gidda et al. 2009; Chen et al. 2011). Interestingly, these GPAT proteins exclusively work bifunctional. GPAT4/6/8 do not only contain a *sn2*-acytransferase but also a phosphatase domain, which enables them to produce *sn2*-MAG. In contrast, monofunctional GPATs lack the phosphatase domain and build *sn2*-lysophosphatidic acid (LPA) (Yang et al. 2010; Yang et al. 2012).

Arabidopsis gpat6 mutants showed normal vegetative growth but abnormal flowers, which coincides with a significant reduction of cutin monomers and lack of nanoridges in this organ (Li-Beisson et al. 2009). GPAT4 and GPAT8 seem to be redundant in function. Only double knockouts (*gpat4x8*) exhibited phenotypes such as reduced rosette growth, a higher water-loss rate and a significant reduction of cutin in stems and leaves (Li et al. 2007). Although, *Atgpat6* and *Atgpat4x8* exhibit distinct morphological phenotypes, likely due to the individual expression pattern of the genes, both mutants reveal reduced levels of C16 cutin monomers, which evidences their common enzymatic preference for C16 fatty acids (Li et al. 2007; Mazurek et al. 2017; Yang et al. 2012).

We hypothesized that the development of the biotrophic pathogen *Hpa* on *Arabidopsis thaliana* is dependent on a functional host-lipid biosynthesis, which simiar to AM symbiosis depends on KASI, GPAT 4, 6 and 8. In this study, we challenged fatty acid as well as lipid biosynthesis mutants of *Arabidopsis*, carrying causative mutations in these genes with the biotrophic pathogen *H. arabidopsidis* (Li et al. 2007; Li-Beisson et al. 2009; Wu and Xue 2010). Based on a combination of microscopic characterization, lipid profiling and gene expression analysis, this study provides evidence that plant fatty acid/lipid biosynthesis is an essential factor for the development of *Hpa* in *Arabidopsis* cotyledons and leaves.

Results:

***H. arabidopsidis* exhibits morphological aberrancies on cotyledons of *A. thaliana* lipid biosynthesis mutants.** To investigate if plant FA/lipid biosynthesis effects oomycetal colonization, we challenged *kasI, gpat6* and *gpat4x8* cotyledons with *Hpa* Noco2 spores. Strikingly, *Hpa* development exhibited drastic morphological aberrancies in all mutants, while its development was normal in wildtype and *kasI* mutant plants complemented with the wildtype. *Hpa* formed regular hyphae and predominantly regular and round-shaped haustoria in wildtype cotyledons. In contrast, in *kasI* mutant cotyledons the hyphae appeared bulbous and significantly thickened and featured a significant higher proportion of morphological altered haustoria (Fig. 1A, B, E). Whereas the majority of haustoria appeared regular round-shaped in wildtype cotyledons, haustoria with multiple lobes (multilobed) were significantly enriched on *kasI* mutants (Fig. 1A, B, E). The exact same phenotypes were observed in two allelic mutants of *gpat6* (Figure 1A, C, F) and a *gpat4x8* line (Figure 1A, D, G).

However, quantitative colonization of *Hpa* seemed not to be affected in any of the mutants on visual inspection, which suggest that the epidermal infection process and the hyphal progression in the mesophyll is not restricted by a dysfunctional plant lipid biosynthesis.

Reproductive success of *Hpa* is compromised in *Arabidopsis* lipid biosynthesis mutants. Conidiophores, the asexual reproductive organs of oomycetes, develop out of hyphal tips in substomatal cavities of *Arabidopsis* leaves. The mature conidiophores emerge through stomata and form tree-shaped sporangiophores, which carry asexual conidiospores (Thines and Kamoun 2010). The number of *Hpa* sporangiophores per cotyledon was significantly reduced on all mutant leaves compared to wildtype controls (Figure 2 A-C). Thus, asexual reproduction of *Hpa* in *kasI, gpat6* and *gpat4x8* mutants is severely affected, which implies that *Hpa* suffers from reduced fitness on these lipid biosynthesis mutants.

Atkasl, Atgpat6* and *Atgpat4x8* showed increased amounts of cell death spots in interaction with *Hpa. Plant induced cell death is a symptom of the defense-related hypersensitive responses (HR), and is recognizable via trypan blue staining by dark-blue dye retention in single cells. To understand if the impaired hyphal and haustorial morphology of *Hpa* might be related to an altered defense response of the fatty acid/lipid bionsythesis mutants, we counted cell death spots which have been in direct contact to oomycetal hyphae or haustoria ("*Hpa*-associated cell death spots") and cell death spots per leaf which have not been associated with *Hpa* hyphae ("non-associated cell death spots") (Figure 3A). No difference was observed in the number of non-associated cell death events in *Hpa*-challenged leaves of any of the tested genotypes (Figure 3B-D). However, the number of *Hpa*-associated cell death spots was significantly higher in leaves of all fatty acid and lipid biosynthesis mutants compared to *Hpa*-infected wildtype leaves (Figure 3B-D), possibly indicating a role of plant lipids in compatibility or containment of defense responses.

Plants evolved different strategies to defend themselves against pathogen attacks (Boller and Felix 2009). Plant perception of pathogen-associated molecular pattern (PAMPs) or plant-derived damage-associated molecular pattern (DAMPs) activates PAMP triggered immunity (PTI), which includes defense marker gene induction and callose deposition around microbial haustoria (Jones and Dangl 2006; Antolín-Llovera

et al. 2012; Gust, Pruitt, and Nurnberger 2017). To test if the higher amount of associated cell death spots in the mutants is due to an altered defense response, we quantified the expression of well-established marker genes, such as *FLG22-INDUCED RECEPTOR-LIKE KINASE 1* (*FRK1*) for flagellin response, *PLANT DEFENSIN 1.2a* (*PDF1.2a*) for jasmonate response, the salicylic acid immune response gene *PATHOGENESIS RELATED GENE 1* (*PR1*) and *GLUTATHIONE S-TRANSFERASE 1* (*GST1*), which is a marker for the reactive oxygen species response (Asai et al. 2002; Glazebrook 2005; Asai et al. 2014; Grant, Yun, and Loake 2000). *FRK1* and *PDF1.2a* did not show significantly altered transcript accumulation patterns in the *kasI* and *gpat6* mutant lines, as compared to wildtype in absence and presence of *Hpa* (Figure S1). Upon *Hpa* infection, the induction of *PR1* is apparently infringed in the *gpat6* background (Figure S1). Further, the transcripts of the reactive oxygen species response gene *GST1* were significantly elevated in *kasI* as compared to the wildtype in non-infected conditions. This might suggest increased ROS accumulation in the *kasI* mutant. However, *GST1* transcript levels in *Hpa*-challenged *kasI* and *gpat6* lines were not significantly altered compared to wildtype. Overall, the results of defense marker gene expression did not provide an explanation for the developmental aberrancies of *Hpa* in the mutant plants. Thus, the phenotype might rather be explained by direct effects on the oomycete than indirect effects through altered plant defense responses.

Lipid profiling of *Hpa*-infected *Arabidopsis* leaves and *Hpa* conidiospores revealed a fatty acid species which is exclusively present in *Hpa*. To characterize the role of KASI and GPAT4/6/8 in determining the lipid composition of *Hpa*-infected and non-infected control plants, we quantified diacylglycerols (DAGs), galactolipids and phospholipids in wildtype and all mutant lines. Profiles of monogalactosyldiacylglycerol (MGDG), phosphatidylcholine (PC) and phosphatidylethanolamine (PE) exhibited a response to *Hpa*-infection. *Hpa*-infected leaves from all tested genotypes showed a slight increase of PCs and PEs as well as a slight decrease of MGDGs (Figure 3A) However, no significant quantitative differences could be detected between treatment and genotypes for any of the tested lipid classes. Further, we also analyzed total fatty acid content in *Hpa*-infected and uninfected leaves of all plant genotypes as well as in *Hpa* conidiophores, which have been extracted from wildtype leaves. The abundance of most FA species did not differ

significantly for all plant genotypes in *Hpa*-challenged conditions, compared to control leaves (Figure 4B). However, the FA species 20:5 could only be detected in *Hpa*-containing material (Figure 4B). Thus, 20:5 FAs seem to be exclusively of *Hpa* origin and not present in uninfected plant material (Figure4B). The relative high abundance of this 20:5 species in total FA profiles of spore extracts, collected from wildtype leaves, strengthens this hypothesis. Moreover, measurements of TAG originating FAs confirmed this finding as 20:5 FA harboring triacylglycerols (TAGs) could exclusively be detected in *Hpa*-infected leaves and spore extracts but not in uninfected leaves (Figure 4C). Thus, 20:5 FA can be used as a marker FA to differentiate lipids of *Hpa* origin from those of plant origin.

Discussion:

The roles of *KASI* and land plant-specific *GPATs 4, 6* and *8* for *Arabidopsis* fatty acid and cutin biosynthesis respectively, have been studied well and corresponding mutants have been characterized (Wu and Xue 2010; Li et al. 2007; Li-Beisson et al. 2009). However, the knowledge about the importance of fatty acid/cutin biosynthesis for microbial interactions in *Arabidopsis* is still narrow. Research on plant-microbe interactions accumulated data suggesting a comprehensive role of plant fatty acids and lipids as drivers for mutualistic as well as pathogenic associations. For example, Wang et al. (2012) found that the hemibiotrophic oomycete *Phytophtora palmivora* forms appressoria *in vitro* when it is exposed to cutin monomers. Accordingly, root colonization by *P. palmivora* was impaired in the *Medicago RAM2* knockout mutant – RAM2 is a paralog of GPAT6 (Wang et al. 2012; Keymer et al. 2017). Recently, it has been shown that *GPAT6* controls antithetically the infection of *P. palmivora* and the necrotrophic fungus *Botrytis cinerea* in tomato. Whereas, *Sigpat6* exhibited increased susceptibility to the hemibiotrophic oomycete *Phytophthora,* the plant mutant showed increased resistance to the necrotoph *Botrytis cinerea* (Fawke et al. 2018). In AM symbiosis lipids have a predominant impact, as the host plant nourishes its fungal partner with lipids that are exclusively produced for this purpose. Interestingly, this transport is perturbed in *ram2* and a *KASI* mutant, called *dis* (Jiang et al. 2017; Luginbuehl et al. 2017; Keymer et al. 2017). Further, Jiang et al. showed that lipid transfer from host to microbe is also the case for the biotrophic fungus *Erysiphe cichoracearum* on *Arabidopsis* leaves (Jiang et al. 2017). Therefore, literature

suggests that the dependence on host-derived lipids or lipid parasitism is a shared phenomenon among diverse microbes (Keymer and Gutjahr 2018).

In our study, mutations in *Arabidopsis KASI, GPAT4,8* and *6* resulted in almost identical impairment of *Hpa* development. This might be surprising as the mutants show drastic morphological differences in their individual plant physiology (Li-Beisson et al. 2009; Li et al. 2007; Wu and Xue 2010). While *kasI* suffers from reduced rosette growth and perturbed chloroplast devision, *gpat4x8* exhibits reduced rosette growth as well as a perturbed cutin layer on stem and leaves (Wu and Xue 2010; Keymer et al. 2017; Li, Beisson, Koo, et al. 2007). *gpat6* mutants do not show any growth defects but lack nanoridge and cutin monomers in the flower (Li-Beisson et al. 2009). However, *KASI, GPAT4,8* and *6* seem to be interconnected as the mutation of *KASI* results in a significantly decreased content of 16:x and 18:x FA containing lipids, *gpat6* mutants display a drastic shortage of C16 cutin monomers but not C18 and *gpat4x8* mutants show significant reductions in both monomers (Li et al. 2007; Li-Beisson et al. 2009; Keymer et al. 2017; Wu and Xue 2010). It is most conceivably that the GPATs act in the same biosynthetic pathway with KASI and that C16 cutin monomers are the common denominator of all tested GPTATs. This enzymatic interconnection might provide the ground for the similar developmental defects of *Hpa* in leaves of these plant mutants.

Haustoria are the primary interface for host-microbe interaction, including nutrient transfer and effector delivery (Hahn et al. 1997; Voegele et al. 2001; Voegele et al. 2006; Struck et al. 1996; Whisson et al. 2007). We observed a significantly higher proportion of multilobed *Hpa* haustoria in *kasI, gpat6* and *gpat4x8* cotyledons compared to *Hpa*-infected wildtype cotyledons. Interestingly, the phenotype of multilobed haustoria of *Hpa* has already been described in *Arabidopsis* mutants of symbiosis signaling homologs (Ried et al. 2018). Additionally, Fawke et al. (2018) also reported a high frequency of aberrantly shaped *Phytophthora* haustoria in tomato *gpat6* leaves (Fawke et al. 2018). Even in wildtype leaves, the proportion of *Hpa* haustoria which appear multilobed increases with progressing time (Ried et al. 2018). Therefore, the alteration of haustorial morphology might be an age-related phenomenon. It remains still unclear, if the morphology of haustoria individually changes over time or if more multilobed haustoria are produced *de novo* at a certain time point. Localization of remorin AtREM2 at the extra-haustorial membrane (EHM) decreased over time and the decline of YFP-emitted fluorescence was linked to the

multilobed morphology (Ried et al. 2018). This suggests that the alteration in haustorial morphology might coincide with changes in protein composition of the EHM. Also, the plant defense mechanism of callose deposition around haustoria is associated with haustorial senescence (Sohn et al. 2007; Caillaud et al. 2014). Callose deposition is a likely consequence of the plant-driven traffic shut-off, which leads to haustorial senescence (Caillaud et al. 2014). In line with these findings, the observed higher proportion of multilobed haustoria on *Arabidopsis kasI, gpat6* and *gpat4x8* (Figure 1) may be due to an early haustorial senescence. In addition to the aberrant haustoria, *Hpa* exhibited also aberrancies regarding its hyphal morphology in *kasI, gpat6* and *gpat4x8* of *Arabidopsis*. In mutant cotyledons hyphae appeared significant thickened and bulbous. To our knowledge, this hyphal phenotype is first described in our study. Interestingly, Ried et al (2018) did not see thickened hyphae in combination with the multilobed haustoria on the tested *Arabidopsis* mutants of CSGs homologs (Ried et al. 2018). Further investigations are required to elucidate the exact cause of both phenotypes. Both phenotypes might be independent from each other but it may also well be that one affects the other.

The increased number of *Hpa*-associated plant cell death spots and the impaired reproductive success of *Hpa* on the tested fatty acid and lipid biosynthesis mutants clearly highlight that *KASI, GPAT4, 6* and *8* do not only affect oomycetal morphology but also *Hpa* performance and physiology.

Hpa colonizing *kasI, gpat6* and *gpat4x8* produced a significantly reduced number of asexually formed sporangiophores. Since sporangiophores emerge from hyphal tipis (Coates and Beynon 2010), the reduced number of sporangiophores might possibly be linked to the hyphal abnormality in the *Arabidopsis* mutants. Alternatively, reproduction might be hindered because of the coinciding increased proportion of defective haustoria, which might negatively influence the hyphal fitness.

Hpa-challenged leaves of *kasI, gpat6* as well as *gpat4x8* exhibited higher numbers of *Hpa*-associated cell death spots. This suggests that *Hpa* fails to suppress plant-mediated hypersensitive response (HR). HR is a vigorous defense response by the plant that culminates in programmed cell death (Boller and Felix 2009). As an obligate biotroph, *Hpa* needs to suppress host-mediated cell death for its own survival (Mendgen and Hahn 2002). Effectors of *Phytophtora* have already been characterized, which suppress cell death response upon colonization (Fawke, Doumane, and Schornack 2015; Bos et al. 2006; King et al. 2014; Deb et al. 2018). Also, *Hpa* effectors

have been identified, that dampen PR1-mediated responsiveness to salicylic acid exclusively in haustoria containing cells and suppress cell death responses in the plant (Asai et al. 2014; Anderson et al. 2012). Therefore, *Hpa* might not be able to suppress HR in the mutants because of defective delivery of corresponding effectors due to a dysfunctional haustorium.

Atgpat6 is characterized by a distorted cuticle layer in sepals and petals of flowers (Li-Beisson et al. 2009). Corresponding to the specific promoter activity of *GPAT4* in leaves and stem, *Atgpat4x8* exhibited tissue specific cuticle layer defects in both organs (Li et al. 2007). A defective cuticle layer has been shown to influence pathogen infection (Fawke et al. 2018; Bessire et al. 2007; Chassot et al. 2007; Blanc et al. 2018). Strikingly, neither *gpat4x8,* nor *gpat6* and *kasI* affected host susceptibility and quantity of *Hpa* colonization, which suggests that *Hpa* infection on *Arabidopsis* is not hindered due to any aberrancies of the leaf surface.

Here we provide evidence that fitness and development of *Hpa* relies on the plant fatty acid and lipid biosynthesis genes *KASI, GPAT6, 4* and *8.* However, elucidating how precisely these plant genes impact *Hpa,* requires further investigations. As profiles of membrane and storage lipids did not exhibit significant differences between wildtype and mutants in control as well as *Hpa*-infected conditions, impairment of *KASI, GPAT4, 6* and *8* seems not to perturb the composition of storage and membrane lipid pools. This supports previous studies that *sn2*-MAGs are primed to be exported (Li, Beisson, Ohlrogge, et al. 2007). Accordingly, this implies an *Hpa*-dependence on specific plant lipids.

As any other microbial colonization, *Hpa* invasion involves signaling as well as membrane synthesis (Dörmann et al. 2014). Therefore, diverse hypothetical scenarios how KASI, GPAT4, 6 and 8 derived lipids interfere with *Hpa* colonization are possible. The aberrancies of *Hpa* haustoria could be based on a shortage of lipids, required for plant EHM synthesis. Further, lipid-derived signaling components are involved in plant response to the invasion of microbes (Chaturvedi et al. 2012; Mandal et al. 2012; Zoeller et al. 2012). Lipids produced via *KASI* and *GAPT4/6/8* could accordingly serve as precursors of signaling molecules that affect either host cell or microbe development. Alternatively, plant-derived lipids could be scavenged directly by *Hpa* and serve as profitable energy-intensive nutrition. Encouraging support for the latter hypothesis is provided by AMS and the pathogenic fungus *Erysiphe cichoracearum*. Lipid scavenging by the microbe has been reported in both cases and furthermore,

associations of the two fungal biotrophs are also impaired on *KASI* plant mutants (Luginbuehl et al. 2017; Jiang et al. 2017; Keymer and Gutjahr 2018; Keymer et al. 2017). In this scenario, both, hyphal and haustorial, aberrancies of *Hpa* in the mutants could be due to stress symptoms from malnutrition. Plant-derived lipids might possibly be transported to the plant and serve as crucial building blocks of oomycetal membranes. The established *Hpa*-marker fatty acid 20:5 will be a valuable tool to dissect the lipid origin and test lipid transport in *Hpa-Arabidopsis* associations in future studies.

All in all, this study demonstrated that plant derived lipids, which are produced via KASI and GPAT4/6/8, are required to sustain development and reproductive success of the biotrophic oomycete *Hpa* in *Arabidopsis.* Moreover, the impairment of *Hpa* interaction on *kasI, gpat6* and *gpat4x8* highlights the function of the respective enzymes as sustained compatibility factors in plant-microbe interactions. Therefore, *KASI, GPAT4, GPAT6* and *GPAT8* can be attributed to the diverse group of susceptibility (S) genes (van Schie and Takken 2014), which promote microbial biotrophy (Baxter et al. 2010).

Material and Methods:

Plant growth and cultivation

All *Arabidopsis thaliana* seeds used in this study were of Col-0 ecotype. Wildtype as well as all mutant seeds (*kasI,* transgenetically complemetented *kasI, gpat6* and gpat4x8) were surface sterilized with 70% EtOH + 0.05% Tween 20 and 100% EtOH, germinated on MS-Medium for 48h at 4°C in the dark followed by 5 – 6 days at 22 °C (8h light/dark). *kasI* and its complemented mutant line were obtained from Hong-Wei Xue (Shanghai Institutes for Biological Science, China) (Wu and Xue 2010), both *gpat6* allelic mutants lines were obtained from Yonghua Li-Beisson (CEA Cadarache, France) (Li-Beisson et al. 2009) and the *gpat4x8* double mutant lines were obtained from (Li, Beisson, Koo, et al. 2007) and sent by Christine Nawrath (University of Lausanne, Switzerland).

Colonization assay with *Hyaloperonospora arabidopsidis*

For inoculation of *Arabidopsis thaliana* cotyledons/leaves with *Hyaloperonospora arabidopsidis* isolate *NoCo*2, wildtype leaves with the sporulating oomycete were harvested seven days after infection into 15 mL reaction tubes containing 10 mL dH_2O. The spore solution was then vortexed for 2s, filtered through a Miracloth filter and

sprayed via a using a spraying gun (Carl Roth, Karlsruhe, Germany) onto 12-day-old plants that had been grown at 18°C under long day conditions (16h light, 85 µmol $m^{-2}s^{-1}$). After inoculation plants were placed into plastic trays covered with wet translucid lids and sealed to maintain high humidity. They were grown in a growth cabinet at 22°C and a 10 h photoperiod with 120 µmol $m^{-2}s^{-1}$ light and 65% relative humidity. Cotyledons (4 dpi) or leaves (4 dpi) of *Arabidopsis* infected with *H. arabidopsidis* were harvested and stained in 0.01 % trypan-blue-lactophenol (10 mL lactic acid, 10 mL glycerol, 10 g phenol, 10 mg trypan blue dissolved in 10 mL distilled water) for 3 min at 96°C and 5h at room temperature, followed by overnight clearing in saturated chloral hydrate (2.5g/mL). Samples were mounted in glycerol for observation using differential interference contrast microscopy. Hyphal thickness measurements were performed using Image J. For dead cell quantification 10 light microscopy images per trypan blue-lactophenol stained cotyledon of five to ten cotyledons per genotype were taken at a magnification of 200x. Dark blue stained spots with dead cells in association with oomycete hyphae and distant from the oomycete were counted on each image.

Real time qRT-PCR

For analysis of transcript levels, plant tissues were rapidly shock frozen in liquid nitrogen. RNA was extracted using the Spectrum Plant Total RNA Kit (www.sigmaaldrich.com). The RNA was treated with Invitrogen DNAse I amp. grade (www.invitrogen.com) and tested for purity by PCR. cDNA synthesis was performed with 500 ng RNA using the Superscript III kit (www.invitrogen.com). qRT-PCR was performed with GoTaq G2 DNA polymerase (Promega), 5 x colorless GoTaq Buffer (Promega) and SYBR Green I (Invitrogen S7563, 10.000x concentrated, 500 µl) - diluted to 100x in DMSO. Primers (Table S2) were designed with primer3 (58). The qPCR reaction was run on an iCycler (Biorad, www.bio-rad.com/) according to manufacturer's instructions. Thermal cycler conditions were: 95°C 2 min, 45 cycles of 95°C 30 sec, 60°C/62°C 30sec and 72°C 20 sec followed by dissociation curve analysis. Expression levels were calculated according to the ΔΔCt method (Rozen and Skaletsky 2000). For each genotype and treatment three to four biological replicates were tested and each sample was represented by two to three technical replicates.

Microscopy

For observation of *Hpa*-infected *Arabidopsis* cotyledons an inverted microscope (Leica DMI6000 B) was used with 10x, 20x and 40x magnification. Images were produced using LAS AF software and analyzed as well as stacked with ImageJ.

Statistics

All statistical analyses were performed and all boxplots were generated in R (www.r-project.org).

References:

Anderson, R. G., M. S. Casady, R. A. Fee, M. M. Vaughan, D. Deb, K. Fedkenheuer, A. Huffaker, E. A. Schmelz, B. M. Tyler, and J. M. McDowell. 2012. 'Homologous RXLR effectors from *Hyaloperonospora arabidopsidis* and *Phytophthora sojae* suppress immunity in distantly related plants', *Plant J*, 72: 882-93.

Antolín-Llovera, Meritxell, Martina K. Ried, Andreas Binder, and Martin Parniske. 2012. 'Receptor kinase signaling pathways in plant-microbe interactions', *Annual Review of Phytopathology*, 50: 451-73.

Asai, Shuta, Ghanasyam Rallapalli, Sophie J. M. Piquerez, Marie-Cécile Caillaud, Oliver J. Furzer, Naveed Ishaque, Lennart Wirthmueller, Georgina Fabro, Ken Shirasu, and Jonathan D. G. Jones. 2014. 'Expression profiling during Arabidopsis/downy mildew interaction reveals a highly-expressed effector that attenuates responses to salicylic acid', *PLoS Pathogen*, 10: e1004443.

Asai, Tsuneaki, Guillaume Tena, Joulia Plotnikova, Matthew R. Willmann, Wan-Ling Chiu, Lourdes Gomez-Gomez, Thomas Boller, Frederick M. Ausubel, and Jen Sheen. 2002. 'MAP kinase signalling cascade in Arabidopsis innate immunity', *Nature*, 415: 977-83.

Baxter, Laura, Sucheta Tripathy, Naveed Ishaque, Nico Boot, Adriana Cabral, Eric Kemen, Marco Thines, Audrey Ah-Fong, Ryan Anderson, Wole Badejoko, Peter Bittner-Eddy, Jeffrey L. Boore, Marcus C. Chibucos, Mary Coates, Paramvir Dehal, Kim Delehaunty, Suomeng Dong, Polly Downton, Bernard Dumas, Georgina Fabro, Catrina Fronick, Susan I. Fuerstenberg, Lucinda Fulton, Elodie Gaulin, Francine Govers, Linda Hughes, Sean Humphray, Rays H. Y. Jiang, Howard Judelson, Sophien Kamoun, Kim Kyung, Harold Meijer, Patrick Minx, Paul Morris, Joanne Nelson, Vipa Phuntumart, Dinah Qutob, Anne Rehmany, Alejandra Rougon-Cardoso, Peter Ryden, Trudy Torto-Alalibo, David Studholme, Yuanchao Wang, Joe Win, Jo Wood, Sandra W. Clifton, Jane Rogers, Guido Van den Ackerveken, Jonathan D. G. Jones, John M. McDowell, Jim Beynon, and Brett M. Tyler. 2010. 'Signatures of adaptation to obligate biotrophy in the *Hyaloperonospora arabidopsidis* genome', *Science*, 330: 1549-51.

Bessire, M., C. Chassot, A. Jacquat, M. Humphry, S. Borel, J. MacDonald-Comber Petetot, J. Metraux, and C. Nawrath. 2007. 'A permeable cuticle in Arabidopsis leads to a strong resistance to *Botrytis cinerea*', *EMBO J*, 28.

Blanc, C., F. Coluccia, F. L'Haridon, M. Torres, M. Ortiz-Berrocal, E. Stahl, P. Reymond, L. Schreiber, C. Nawrath, J. P. Metraux, and M. Serrano. 2018. 'The cuticle mutant eca2 modifies plant defense responses to biotrophic and necrotrophic pathogens and herbivory insects', *Mol Plant Microbe Interact*, 31: 344-55.

Boller, T., and G. Felix. 2009. 'A renaissance of elicitors: perception of microbe-associated molecular patterns and danger signals by pattern-recognition receptors', *Annu Rev Plant Biol*, 60: 379-406.

Bos, J. I., T. D. Kanneganti, C. Young, C. Cakir, E. Huitema, J. Win, M. R. Armstrong, P. R. Birch, and S. Kamoun. 2006. 'The C-terminal half of *Phytophthora infestans* RXLR effector AVR3a is sufficient to trigger R3a-mediated hypersensitivity and suppress INF1-induced cell death in *Nicotiana benthamiana*', *Plant J*, 48: 165-76.

Brands, M., V. Wewer, A. Keymer, C. Gutjahr, and P. Dörmann. 2018. 'The *Lotus japonicus* acyl-acyl carrier protein thioesterase FatM is required for mycorrhiza formation and lipid accumulation of *Rhizophagus irregularis*', *Under Review*.

Bravo, Armando, Mathias Brands, Vera Wewer, Peter Dörmann, and Maria J. Harrison. 2017. 'Arbuscular mycorrhiza-specific enzymes FatM and RAM2 fine-tune lipid biosynthesis to promote development of arbuscular mycorrhiza', *New Phytol*, 214: 1631-45.

Caillaud, M. C., L. Wirthmueller, J. Sklenar, K. Findlay, S. J. Piquerez, A. M. Jones, S. Robatzek, J. D. Jones, and C. Faulkner. 2014. 'The plasmodesmal protein PDLP1 localises to haustoria-associated membranes during downy mildew infection and regulates callose deposition', *PLoS Pathogen*, 10: e1004496.

Carella, P., A. Gogleva, M. Tomaselli, C. Alfs, and S. Schornack. 2018. 'Phytophthora palmivora establishes tissue-specific intracellular infection structures in the earliest divergent land plant lineage', *PNAS*, 115: E3846-E55.

Chassot, C., C. Nawrath, and J. P. Metraux. 2007. 'Cuticular defects lead to full immunity to a major plant pathogen', *Plant J*, 49: 972-80.

Chaturvedi, R., B. Venables, R. A. Petros, V. Nalam, M. Li, X. Wang, L. J. Takemoto, and J. Shah. 2012. 'An abietane diterpenoid is a potent activator of systemic acquired resistance', *Plant J*, 71: 161-72.

Chen, X., C. L. Snyder, M. Truksa, S. Shah, and R. J. Weselake. 2011. 'sn-Glycerol-3-phosphate acyltransferases in plants', *Plant Signaling and Behaviour*, 6: 1695-9.

Coates, M. E., and J. L. Beynon. 2010. 'Hyaloperonospora Arabidopsidis as a pathogen model', *Annu Rev Phytopathol*, 48: 329-45.

Deb, D., R. G. Anderson, T. How-Yew-Kin, B. M. Tyler, and J. M. McDowell. 2018. 'Conserved RxLR effectors from oomycetes *Hyaloperonospora arabidopsidis* and *Phytophthora sojae* suppress PAMP- and Effector-Triggered Immunity in diverse plants', *Mol Plant Microbe Interact*, 31: 374-85.

Dick. 2001. *Straminipilous fungi: Systematics of the Peronosporomycetes including accounts of the marine Straminipilous protists, the Plasmodiophorids and similar organisms* (**Dordrecht/Boston/London: Kluwer Academic Publishers**).

Dörmann, Peter, Hyeran Kim, Thomas Ott, Paul Schulze-Lefert, Marco Trujillo, Vera Wewer, and Ralph Hückelhoven. 2014. 'Cell-autonomous defense, re-organization and trafficking of membranes in plant–microbe interactions', *New Phytol*, 204: 815-22.

Fawke, S., M. Doumane, and S. Schornack. 2015. 'Oomycete interactions with plants: infection strategies and resistance principles', *Microbiol Mol Biol Rev*, 79: 263-80.

Fawke, S., T. A. Torode, A. Gogleva, E. A. Fich, I. Sørensen, T. Yunusov, Rose J. K. C., and S. Schornack. 2018. 'Glycerol phosphate acyltransferase 6 controls filamentous pathogen interactions and cell wall properties of the tomato and *Nicotiana benthamiana* leaf epidermis', *bioRxiv*.

Gidda, Satinder K., Jay M. Shockey, Steven J. Rothstein, John M. Dyer, and Robert T. Mullen. 2009. 'Arabidopsis thaliana GPAT8 and GPAT9 are localized to the ER and possess distinct ER retrieval signals: Functional divergence of the dilysine ER retrieval motif in plant cells', *Plant Physiology and Biochemistry*, 47: 867-79.

Glazebrook, Jane. 2005. 'Contrasting mechanisms of defence against biotrophic and necrotrophic pathogens', *Annu. Rev. Phytopathol.*, 43: 205-27.

Grant, John J., Byung-Wook Yun, and Gary J. Loake. 2000. 'Oxidative burst and cognate redox signalling reported by luciferase imaging: identification of a signal network that functions independently of ethylene, SA and Me-JA but is dependent on MAPKK activity', *Plant J*, 24: 569-82.
Gust, A. A., R. Pruitt, and T. Nurnberger. 2017. 'Sensing Danger: Key to activating plant immunity', *Trends Plant Sci*, 22: 779-91.
Gutjahr, Caroline, and Martin Parniske. 2013. 'Cell and developmental biology of the arbuscular mycorrhiza symbiosis', *Ann Rev Cell Dev Biol*, 29: 593-617.
Hahn, M., U. Neef, C. Struck, M. Göttfert, and K. Mendgen. 1997. 'A putative amino acid transporter is specifically expressed in haustoria of the rust fungus *Uromyces fabae*', *MPMI*, 10.
Jiang, Y., W. Wang, Q. Xie, N. Liu, L. Liu, D. Wang, X. Zhang, C. Yang, X. Chen, D. Tang, and E. Wang. 2017. 'Plants transfer lipids to sustain colonization by mutalistic mycorrhizial and parasitic fungi', *Science*, 356: 1172-75.
Jones, JD, and JL Dangl. 2006. 'The plant immune system', *Nature*, 444: 323 - 29.
Judelson, H. S. 2012. 'Dynamics and innovations within oomycete genomes: insights into biology, pathology, and evolution', *Eukaryot Cell*, 11: 1304-12.
Judelson, H. S. 2017. 'Metabolic diversity and novelties in the oomycetes', *Ann Rev Cell Dev Biol*, 71: 21-39.
Kamoun, S., O. Furzer, J. D. Jones, H. S. Judelson, G. S. Ali, R. J. Dalio, S. G. Roy, L. Schena, A. Zambounis, F. Panabieres, D. Cahill, M. Ruocco, A. Figueiredo, X. R. Chen, J. Hulvey, R. Stam, K. Lamour, M. Gijzen, B. M. Tyler, N. J. Grunwald, M. S. Mukhtar, D. F. Tome, M. Tor, G. Van Den Ackerveken, J. McDowell, F. Daayf, W. E. Fry, H. Lindqvist-Kreuze, H. J. Meijer, B. Petre, J. Ristaino, K. Yoshida, P. R. Birch, and F. Govers. 2015. 'The Top 10 oomycete pathogens in molecular plant pathology', *Mol Plant Pathol*, 16: 413-34.
Keymer, A., and C. Gutjahr. 2018. 'Cross-kingdom lipid transfer in arbuscular mycorrhiza symbiosis and beyond', *Curr Opin Plant Biol*, 44: 137-44.
Keymer, A., P. Pimprikar, V. Wewer, C. Huber, M. Brands, S. L. Bucerius, P. M. Delaux, V. Klingl, E. V. Ropenack-Lahaye, T. L. Wang, W. Eisenreich, P. Dormann, M. Parniske, and C. Gutjahr. 2017. 'Lipid transfer from plants to arbuscular mycorrhiza fungi', *eLife*, 6: doi: 10.7554/eLife.29107.
King, S. R., H. McLellan, P. C. Boevink, M. R. Armstrong, T. Bukharova, O. Sukarta, J. Win, S. Kamoun, P. R. Birch, and M. J. Banfield. 2014. '*Phytophthora infestans* RXLR effector PexRD2 interacts with host MAPKKK epsilon to suppress plant immune signaling', *Plant Cell*, 26: 1345-59.
Koch, E., and A. Slusarenko. 1990. '*Arabidopsis* is susceptible to infection by a downy mildew fungus', *Plant Cell*, 2: 437.
Krings, M., T. N. Taylor, and N. Dotzler. 2011. 'The fossil record of the Peronosporomycetes (Oomycota)', *Mycologia*, 103: 455-7.
Li, Y. , F. Beisson, A. J. K. Koo, I. Molina, M. Pollard, and J. Ohlrogge. 2007. 'Identification of acyltransferases required for cutin biosynthesis and production of cutin with suberin-like monomers', *PNAS* 104.
Li, Y., F. Beisson, J. Ohlrogge, and M. Pollard. 2007. 'Monoacylglycerols are components of root waxes and can be produced in the aerial cuticle by ectopic expression of a suberin-associated acyltransferase', *Plant Physiol*, 144: 1267–77.
Li-Beisson, Y., J. Neunzig, Y. Lee, and K. Philippar. 2017. 'Plant membrane-protein mediated intracellular traffic of fatty acids and acyl lipids', *Curr Opin Plant Biol*, 40: 138-46.

Li-Beisson, Yonghua, Mike Pollard, Vincent Sauveplane, Franck Pinot, John Ohlrogge, and Fred Beisson. 2009. 'Nanoridges that characterize the surface morphology of flowers require the synthesis of cutin polyester', *PNAS*, 106: 22008.

Li-Beisson, Yonghua, Basil Shorrosh, Fred Beisson, Mats X. Andersson, Vincent Arondel, Philip D. Bates, Sébastien Baud, David Bird, Allan DeBono, Timothy P. Durrett, Rochus B. Franke, Ian A. Graham, Kenta Katayama, Amélie A. Kelly, Tony Larson, Jonathan E. Markham, Martine Miquel, Isabel Molina, Ikuo Nishida, Owen Rowland, Lacey Samuels, Katherine M. Schmid, Hajime Wada, Ruth Welti, Changcheng Xu, Rémi Zallot, and John Ohlrogge. 2010. 'Acyl-Lipid Metabolism', *The Arabidopsis Book*: e0133.

Luginbuehl, L.H., G.N. Menard, S. Kurup, H. Van Erp, G.V. Radhakrishnan, A. Breakspear, G.E.D. Oldroyd, and P.J. Eastmond. 2017. 'Fatty acids in arbuscular mycorrhizal fungi are synthesized by the host plant', *Science*, 6: 763-75.

Mandal, M. K., A. C. Chandra-Shekara, R. D. Jeong, K. Yu, S. Zhu, B. Chanda, D. Navarre, A. Kachroo, and P. Kachroo. 2012. 'Oleic acid-dependent modulation of NITRIC OXIDE ASSOCIATED1 protein levels regulates nitric oxide-mediated defense signaling in *Arabidopsis*', *Plant Cell*, 24: 1654-74.

Mauch-Mani, Brigitte, and Alan J. Slusarenko. 1993. '*Arabidopsis* as a model host for studying plant-pathogen interactions', *Trends in Microbiology*, 1: 265-70.

Mazurek, S., I. Garroum, J. Daraspe, D. De Bellis, V. Olsson, A. Mucciolo, M. A. Butenko, B. M. Humbel, and C. Nawrath. 2017. 'Connecting the molecular structure of cutin to ultrastructure and physical properties of the cuticle in petals of *Arabidopsis*', *Plant Physiol*, 173: 1146-63.

Mendgen, Kurt, and Matthias Hahn. 2002. 'Plant infection and the establishment of fungal biotrophy', *Trends in Plant Science*, 7: 352-56.

Parniske, Martin. 2000. 'Intracellular accommodation of microbes by plants: a common developmental program for symbiosis and disease?', *Current Opinion in Plant Biology*, 3: 320-28.

Rey, Thomas, and Sebastian Schornack. 2013. 'Interactions of beneficial and detrimental root-colonizing filamentous microbes with plant hosts', *Genome Biology*, 14: 121.

Ried, Martina Katharina, Aline Banhara, Andreas Binder, Fang-Hu Hwu, Andrea A. Gust, Caroline Höfle, Ralph Hückelhoven, Thorsten Nürnberger, and Martin Parniske. 2018. 'Symbiosis-related genes sustain the development of a downy mildew pathogen on *Arabidopsis thaliana*', *bioRxiv*.

Rozen, S, and HJ Skaletsky. 2000. 'Primer3 on the WWW for general users and for biologist programmers.' in S Krawets and S Misener (eds.), *Bioinformatics Methods and Protocols: Methods in Molecular Biology.* (Humana Press: Totwana, NJ, USA).

Slusarenko, Alan J., and Nikolaus L. Schlaich. 2003. 'Downy mildew of *Arabidopsis thaliana* caused by *Hyaloperonospora parasitica* (formerly *Peronospora parasitica*)', *Molecular Plant Pathology*, 4: 159-70.

Sohn, K. H., R. Lei, A. Nemri, and J. D. Jones. 2007. 'The downy mildew effector proteins ATR1 and ATR13 promote disease susceptibility in *Arabidopsis thaliana*', *Plant Cell*, 19: 4077-90.

Soylu, E. M., and S. Soylu. 2003. 'Light and electron microscopy of the compatible interaction between *Arabidopsis* and the downy mildew pathogen *Peronospora parasitica*', *Journal of Phytopathology*, 151: 300-06.

Struck, C., M. Hahn, and K. Mendgen. 1996. 'Plasma membrane H+-ATPase activity in spores, germ tubes, and haustoria of the rust fungus *Uromyces viciae-fabae*', *Fungal Genetics and Biology*.

Thines, Marco, and Sophien Kamoun. 2010. 'Oomycete–plant coevolution: recent advances and future prospects', *Current Opinion in Plant Biology*, 13: 427-33.

Tisserant, Emilie, Mathilde Malbreil, Alan Kuo, Annegret Kohler, Aikaterini Symeonidi, Raffaella Balestrini, Philippe Charron, Nina Duensing, Nicolas Frei dit Frey, Vivienne Gianinazzi-Pearson, Luz B. Gilbert, Yoshihiro Handa, Joshua R. Herr, Mohamed Hijri, Raman Koul, Masayoshi Kawaguchi, Franziska Krajinski, Peter J. Lammers, Frederic G. Masclaux, Claude Murat, Emmanuelle Morin, Steve Ndikumana, Marco Pagni, Denis Petitpierre, Natalia Requena, Pawel Rosikiewicz, Rohan Riley, Katsuharu Saito, Hélène San Clemente, Harris Shapiro, Diederik van Tuinen, Guillaume Bécard, Paola Bonfante, Uta Paszkowski, Yair Y. Shachar-Hill, Gerald A. Tuskan, Peter W. Young, Ian R. Sanders, Bernard Henrissat, Stefan A. Rensing, Igor V. Grigoriev, Nicolas Corradi, Christophe Roux, and Francis Martin. 2013. 'Genome of an arbuscular mycorrhizal fungus provides insight into the oldest plant symbiosis', *PNAS*: 20117–22.

van Schie, C. C., and F. L. Takken. 2014. 'Susceptibility genes 101: how to be a good host', *Annu Rev Phytopathol*, 52: 551-81.

Voegele, R. T., S. Wirsel, U. Möll, M. Lechner, and K. Mendgen. 2006. 'Cloning and characterization of a novel invertase from the obligate biotroph *Uromyces fabae* and analysis of expression patterns of host and pathogen invertases in the course of infection', *MPMI*, 19.

Voegele, R.T., C. Struck, M. Hahn, and K. Mendgen. 2001. 'The role of haustoria in sugar supply during infection of broad bean by the rust fungus *Uromyces fabae*', *PNAS*, 98.

Wang, Ertao, Sebastian Schornack, JF Marsh, Enrico Gobbato, Benjamin Schwessinger, Peter Eastmond, Michael Schultze, Sophien Kamoun, and GED Oldroyd. 2012. 'A common signaling process that promotes mycorrhizal and oomycete colonization of plants', *Cur Biol*, 22: 2242-46.

Wewer, V., M. Brands, and P. Dormann. 2014. 'Fatty acid synthesis and lipid metabolism in the obligate biotrophic fungus Rhizophagus irregularis during mycorrhization of Lotus japonicus', *Plant J*, 79: 398-412.

Whisson, SC, PC Boevink, L Moleleki, AO Avrova, JG Morales, EM Gilroy, MR Armstrong, S Grouffaud, P van West, S Chapman, I Hein, IK Toth, L Pritchard, and PR Birch. 2007. 'A translocation signal for delivery of oomycete effector proteins into host plant cells', *Nature*, 450: 115 - 18.

Wu, GZ., and HW. Xue. 2010. '*Arabidopsis* β-Ketoacyl-[Acyl Carrier Protein] synthase I is crucial for fatty acid synthesis and plays a role in chloroplast division and embryo development', *Plant Cell*, 22: 3726-44.

Yang, Weili, Mike Pollard, Yonghua Li-Beisson, Fred Beisson, Michael Feig, and John Ohlrogge. 2010. 'A distinct type of glycerol-3-phosphate acyltransferase with *sn*-2 preference and phosphatase activity producing 2-monoacylglycerol', *PNAS*, 107: 12040-45.

Yang, Weili, Jeffrey P. Simpson, Yonghua Li-Beisson, Fred Beisson, Mike Pollard, and John B. Ohlrogge. 2012. 'A land-plant-specific Glycerol-3-Phosphate Acyltransferase family in Arabidopsis: Substrate specificity, sn-2 preference, and evolution', *Plant Physiology*, 160: 638-52.

Zoeller, M., N. Stingl, M. Krischke, A. Fekete, F. Waller, S. Berger, and M. J. Mueller. 2012. 'Lipid profiling of the *Arabidopsis* hypersensitive response reveals specific lipid peroxidation and fragmentation processes: biogenesis of pimelic and azelaic acid', *Plant Physiol*, 160: 365-78.

Figures:

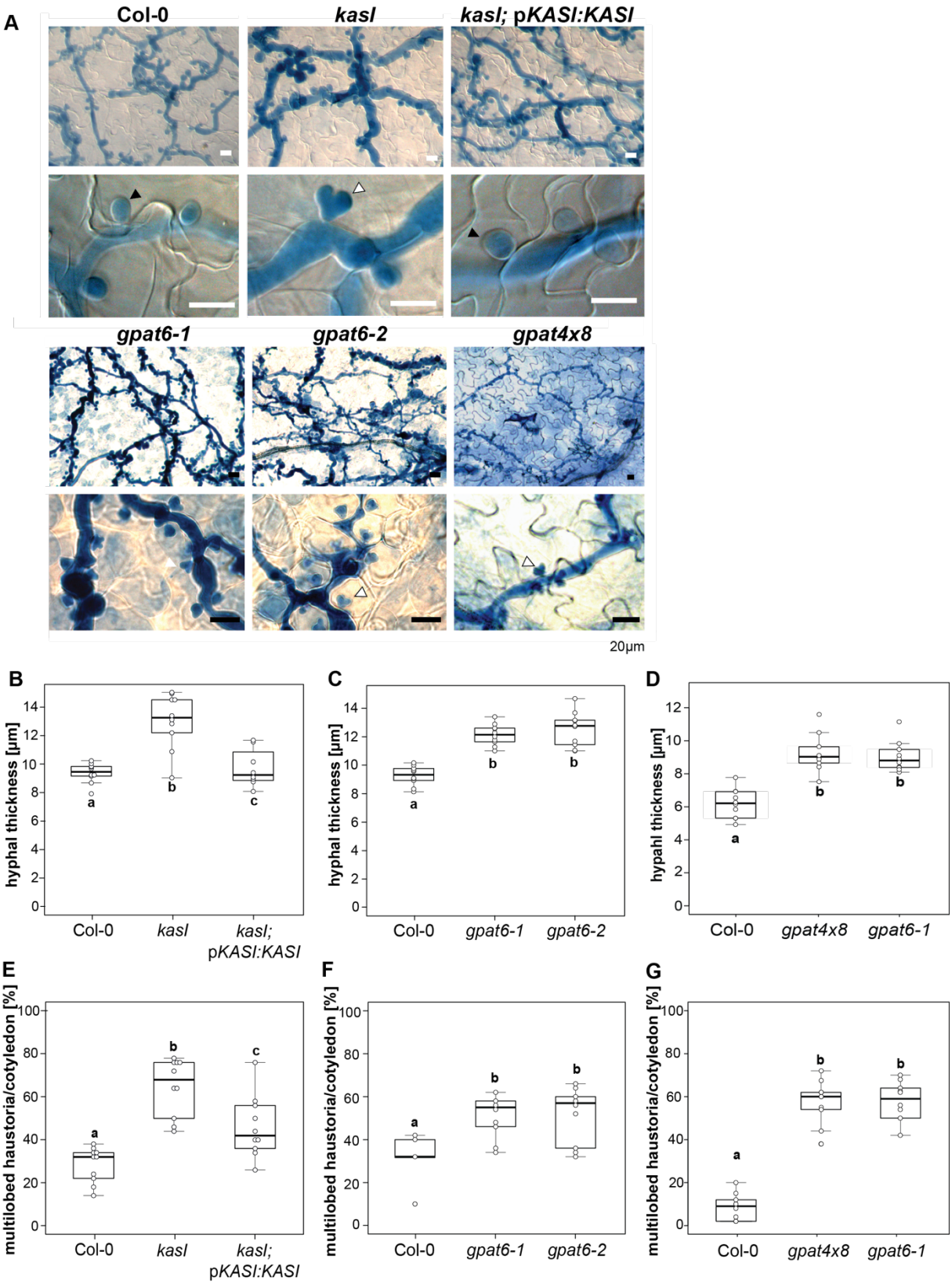
A
Col-0
kasl
kasl; pKASI:KASI
gpat6-1
gpat6-2
gpat4x8
20µm
B
hyphal thickness [µm]
Col-0
kasl
kasl; pKASI:KASI
C
hyphal thickness [µm]
Col-0
gpat6-1
gpat6-2
D
hypahl thickness [µm]
Col-0
gpat4x8
gpat6-1
E
multilobed haustoria/cotyledon [%]
Col-0
kasl
kasl; pKASI:KASI
F
multilobed haustoria/cotyledon [%]
Col-0
gpat6-1
gpat6-2
G
multilobed haustoria/cotyledon [%]
Col-0
gpat4x8
gpat6-1

Figure 1: *Arabidopsis* lipid biosynthesis genes are required for *H. arabidopsidis* development

(A) *H. arabidopsidis* colonization pattern in cotyledons of *A. thaliana* Col-0 wildtype, *kasI,* transgenically complemented *kasI (*p*KASI:KASI),* two allelic *gpat6* mutants (*gpat6-1* and *gpat6-2*) and the *gpat4x8* double mutant at 4 days post infection (dpi). *Hpa* structures were stained with trypan blue-lactophenol. First and third panel:In wildtype and the complemented *kasI* line, *Hpa* hyphae were straight and slim, whereas they were thickened and bulbous on the mutant plants of *kasI, gpat6* and *gpat4x8.* Second and fourth panel: Round-shaped haustoria in wildtype and complemented *kasI* (black arrowhead) and multilobed haustoria (white arrowhead) in the *kasI, gpat6* and *gpat4x8* mutants. (B-D) Hyphal thickness of *Hpa* in *kasI* mutant, transgenically complemented *kasI* and wildtype (ANOVA; posthoc Tukey; n=28; $p \leq 0.001$; $F_{2,25}$=20,03) (B), in two *Atgpat6* allelic mutant lines and wildtype (ANOVA; posthoc Tukey; n=30; $p \leq 0.001$; $F_{2,275}$=38,33) (C) and in the double mutant *Atgpat4x8, Atgpat6-1* and wildtype (ANOVA; posthoc Tukey; n=30; $p \leq 0.001$; $F_{2,27}$=29.68) (D). (B-D) Hyphal thickness was measured on 25 independent hyphae per cotyledon and 8-10 cotyledons per genotype. Different letters indicate significant differences (E-G) Proportion of multilobed *Hpa* haustoria in *kasI,* complemented *kasI* and wildtype (ANOVA; posthoc Tukey; n=30; $p \leq 0.001$; $F_{2,27}$=21,57) (E), in *gpat6-1, gpat6-2* and wildtype (ANOVA; posthoc Tukey; n=30; $p \leq 0.001$; $F_{2,27}$=9,526) (F) and in *gpat4x8, gpat6-1* and wildtype (ANOVA; posthoc Tukey; n=30; $p \leq 0.001$; $F_{2,27}$=108.6) (G). (E-G) 50 haustoria per cotyledon were counted on 10 independent cotyledons per genotype. Different letters indicate significant differences.

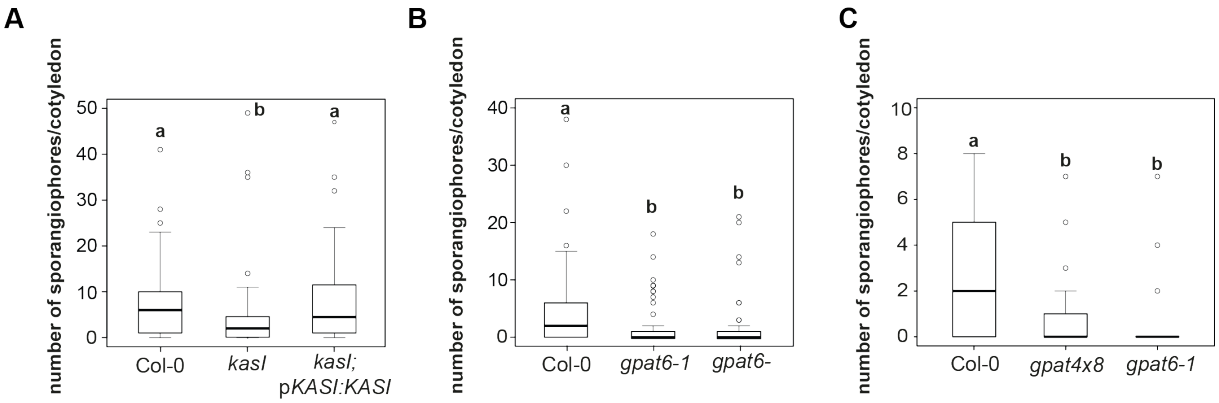

Figure 2: Reproductive success is significantly impaired on cotyledons of *Arabidopsis* mutants.

(A-C) Reproductive success of *Hpa* is reduced in the *kasI, gpat6* and the *gpat4x8* mutants. Box-plots represent the number of sporangiophores per infected cotyledon on 50 cotyledons of *Arabidopsis* wildtype (Col-0) and all tested mutant lines 4 dpi with *Hpa* isolate NoCo2. Dots: outliers. Different letters indicate significant differences ($p \leq 0.05$ (A), $p \leq 0.01$ (B & C), Kruskal-Wallis test followed by Bonferroni-Holm correction).

(D-F) Mean number of cell death spots per cotyledon. A significantly increased number of cell death spots that were directly associated with *Hpa* hyphae in all tested mutant lines compared to Col-0 wildtype and the transgenetically complemented *kasI* mutant (ANOVA; posthoc Tukey; n=15; (D): $p \leq 0.05$, $F_{2,12}$(associated) = 4.501, $F_{2,12}$(random) = 0.01; (E): $p \leq 0.1$ $F_{2,12}$(associated) = 12.04, $F_{2,12}$(random) = 0.881 (F): $p \leq 0.05$ $F_{2,12}$(associated) = 6.916, $F_{2,12}$(random) = 2.015). However, the number of randomly distributed cell death spots that were not associated with *Hpa* hyphae did not differ among the genotypes.

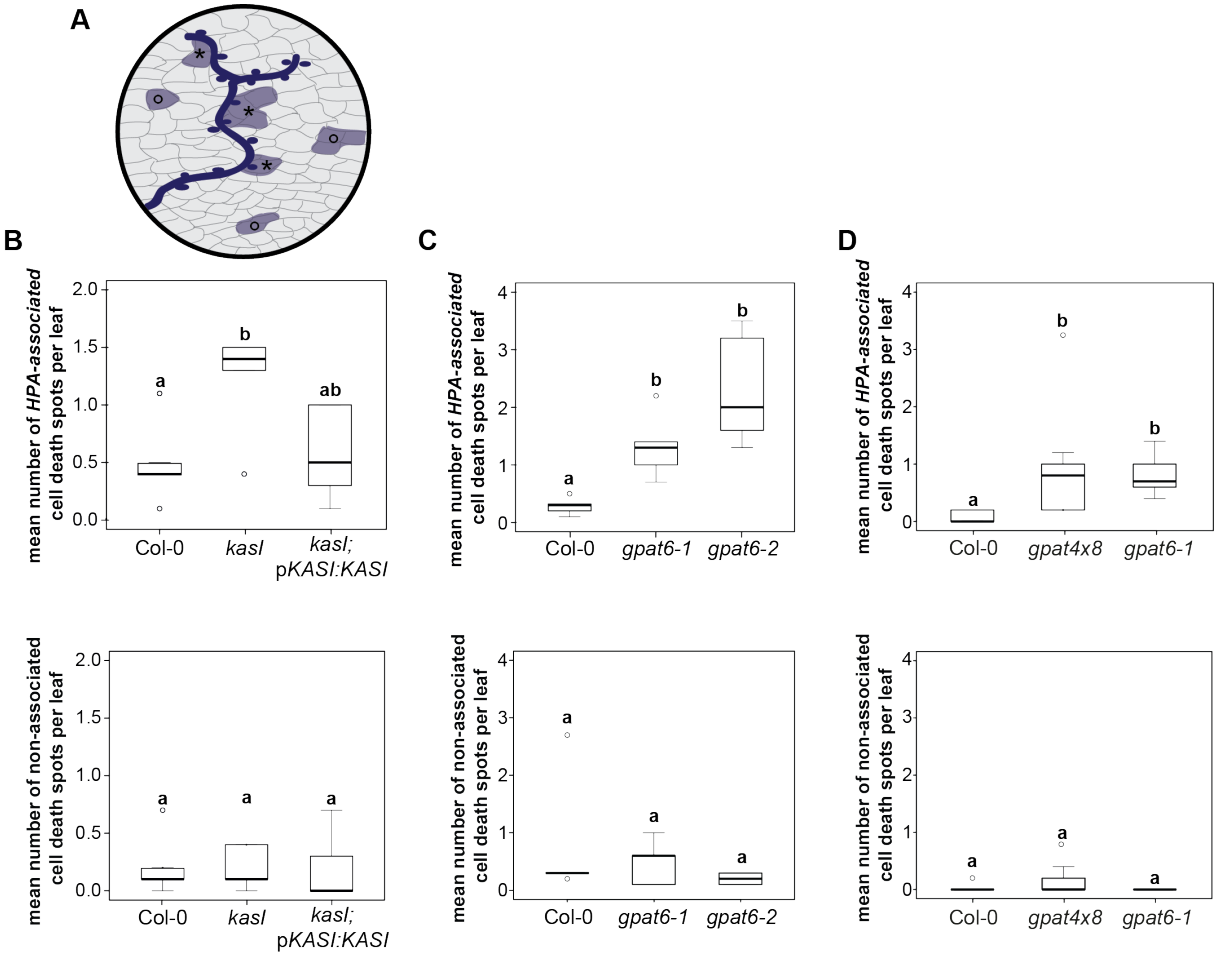

Figure 3: Number of *Hpa*-associated cell death spots is significantly altered in *Arabidopsis* mutants.

(A) Schematic representation of *Hpa*-associated cell death spots (*) and non-associated cell death spots (°), recognizable via trypan blue staining by dark-blue dye retention in single cells. (B-C) Mean number of cell death spots per cotyledon. A significantly increased number of cell death spots that were directly associated with *Hpa* hyphae in all tested mutant lines compared to Col-0 wildtype and the transgenetically complemented *kasI* mutant (ANOVA; posthoc Tukey; n=15; (D): $p \leq 0.05$, $F_{2,12}$(associated) = 4.501, $F_{2,12}$(random) = 0.01; (E): $p \leq 0.1$ $F_{2,12}$(associated) = 12.04, $F_{2,12}$(random) = 0.881 (F): $p \leq 0.05$ $F_{2,12}$(associated) = 6.916, $F_{2,12}$(random) = 2.015). However, the number of randomly distributed cell death spots that were not associated with *Hpa* hyphae did not differ among the genotypes.

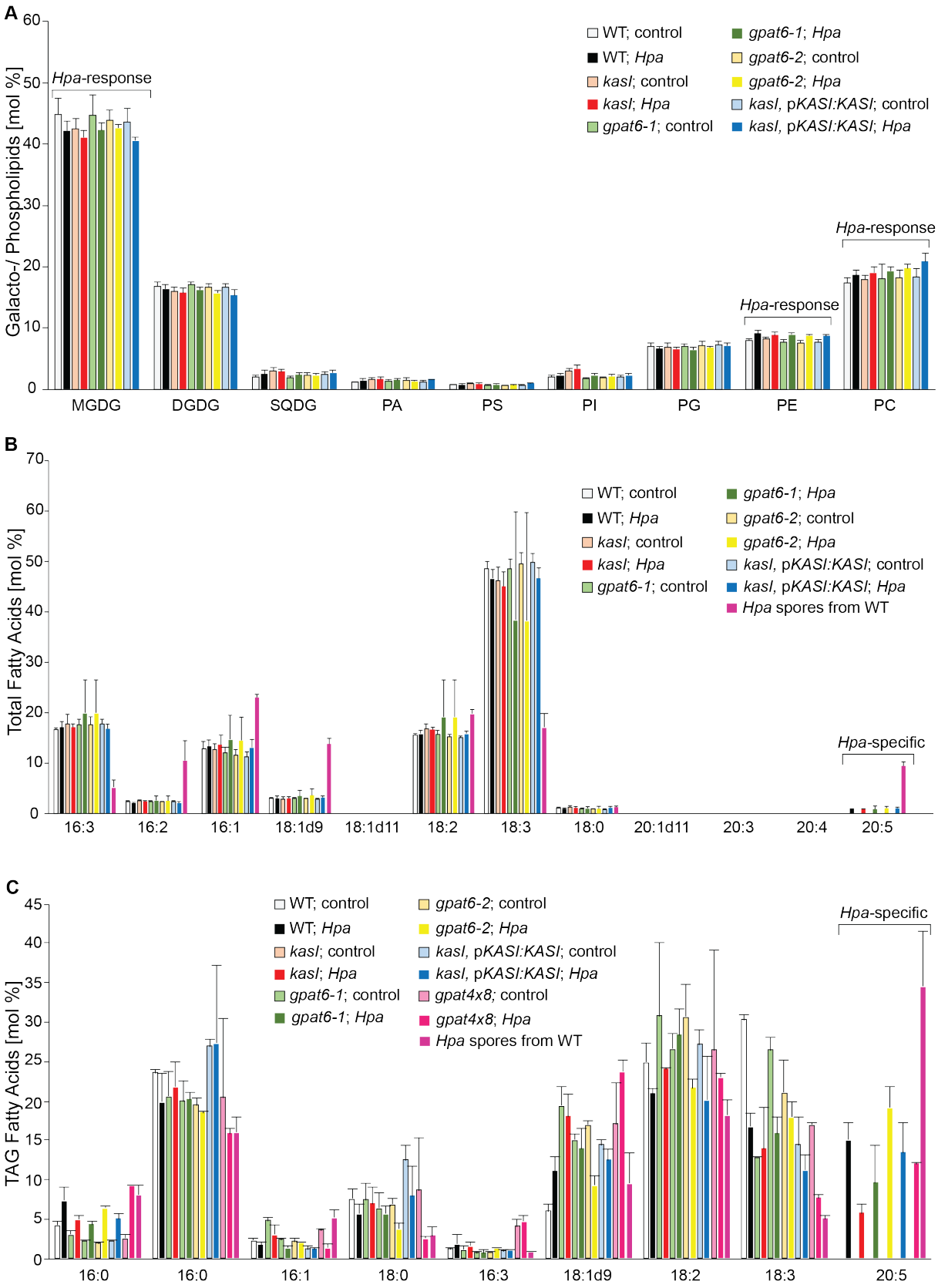
A
Galacto-/ Phospholipids [mol %]
Hpa-response
Hpa-response
Hpa-response
WT; control
WT; Hpa
kasI; control
kasI; Hpa
gpat6-1; control
gpat6-1; Hpa
gpat6-2; control
gpat6-2; Hpa
kasI, pKASI:KASI; control
kasI, pKASI:KASI; Hpa
MGDG
DGDG
SQDG
PA
PS
PI
PG
PE
PC
B
Total Fatty Acids [mol %]
Hpa-specific
WT; control
WT; Hpa
kasI; control
kasI; Hpa
gpat6-1; control
gpat6-1; Hpa
gpat6-2; control
gpat6-2; Hpa
kasI, pKASI:KASI; control
kasI, pKASI:KASI; Hpa
Hpa spores from WT
16:3
16:2
16:1
18:1d9
18:1d11
18:2
18:3
18:0
20:1d11
20:3
20:4
20:5
C
TAG Fatty Acids [mol %]
Hpa-specific
WT; control
WT; Hpa
kasI; control
kasI; Hpa
gpat6-1; control
gpat6-1; Hpa
gpat6-2; control
gpat6-2; Hpa
kasI, pKASI:KASI; control
kasI, pKASI:KASI; Hpa
gpat4x8; control
gpat4x8; Hpa
Hpa spores from WT
16:0
16:0
16:1
18:0
16:3
18:1d9
18:2
18:3
20:5

Figure3: Lipid profiles of control (mock inoculated) and *Hpa*-challenged *Arabidopsis* leaves and identification of a *Hpa*-marker. (A) Total Galacto- and Phospholipids in control and *Hpa*-challenged leaves of *Arabidopsis* wildtype, *kasI, gpat6-1, gpat6-2* and of a transgenetically complemented *kasI* line. PE and PC exhibits a *Hpa*-induced increase whereas MGDG exhibits an *Hpa*-induced decrease among all tested genotypes (B) Profiles of total fatty acid species. 20:5 FA was exclusively detected in *Hpa* containing material. (A-B) Means of 5 biological replicates per treatment and genotype. (C) Profiles of TAG originating fatty acid species. 20:5 harboring TAGs were exclusively detected in *Hpa* containing material. Means of 2 biological replicates per treatment and genotype.

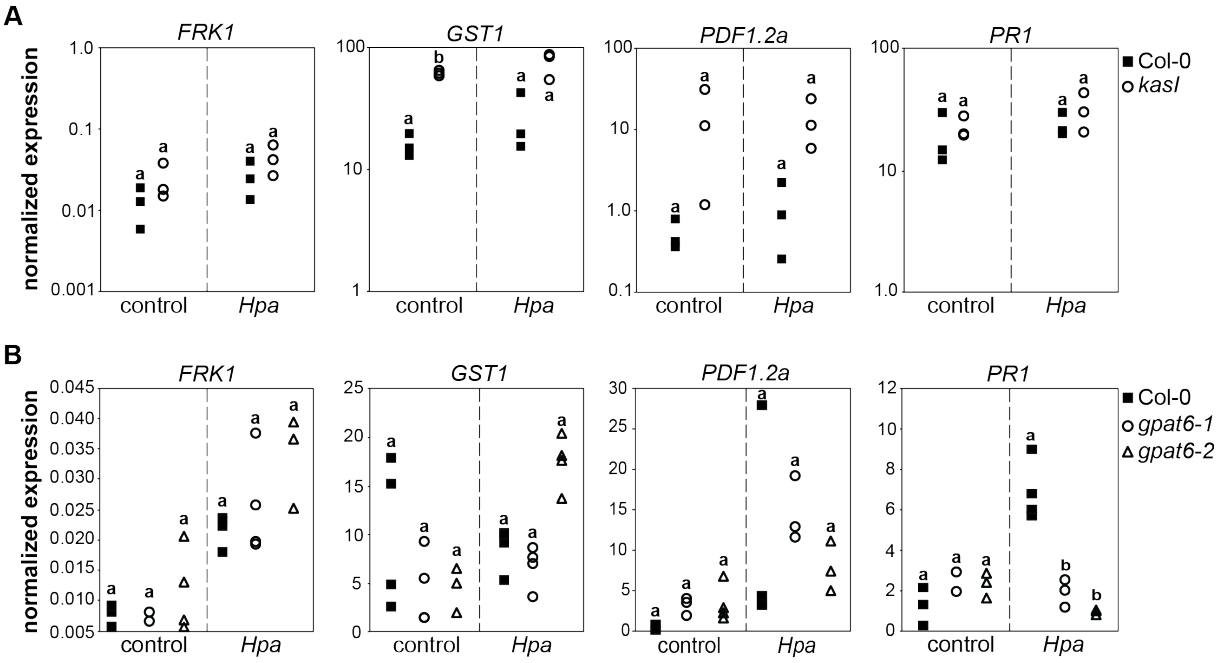

Figure S1: Transcript accumulation of *FRK1, GST1, PDF1.2a* and *PR1* in control (mock inoculated) and *Hpa* colonized leaves of Arabidopsis wildtype, *kasI* and *gpat6* as assessed by qPCR. Expression values were normalized to those of the constitutively expressed gene *PP2A*. Different letters indicate significant differences (ANOVA; posthoc Tukey; (A) n=6; $p \leq 0.001$; $F_{1,4}$(GST1, mock) =310.02 (B) n = 11; $p \leq 0.05$; $F_{2,8}$(PR1,*Hpa*) = 4.411).

qPCR of *AtFRK*	FRK_F FRK_R	ATCTTCGCTTGGAGCTTCTC TGCAGCGCAAGGACTAGAG
qPCR of *AtGST1*	GST1_F GST1_R	TAATAAAAGTGGCGATGACC ACATTCAAATCAAACACTCG
qPCR of *AtPDF1.2a*	PDF1.2a_F PDF1.2a_R	TGCTACCATCATCACCTTCCTT TAACATGGGACGTAACAGATACAT
qPCR of *AtPR1*	PR1_F PR1_R	TTCTTCCCTCGAAAGCTCAA AAGGCCCACCAGAGTGTATG
qPCR of *AtPP2A*	PP2A_F PP2A_R	TAACGTGGCCAAAATGATGC GTTCTCCACAACCGATTGGT

Table S1: Primers used in this study

IX. General Discussion:

1. The paradigm shift: Lipids are transferred from plants to AMF

There is little doubt, that the driving force of plant mutualistic interaction with *Glomeromycotina* fungi is the reciprocal exchange of nutrients. Therefore, the discovery of lipids as an additional cargo from plant to fungus is of great value for future AM research. This finding might harbor great potential to achieve a more efficient application of AMS for a modern and sustainable agriculture.

Independent investigations of AM fungal genomes revealed the absence of *de novo* fatty acid synthase complexes und thus weakened the previous paradigm that plant carbohydrates are the exclusive cargo, which is transported to the fungal partner (Wewer et al. 2014; Ropars et al. 2016; Salvioli et al. 2016; Tang et al. 2016). In line with this, the involvement of plant lipid biosynthesis in AMS has become an important scope to elucidate within the last years.

Different studies showed that a significant number of lipid biosynthesis genes is induced in arbuscocytes and several of these genes are exclusively present in AM-host plants (Gaude et al. 2012; Bravo et al. 2016; Gaude et al. 2012). These findings lead to the hypothesis that AM-competent plants might have evolved an AM-specific lipid biosynthesis pathway in order to nourish the fungal partner. First, Wang et al. published that a mutation in the AM-specific *GPAT6* paralog *RAM2* impairs AM development in *Medicago* (Wang et al. 2012). Suitably, further research discovered *dis* and *fatm* as additional AM-specific fatty acid plant mutants (Keymer et al. 2017; Bravo et al. 2016). All identified mutants exhibit similar phenotypes, characterized by impaired arbuscule branching (Figure 4A), a significantly reduced percentage of fungal colonization and a severe reduction in the number of lipid-containing vesicles in the mycelium of associated AMF, suggesting a shortage of lipids, which coincides eventually with the lack of 16:0 FA (palmitic acid) and 16:1ω5 FA (palmitvaccenic acid) containing lipids (Bravo et al. 2017; Keymer et al. 2017; Brands et al. 2018; Jiang et al. 2017; Luginbuehl et al. 2017).

Direct lipid transport from plant to fungus was shown by three different laboratories independently, following different experimental approaches. The authors of two studies used an elegant synthetic approach and took advantage of the *Umbellularia californica* fatty acyl-ACP thioesterase (UcFatB), which terminates FA chain elongation after 12

carbon units and consequently produces 12:0 FA (lauric acid) (Figure 4B) (Voelker et al. 1992). Since lauric acid hardly occurs in colonized *Medicago* roots it can be used as an unequivocal tracer for cross-organismal lipid fluxes. Expression of *UcFatB* resulted in significantly enhanced levels of lauroyl groups in colonized roots, in the fungal extraradical mycelium (ERM) and spores (Jiang et al. 2017; Luginbuehl et al. 2017). Detection of plant-produced lauroyl groups in fungus-exclusive compartments demonstrated that lipids are transported from plant to the associated fungus (Figure 4C). In *Mtram2* mutants, expressing *UcFatB,* elevated lauroyl group levels could be detected in colonized roots but not in the associated fungal ERM, which indicates that tracer transfer is impaired in this mutant (Figure 4C) (Jiang et al. 2017). Possibly, transfer is not detected due to insufficient 12:0 sn2-MAGs production, which is performed by RAM2.

Further, Luginbuehl et al. provided genetic evidence for lipid transport by not manipulating plant lipid pathways but exploiting the fact that sucrose and acetate are used for plant FA biosynthesis via two different routes (Figure 4B). Located in the plastids, the acetyl coenzyme A synthase (ACS) is an enzyme crucial for acetate use in FA synthesis but not involved in plant FA synthesis from sucrose (Lin and Oliver 2008). Since FAs can be produced independently of acetate, *acs* mutants of *Medicago* develop normal and show no impairment in AM symbiosis. Radiolabeling of *acs* mutants with ^{14}C acetate showed strong reduction of ^{14}C-labeld acyl groups compared to labeling wildtype plants (Luginbuehl et al. 2017). Feeding mycorrhizal wildtype and *acs* plants with ^{14}C acetate as well as ^{14}C sucrose, followed by an analysis of labeled triacylglycerols in the fungal ERM, allowed the conclusion that lipid transfer depends on the plant's genetic background. Fungal spores showed almost no radiolabel, when the ^{14}C-acetate fed plant was an *acs* mutant. However, when ^{14}C sucrose was provided as substrate to wildtype and *acs Medicago* plants, levels of ^{14}C radiolabeling did not differ in spores associated to either *acs* or wildtype plants.

In this work (Paper I), lipid transport in AMS was detected via an alternative technique called isotopolog profiling. This approach is not based on genetically engineering of the plant but on directly measuring endogenous FAs, which are labelled with an isotope tracer. 16:0 as well as 16:1ω5 FAs occur in large quantities in AMF in form of triacylglycerols. Thus, both could be used as markers in roots and in the associated ERM. Furthermore, 16:1ω5 is exclusively produced by AMF and not present in plants or any other fungal species (Graham et al. 1995; Bentivenga and Morton 1996; Madan

et al. 2002). Hence, this FA species allows a distinction between both organisms, even in colonized roots in which substances like FA/lipids from both symbiotic partners are intermingled. Roots were fed with $^{13}C_6$-glucose which is used together with photosynthetically fixed ^{12}C-glucose for FA synthesis. Both carbon isotopes are randomly incorporated into the marker FAs, which results in a FA-specific cocktail of isotopologs. The isotopologs of one specific FA species are identical in their molecular structure but different in their composition of carbon isotopes (Figure 4D). Quantification of all isotopologs by mass spectrometry, followed by plotting the relative quantity of all represented isotopologs, results in a display of distinctive isotopolog patterns. In *Lotus* wildtype, the 16:0 FA patterns were close to identical between non-colonized and colonized roots and the associated ERM (Keymer et al. 2017). Strikingly, the pattern was also conserved in the fungus specific 16:1ω5 FA (Keymer et al. 2017). The pattern conservation in *Lotus* wildtype and the associated ERM was a strong hint towards transport of 16:0 FA containing lipids from plant to fungus. However, this preservation could also be explained by an underlying biophysical law of fluxes, which influences fluxes or enzymatic activities, which leads to the same pattern in each organism. To rule out this doubt, root organ cultures of *Daucus carota* were labeled with $^{13}C_6$-glucose, which resulted in 16:0 FA isotopolog profiles, which were different from *Lotus,* but conserved among non-colonized and colonized roots as well as ERM and also mirrored by all 16:1ω5 FA pattern (Keymer et al. 2017) (Figure 4E). The plant species dependent conservation of isotopolog pattern in the host plant and fungus indicates that all lipids originated from the same pool, which is build up by the plant and determines the fungal pool. The isotopolog profiles of AM-specific lipid mutants are consistent with this interpretation. The palmitic acid (16:0) pattern of non-colonized and colonized *dis* and *ram2* mutants were identical with wildtype pattern, showing that $^{13}C_6$-glucose incorporation and conversion to 16:0 FA is AM-independent and unaffected by the respective mutations. However, hardly any FA was transported to the fungus from the mutant roots. This was observed by very low amounts of labeled 16:0 and 16:1ω5 FA in the mutant associated ERM, very low amounts of labeled 16:1ω5 FA in the IRM and a complete breakdown of the isotopolog pattern conservation (Figure 4E). All in all, these data indicate, that colonized wildtype plants determine the fungal isotopolog pattern by direct lipid transport, which is impaired in AM-specific lipid biosynthesis mutants (Keymer et al. 2017).

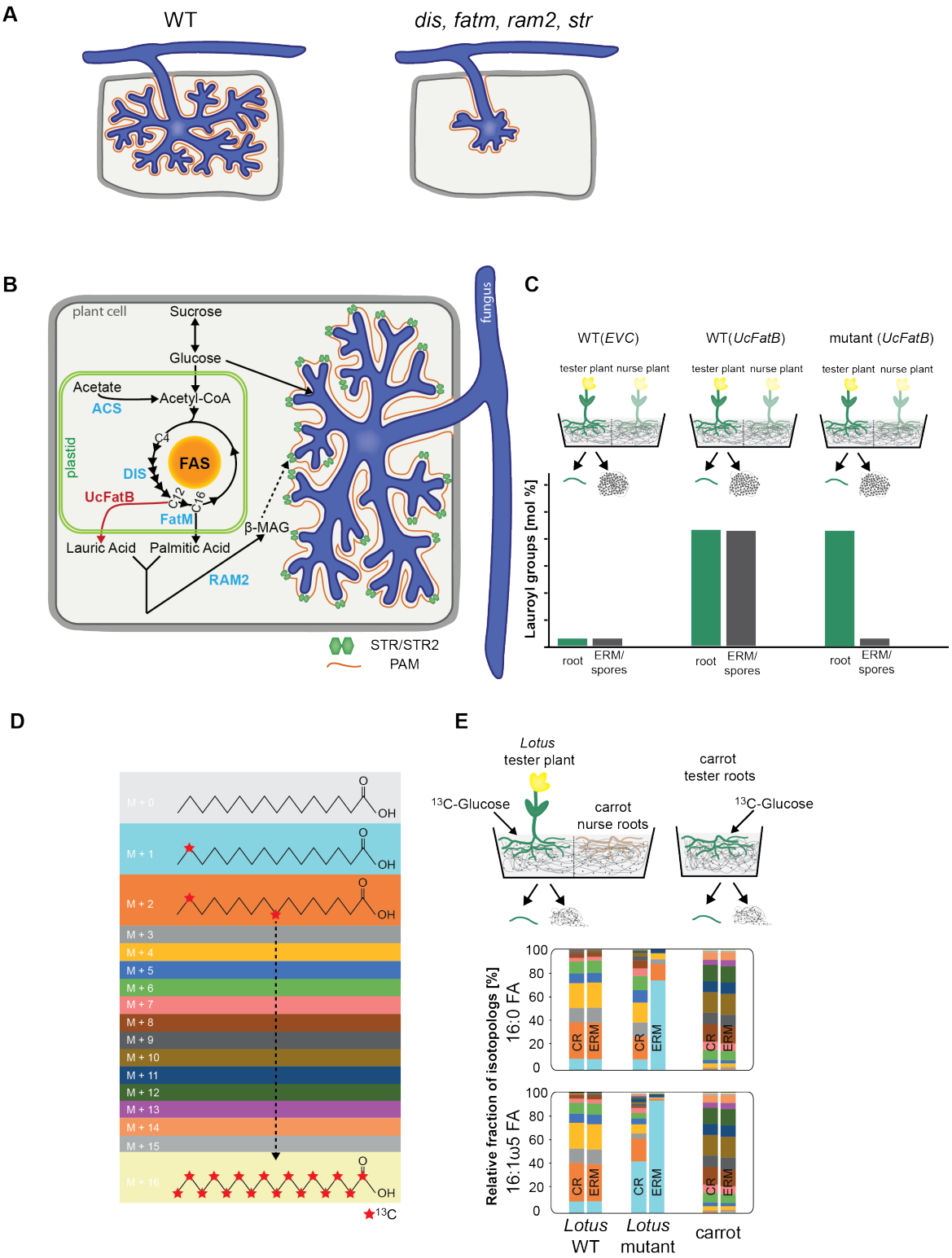

Figure 4: Arbuscule phenotype of AM-specific lipid mutant plants and schematic representation of experimental approaches, which demonstrated lipid transfer from plant to fungus.

(A) Fully branched arbuscules in a wildtype root (left) and stunted arbuscule in roots of AM-specific lipid biosynthesis mutants and the *str* mutant (right). (B) Model of AM-specific lipid biosynthesis pathway in a plant cell hosting an arbuscule. The red arrow illustrates the synthetic deviation of the pathway by transgenic expression of *UcFatB* in *Medicago* hairy roots. (C) Illustration of the growth system used by Luginbuehl et al. (2017) and Jiang et al. (2017), and schematic representation of the results obtained from the quantification of lauroyl groups in colonized roots and fungal ERM/spores upon transgenic expression of *UcFatB*. Tester plant were grown in presence of nurse plants to ensure

sufficient colonization of the lipid biosynthesis mutants. (D) Schematic representation of palmitic acid isotopologs. The isotopologs are quantified by mass spectrometry resulting in a specific isotopolog pattern. (E) Two compartment Petri dish system used by Keymer et al. for isotope labeling (top) and schematic representation of isotopolog pattern in colonized roots and ERM with spores, revealing that *Lotus* wildtype and carrot hairy roots determine the FA isotopolog pattern in the fungus, while the pattern is disturbed in ERM associated with AM-specific lipid biosynthesis mutants. (Figure from Keymer and Gutjahr, 2018)

2. Transcriptional regulation of the AM-specific lipid biosynthesis pathway

The transcription factor RAM1 might be a key player in the transcriptional regulation of the AM-specific lipid machinery. Similar to *Lotus dis* and *ram2* mutants, colonized *Ljram1* mutants are also impaired in the AM-specific accumulation of marker lipids (Keymer et al. 2017). Further, *DIS, KASIII, FatM, RAM2* and *STR* are not induced in *ram1* (Wang et al. 2012; Park et al. 2015; Pimprikar et al. 2016; Luginbuehl et al. 2017; Keymer et al. 2017). These results are accumulating evidence, that plants have evolved an AM-specific *RAM1*-dependent regulatory module for lipid production and delivery to the fungus in arbuscoytes.

Recent data suggests that transcription factors of the AP2/ERF superfamily play a crucial role in the transcriptional regulation of lipid biosynthesis genes. *WRI5 a, b* and c are exclusively found in genomes of AM-competent plant and are homologues to the WRINKLED transcription factors, which regulate late glycolysis and lipid biosynthesis in *Arabidopsis* (Cernac and Benning 2004; To et al. 2012; Luginbuehl et al. 2017; Jiang et al. 2018). RNAi-meditated silencing of *WRI5a* in *Medicago truncatula* caused a significantly reduced total root length colonization and frequency of arbuscule (Jiang et al. 2018). Moreover, similar to WRINKELD in *Arabidopsis,* artificial expression of *Medicago WRI5 a-c* in *N. benthamiana* resulted in the accumulation of TAGs (Luginbuehl et al. 2017). *In vitro* experiments showed binding of WRIa to the AW motif in the *STR* promoter and the same is most probably the case for the promoter of *PT4* (Jiang et al. 2018). Overexpression of *WRI5a* enhances the expression of fatty acid biosynthesis genes as well as lipid and phosphate transfer genes (Jiang et al. 2018). Strikingly, the two regulators, RAM1 and WRI5a, seem to be interconnected in a positive feedback loop, as overexpression of *RAM1* promotes *WRI5a* expression and the same is true the other way around (Jiang et al. 2018; Luginbuehl et al. 2017). All in all, these data suggest, that WRI5 a-c may be RAM1-dependend transcriptional regulators of lipid metabolism and bidirectional nutrient transfer via binding of WRI5 a-

c to AW-motifs in the promoter regions of AM-specific genes (Luginbuehl et al. 2017; Jiang et al. 2018).

In addition to WRI a-c, another AP2 family transcriptional factor, CBX1, was identified recently in *Lotus japonicus*. Similar to RNAi-silenced *WRI5a* plants, LORE1 retrotransposon insertion mutants of *CBX1* are impaired in root fungal length colonization and exhibit a significantly reduced arbuscule frequency (Xue et al. 2018). CBX1 seems to be critical for a variety of AM-specific responses as this regulator has been shown via ChipSeq to target 43 mycorrhiza-inducible genes (Xue et al. 2018). Similar to WRI5 a-c, CBX1 possesses the ability to regulate AM-specific genes of diverse functions including genes with prominent roles in phosphate uptake and AM-specific lipid biosynthesis. In line with this, genome wide studies, heterologous expression and DNA binding assays confirmed the WRI-typical binding of CBX1 to the AW box, which is enriched in lipid biosynthesis genes (Jiang et al. 2018; Xue et al. 2018). Moreover, the CBX1 binding to an additional cis-regulatory motif has been identified (Xue et al. 2018). Several mycorrhiza-induced genes harbor an evolutionary conserved motif, called CTTC CRE (CTTCTTGTTC, alternatively named “MYCS,” TTTCTTGTTCT), in their promotor regions (Chen et al. 2011; Lota et al. 2013; An et al. 2018). A quadruple tandem repeat of the CTTC CRE element fused to the 35s minimal promoter is sufficient to drive *GUS* or *mCherry* expression in the arbuscocyte (Xue et al. 2018). Xue et al. could show binding of CBX1 to the CTTC CRE motif of the PT4 promoter by *in vitro* and *in vivo* assays (Xue et al. 2018). In sum, CBX1 seems to be another core transcriptional regulator for a broad spectrum of AM-specific responses including key processes like lipid biosynthesis and phosphate uptake.

3. Evolution of arbuscular mycorrhiza symbiosis

Arbuscular mycorrhiza symbiosis probably represents a key innovation, which enabled plant migration to land (Bonfante and Genre 2008; Wang et al. 2010). The discovery of 450 My-old fossilized AM-alike spores and the occurrence of AMS in all major linages of extant land plants except most mosses supports the idea that an algal ancestor of land plants was preadapted for AMS (Delaux et al. 2015). Further, the presence of AM signaling genes in algae confirms the early preadaptation to AM associations. Rounds of genome duplications led to the acquisition of additional AM-serving pathways and gradually refined the ability to establish a fully functional AMS

(Delaux et al. 2015). Given that assumption, AMS-ability must have emerged monophyletically. Several phylogenetic studies on AM related plant genes agree on the “mycorrhizial landing” hypothesis, which claims the AMS contribution to plant land colonization and subsequently, the early adaptation of plants for AMS. Accordingly, a set of AM-conserved genes in plant species of different clades was identified (Wang et al. 2010; Favre et al. 2014; Delaux et al. 2015; Bravo et al. 2016; An et al. 2018). AM-conserved genes are represented in diverse functional categories facilitating AM-specific signaling, transport, transcription and metabolic processes. In angiosperms, the loss of AM competence, for example in *Brassicales,* consistently resulted in the independent loss of these genes, supporting the idea that the individual gene function is specifically linked to AM symbiosis (Delaux et al. 2014). A good example are the described lipid biosynthesis genes, *DIS, FatM* and *RAM2.* Their exclusive presence in AM-competent plants implicates an AM-exclusive lipid biosynthesis pathway to nourish the microbial partner (Wang et al. 2012; Bravo et al. 2016; Keymer et al. 2017; Brands et al. 2018; An et al. 2018).

The high conservation degree of the genetic machinery, which enables AMS across such a wide range of evolutionary plant divergence, can possibly be explained by the comparatively small number of *Glomeromycotina* species. Around 270 *Glomeromycotinan* species establish AMS with about 80% of all land plants. Hence. the evolutionary space of mycorrhizial plant genes may be strictly dictated by the small species number of AM fungi, which let mycorrhizal plant genes not diversify much during more than 450 million years of evolution (Redecker et al. 2000; Wang et al. 2010; Crossay et al. 2017). However, the highly conserved genes all refer to basic functions of symbiosis, such as basic features of colonization and nutrient exchange. Therefore, it might be worth focusing on pattern and effector recognition genes, which are usually very variable, in order to extent the knowledge about the conservation degree of AMS plant genes.

The putative preadaptation of algal land plant ancestors for AMS is tempting to be interpreted as a general predisposition event of plant-microbe interactions on Earth. The beneficial RNS clearly evolved from the more ancient AMS and the two associations share many genes, foremost in the early stages of plant-microbe communication (Kistner and Parniske 2002; Stracke et al. 2002; Kistner et al. 2005; Wang et al. 2010; Oldroyd 2013).

However, our understanding if also detrimental microbes exploit this symbiotic program of most land plants for their plant colonization is still limited. Nevertheless, publications about morphological similarities and common signaling principles between AMS, RNS and other plant-microbe interactions already gave rise to hypothesis about a common mechanism for the establishment of diverse plant-microbe interactions (Rey and Schornack 2013; Parniske 2000; Evangelisti et al. 2014; Kloppholz et al. 2011; Bago et al. 2002; Rey and Jacquet 2018). Emerging studies, showing that either mutations in AM-specific genes of AM-competent plants or in *Arabidopsis* homologs of AM-specific genes perturb the interaction of pathogenic microbes, are pioneer work for in-depth investigations of putative common molecular principles of diverse detrimental as well as beneficial plant-microbe associations (Wang et al. 2012; Rey et al. 2015; Ried et al. 2018; Jiang et al. 2017). The results of this thesis indicate, that plant fatty acid and lipid biosynthesis is of conserved importance for plant interactions with the symbiotic fungus *R. irregularis* as well as for detrimental association with the oomycete *H. arabidopsidis.* Though, the molecular basis for the impairment of *Hpa* on *kasI, gpat6* and *gpat4x8 Arabidopsis* mutants still needs to be identified, the obtained results are encouraging support that different hyphal biotrophs seem to depend on similar host plant processes for their own developmental success.

4. Cross-kingdom lipid transfer occurs in several interorganismic associations

Genomes of fungi from all clades harbor genes encoding subunits of the multi-functional FA synthase complex (FASI) (Wewer et al. 2014; Bukhari et al. 2014; Tisserant et al. 2013). This implies that FASI was likely present in the last common ancestor of extant fungi and that AMF might have lost the ability to *de novo* synthesize FAs secondarily after host-derived lipid transfer had evolved (James et al. 2006). *De novo* FA synthesis consumes big amounts of ATP and reducing equivalents NADPH. Thus, it is considered to be a very energy demanding process (Wewer et al. 2014). Therefore, it is favorable for the organism to outsource this process to the host. This might be the main argument why also biotrophic fungal plant pathogens might profit from host FA biosynthesis. The obligate biotrophic fungus, *Erysiphe cichoracearum,* causing powdery mildew symptoms on leaves, induces expression of FA synthesis genes in *Arabidopsis* and bleeds plant FAs, as shown by lauric fatty acid quantification

in *UcFatB* transformed *Arabidopsis* and in *E. cichoracearum* spores, associated to these transgenic plants (Jiang et al. 2017). The close relatives, *Erysiphe necator* and *Erysiphe* graminis possess genes encoding FASI complex subunits and this is highly likely for *E. cichoracearum* as well (Spanu et al. 2010; Jones et al. 2014). Thus, it is tempting to speculate that biotrophic fungi exploit host FA biosynthesis independently from their own ability to produce FAs by themselves in order to reduce energy expenditure (lipid parasitism). The genome of *Ustilago maydis* harbors FASI genes and the fungus can also be cultivated axenically (Teichmann et al. 2007). Notably, upon maize infection lipid biosynthesis genes are strongly upregulated in both, the host plant and the fungus (Doehlemann et al. 2008; Lanver et al. 2018). One can argue that the induction of lipid metabolism on both sides is only due to fungal growth and tumor and/or peri-fungal membrane formation, on the other hand, these expression patterns may also indicate that lipids are provided by the host plant to *U. maydis.* Further, host-lipid exploitation is likely also a feature of oomycete-plant interactions. For example, infection of *Nicotiana benthamiana* by the hemibiotrophic oomycete *Phytophthora* induces expression of *GPAT6* and *Phytophthora* exhibited a high frequency of misshaped haustoria in the *gpat6* mutant of tomato. However, the increased susceptibility of *Phytophthora* in *gpat6* mutants of tomato and *N. benthaminana* might be counterintuitive to argue that plant derived lipids are of advantageous effect for *Phytophthora* (Fawke et al. 2018). More obvious seems the impact of plant lipid biosynthesis for biotrophic oomycetes. Strikingly, the obligate biotroph *Hpa* is severely hindered in development and reproduction when infecting the fatty acid and lipid biosynthesis mutants *kasI, gpat6* and *gpat4x8* of *Arabidopsis* (Manuscript I). Even if genome data of *Hpa* indicate the competence for *de novo* fatty acid synthesis (Baxter et al. 2010), the impairment of *Hpa* development on *kasI, gpat6* and *gpat4x8* mutants suggests that *Hpa* fitness depends on an intact host lipid biosynthesis machinery. Certainly, the basis for this impairment has to be identified and direct lipid transfer remains to be tested for plant interactions with the oomycetes like *Hpa* and *Phytophthora* as well as interactions with the biotrophic fungus *Ustilago*. Nevertheless, the listed results may already indicate that lipid transfer from host to microbe may be a more widespread phenomenon in plant-fungal/oomycetal interactions and not exclusively restricted to AMS.

The impotence to produce FA *de novo* is not restricted to AMF. Yeasts belonging to the *Malassezia* spp. also lack FASI encoding genes. These lipid-depended fungi are

representatives of the human and animal skin microbiota, typically found in regions rich in sebaceous glands associated to dandruff (Xu et al. 2007; Triana et al. 2017). Furthermore, the genome of the *Plasmodiophorid, Plasmodiophora brassicae,* an obligate biotrophic protist in the eukaryotic kingdom *Rhizaria,* which causes clubroot, a major disease of *Brassica* oil and vegetable crops worldwide, lacks fatty acid synthesis genes. This loss obviously makes *P. brassicae* fully dependent on lipid scavenging (Schwelm et al. 2015). In the genomes of both, *P. brassicae* and *Malassezia* spp., the reliance to assimilate FAs from external sources is indicated by the presence of multiple genes encoding phospholipases and secreted lipases (Xu et al. 2007; Schwelm et al. 2015; Triana et al. 2015; Wu et al. 2015).

Apicomplexans, comprising a large group of unicellular eukaryotic animal parasites, such as *Toxoplasma, Leishmania, Plasmodium* and *Trypanosoma,* selectively exploit host lipids for their own requirement – no matter whether they are competent to produce FAs on their own or not (Mazumdar and Striepen 2007; Rub et al. 2013). The majority of these intracellular protozoan parasites lives inside the host cell and akin to AMF and other biotrophic plant-pathogenic microbes, they are surrounded by a host-derived membrane, the parasite vacuolar membrane (PVM), across which the host cargo is transferred. *Apicomplexans* scavenge a variety of lipids via a diversity of mechanisms, which are not yet fully understood (Rub et al. 2013). Recent evidence suggests that host derived lipid bodies enter the PVM and may serve as lipid sources (Toledo et al. 2016).

Also, bacterial plant pathogens, called phytoplasms, endosymbiotic bacteria of insects and pathogenic bacteria of humans have been proven to depend on host lipid transfer (Oshima et al. 2004; Elwell et al. 2011; Herren et al. 2014; Paredes et al. 2016). Strikingly, *Spiroplasma poulsonii,* naturally associated to *Drosophila melanogaster,* depletes lipids from the host hemolymph. Similar to AMF, *S. poulsonii* proliferation is restricted by the availability of host-derived lipids (Bravo et al. 2017; Keymer et al. 2017; Herren et al. 2014). This association appears to be mutualistic as these endosymbiotic bacteria protect *Drosophila* as well as other insects against a range of parasitoid wasps, which notably also have lost to synthesize FAs from *de novo,* probably as an evolutionary consequence of their parasitoid lifestyle (Paredes et al. 2016; Visser et al. 2010).

In summary, the dependence on host lipids and lipid parasitism has evolved, probably independently, multiple times (Table 1) and may turn out to be more widespread than

currently known. Although, outsourcing fundamental processes like *de novo* fatty acid synthesis to the host intensifies the dependence and can be seen as a driver towards true biotrophy, it can also be interpreted as a stringent and energy saving consequence of environmental compensation (Visser et al. 2010). All in all, no matter if parasitic or truly mutualistic, diverse microbes exploit host lipids for their own energy efficiency (lipid parasitism) or even rely exclusively on the external lipid source (lipid dependence).

Microbe	Kingdom	Host	Able to synthesize FAs	References
Chlamydia	bacteria	mammals	Yes	(Elwell et al. 2011; Hackstadt T. 1995)
Spiroplasma	bacteria	insects	No	(Herren et al. 2014)
Erysiphae	mycota	plants	Yes	(Jiang et al. 2017)
Glomeromycotina	mycota	plants	No	(Jiang et al. 2017; Luginbuehl et al. 2017; Keymer et al. 2017)
Malassezia	mycota	mammals	No	(Triana et al. 2017; Wu et al. 2015)
Ustilago	mycota	plants	Yes	(Doehlemann et al. 2008; Lanver et al. 2018)
Phytophthora	straminipila	plants	Yes	(Fawke et al. 2018)
Hyaloperonospora	straminipila	plants	Yes	(Manuscript I)
Leishmania	protists	mammals	Yes	(Rub et al. 2013)
Plasmodiophorid	protists	plants	No	(Schwelm et al. 2015)
Plasmodium	protists	mammals	Yes	(Jackson et al. 2004; Itoe et al. 2014)
Theileria	protists	mammals	No	(Mazumdar and Striepen 2007; Gardner et al. 2005)
Toxoplasma	protists	mammals	Yes	(Charron and Sibley 2002; Coppens 2006; Mazumdar and Striepen 2007)
Trypanosma	protists	mammals	Yes	(Toledo et al. 2016; Melo et al. 2003)

Table 1: Organisms associated with their host in order to exploit lipids. Bright colors indicate interactions, with reported lipid scavenging from the host. Faint colors indicate interactions, for which circumstantial evidence suggest lipid dependence or lipid parasitism. The ability to produce FA is based on the presence of fatty acid synthase genes in respective genomes. (modified table from Keymer and Gutjahr; COPB (2018))

X. Outlook

This doctoral work has shown that lipids are transported from wildtype *Lotus japonicus* plants to the associated AM fungus and characterized *DIS, RAM2* and *FatM* as essential components of an AM-specific lipid biosynthesis pathway. The next challenging questions to be addressed will be the transcriptional regulation of AM-specific lipid biosynthesis in host plants (see IX.2), the identification of the exact lipid cargo that is transported and the transfer mechanism via which the lipid cargo is sent to the fungus. Moreover, in the light of the biological market theory, it will be of great scientific value to gain insights into the relative amounts of translocated carbohydrates and lipids.

16:0 sn2-MAG appears to be a likely candidate-lipid to serve as cargo and to be exported from the plant cell. This compound is likely the most abundant product of RAM2, which is so far the most downstream enzyme of the AM-specific lipid biosynthesis pathway. Furthermore, lipid profiles of colonized *dis, fatm* and *ram2* mutants show a massive shortage of 16:0 sn2-MAGs (Keymer et al. 2017; Brands et al. 2018; Bravo et al. 2017). Interestingly, acetylation of glycerol on the sn2 position via land plant-specific GPATs results in sn2-MAGs, which comprise a specific group of lipids, that are apparently not used for storage or membrane lipid synthesis, but have been reported to be exported to cell surfaces to serve as precursors of suberin and cutin biosynthesis in plants (Li et al. 2007; Yang et al. 2012). Thus, sn2-MAGs represent a convenient vehicle to redirect FAs from the plant storage and membrane lipid biosynthesis towards export. Moreover, significant amounts of sn2-MAGs were also found in the ERM of AMF and a fungal monoacylglyceride lipase (*MGL1*) has been identified to be highly expressed in the arbuscule (Brands et al. 2018; Kameoka H. 2018). This suggests that MAG is not only a favorable transport cargo within the fungal mycelium but may also be metabolized directedly in the arbuscule, once it is received by the fungus.

Concerning the mechanism of transfer, many scenarios appear conceivable and transfer might not happen via one exclusive route but possibly in different ways. A reasonable candidate to pump lipids from the plant cell into the peri-arbuscular space is the AM-specific PAM-localized ABCG transporter heterocomplex STR/STR2 (Zhang et al. 2010; Gutjahr et al. 2012). As support of this hypothesis, the AM phenotype of *str* resembles that of AM-specific lipid biosynthesis mutants with regard to the

morphological discrepancies of the fungal structures and to the lipid profiles of colonized roots (Bravo et al. 2017; Keymer et al. 2017; Jiang et al. 2017; Zhang et al. 2010; Gutjahr et al. 2012). Notably, *str* mutants in *Medicago* and *Lotus* are to the same extent unable to transport lipids to the fungus as *dis* and *ram2* mutants (Jiang et al. 2017; Keymer et al. 2017). Furthermore, the lipid, especially sn2-MAG, transport ability for ABCG transporters has already been highlighted. Genetic evidence suggests, that *Arabidopsis* ABCG transporters facilitate sn2-MAG export for leaf cuticle formation (Pighin et al. 2004; Panikashvili et al. 2011; Yeats et al. 2012). Further, a mammalian host-derived ABC transporter, which is located in the PVM, is known to transport cholesterol to *Toxoplasma* (Rub et al. 2013; Bottova et al. 2009). In addition to direct transport via the ABCG transporter complex STR/STR2 at the PAM, lipids might also be shuffled as cargo of extracellular vesicles (EV) into the PAS. The relevance of EV in plant-microbe interactions is poorly understood. However, it has been shown, that the formation of multivesicular bodies (MVBs), the precursors of EVs, is enhanced upon fungal infection of pathogenic powdery mildew fungi (An et al. 2006; An et al. 2006), which indicates their relevance in plant-microbe interactions. In current research concepts MVBs/EVs are predominately affiliated to pathogenicity or defense response for example to mediate small RNA transport (Samuel et al. 2015; Cai et al. 2018), but these structures are also capable to transport lipids (Rutter and Innes 2018; Rub et al. 2013). One could assume that ABCG transporters like STR/STR2 might also facilitate lipid loading of EVs. Lipid uptake from the PAS on the fungal site is hardly studied. So far, only fungal ABC transporters have been identified, which are expressed in the IRM, and therefore, might mediate lipid uptake from the PAS into the fungal cytoplasm (Tisserant et al. 2012; Tang et al. 2016).

Future research on the *Hpa-Arabidopsis* interaction is required to identify the basis for the developmental impairment of *Hpa* on *Arabidopsis* fatty acid/lipid biosynthesis mutants of *KASI, GPAT4/8* and *6.* As any other microbial colonization, *Hpa* infection and development requires signaling and membrane synthesis (Dörmann et al. 2014). Thus, various involvements of KASI and GPAT4/6/8 seem plausible. Lipid-derived signaling components are involved in the plant response to the invasion of microbes (Chaturvedi et al. 2012; Mandal et al. 2012; Zoeller et al. 2012). Accordingly, lipids produced by KASI, GPAT4, 6 and 8 could be required to produce precursors of signaling molecules that affect either the host cell or the microbe. Alternatively, lipids produced via these enzymes could also serve as building blocks for EHM membrane

synthesis, which might explain the aberrancies of *Hpa* haustoria in the respective challenged *Arabidopsis* mutants. With respect to the AM results of this thesis obtained for AM symbiosis, it might also be likely that the pathogenic biotroph *Hpa* exploits host-derived lipids. Though, *Hpa* seems to be FA and lipid prototroph (Baxter et al. 2010), lipid parasitism might be a favorable strategy for energy efficiency. Therefore, challenging the hypothesis of plant-derived lipid transfer to the pathogen in future studies appears worthwhile.

In conclusion, this work elucidated the importance of plant-derived lipids for AMS and further contributed to the understanding of host-derived lipids as common compatibility factors for different host-microbe interactions. Moreover, this thesis in combination with emerging knowledge from literature indicates an overlap of morphological principles between diverse plant interactions with filamentous microbes. If also molecular principles are shared, remains to be shown in successive studies.

XI. References:

Abrahamian, M., A. M. Ah-Fong, C. Davis, K. Andreeva, and H. S. Judelson. 2016. 'Gene expression and silencing studies in *Phytophthora infestans* reveal infection-specific nutrient transporters and a role for the nitrate reductase pathway in plant pathogenesis', *PLoS Pathogen*, 12: e1006097.

Ah-Fong, A. M. V., J. Shrivastava, and H. S. Judelson. 2017. 'Lifestyle, gene gain and loss, and transcriptional remodeling cause divergence in the transcriptomes of *Phytophthora infestans* and *Pythium ultimum* during potato tuber colonization', *BMC Genomics*, 18: 764.

Akiyama, K, KI Matsuzaki, and H Hayashi. 2005. 'Plant sesquiterpenes induce hyphal branching in arbuscular mycorrhizal fungi', *Nature*, 435: 824-27.

Al-Babili, Salim, and Harro J. Bouwmeester. 2015. 'Strigolactones, a novel carotenoid-derived plant hormone', *Annual Review of Plant Biology*, 66: 161-86.

Alexander, T., R. Meier, R. Toth, and H. Weber. 1988. 'Dynamics of arbuscule development and degeneration in mycorrhizas of *Triticum aestivum* L. and *Avena sativa* L. with reference to *Zea mays* L.', *New Phytol*, 110: 363-70.

Allen, James W., and Yair Shachar-Hill. 2009. 'Sulfur transfer through an arbuscular mycorrhiza', *Plant Physiol.*, 149: 549-60.

Allen, M. F., W. Swenson, J. I. Querejeta, L. M. Egerton-Warburton, and K. K. Treseder. 2003. 'Ecology of mycorrhizae: A conceptual framework for complex interactions among plants and fungi', *Annual Review of Phytopathology*, 41: 271-303.

Alvey, Liz, and Nicholas P. Harberd. 2004. 'DELLA proteins: integrators of multiple plant growth regulatory inputs?', *Physiologia Plantarum*, 123: 153-60.

Ames, R. N., C. P. P. Reid, L. K. Porter, and C. Cambardella. 1983. 'Hyphal uptake and transport of nitrogen from two 15N-labelled sources by *Glomus mosseae,* a vesicular-arbuscular mycorrhizal fungus', *New Phytol*, 95: 381-96.

An, J., M. Sun, R. van Velzen, C. Ji, Z. Zheng, E. Limpens, T. Bisseling, X. Deng, S. Xiao, and Z. Pan. 2018. 'Comparative transcriptome analysis of *Poncirus trifoliata* identifies a core set of genes involved in arbuscular mycorrhizal symbiosis', *J Exp Bot*, 69: 5255-64.

An, Q., K. Ehlers, K. H. Kogel, A. J. van Bel, and R. Huckelhoven. 2006. 'Multivesicular compartments proliferate in susceptible and resistant MLA12-barley leaves in response to infection by the biotrophic powdery mildew fungus', *New Phytol*, 172: 563-76.

An, Q., R. Huckelhoven, K. H. Kogel, and A. J. van Bel. 2006. 'Multivesicular bodies participate in a cell wall-associated defence response in barley leaves attacked by the pathogenic powdery mildew fungus', *Cell Microbiol*, 8: 1009-19.

Antolín-Llovera, Meritxell, Martina K Ried, and Martin Parniske. 2014. 'Cleavage of the SYMBIOSIS RECEPTOR-LIKE KINASE ectodomain promotes complex formation with Nod Factor Receptor 5', *Current Biology*, 24: 422-27.

Asai, Shuta, Ghanasyam Rallapalli, Sophie J. M. Piquerez, Marie-Cécile Caillaud, Oliver J. Furzer, Naveed Ishaque, Lennart Wirthmueller, Georgina Fabro, Ken Shirasu, and Jonathan D. G. Jones. 2014. 'Expression profiling during Arabidopsis/downy mildew interaction reveals a highly-expressed effector that attenuates responses to salicylic acid', *PLoS Pathogen*, 10: e1004443.

Auge, R. M. 2001. 'Water relations, drought and vesicular-arbuscular mycorrhizal symbiosis', *Mycorrhiza*.

Bago, B, PE Pfeffer, and Y Shachar-Hill. 2000. 'Carbon metabolism and transport in arbuscular mycorrhizas', *Plant Physiol*, 124: 949-57.
Bago, B., and G. Bécard. 2002. 'Bases of the obligate biotrophy of arbuscular mycorrhizal fungi.' in Silvio Gianinazzi, Hannes Schüepp, José Miguel Barea and Kurt Haselwandter (eds.), *Mycorrhizal Technology in Agriculture: From Genes to Bioproducts* (Birkhäuser Basel: Basel).
Bago, B., H. Vierheilig, Y. PichÉ, and C. AzcÓN-Aguilar. 1996. 'Nitrate depletion and pH changes induced by the extraradical mycelium of the arbuscular mycorrhizal fungus *Glomus intraradices* grown in monoxenic culture', *New Phytol*, 133: 273-80.
Bago, Berta, Philip E. Pfeffer, Jehad Abubaker, Jeongwon Jun, James W. Allen, Janine Brouillette, David D. Douds, Peter J. Lammers, and Yair Shachar-Hill. 2003. 'Carbon export from arbuscular mycorrhizal roots involves the translocation of carbohydrate as well as lipid', *Plant Physiol*, 131: 1496-507.
Bago, Berta, Warren Zipfel, Rebecca M. Williams, Jeongwon Jun, Raoul Arreola, Peter J. Lammers, Philip E. Pfeffer, and Yair Shachar-Hill. 2002. 'Translocation and utilization of fungal storage lipid in the arbuscular mycorrhizal symbiosis', *Plant Physiol*, 128: 108-24.
Baier, MC, M Keck, V Gödde, K Niehaus, H Küster, and N Hohnjec. 2010. 'Knockdown of the symbiotic sucrose synthase *MtSucS1* affects arbuscule maturation and maintenance in mycorrhizal roots of *Medicago truncatula*', *Plant Physiol.*, 152: 1000-14.
Bailey, Kate, Volkan Çevik, Nicholas Holton, Jane Byrne-Richardson, Kee Hoon Sohn, Mary Coates, Alison Woods-Tör, H. Murat Aksoy, Linda Hughes, Laura Baxter, Jonathan D. G. Jones, Jim Beynon, Eric B. Holub, and Mahmut Tör. 2011. 'Molecular cloning of *ATR5* Emoy2 from *Hyaloperonospora arabidopsidis*, an avirulence determinant that triggers RPP5-mediated defense in *Arabidopsis*', *Molecular Plant-Microbe Interactions*, 24: 827-38.
Bais, Harsh P., Tiffany L. Weir, Laura G. Perry, Simon Gilroy, and Jorge M. Vivanco. 2006. 'The role of root exudates in Rhizosphere interactions with plants and other organisms ', *Annual Review of Plant Biology*, 57: 233-66.
Balestrini, Raffaella, Jorge Gómez-Ariza, Luisa Lanfranco, and Paola Bonfante. 2007. 'Laser microdissection reveals that transcripts for five plant and one fungal phosphate transporter genes are contemporaneously present in arbusculated cells', *Molecular Plant-Microbe Interactions*, 20: 1055-62.
Balzergue, Coline, Virginie Puech-Pagès, Guillaume Bécard, and Soizic F. Rochange. 2010. 'The regulation of arbuscular mycorrhizal symbiosis by phosphate in pea involves early and systemic signalling events', *Journal of Experimental Botany*, 62: 1049-60.
Bardgett, Richard D., and Wim H. van der Putten. 2014. 'Belowground biodiversity and ecosystem functioning', *Nature*, 515: 505.
Bary, A. de. 1879. 'Die Erscheinung der Symbiose', *Trübner Verlag*.
Baxter, Laura, Sucheta Tripathy, Naveed Ishaque, Nico Boot, Adriana Cabral, Eric Kemen, Marco Thines, Audrey Ah-Fong, Ryan Anderson, Wole Badejoko, Peter Bittner-Eddy, Jeffrey L. Boore, Marcus C. Chibucos, Mary Coates, Paramvir Dehal, Kim Delehaunty, Suomeng Dong, Polly Downton, Bernard Dumas, Georgina Fabro, Catrina Fronick, Susan I. Fuerstenberg, Lucinda Fulton, Elodie Gaulin, Francine Govers, Linda Hughes, Sean Humphray, Rays H. Y. Jiang, Howard Judelson, Sophien Kamoun, Kim Kyung, Harold Meijer, Patrick Minx, Paul Morris, Joanne Nelson, Vipa Phuntumart, Dinah Qutob, Anne Rehmany, Alejandra Rougon-Cardoso, Peter Ryden, Trudy Torto-

Alalibo, David Studholme, Yuanchao Wang, Joe Win, Jo Wood, Sandra W. Clifton, Jane Rogers, Guido Van den Ackerveken, Jonathan D. G. Jones, John M. McDowell, Jim Beynon, and Brett M. Tyler. 2010. 'Signatures of adaptation to obligate biotrophy in the *Hyaloperonospora arabidopsidis* genome', *Science*, 330: 1549-51.

Benedetto, A., F. Magurno, P. Bonfante, and L. Lanfranco. 2005. 'Expression profiles of a phosphate transporter gene (*GmosPT*) from the endomycorrhizal fungus *Glomus mosseae*', *Mycorrhiza*, 15: 620-27.

Bentivenga, S. P., and J. B. Morton. 1996. 'Congruence of fatty acid methyl ester profiles and morphological characters of arbuscular mycorrhizal fungi in *Gigasporaceae*', *Proc Natl Acad Sci USA*, 93: 5659-62.

Berruti, Andrea, Erica Lumini, Raffaella Balestrini, and Valeria Bianciotto. 2016. 'Arbuscular mycorrhizal fungi as natural biofertilizers: Let's benefit from past successes', *Frontiers in Microbiology*, 6.

Besserer, A, V Puech-Pagés, and P Kiefer, Gomez-Roldan, V, Jauneau, A, Roy, S, Portais, JC, Roux, C, Bécard, G, Séjalon-Delmas, N. 2006. 'Strigolactones stimulate arbuscular mycorrhizal fungi by activating mitochondria', *PLoS Biology*, 4: e226. DOI: 10.1371/journal.pbio.0040226.

Besserer, Arnaud, Guillaume Becard, Alain Jauneau, Christophe Roux, and Nathalie Sejalon-Delmas. 2008. 'GR24, a synthetic analog of strigolactones, stimulates the mitosis and growth of the arbuscular mycorrhizal fungus *Gigaspora rosea* by boosting its energy metabolism.', *Plant Physiol*, 148: 402-13.

Binder, A, and M Parniske. 2013. 'The nuclear pore complex in symbiosis and pathogen defence', *Annual Plant Reviews*, 46: 229-54.

Blee, K. A., and A. J. Anderson. 1998. 'Regulation of arbuscule formation by carbon in the plant', *Plant J.*, 16.

Bolle, Cordelia. 2004. 'The role of GRAS proteins in plant signal transduction and development', *Planta*, 218: 683-92.

Boller, T., and G. Felix. 2009. 'A renaissance of elicitors: perception of microbe-associated molecular patterns and danger signals by pattern-recognition receptors', *Annu Rev Plant Biol*, 60: 379-406.

Bonfante, P., and A. Genre. 2015. 'Arbuscular mycorrhizal dialogues: do you speak 'plantish' or 'fungish'?', *Trends Plant Sci*, 20: 150-4.

Bonfante, Paola, and Andrea Genre. 2008. 'Plants and arbuscular mycorrhizal fungi: an evolutionary-developmental perspective', *Trends Plant Sci*, 13: 492-98.

Bonfante, Paola, Andrea Genre, Antonella Faccio, Isabella Martini, Leif Schauser, Jens Stougaard, Judith Webb, and Martin Parniske. 2000. 'The *Lotus japonicus LjSym4* gene is required for the successful symbiotic infection of root epidermal cells', *Molecular Plant-Microbe Interactions*, 13: 1109-20.

Bonfante-Fasolo, S. Scannerini and P. 1983. 'Comparative ultrastructural analysis of mycorrhizal associations', *Canadian Journal of Botany*, 61.

Bottova, I., A. B. Hehl, S. Stefanic, G. Fabrias, J. Casas, E. Schraner, J. Pieters, and S. Sonda. 2009. 'Host cell P-glycoprotein is essential for cholesterol uptake and replication of *Toxoplasma gondii*', *J Biol Chem*, 284: 17438-48.

Bozkurt, Tolga O., Sebastian Schornack, Mark J. Banfield, and Sophien Kamoun. 2012. 'Oomycetes, effectors, and all that jazz', *Current Opinion in Plant Biology*, 15: 483-92.

Brands, M., V. Wewer, A. Keymer, C. Gutjahr, and P. Dörmann. 2018. 'The *Lotus japonicus* acyl-acyl carrier protein thioesterase FatM is required for mycorrhiza formation and lipid accumulation of *Rhizophagus irregularis*', *Under Review*.

Braunberger, P. G., M. H. Miller, and R. L. Peterson. 1991. 'Effect of phosphorous nutrition on morphological characteristrics of vesicular-arbuscular mycorrhizal colonization of maize', *New Phytol*, 119: 107-13.
Bravo, A, T York, N Pumplin, LA Mueller, and MJ Harrison. 2016. 'Genes conserved for arbuscular mycorrhizal symbiosis identified through phylogenomics', *Nature Plants*, 2: doi: 10.1038/NPLANTS.2015.208.
Bravo, Armando, Mathias Brands, Vera Wewer, Peter Dörmann, and Maria J. Harrison. 2017. 'Arbuscular mycorrhiza-specific enzymes FatM and RAM2 fine-tune lipid biosynthesis to promote development of arbuscular mycorrhiza', *New Phytol*, 214: 1631-45.
Breakspear, Andrew, Chengwu Liu, Sonali Roy, Nicola Stacey, Christian Rogers, Martin Trick, Giulia Morieri, Kirankumar S. Mysore, Jiangqi Wen, Giles E. D. Oldroyd, J. Allan Downie, and Jeremy D. Murray. 2014. 'The Root Hair "Infectome" of *Medicago truncatula* uncovers changes in cell cycle genes and reveals a requirement for auxin signaling in rhizobial infection', *Plant Cell*.
Breuillin, Florence, Jonathan Schramm, Mohammad Hajirezaei, Amir Ahkami, Patrick Favre, Uwe Druege, Bettina Hause, Marcel Bucher, Tobias Kretzschmar, Eligio Bossolini, Cris Kuhlemeier, Enrico Martinoia, Philipp Franken, Uwe Scholz, and Didier Reinhardt. 2010. 'Phosphate systemically inhibits development of arbuscular mycorrhiza in *Petunia hybrida* and represses genes involved in mycorrhizal functioning', *Plant J*, 64: 1002-17.
Breuillin-Sessoms, Florence, Daniela S. Floss, S. Karen Gomez, Nathan Pumplin, Yi Ding, Veronique Levesque-Tremblay, Roslyn D. Noar, Dierdra A. Daniels, Armando Bravo, James B. Eaglesham, Vagner A. Benedito, Michael K. Udvardi, and Maria J. Harrison. 2015. 'Suppression of arbuscule degeneration in *Medicago truncatula phosphate transporter4* mutants is dependent on the ammonium transporter 2 family protein AMT2;3', *Plant Cell*, 27: 1352-66.
Brundrett, M. C., and L. Tedersoo. 2018. 'Evolutionary history of mycorrhizal symbioses and global host plant diversity', *New Phytol*: doi: 10.1111/nph.14976.
Brussaard, Lijbert. 1997. 'Biodiversity and ecosystem functioning in soil', *Ambio*, 26: 563-70.
Buée, M, M Rossignol, A Jauneau, R Ranjeva, and G Bécard. 2000. 'The pre-symbiotic growth of arbuscular mycorrhizal fungi is induced by a branching factor partially purified from from plant root exsudates.', *Molecular Plant-Microbe Interactions*, 13: 693-98.
Buendia, Luis, Tongming Wang, Ariane Girardin, and Benoit Lefebvre. 2015. 'The LysM receptor-like kinase SlLYK10 regulates the arbuscular mycorrhizal symbiosis in tomato', *New Phytol*, 210: 184-95.
Bukhari, H. S., R. P. Jakob, and T. Maier. 2014. 'Evolutionary origins of the multienzyme architecture of giant fungal fatty acid synthase', *Structure*, 22: 1775-85.
Busby, P. E., C. Soman, M. R. Wagner, M. L. Friesen, J. Kremer, A. Bennett, M. Morsy, J. A. Eisen, J. E. Leach, and J. L. Dangl. 2017. 'Research priorities for harnessing plant microbiomes in sustainable agriculture', *PLoS Biology*, 15: e2001793.
Cai Q, Qiao L, Wang M, He B, Lin, FM, Palmquist J, Huang HD, Jin H. 2018. 'Plants send small RNAs in extracellular vesicles to fungal pathogen to silence virulence genes', *Science*.
Cai, Qiang, Lulu Qiao, Ming Wang, Baoye He, Feng-Mao Lin, Jared Palmquist, Sienna-Da Huang, and Hailing Jin. 2018. 'Plants send small RNAs in

extracellular vesicles to fungal pathogen to silence virulence genes', *Science*, 360: 1126.
Caillaud, Marie-Cécile, Shuta Asai, Ghanasyam Rallapalli, Sophie Piquerez, Georgina Fabro, and Jonathan D. G. Jones. 2013. 'A downy mildew effector attenuates salicylic acid–triggered immunity in arabidopsis by interacting with the host mediator complex', *PLoS Biology*, 11: e1001732.
Camps, Céline, Marie-Françoise Jardinaud, David Rengel, Sébastien Carrère, Christine Hervé, Frédéric Debellé, Pascal Gamas, Sandra Bensmihen, and Clare Gough. 2015. 'Combined genetic and transcriptomic analysis reveals three major signalling pathways activated by Myc-LCOs in *Medicago truncatula*', *New Phytol*, 208: 224-40.
Capoen, Ward, Jongho Sun, Derin Wysham, Marisa S. Otegui, Muthusubramanian Venkateshwaran, Sibylle Hirsch, Hiroki Miwa, J. Allan Downie, Richard J. Morris, Jean-Michel Ané, and Giles E. D. Oldroyd. 2011. 'Nuclear membranes control symbiotic calcium signaling of legumes', *PNAS*, 108: 14348-53.
Carbonnel, Samy, and Caroline Gutjahr. 2014. 'Control of arbuscular mycorrhiza development by nutrient signals', *Front Plant Sci*, 5.
Casieri, Leonardo, Karine Gallardo, and Daniel Wipf. 2012. 'Transcriptional response of *Medicago truncatula* sulphate transporters to arbuscular mycorrhizal symbiosis with and without sulphur stress', *Planta*, 235: 1431-47.
Cernac, A., and C. Benning. 2004. 'WRINKLED1 encodes an AP2/EREB domain protein involved in the control of storage compound biosynthesis in *Arabidopsis*', *Plant J*, 40: 575-85.
Chabaud, Mireille, Andrea Genre, Björn J. Sieberer, Antonella Faccio, Joëlle Fournier, Mara Novero, David G. Barker, and Paola Bonfante. 2011. 'Arbuscular mycorrhizal hyphopodia and germinated spore exudates trigger Ca2+ spiking in the legume and nonlegume root epidermis', *New Phytol*, 189: 347-55.
Charpentier, Myriam, Rolf Bredemeier, Gerhard Wanner, Naoya Takeda, Enrico Schleiff, and Martin Parniske. 2008. '*Lotus japonicus* CASTOR and POLLUX are ion channels essential for perinuclear calcium spiking in legume root endosymbiosis', *Plant Cell*, 20: 3467-79.
Charpentier, Myriam, Jongho Sun, Teresa Vaz Martins, Guru V. Radhakrishnan, Kim Findlay, Eleni Soumpourou, Julien Thouin, Anne-Aliénor Véry, Dale Sanders, Richard J. Morris, and Giles E. D. Oldroyd. 2016. 'Nuclear-localized cyclic nucleotide–gated channels mediate symbiotic calcium oscillations', *Science*, 352: 1102.
Charron, Audra J., and L. David Sibley. 2002. 'Host cells: mobilizable lipid resources for the intracellular parasite *Toxoplasma gondii*', *J Cell Sci*, 115: 3049-59.
Chaturvedi, R., B. Venables, R. A. Petros, V. Nalam, M. Li, X. Wang, L. J. Takemoto, and J. Shah. 2012. 'An abietane diterpenoid is a potent activator of systemic acquired resistance', *Plant J*, 71: 161-72.
Chen, Aiqun, Mian Gu, Shubin Sun, Lingling Zhu, Shuai Hong, and Guohua Xu. 2011. 'Identification of two conserved cis-acting elements, MYCS and P1BS, involved in the regulation of mycorrhiza-activated phosphate transporters in eudicot species', *New Phytol*, 189: 1157-69.
Chen, E. C., S. Mathieu, A. Hoffrichter, K. Sedzielewska-Toro, M. Peart, A. Pelin, S. Ndikumana, J. Ropars, S. Dreissig, J. Fuchs, A. Brachmann, and N. Corradi. 2018. 'Single nucleus sequencing reveals evidence of inter-nucleus recombination in arbuscular mycorrhizal fungi', *eLife*, 7.

Chen, X., G. Shen, Y. Wang, X. Zheng, and Y. Wang. 2007. 'Identification of *Phytophthora sojae* genes upregulated during the early stage of soybean infection', *FEMS Microbiol Lett*, 269: 280-8.
Clark, J. S. C., and P. T. N. Spencer-Phillips. 1993. 'Accumulation of photoassimilate by *Peronospora viciae* (Berk.) Casp. and leaves of *Pisum sativum* L.: evidence for nutrient uptake via intercellular hyphae', *New Phytol*, 124: 107-19.
Coates, Mary E., and Jim L. Beynon. 2010. '*Hyaloperonospora arabidopsidis* as a pathogen model', *Annual Review of Phytopathology*, 48: 329-45.
Compant, Stéphane, Christophe Clément, and Angela Sessitsch. 2010. 'Plant growth-promoting bacteria in the rhizo- and endosphere of plants: Their role, colonization, mechanisms involved and prospects for utilization', *Soil Biology and Biochemistry*, 42: 669-78.
Coppens, I. 2006. 'Contribution of host lipids to *Toxoplasma* pathogenesis', *Cell Microbiol*, 8: 10.1111/j.462-5822.2005.00647.x.
Corradi, Nicolas, and Andreas Brachmann. 2017. 'Fungal mating in the most widespread plant symbionts?', *Trends Plant Sci*, 22: 175-83.
Crossay, T., C. Antheaume, D. Redecker, L. Bon, N. Chedri, C. Richert, L. Guentas, Y. Cavaloc, and H. Amir. 2017. 'New method for the identification of arbuscular mycorrhizal fungi by proteomic-based biotyping of spores using MALDI-TOF-MS', *Sci Rep*, 7: 14306.
Cruz, Cristina, Helge Egsgaard, Carmen Trujillo, Per Ambus, Natalia Requena, Maria Amélia Martins-Loução, and Iver Jakobsen. 2007. 'Enzymatic evidence for the key role of arginine in nitrogen translocation by arbuscular mycorrhizal fungi', *Plant Physiol*, 144: 782.
Czaja, Lisa F., Claudia Hogekamp, Patrick Lamm, Fabienne Maillet, Eduardo Andres Martinez, Eric Samain, Jean Dénarié, Helge Küster, and Natalija Hohnjec. 2012. 'Transcriptional responses toward diffusible signals from symbiotic microbes reveal MtNFP- and MtDMI3-dependent reprogramming of host gene expression by arbuscular mycorrhizal fungal lipochitooligosaccharides', *Plant Physiol*, 159: 1671-85.
Davière, J.-M., and P. Achard. 2016. 'A pivotal role of DELLAs in regulating multiple hormone signals', *Molecular Plant*, 9: 10-20.
Davière, Jean-Michel, and Patrick Achard. 2013. 'Gibberellin signaling in plants', *Development*, 140: 1147-51.
Dean, R., J. A. Van Kan, Z. A. Pretorius, K. E. Hammond-Kosack, A. Di Pietro, P. D. Spanu, J. J. Rudd, M. Dickman, R. Kahmann, J. Ellis, and G. D. Foster. 2012. 'The Top 10 fungal pathogens in molecular plant pathology', *Mol Plant Pathol*, 13: 414-30.
Delaux, Pierre-Marc, Guru V. Radhakrishnan, Dhileepkumar Jayaraman, Jitender Cheema, Mathilde Malbreil, Jeremy D. Volkening, Hiroyuki Sekimoto, Tomoaki Nishiyama, Michael Melkonian, Lisa Pokorny, Carl J. Rothfels, Heike Winter Sederoff, Dennis W. Stevenson, Barbara Surek, Yong Zhang, Michael R. Sussman, Christophe Dunand, Richard J. Morris, Christophe Roux, Gane Ka-Shu Wong, Giles E. D. Oldroyd, and Jean-Michel Ané. 2015. 'Algal ancestor of land plants was preadapted for symbiosis', *PNAS*, 112: 13390-95.
Delaux, Pierre-Marc, Kranthi Varala, Patrick P. Edger, Gloria M. Coruzzi, J. Chris Pires, and Jean-Michel Ané. 2014. 'Comparative phylogenomics uncovers the impact of symbiotic associations on host genome evolution', *PLoS Genetics.*, 10: e1004487.
Delaux, PM, N Séjalon-Delmas, G Bécard, and JM Ané. 2013. 'Evolution of the plant-microbe symbiotic "toolkit"', *Trends Plant Sci*.

Demchenko, K, T Winzer, J Stougaard, M Parniske, and K Pawlowski. 2004. 'Distinct roles of *Lotus japonicus SYMRK* and *SYM15* in root colonization and arbuscule formation', *New Phytol*, 163: 381-92.
Devers, Emanuel, Julia Teply, Armin Reinert, Nicole Gaude, and Franziska Krajinski. 2013. 'An endogenous artificial microRNA system for unraveling the function of root endosymbioses related genes in Medicago truncatula', *BMC Plant Biology*, 13: 82.
Dick. 2001. *Straminipilous fungi: Systematics of the Peronosporomycetes including accounts of the marine Straminipilous protists, the Plasmodiophorids and similar organisms* (Dordrecht/Boston/London: Kluwer Academic Publishers).
Dickson, S. 2004. 'The Arum-Paris continuum of mycorrhizal symbioses', *New Phytol*, 163: 187-200.
Dodds, Peter N., Maryam Rafiqi, Pamela H. P. Gan, Adrienne R. Hardham, David A. Jones, and Jeffrey G. Ellis. 2009. 'Effectors of biotrophic fungi and oomycetes: pathogenicity factors and triggers of host resistance', *New Phytol*, 183: 993-1000.
Doehlemann, G., R. Wahl, R. J. Horst, L. M. Voll, B. Usadel, F. Poree, M. Stitt, J. Pons-Kuhnemann, U. Sonnewald, R. Kahmann, and J. Kamper. 2008. 'Reprogramming a maize plant: transcriptional and metabolic changes induced by the fungal biotroph *Ustilago maydis*', *Plant J*, 56: 181-95.
Dörmann, Peter, Hyeran Kim, Thomas Ott, Paul Schulze-Lefert, Marco Trujillo, Vera Wewer, and Ralph Hückelhoven. 2014. 'Cell-autonomous defense, re-organization and trafficking of membranes in plant–microbe interactions', *New Phytol*, 204: 815-22.
Douds, David D., Philip E. Pfeffer, and Yair Shachar-Hill. 2000. 'Application of in vitro methods to study carbon uptake and transport by AM fungi', *Plant and Soil*, 226: 255-61.
El Ghachtouli, N., J. Martin-Tanguy, M. Paynot, and S. Gianinazzi. 1996. 'First-report of the inhibition of arbuscular mycorrhizal infection of *Pisum sativum* by specific and irreversible inhibition of polyamine biosynthesis or by gibberellic acid treatment', *FEBS letters*, 385: 189-92.
Elwell, Cherilyn A., Shaobo Jiang, Jung Hwa Kim, Albert Lee, Torsten Wittmann, Kentaro Hanada, Paul Melancon, and Joanne N. Engel. 2011. '*Chlamydia trachomatis* co-opts GBF1 and CERT to acquire host sphingomyelin for distinct roles during intracellular development', *PLoS Pathogen*, 7: doi: 10.1371/journal.ppat.1002198.
Evangelisti, E., T. Rey, and S. Schornack. 2014. 'Cross-interference of plant development and plant–microbe interactions', *Current Opinion in Plant Biology*, 20.
Ezawa T, Hayatsu M, Saito M. 2005. 'A new hypothesis on the strategy for acquisition of phosphorus in arbuscular mycorrhiza: Up-regulation of secreted acid phosphatase gene in the host plant', *MPMI*, 18.
Ezawa, Tatsuhiro, R. Cavagnaro Timothy, E. Smith Sally, F. Andrew Smith, and Ryo Ohtomo. 2003. 'Rapid accumulation of polyphosphate in extraradical hyphae of an arbuscular mycorrhizal fungus as revealed by histochemistry and a polyphosphate kinase/luciferase system', *New Phytol*, 161: 387-92.
Favre, Patrick, Laure Bapaume, Eligio Bossolini, Mauro Delorenzi, Laurent Falquet, and Didier Reinhardt. 2014. 'A novel bioinformatics pipeline to discover genes related to arbuscular mycorrhizal symbiosis based on their evolutionary conservation pattern among higher plants', *BMC Plant Biology*, 14: 333.

Fawke, S., T. A. Torode, A. Gogleva, E. A. Fich, I. Sørensen, T. Yunusov, Rose J. K. C., and S. Schornack. 2018. 'Glycerol phosphate acyltransferase 6 controls filamentous pathogen interactions and cell wall properties of the tomato and *Nicotiana benthamiana* leaf epidermis', *bioRxiv*.
Feng, G., Song, Y. C., Li, X. L., Christie, P. 2003. 'Contribution of arbuscular mycorrhizal fungi to utilization of organic sources of phosphorus by red clover in a calcareous soil', *Applied Soil Ecology*.
Fester, T, D Strack, and B Hause. 2001. 'Reorganization of tobacco root plastids during arbuscule development', *Planta*, 213: 864-68.
Fierer, N., M. S. Strickland, D. Liptzin, M. A. Bradford, and C. C. Cleveland. 2009. 'Global patterns in belowground communities', *Ecol Lett*, 12: 1238-49.
Fiorilli, Valentina, Luisa Lanfranco, and Paola Bonfante. 2013. 'The expression of *GintPT*, the phosphate transporter of *Rhizophagus irregularis*, depends on the symbiotic status and phosphate availability', *Planta*, 237: 1267-77.
Fitter, A. H.; Moyersoen, B. 1996. 'Evolutionary trends in root-microbe symbioses', *Philosophical Transactions of the Royal Society B: Biological Sciences*, 351: 1367-75.
Floss, Daniela S., S. Karen Gomez, Hee-Jin Park, Allyson M. MacLean, Lena M. Müller, Kishor K. Bhattarai, Veronique Lévesque-Tremblay, Ignacio E. Maldonado-Mendoza, and Maria J. Harrison. 2017. 'A transcriptional program for arbuscule degeneration during am symbiosis is regulated by MYB1', *Current Biology*.
Floss, Daniela S., Julien G. Levy, Véronique Lévesque-Tremblay, Nathan Pumplin, and Maria J. Harrison. 2013. 'DELLA proteins regulate arbuscule formation in arbuscular mycorrhizal symbiosis', *PNAS*, 110: E5025-E34.
Friesen, Maren L., Stephanie S. Porter, Scott C. Stark, Eric J. von Wettberg, Joel L. Sachs, and Esperanza Martinez-Romero. 2011. 'Microbially mediated plant functional traits', *Annual Review of Ecology, Evolution, and Systematics*, 42: 23-46.
Gallego-Bartolomé, Javier, Eugenio G. Minguet, Federico Grau-Enguix, Mohamad Abbas, Antonella Locascio, Stephen G. Thomas, David Alabadí, and Miguel A. Blázquez. 2012. 'Molecular mechanism for the interaction between gibberellin and brassinosteroid signaling pathways in *Arabidopsis*', *PNAS*, 109: 13446.
Gardner, Malcolm J., Richard Bishop, Trushar Shah, Etienne P. de Villiers, Jane M. Carlton, Neil Hall, Qinghu Ren, Ian T. Paulsen, Arnab Pain, Matthew Berriman, Robert J. M. Wilson, Shigeharu Sato, Stuart A. Ralph, David J. Mann, Zikai Xiong, Shamira J. Shallom, Janice Weidman, Lingxia Jiang, Jeffery Lynn, Bruce Weaver, Azadeh Shoaibi, Alexander R. Domingo, Delia Wasawo, Jonathan Crabtree, Jennifer R. Wortman, Brian Haas, Samuel V. Angiuoli, Todd H. Creasy, Charles Lu, Bernard Suh, Joana C. Silva, Teresa R. Utterback, Tamara V. Feldblyum, Mihaela Pertea, Jonathan Allen, William C. Nierman, Evans L. N. Taracha, Steven L. Salzberg, Owen R. White, Henry A. Fitzhugh, Subhash Morzaria, J. Craig Venter, Claire M. Fraser, and Vishvanath Nene. 2005. 'Genome sequence of *Theileria parva*, a Bovine pathogen that transforms lymphocytes', *Science*, 309: 134-37.
Gaude, N., S. Bortfeld, N. Duensing, M. Lohse, and F. Krajinski. 2012. 'Arbuscule-containing and non-colonized cortical cells of mycorrhizal roots undergo extensive and specific reprogramming during arbuscular mycorrhizal development', *Plant J*, 69: 510-28.
Gaude, N., WX. Schulze, P. Franken, and F. Krajinski. 2012. 'Cell type-specific protein and transcription profiles implicate periarbuscular membrane synthesis

as an important carbon sink in the mycorrhizal symbiosis', *Plant Signal Behav*, 7: 461-64.
Genre, A, M Chabaud, C Balzergue, V Puech-Pages, M Novero, T Rey, J Fournier, S Rochange, G Becard, P Bonfante, and DG Barker. 2013. 'Short-chain chitin oligomers from arbuscular mycorrhizal fungi trigger nuclear Ca(2+) spiking in *Medicago truncatula* roots and their production is enhanced by strigolactone', *New Phytol*, 198: 190 - 202.
Genre, A, M Chabaud, T Timmers, P Bonfante, and DG Barker. 2005. 'Arbuscular mycorrhizal fungi elicit a novel intracellular apparatus in *Medicago truncatula* root epidermal cells before infection', *Plant Cell*, 17: 3489 - 99.
Genre, A, Sergey Ivanov, M Fendrych, A Faccio, V Zarsky, T Bisseling, and P Bonfante. 2012. 'Multiple exocytotic markers accumulate at the sites of perifungal membrane biogenesis in arbuscular mycorrhizas', *Plant and Cell Physiol*, 53: 244-55.
Genre, Andrea, Mireille Chabaud, Antonella Faccio, David G. Barker, and Paola Bonfante. 2008. 'Prepenetration apparatus assembly precedes and predicts the colonization patterns of arbuscular mycorrhizal fungi within the root cortex of both *Medicago truncatula* and *Daucus carota*', *Plant Cell*, 20: 1407-20.
Genre, Andrea, Giuseppe Ortu, Chiara Bertoldo, Elena Martino, and Paola Bonfante. 2009. 'Biotic and abiotic stimulation of root epidermal cells reveals common and specific responses to arbuscular mycorrhizal fungi', *Plant Physiol*, 149: 1424-34.
Gherbi, Hassen, Katharina Markmann, Sergio Svistoonoff, Joan Estevan, Daphne Autran, Gabor Giczey, Florence Auguy, Benjamin Peret, Laurent Laplaze, Claudine Franche, Martin Parniske, and Didier Bogusz. 2008. 'SymRK defines a common genetic basis for plant root endosymbioses with arbuscular mycorrhiza fungi, rhizobia, and *Frankia* bacteria', *PNAS*: 0710618105.
Gianinazzi, Silvio, Armelle Gollotte, Marie-Noëlle Binet, Diederik Tuinen, Dirk Redecker, and Daniel Wipf. 2010. 'Agroecology: the key role of arbuscular mycorrhizas in ecosystem services', *Mycorrhiza*, 20: 519-30.
Gianinazzi-Pearson, V., C. Arnould, M. Oufattole, M. Arango, and S. Gianinazzi. 2000. 'Differential activation of H+-ATPase genes by an arbuscular mycorrhizal fungus in root cells of transgenic tobacco', *Planta*, 211: 609-13.
Gobbato, Enrico, JF Marsh, Tatiana Vernié, Ertao Wang, Fabienne Maillet, Jiyoung Kim, JB Miller, Jongho Sun, SA Bano, Pascal Ratet, KS Mysore, Jean DÈnarié, Michael Schultze, and GED Oldroyd. 2012. 'A GRAS-type transcription factor with a specific function in mycorrhizal signaling', *Current Biology*, 22: 2236-41.
Gobbato, Enrico, Ertao Wang, Gillian Higgins, Syeda Asma Bano, Christine Henry, Michael Schultze, and Giles E. D. Oldroyd. 2013. '*RAM1* and *RAM2* function and expression during arbuscular mycorrhizal symbiosis and *Aphanomyces euteiches* colonization', *Plant Signaling & Behavior*, 8: e26049.
Gohre, V., and U. Paszkowski. 2006. 'Contribution of the arbuscular mycorrhizal symbiosis to heavy metal phytoremediation', *Planta*, 223: 1115-22.
Gomez, S Karen, Helene Javot, Prasit Deewatthanawong, Ivone Torres-Jerez, Yuhong Tang, Elison Blancaflor, Michael Udvardi, and Maria Harrison. 2009. '*Medicago truncatula* and *Glomus intraradices* gene expression in cortical cells harboring arbuscules in the arbuscular mycorrhizal symbiosis', *BMC Plant Biology*, 9: 10.

Govindarajulu, M, PE Pfeffer, H Jin, and J Abubaker, Douds, DD, Allen, JW, Bücking, H, Lammers, PJ, Shachar-Hill, Y. 2005. 'Nitrogen transfer in the arbuscular mycorrhizal symbiosis', *Nature*, 435: 819-23.

Graham, J. A., N. C. Hodge, and J. B. Morton. 1995. 'Fatty Acid methyl ester profiles for characterization of glomalean fungi and their endomycorrhizae.', *Appl Environ Microbiol*, 61: 58-64.

Griesmann, M., Y. Chang, X. Liu, Y. Song, G. Haberer, M. B. Crook, B. Billault-Penneteau, D. Lauressergues, J. Keller, L. Imanishi, Y. P. Roswanjaya, W. Kohlen, P. Pujic, K. Battenberg, N. Alloisio, Y. Liang, H. Hilhorst, M. G. Salgado, V. Hocher, H. Gherbi, S. Svistoonoff, J. J. Doyle, S. He, Y. Xu, S. Xu, J. Qu, Q. Gao, X. Fang, Y. Fu, P. Normand, A. M. Berry, L. G. Wall, J. M. Ane, K. Pawlowski, X. Xu, H. Yang, M. Spannagl, K. F. X. Mayer, G. K. Wong, M. Parniske, P. M. Delaux, and S. Cheng. 2018. 'Phylogenomics reveals multiple losses of nitrogen-fixing root nodule symbiosis', *Science*, 361.

Groth, M; , N Takeda, J Perry, H Uchida, S Dräxl, A Brachmann, S Sato, S Tabata, M Kawaguchi, TL Wang, and M Parniske. 2010. '*NENA*, a *Lotus japonicus* homologue of *Sec13*, is required for rhizodermal infection by arbuscular mycorrhizal fungi but dispensable for cortical endosymbiotic development', *Plant Cell*, 22: 2509-26.

Groth, M., S. Kosuta, C. Gutjahr, K. Haage, S. L. Hardel, M. Schaub, A. Brachmann, S. Sato, S. Tabata, K. Findlay, T. L. Wang, and M. Parniske. 2013. 'Two Lotus japonicus symbiosis mutants impaired at distinct steps of arbuscule development', *Plant J*, 75: 117-29.

Gutjahr, C, M Novero, M Guether, O Montanari, M Udvardi, and P Bonfante. 2009. 'Presymbiotic factors released by the arbuscular mycorrhizal fungus *Gigaspora margarita* induce starch accumulation in *Lotus japonicus* roots', *New Phytol*, 183: 53-61.

Gutjahr, C., and M. Parniske. 2017. 'Cell Biology: Control of Partner Lifetime in a Plant-Fungus Relationship', *Curr Biol*, 27: R420-R23.

Gutjahr, Caroline, Mari Banba, Vincent Croset, Kyungsook An, Akio Miyao, Gynheung An, Hirohiko Hirochika, Haruko Imaizumi-Anraku, and Uta Paszkowski. 2008. 'Arbuscular mycorrhiza-specific signaling in rice transcends the common symbiosis signaling pathway', *Plant Cell*, 20: 2989-3005.

Gutjahr, Caroline, Enrico Gobbato, Jeongmin Choi, Michael Riemann, Matthew G. Johnston, William Summers, Samy Carbonnel, Catherine Mansfield, Shu-Yi Yang, Marina Nadal, Ivan Acosta, Makoto Takano, Wen-Biao Jiao, Korbinian Schneeberger, Krystyna A. Kelly, and Uta Paszkowski. 2015. 'Rice perception of symbiotic arbuscular mycorrhizal fungi requires the karrikin receptor complex', *Science*, 350: 1521-24.

Gutjahr, Caroline, and Martin Parniske. 2013. 'Cell and developmental biology of the arbuscular mycorrhiza symbiosis', *Ann Rev Cell Dev Biol*, 29: 593-617.

Gutjahr, Caroline, Dragica Radovanovic, Jessika Geoffroy, Quan Zhang, Heike Siegler, Marco Chiapello, Leonardo Casieri, Kyungsook An, Gynheung An, Emmanuel Guiderdoni, Chellian Santhosh Kumar, Venkatesan Sundaresan, Maria J. Harrison, and Uta Paszkowski. 2012. 'The half-size ABC transporters STR1 and STR2 are indispensable for mycorrhizal arbuscule formation in rice', *Plant J*, 69: 906-20.

Hackstadt T., Scidmore M. A., Rockey D. D. 1995. 'Lipid metabolism in *Chlamydia trachomatis*-infected cells: Directed trafficking of Golgi-derived sphingolipids to the chlamydial inclusion', *PNAS*, 92: 4877-81.

Handa, Yoshihiro, Hiroyo Nishide, Naoya Takeda, Yutaka Suzuki, Masayoshi Kawaguchi, and Katsuharu Saito. 2015. 'RNA-seq transcriptional profiling of an arbuscular mycorrhiza provides insights into regulated and coordinated gene expression in *Lotus japonicus* and *Rhizophagus irregularis*', *Plant and Cell Physiology*, 56: 1490-511.
Hardham, Adrienne R. 2006. 'Cell biology of plant–oomycete interactions', *Cellular Microbiology*, 9: 31-39.
Harrison, Maria J., and Marianne L. van Buuren. 1995. 'A phosphate transporter from the mycorrhizal fungus *Glomus versiforme*', *Nature*, 378: 626-29.
Harrison, MJ. 2005. 'Signaling in the mycorrhizal symbiosis', *Annual Reviews in Microbiology*, 59: 19-42.
Harrison, MJ, GR Dewbre, and J Liu. 2002. 'A phosphate transporter of *Medicago truncatula* involved in the acquisition of phosphate released by arbuscular mycorrhizal fungi.', *Plant Cell*, 14: 2413-29.
Hawkins, Heidi-Jayne, Anders Johansen, and Eckhard George. 2000. 'Uptake and transport of organic and inorganic nitrogen by arbuscular mycorrhizal fungi', *Plant and Soil*, 226: 275-85.
Heck, Carolin, Hannah Kuhn, Sven Heidt, Stefanie Walter, Nina Rieger, and Natalia Requena. 2016. 'Symbiotic fungi control plant root cortex development through the novel GRAS transcription factor MIG1', *Current Biology*.
Helber, Nicole, Kathrin Wippel, Norbert Sauer, Sara Schaarschmidt, Bettina Hause, and Natalia Requena. 2011. 'A versatile monosaccharide transporter that operates in the arbuscular mycorrhizal fungus *Glomus* sp is crucial for the symbiotic relationship with plants', *Plant Cell*, 23: 3812-23.
Herren, J. K., J. C. Paredes, F. Schupfer, K. Arafah, P. Bulet, and B. Lemaitre. 2014. 'Insect endosymbiont proliferation is limited by lipid availability', *eLife*, 3: doi: 10.7554/eLife.02964.
Hijikata, Nowaki, Masatake Murase, Chiharu Tani, Ryo Ohtomo, Mitsuru Osaki, and Tatsuhiro Ezawa. 2010. 'Polyphosphate has a central role in the rapid and massive accumulation of phosphorus in extraradical mycelium of an arbuscular mycorrhizal fungus', *New Phytol*, 186: 285-89.
Hirano, Yoshinori, Masahiro Nakagawa, Tomoe Suyama, Kohji Murase, Maya Shirakawa, Seiji Takayama, Tai-ping Sun, and Toshio Hakoshima. 2017. 'Structure of the SHR–SCR heterodimer bound to the BIRD/IDD transcriptional factor JKD', *Nature Plants*, 3: 17010.
Hohnjec, Natalija, Lisa F. Czaja-Hasse, Claudia Hogekamp, and Helge Küster. 2015. 'Pre-announcement of symbiotic guests: transcriptional reprogramming by mycorrhizal lipochitooligosaccharides shows a strict co-dependency on the GRAS transcription factors NSP1 and RAM1', *BMC Genomics*, 16: 994.
Hohnjec, Natalija, Andreas M. Perlick, Alfred Pühler, and Helge Küster. 2003. 'The *Medicago truncatula* sucrose synthase gene *MtSucS1* is activated both in the infected region of root nodules and in the cortex of roots colonized by arbuscular mycorrhizal fungi', *Molecular Plant-Microbe Interactions*, 16: 903-15.
Hong, JeonJ, Yong-Soon Park, Armando Bravo, KishorK Bhattarai, DierdraA Daniels, and MariaJ Harrison. 2012. 'Diversity of morphology and function in arbuscular mycorrhizal symbioses in *Brachypodium distachyon*', *Planta*, 236: 851-65.
Horváth, Beatrix, Li Huey Yeun, Ágota Domonkos, Gábor Halász, Enrico Gobbato, Ferhan Ayaydin, Krisztina Miró, Sibylle Hirsch, Jongho Sun, Million Tadege, Pascal Ratet, Kirankumar S. Mysore, Jean-Michel Ané, Giles E. D. Oldroyd, and Péter Kaló. 2011. '*Medicago truncatula* IPD3 is a member of the common

symbiotic signaling pathway required for rhizobial and mycorrhizal symbioses', *Molecular Plant-Microbe Interactions*, 24: 1345-58.
Itoe, M. A., J. L. Sampaio, G. G. Cabal, E. Real, V. Zuzarte-Luis, S. March, S. N. Bhatia, F. Frischknecht, C. Thiele, A. Shevchenko, and M. M. Mota. 2014. 'Host cell phosphatidylcholine is a key mediator of malaria parasite survival during liver stage infection', *Cell Host Microbe*, 16: 778-86.
Ivanov, Sergey, Elena E. Fedorova, Erik Limpens, Stephane De Mita, Andrea Genre, Paola Bonfante, and Ton Bisseling. 2012. 'Rhizobium–legume symbiosis shares an exocytotic pathway required for arbuscule formation', *PNAS*, 109: 8316-21.
Jackson, K. E., N. Klonis, D. J. Ferguson, A. Adisa, C. Dogovski, and L. Tilley. 2004. 'Food vacuole-associated lipid bodies and heterogeneous lipid environments in the malaria parasite, *Plasmodium falciparum*', *Mol Microbiol*, 54: 109-22.
James, T. Y., F. Kauff, C. L. Schoch, P. B. Matheny, V. Hofstetter, C. J. Cox, G. Celio, C. Gueidan, E. Fraker, J. Miadlikowska, H. T. Lumbsch, A. Rauhut, V. Reeb, A. E. Arnold, A. Amtoft, J. E. Stajich, K. Hosaka, G. H. Sung, D. Johnson, B. O'Rourke, M. Crockett, M. Binder, J. M. Curtis, J. C. Slot, Z. Wang, A. W. Wilson, A. Schussler, J. E. Longcore, K. O'Donnell, S. Mozley-Standridge, D. Porter, P. M. Letcher, M. J. Powell, J. W. Taylor, M. M. White, G. W. Griffith, D. R. Davies, R. A. Humber, J. B. Morton, J. Sugiyama, A. Y. Rossman, J. D. Rogers, D. H. Pfister, D. Hewitt, K. Hansen, S. Hambleton, R. A. Shoemaker, J. Kohlmeyer, B. Volkmann-Kohlmeyer, R. A. Spotts, M. Serdani, P. W. Crous, K. W. Hughes, K. Matsuura, E. Langer, G. Langer, W. A. Untereiner, R. Lucking, B. Budel, D. M. Geiser, A. Aptroot, P. Diederich, I. Schmitt, M. Schultz, R. Yahr, D. S. Hibbett, F. Lutzoni, D. J. McLaughlin, J. W. Spatafora, and R. Vilgalys. 2006. 'Reconstructing the early evolution of fungi using a six-gene phylogeny', *Nature*, 443: 818-22.
Javot, H, N Pumplin, and M Harrison. 2007. 'Phosphate in the arbuscular mycorrhizal symbiosis: transport properties and regulatory roles', *Plant Cell and Environment*, 30: 310-22.
Javot, H., R. Varma Penmetsa, N. Terzaghi, D. R. Cook, and M. J. Harrison. 2007. 'A *Medicago truncatula* phosphate transporter indispensible for the arbuscular mycorrhizal symbiosis', *PNAS*, 104: 1720-25.
Javot, Hélène, R. Varma Penmetsa, Florence Breuillin, Kishor K. Bhattarai, Roslyn D. Noar, S. Karen Gomez, Quan Zhang, Douglas R. Cook, and Maria J. Harrison. 2011. '*Medicago truncatula mtpt4* mutants reveal a role for nitrogen in the regulation of arbuscule degeneration in arbuscular mycorrhizal symbiosis', *Plant J*, 68: 954-65.
Jiang, Y., W. Wang, Q. Xie, N. Liu, L. Liu, D. Wang, X. Zhang, C. Yang, X. Chen, D. Tang, and E. Wang. 2017. 'Plants transfer lipids to sustain colonization by mutalistic mycorrhizial and parasitic fungi', *Science*, 356: 1172-75.
Jiang, Y., Q. Xie, W. Wang, J. Yang, X. Zhang, N. Yu, Y. Zhou, and E. Wang. 2018. '*Medicago* AP2-domain transcription factor WRI5a is a master regulator of lipid biosynthesis and transfer during mycorrhizal symbiosis', *Mol Plant*.
Jin, Y., Z. Chen, J. Yang, K. S. Mysore, J. Wen, J. Huang, N. Yu, and E. Wang. 2018. 'IPD3 and IPD3L function redundantly in rhizobial and mycorrhizal symbioses', *Front Plant Sci*, 9: 267.
Jin, Yue, Huan Liu, Dexian Luo, Nan Yu, Wentao Dong, Chao Wang, Xiaowei Zhang, Huiling Dai, Jun Yang, and Ertao Wang. 2016. 'DELLA proteins are common components of symbiotic rhizobial and mycorrhizal signalling pathways', *Nature Communications*, 7: 12433.

Jones, JD, and JL Dangl. 2006. 'The plant immune system', *Nature*, 444: 323 - 29.
Jones, L., S. Riaz, A. Morales-Cruz, K. Amrine, B. McGuire, D. Gubler, A. Walker, and D. Cantu. 2014. 'Adaptive genomic structural variation in the grape powdery mildew pathogen, *Erysiphe necator*', *BMC Genomics*, 15: doi: 10.1186/471-2164-15-1081.
Judelson, H. S. 2017. 'Metabolic diversity and novelties in the oomycetes', *Ann Rev Cell Dev Biol*, 71: 21-39.
Kamel, Laurent, Michelle Keller-Pearson, Christophe Roux, and Jean-Michel Ané. 2016. 'Biology and evolution of arbuscular mycorrhizal symbiosis in the light of genomics', *New Phytol*, 213: 531-36.
Kameoka H., Maeda T., Okuma N., Kawaguchi M. 2018. 'Cell type-specific regulation of nutrient absorption, metabolism and transfer in arbuscular mycorrhizal fungi', *bioRxiv*.
Kamoun, S., O. Furzer, J. D. Jones, H. S. Judelson, G. S. Ali, R. J. Dalio, S. G. Roy, L. Schena, A. Zambounis, F. Panabieres, D. Cahill, M. Ruocco, A. Figueiredo, X. R. Chen, J. Hulvey, R. Stam, K. Lamour, M. Gijzen, B. M. Tyler, N. J. Grunwald, M. S. Mukhtar, D. F. Tome, M. Tor, G. Van Den Ackerveken, J. McDowell, F. Daayf, W. E. Fry, H. Lindqvist-Kreuze, H. J. Meijer, B. Petre, J. Ristaino, K. Yoshida, P. R. Birch, and F. Govers. 2015. 'The Top 10 oomycete pathogens in molecular plant pathology', *Mol Plant Pathol*, 16: 413-34.
Kanamori, Norihito, Lene Heegaard Madsen, Simona Radutoiu, Mirela Frantescu, Esben M. H. Quistgaard, Hiroki Miwa, J. Allan Downie, Euan K. James, Hubert H. Felle, Line Lindegaard Haaning, Torben Heick Jensen, Shusei Sato, Yasukazu Nakamura, Satoshi Tabata, Niels Sandal, and Jens Stougaard. 2006. 'A nucleoporin is required for induction of Ca2+ spiking in legume nodule development and essential for rhizobial and fungal symbiosis', *PNAS*, 103: 359-64.
Kevei, Zoltán, Géraldine Lougnon, Peter Mergaert, Gábor V. Horváth, Attila Kereszt, Dhileepkumar Jayaraman, Najia Zaman, Fabian Marcel, Krzysztof Regulski, György B. Kiss, Adam Kondorosi, Gabriella Endre, Eva Kondorosi, and Jean-Michel Ané. 2007. '3-Hydroxy-3-Methylglutaryl Coenzyme A Reductase1 interacts with NORK and is crucial for nodulation in *Medicago truncatula*', *Plant Cell*, 19: 3974.
Keymer, A., P. Pimprikar, V. Wewer, C. Huber, M. Brands, S. L. Bucerius, P. M. Delaux, V. Klingl, E. V. Ropenack-Lahaye, T. L. Wang, W. Eisenreich, P. Dormann, M. Parniske, and C. Gutjahr. 2017. 'Lipid transfer from plants to arbuscular mycorrhiza fungi', *eLife*, 6: doi: 10.7554/eLife.29107.
Kiers, ET, M Duhamel, Y Beesetty, JA Mensah, O Franken, E Verbruggen, CR Fellbaum, GA Kowalchuk, MM Hart, A Bago, TM Palmer, SA West, P Vandenkoornhuyse, J Jansa, and H Bucking. 2011. 'Reciprocal rewards stabilize cooperation in the mycorrhizal symbiosis', *Science*, 333: 880 - 82.
Kikuchi, Yusuke, Nowaki Hijikata, Kaede Yokoyama, Ryo Ohtomo, Yoshihiro Handa, Masayoshi Kawaguchi, Katsuharu Saito, and Tatsuhiro Ezawa. 2014. 'Polyphosphate accumulation is driven by transcriptome alterations that lead to near-synchronous and near-equivalent uptake of inorganic cations in an arbuscular mycorrhizal fungus', *New Phytol*, 204: 638-49.
Kistner, C, and M Parniske. 2002. 'Evolution of signal transduction in intracellular symbiosis.', *Trends Plant Sci*, 7.
Kistner, C., T. Winzer, A. Pitzschke, L. Mulder, S. Sato, T. Kaneko, S. Tabata, N. Sandal, J. Stougaard, K. J. Webb, K. Szczyglowski, and M. Parniske. 2005.

'Seven *Lotus japonicus* genes required for transcriptional reprogramming of the root during fungal and bacterial symbiosis', *Plant Cell*, 17: 2217-29.
Kloppholz, Silke, Hannah Kuhn, and Natalia Requena. 2011. 'A secreted fungal effector of *Glomus intraradices* promotes symbiotic biotrophy', *Current Biology*, 21: 1204-09.
Kobae, Yoshihiro, and Shingo Hata. 2010. 'Dynamics of periarbuscular membranes visualized with a fluorescent phosphate transporter in arbuscular mycorrhizal roots of rice', *Plant Cell Physiology*, 51: 341-53.
Kobae, Yoshihiro, Yosuke Tamura, Shoko Takai, Mari Banba, and Shingo Hata. 2010. 'Localized expression of arbuscular mycorrhiza-inducible ammonium transporters in soybean', *Plant Cell Physiology*, 51: 1411-15.
Kobayashi, Yuuki, Taro Maeda, Katsushi Yamaguchi, Hiromu Kameoka, Sachiko Tanaka, Tatsuhiro Ezawa, Shuji Shigenobu, and Masayoshi Kawaguchi. 2018. 'The genome of *Rhizophagus clarus* HR1 reveals a common genetic basis for auxotrophy among arbuscular mycorrhizal fungi', *BMC Genomics*, 19: 465.
Koch, E., and A. Slusarenko. 1990. '*Arabidopsis* is susceptible to infection by a downy mildew fungus', *Plant Cell*, 2: 437.
Koegel, Sally, Nassima Ait Lahmidi, Christine Arnould, Odile Chatagnier, Florian Walder, Kurt Ineichen, Thomas Boller, Daniel Wipf, Andres Wiemken, and Pierre-Emmanuel Courty. 2013. 'The family of ammonium transporters (AMT) in Sorghum bicolor: two AMT members are induced locally, but not systemically in roots colonized by arbuscular mycorrhizal fungi', *New Phytol*, 198: 853-65.
Kojima, Tomoko, and Masanori Saito. 2004. 'Possible involvement of hyphal phosphatase in phosphate efflux from intraradical hyphae isolated from mycorrhizal roots colonized by *Gigaspora margarita*', *Mycological research*, 108: 610-15.
Kosuta, S, M Chabaud, G Lougnon, C Gough, J Dénarié, DG Barker, and G Becard. 2003. 'A diffusible factor from arbuscular mycorrhizal fungi induces symbiosis-specific *MtENOD11* expression in roots of *Medicago truncatula*', *Plant Physiol*, 131: 952-62.
Kosuta, Sonja, Saul Hazledine, Jongho Sun, Hiroki Miwa, Richard J. Morris, J. Allan Downie, and Giles E. D. Oldroyd. 2008. 'Differential and chaotic calcium signatures in the symbiosis signaling pathway of legumes', *PNAS*, 105: 9823-28.
Krajinski, Franziska, Pierre-Emmanuel Courty, Daniela Sieh, Philipp Franken, Haoqiang Zhang, Marcel Bucher, Nina Gerlach, Igor Kryvoruchko, Daniela Zoeller, Michael Udvardi, and Bettina Hause. 2014. 'The H+-ATPase HA1 of *Medicago truncatula* Is essential for phosphate transport and plant growth during arbuscular mycorrhizal symbiosis', *Plant Cell*, 26: 1808.
Kretzschmar, Tobias, Wouter Kohlen, Joelle Sasse, Lorenzo Borghi, Markus Schlegel, Julien B. Bachelier, Didier Reinhardt, Ralph Bours, Harro J. Bouwmeester, and Enrico Martinoia. 2012. 'A petunia ABC protein controls strigolactone-dependent symbiotic signalling and branching', *Nature*, 483: 341-44.
Krings, M., T. N. Taylor, and N. Dotzler. 2011. 'The fossil record of the Peronosporomycetes (Oomycota)', *Mycologia*, 103: 455-7.
Kuhn, H., H. Küster, and N. Requena. 2010. 'Membrane steroid-binding protein 1 induced by a diffusible fungal signal is critical for mycorrhization in *Medicago truncatula*', *New Phytol*, 185: 716-33.

Kuhn, H., M. Kwaaitaal, S. Kusch, J. Acevedo-Garcia, H. Wu, and R. Panstruga. 2016. 'Biotrophy at its best: Novel findings and unsolved mysteries of the *Arabidopsis*-Powdery Mildew pathosystem', *Arabidopsis Book*, 14: e0184.

Lanfranco, L., P. Bonfante, and A. Genre. 2016. 'The mutualistic interaction between plants and arbuscular mycorrhizal fungi', *Microbiology Spectrum*.

Lanfranco, L., V. Fiorilli, and C. Gutjahr. 2018. 'Partner communication and role of nutrients in the arbuscular mycorrhizal symbiosis', *New Phytol*.

Lanfranco, L., J. Young, and W. Peter. 2012. 'Genetic and genomic glimpses of the elusive arbuscular mycorrhizal fungi', *Current Opinion in Plant Biology*, 15: 454-61.

Lanver, D., A. N. Muller, P. Happel, G. Schweizer, F. B. Haas, M. Franitza, C. Pellegrin, S. Reissmann, J. Altmuller, S. A. Rensing, and R. Kahmann. 2018. 'The biotrophic development of *Ustilago maydis* studied by RNAseq analysis', *Plant Cell*: doi:10.1105/tpc.17.00764.

Leigh, Joanne, Angela Hodge, and Alastair H. Fitter. 2008. 'Arbuscular mycorrhizal fungi can transfer substantial amounts of nitrogen to their host plant from organic material', *New Phytol*, 181: 199-207.

Levy, Julien, Cecile Bres, Rene Geurts, Boulos Chalhoub, Olga Kulikova, Gerard Duc, Etienne-Pascal Journet, Jean-Michel Ane, Emmanuelle Lauber, Ton Bisseling, Jean Denarie, Charles Rosenberg, and Frederic Debelle. 2004. 'A putative Ca2+ and calmodulin-dependent protein kinase required for bacterial and fungal symbioses', *Science*, 303: 1361-64.

Li, Y., F. Beisson, J. Ohlrogge, and M. Pollard. 2007. 'Monoacylglycerols are components of root waxes and can be produced in the aerial cuticle by ectopic expression of a suberin-associated acyltransferase', *Plant Physiol*, 144: 1267–77.

Lin, M., and D. J. Oliver. 2008. 'The role of acetyl-coenzyme a synthetase in *Arabidopsis*', *Plant Physiol*, 147: 1822-9.

Liu, Jinyuan, Ignacio Maldonado-Mendoza, Melina Lopez-Meyer, Foo Cheung, Christopher D. Town, and Maria J. Harrison. 2007. 'Arbuscular mycorrhizal symbiosis is accompanied by local and systemic alterations in gene expression and an increase in disease resistance in the shoots', *Plant J*, 50: 529-44.

Lohse, S, W Schliemann, C Ammer, J Kopka, D Strack, and T Fester. 2005. 'Organization and metabolism of plastids and mitochondria in arbuscular mycorrhizal roots of *Medicago truncatula*', *Plant Physiol*, 139: 329-40.

López-Pedrosa, Agustín, Manuel González-Guerrero, Ascensión Valderas, Concepción Azcón-Aguilar, and Nuria Ferrol. 2006. '*GintAMT1* encodes a functional high-affinity ammonium transporter that is expressed in the extraradical mycelium of *Glomus intraradices*', *Fungal Genetics and Biology*, 43: 102-10.

Lota, F., S. Wegmuller, B. Buer, S. Sato, A. Brautigam, B. Hanf, and M. Bucher. 2013. 'The cis-acting CTTC-P1BS module is indicative for gene function of LjVTI12, a Qb-SNARE protein gene that is required for arbuscule formation in Lotus japonicus', *Plant J*, 74: 280-93.

Lu, YJ, S Schornack, T Spallek, N Geldner, J Chory, S Schellmann, K Schumacher, S Kamoun, and S Robatzek. 2012. 'Patterns of plant subcellular responses to successful oomycete infections reveal differences in host cell reprogramming and endocytic trafficking', *Cell Microbiol*, 14: 682 - 97.

Luginbuehl, L.H., G.N. Menard, S. Kurup, H. Van Erp, G.V. Radhakrishnan, A. Breakspear, G.E.D. Oldroyd, and P.J. Eastmond. 2017. 'Fatty acids in

arbuscular mycorrhizal fungi are synthesized by the host plant', *Science*, 6: 763-75.
MacLean, A. M.; Bravo, A.; Harrison, M. J. 2017. 'Plant signaling and metabolic pathways enabling arbuscular mycorrhizal symbiosis', *Plant Cell*, 29: 2319-35.
Madan, R., C. Pankhurst, B. Hawke, and S. Smith. 2002. 'Use of fatty acids for identification of AM fungi and estimation of the biomass of AM spores in soil', *Soil Biol Biochem*, 34: 125-28.
Maekawa, Takaki, Makoto Maekawa-Yoshikawa, Naoya Takeda, Haruko Imaizumi-Anraku, Yoshikatsu Murooka, and Makoto Hayashi. 2009. 'Gibberellin controls the nodulation signaling pathway in *Lotus japonicus*', *Plant J*, 58: 183-94.
Maillet, Fabienne, Verena Poinsot, Olivier Andre, Virginie Puech-Pages, Alexandra Haouy, Monique Gueunier, Laurence Cromer, Delphine Giraudet, Damien Formey, Andreas Niebel, Eduardo Andres Martinez, Hugues Driguez, Guillaume Becard, and Jean Denarie. 2011. 'Fungal lipochitooligosaccharide symbiotic signals in arbuscular mycorrhiza', *Nature*, 469: 58-63.
Maldonado-Mendoza, Ignacio E., Gary R. Dewbre, and Maria J. Harrison. 2001. 'A phosphate transporter gene from the extraradical mycelium of an arbuscular mycorrhizal fungus *Glomus intraradices* is regulated in response to phosphate in the environment', *Molecular Plant-Microbe Interactions*, 14: 1140-48.
Mandal, M. K., A. C. Chandra-Shekara, R. D. Jeong, K. Yu, S. Zhu, B. Chanda, D. Navarre, A. Kachroo, and P. Kachroo. 2012. 'Oleic acid-dependent modulation of NITRIC OXIDE ASSOCIATED1 protein levels regulates nitric oxide-mediated defense signaling in *Arabidopsis*', *Plant Cell*, 24: 1654-74.
Markmann, K., G. Giczey, and M. Parniske. 2008. 'Functional adaptation of a plant receptor- kinase paved the way for the evolution of intracellular root symbioses with bacteria', *PLoS Biology*, 6: e68.
Marschner, H. , and B. Dell. 1994. 'Nutrient uptake in mycorrhizail symbiosis', *Plant and Soil*, 159.
Marschner, Horst, Eckhard George, and Volker Römheld. 1995. Horst Marschner (ed.), *Mineral Nutrition of Higher Plants (Second Edition)* (Academic Press: London).
Martin, F. M.; Uroz, S.; Barker, D. G. 2017. 'Ancestral alliances: Plant mutualistic symbioses with fungi and bacteria', *Science*, 356.
Mauch-Mani, Brigitte, and Alan J. Slusarenko. 1993. '*Arabidopsis* as a model host for studying plant-pathogen interactions', *Trends in Microbiology*, 1: 265-70.
Mazumdar, J., and B. Striepen. 2007. 'Make it or take it: fatty acid metabolism of apicomplexan parasites', *Eukaryot Cell*, 6: 1727-35.
McGowan, Jamie, and David A. Fitzpatrick. 2017. 'Genomic, network, and phylogenetic analysis of the oomycete effector arsenal', *mSphere*, 2.
Melo, R. C. N., H. D'Ávila, D. L. Fabrino, P. E. Almeida, and P. T. Bozza. 2003. 'Macrophage lipid body induction by Chagas disease in vivo: putative intracellular domains for eicosanoid formation during infection', *Tissue Cell*, 35: 59-67.
Mendes, Rodrigo, Marco Kruijt, Irene de Bruijn, Ester Dekkers, Menno van der Voort, Johannes H. M. Schneider, Yvette M. Piceno, Todd Z. DeSantis, Gary L. Andersen, Peter A. H. M. Bakker, and Jos M. Raaijmakers. 2011. 'Deciphering the Rhizosphere microbiome for disease-suppressive bacteria', *Science*, 332: 1097.
Mendgen, Kurt, and Matthias Hahn. 2002. 'Plant infection and the establishment of fungal biotrophy', *Trends Plant Sci*, 7: 352-56.

Messinese, E, JW Mun, LH Yeun, D Jayaraman, P Rougé, A Barre, G Lougnon, S Schornack, JJ Bono, DR Cook, and JM Ané. 2007. 'A novel nuclear protein interacts with the symbiotic DMI3 calcium and calmodulin dependent protein kinase of *Medicago truncatula*', *Molecular Plant-Microbe Interactions*, 20: 912-21.

Miller, J. Benjamin, Amitesh Pratap, Akira Miyahara, Liang Zhou, Stephen Bornemann, Richard J. Morris, and Giles E.D. Oldroyd. 2013. 'Calcium/calmodulin-dependent protein kinase is negatively and positively regulated by calcium, providing a mechanism for decoding calcium responses during symbiosis signaling', *Plant Cell*, 25: 5053-66.

Mims, C. W., E. A. Richardson, B. F. Holt Iii, and J. L. Dangl. 2004. 'Ultrastructure of the host–pathogen interface in *Arabidopsis thaliana* leaves infected by the downy mildew *Hyaloperonospora parasitica*', *Canadian Journal of Botany*, 82: 1001-08.

Mitra, Raka M., Cynthia A. Gleason, Anne Edwards, James Hadfield, J. Allan Downie, Giles E. D. Oldroyd, and Sharon R. Long. 2004. 'From The Cover: A Ca2+/calmodulin-dependent protein kinase required for symbiotic nodule development: Gene identification by transcript-based cloning', *PNAS*, 101: 4701-05.

Miyata, K, Kozaki, T, Kouzai, Y, Ozawa, K, Ishii, K, Asamizu, E, Okabe, Y, Umehara, Y, Miyamoto, A, Kobae, Y, Akiyama, K, Kakua, H, Nishizawa, Y, Shibuyaa, N, Nakagawaa, T. 2014. 'Bifunctional plant receptor, OsCERK1, regulates both chitin-triggered immunity and arbuscular mycorrhizal symbiosis in rice', *Plant and Cell Physiology*.

Moscatiello, R., S. Sello, M. Novero, A. Negro, P. Bonfante, and L. Navazio. 2014. 'The intracellular delivery of TAT-aequorin reveals calcium-mediated sensing of environmental and symbiotic signals by the arbuscular mycorrhizal fungus *Gigaspora margarita*', *New Phytol*, 203: 1012-20.

Müller, D. B., C. Vogel, Y. Bai, and J. A. Vorholt. 2016. 'The Plant Microbiota: Systems-Level insights and perspectives', *Annu Rev Genet*, 50: 211-34.

Nadal, M., R. Sawers, S. Naseem, B. Bassin, C. Kulicke, A. Sharman, G. An, K. An, K. R. Ahern, A. Romag, T. P. Brutnell, C. Gutjahr, N. Geldner, C. Roux, E. Martinoia, J. B. Konopka, and U. Paszkowski. 2017. 'An N-acetylglucosamine transporter required for arbuscular mycorrhizal symbioses in rice and maize', *Nature Plants*, 3: 17073.

Navazio, L, R Moscatiello, and A Genre, Novero, M, Baldan, B, Bonfante, P, Mariani, P. 2007. 'A diffusible signal from arbuscular mycorrhizal fungi elicits a transient cytosolic calcium elevation in host plant cells', *Plant Physiol*, 114: 673-81.

Nielsen, Uffe N., Diana H. Wall, and Johan Six. 2015. 'Soil biodiversity and the environment', *Annual Review of Environment and Resources*, 40: 63-90.

Nouri, Eva, Florence Breuillin-Sessoms, Urs Feller, and Didier Reinhardt. 2014. 'Phosphorus and nitrogen regulate arbuscular mycorrhizal symbiosis in *Petunia hybrida*', *PLoS One*, 9: e90841.

Nussaume, Laurent, Satomi Kanno, Hélène Javot, Elena Marin, Tomoko M. Nakanishi, and Marie-Christine Thibaud. 2011. 'Phosphate import in plants: Focus on the PHT1 transporters', *Front Plant Sci*, 2.

Oláh, Boglárka, Christian Brière, Guillaume Bécard, Jean Dénarié, and Clare Gough. 2005. 'Nod factors and a diffusible factor from arbuscular mycorrhizal fungi stimulate lateral root formation in *Medicago truncatula* via the DMI1/DMI2 signalling pathway', *Plant J*, 44: 195-207.

Oldroyd, G. E., and J. A. Downie. 2008. 'Coordinating nodule morphogenesis with rhizobial infection in legumes', *Annu Rev Plant Biol*, 59.
Oldroyd, GE. 2013. 'Speak, friend, and enter: signalling systems that promote beneficial symbiotic associations in plants', *Nat. Rev. Microbiol.*, 11: 252-63.
Olsson, Pål Axel, Ingrid M. van Aarle, William G. Allaway, Anne E. Ashford, and Hervé Rouhier. 2002. 'Phosphorus effects on metabolic processes in monoxenic arbuscular mycorrhiza cultures', *Plant Physiol*, 130: 1162.
Op den Camp, Rik, Arend Streng, Stéphane De Mita, Qingqin Cao, Elisa Polone, Wei Liu, Jetty S. S. Ammiraju, Dave Kudrna, Rod Wing, Andreas Untergasser, Ton Bisseling, and René Geurts. 2011. 'LysM-type mycorrhizal receptor recruited for rhizobium symbiosis in nonlegume *Parasponia*', *Science*, 331: 909-12.
Oshima, K., S. Kakizawa, H. Nishigawa, H. Y. Jung, W. Wei, S. Suzuki, R. Arashida, D. Nakata, S. Miyata, M. Ugaki, and S. Namba. 2004. 'Reductive evolution suggested from the complete genome sequence of a plant-pathogenic phytoplasma', *Nat Genet*, 36: 27-9.
Panikashvili, David, Jian Xin Shi, Lukas Schreiber, and Asaph Aharoni. 2011. 'The *Arabidopsis* ABCG13 transporter is required for flower cuticle secretion and patterning of the petal epidermis', *New Phytol*, 190: 113-24.
Paredes, Juan C., Jeremy K. Herren, Fanny Schüpfer, and Bruno Lemaitre. 2016. 'The role of lipid competition for endosymbiont-mediated protection against parasitoid wasps in *Drosophila*', *mBio*, 7: doi: 10.1128/mBio.01006-16.
Park, Hee-Jin, Daniela S Floss, Veronique Levesque-Tremblay, Armando Bravo, and Maria J. Harrison. 2015. 'Hyphal branching during arbuscule development requires RAM1', *Plant Physiol*, 169: 2774-88.
Parniske, M. 2008. 'Arbuscular mycorrhiza: the mother of plant root endosymbioses', *Nat. Rev. Microbiol.*, 6: 763-75.
Parniske, Martin. 2000. 'Intracellular accommodation of microbes by plants: a common developmental program for symbiosis and disease?', *Current Opinion in Plant Biology*, 3: 320-28.
Paszkowski, U, S Kroken, C Roux, and SP Briggs. 2002. 'Rice phosphate transporters include an evolutionarily divergent gene specifically activated in arbuscular mycorrhizal symbiosis', *PNAS*, 99: 13324-29.
Pel, Michiel J. C., Paul C. A. Wintermans, Adriana Cabral, Bjorn J. M. Robroek, Michael F. Seidl, Jaqueline Bautor, Jane E. Parker, Guido Van den Ackerveken, and Corné M. J. Pieterse. 2014. 'Functional analysis of *Hyaloperonospora arabidopsidis* RXLR effectors', *PLoS One*, 9: e110624.
Peng, J., and N. P. Harberd. 1993. 'Derivative alleles of the *Arabidopsis* gibberellin-insensitive (gai) mutation confer a wild-type phenotype', *Plant Cell*, 5: 351.
Pérez-de-Luque, Alejandro, Stefanie Tille, Irene Johnson, David Pascual-Pardo, Jurriaan Ton, and Duncan D. Cameron. 2017. 'The interactive effects of arbuscular mycorrhiza and plant growth-promoting rhizobacteria synergistically enhance host plant defences against pathogens', *Scientific Reports*, 7: 16409.
Pfeffer, Philip E., David D. Douds, Guillaume Bécard, and Yair Shachar-Hill. 1999. 'Carbon uptake and the metabolism and transport of lipids in an arbuscular mycorrhiza', *Plant Physiol*, 120: 587-98.
Pighin, Jamie A., Huanquan Zheng, Laura J. Balakshin, Ian P. Goodman, Tamara L. Western, Reinhard Jetter, Ljerka Kunst, and A. Lacey Samuels. 2004. 'Plant cuticular lipid export requires an ABC transporter', *Science*, 306: 702.
Pimprikar, P, S Carbonnel, M Paries, K Katzer, V Klingl, M Bohmer, L Karl, D Floss, MJ Harrison, M Parniske, and C Gutjahr. 2016. 'A CCaMK-CYCLOPS-DELLA

complex regulates transcription of RAM1, a central regulator of arbuscule branching', *Current Biology*, 26: 987-98.
Pimprikar, Priya, and Caroline Gutjahr. 2018. 'Transcriptional regulation of arbuscular mycorrhiza development', *Plant and Cell Physiology*, 59: 678-95.
Poirier, Yves, and Marcel Bucher. 2002. 'Phosphate transport and homeostasis in *Arabidopsis*', *The Arabidopsis Book / American Society of Plant Biologists*, 1: e0024.
Popova, Yulia, Palvannan Thayumanavan, Elena Lonati, Margarida Agrochão, and Johan M. Thevelein. 2010. 'Transport and signaling through the phosphate-binding site of the yeast Pho84 phosphate transceptor', *PNAS*.
Pumplin, Nathan, and Maria J. Harrison. 2009. 'Live-cell imaging reveals periarbuscular membrane domains and organelle location in *Medicago truncatula* roots during arbuscular mycorrhizal symbiosis', *Plant Physiol*, 151: 809-19.
Rausch, Christine, Pierre Daram, Silvia Brunner, Jan Jansa, Maryse Laloi, Georg Leggewie, Nikolaus Amrhein, and Marcel Bucher. 2001. 'A phosphate transporter expressed in arbuscule-containing cells in potato', *Nature*, 414: 462.
Read, D. J., and J. Perez-Moreno. 2003. 'Mycorrhizas and nutrient cycling in ecosystems – a journey towards relevance?', *New Phytol*, 157: 475-92.
Redecker, D , R Kodner, and LE Graham. 2000. 'Glomalean fungi from the Ordovician', *Science*, 289: 1920-21.
Remy, W., T. N. Taylor, H. Hass, and H. Kerp. 1994. 'Four hundred-million-year-old vesicular arbuscular mycorrhizae', *PNAS*, 91: 11841-43.
Rey, T, A Nars, M Bonhomme, A Bottin, S Huguet, S Balzergue, MF Jardinaud, JJ Bono, J Cullimore, B Dumas, C Gough, and C Jacquet. 2013. 'NFP, a LysM protein controlling Nod factor perception, also intervenes in *Medicago truncatula* resistance to pathogens', *New Phytol*, 198: 875 - 86.
Rey , T., Chatterjee, M. Buttay, J. Toulotte, and S. Schornack. 2015. '*Medicago truncatula* symbiosis mutants affected in the interaction with a biotrophic root pathogen', *New Phytol*, 206.
Rey, T., and C. Jacquet. 2018. 'Symbiosis genes for immunity and vice versa', *Current Opinion in Plant Biology*, 44: 64-71.
Rey, Thomas, and Sebastian Schornack. 2013. 'Interactions of beneficial and detrimental root-colonizing filamentous microbes with plant hosts', *Genome Biology*, 14: 121.
Rich, M. K., P. E. Courty, C. Roux, and D. Reinhardt. 2017. 'Role of the GRAS transcription factor ATA/RAM1 in the transcriptional reprogramming of arbuscular mycorrhiza in *Petunia hybrida*', *BMC Genomics*, 18: 589.
Rich, Mélanie K., Martine Schorderet, Laure Bapaume, Laurent Falquet, Patrice Morel, Michiel Vandenbussche, and Didier Reinhardt. 2015. 'The *Petunia* GRAS transcription factor ATA/RAM1 regulates symbiotic gene expression and fungal morphogenesis in arbuscular mycorrhiza', *Plant Physiol*, 168: 788-97.
Ried, Martina Katharina, Aline Banhara, Andreas Binder, Fang-Hu Hwu, Andrea A. Gust, Caroline Höfle, Ralph Hückelhoven, Thorsten Nürnberger, and Martin Parniske. 2018. 'Symbiosis-related genes sustain the development of a downy mildew pathogen on *Arabidopsis thaliana*', *bioRxiv*.
Rodenburg, S. Y. A., M. F. Seidl, D. de Ridder, and F. Govers. 2018. 'Genome-wide characterization of Phytophthora infestans metabolism: a systems biology approach', *Mol Plant Pathol*, 19: 1403-13.

Ropars, Jeanne, Kinga Sędzielewska Toro, Jessica Noel, Adrian Pelin, Philippe Charron, Laurent Farinelli, Timea Marton, Manuela Krüger, Jörg Fuchs, Andreas Brachmann, and Nicolas Corradi. 2016. 'Evidence for the sexual origin of heterokaryosis in arbuscular mycorrhizal fungi', *Nat Microbiol*, 1: doi:10.1038/nmicrobiol.2016.33.

Roth, R., M. Chiapello, H. Montero, P. Gehrig, J. Grossmann, K. O'Holleran, D. Hartken, F. Walters, S. Y. Yang, S. Hillmer, K. Schumacher, S. Bowden, M. Craze, E. J. Wallington, A. Miyao, R. Sawers, E. Martinoia, and U. Paszkowski. 2018. 'A rice Serine/Threonine receptor-like kinase regulates arbuscular mycorrhizal symbiosis at the peri-arbuscular membrane', *Nat Commun*, 9: 4677.

Roth, Ronelle, and Uta Paszkowski. 2017. 'Plant carbon nourishment of arbuscular mycorrhizal fungi', *Current Opinion in Plant Biology*, 39: 50-56.

Roux, B., N. Rodde, M. F. Jardinaud, T. Timmers, L. Sauviac, and L. Cottret. 2014. 'An integrated analysis of plant and bacterial gene expression in symbiotic root nodules using laser-capture microdissection coupled to RNA sequencing', *Plant J*, 77.

Rub, A., M. Arish, S. A. Husain, N. Ahmed, and Y. Akhter. 2013. 'Host-lipidome as a potential target of protozoan parasites', *Microbes Infect*, 15: 649-60.

Ruiz-Lozano, J. M. 2003. 'Arbuscular mycorrhizal symbiosis and alleviation of osmotic stress. New perspectives for molecular studies', *Mycorrhiza*, 13: 309-17.

Rutter, B. D., and R. W. Innes. 2018. 'Extracellular vesicles as key mediators of plant-microbe interactions', *Current Opinion in Plant Biology*, 44: 16-22.

Saito, K, M Yoshikawa, K Yano, H Miwa, H Uchida, E Azamizu, S Sato, S Tabata, H Imaizumi-Anraku, Y Umehara, H Kouchi, Y Murooka, K Szczyglowski, JA Downie, M Parniske, M Hayashi, and M Kawaguchi. 2007. 'NUCLEOPORIN85 is required for calcium spiking, fungal and bacterial symbiosis and seed production in *Lotus japonicus*', *Plant Cell*, 19: 610-24.

Salanoubat, M., S. Genin, F. Artiguenave, J. Gouzy, S. Mangenot, M. Arlat, A. Billault, P. Brottier, J. C. Camus, L. Cattolico, M. Chandler, N. Choisne, C. Claudel-Renard, S. Cunnac, N. Demange, C. Gaspin, M. Lavie, A. Moisan, C. Robert, W. Saurin, T. Schiex, P. Siguier, P. Thébault, M. Whalen, P. Wincker, M. Levy, J. Weissenbach, and C. A. Boucher. 2002. 'Genome sequence of the plant pathogen *Ralstonia solanacearum*', *Nature*, 415: 497.

Salvioli, Alessandra, Stefano Ghignone, Mara Novero, Lorella Navazio, Francesco Venice, Paolo Bagnaresi, and Paola Bonfante. 2016. 'Symbiosis with an endobacterium increases the fitness of a mycorrhizal fungus, raising its bioenergetic potential', *ISME J*, 10: 130-44.

Samuel, M., M. Bleackley, M. Anderson, and S. Mathivanan. 2015. 'Extracellular vesicles including exosomes in cross kingdom regulation: a viewpoint from plant-fungal interactions', *Front Plant Sci*, 6: 766.

Sato, Takumi, Tatsuhiro Ezawa, Weiguo Cheng, and Keitaro Tawaraya. 2015. 'Release of acid phosphatase from extraradical hyphae of arbuscular mycorrhizal fungus *Rhizophagus clarus*', *Soil Science and Plant Nutrition*, 61: 269-74.

Schaarschmidt, Sara, Mari-Cruz Gonzalez, Thomas Roitsch, Dieter Strack, Uwe Sonnewald, and Bettina Hause. 2007. 'Regulation of arbuscular mycorrhization by carbon. The symbiotic interaction cannot be improved by increased carbon availability accomplished by root-specifically enhanced invertase activity', *Plant Physiol*, 143: 1827-40.

Schaarschmidt, Sara, Thomas Roitsch, and Bettina Hause. 2006. 'Arbuscular mycorrhiza induces gene expression of the apoplastic invertase *LIN6* in tomato (*Lycopersicon esculentum*) roots', *Journal of Experimental Botany*, 57: 4015-23.
Schachtman, Daniel P., Robert J. Reid, and S. M. Ayling. 1998. 'Phosphorus uptake by plants: From soil to cell', *Plant Physiol*, 116: 447.
Schornack, Sebastian, Mireille van Damme, Tolga O. Bozkurt, Liliana M. Cano, Matthew Smoker, Marco Thines, Elodie Gaulin, Sophien Kamoun, and Edgar Huitema. 2010. 'Ancient class of translocated oomycete effectors targets the host nucleus', *PNAS*, 107: 17421.
Schüßler, A, D Schwarzott, and C Walker. 2001. 'A new fungal phylum *Glomeromycota*: phylogeny and evolution', *Mycological research*, 105: 1413-21.
Schwelm, A., J. Fogelqvist, A. Knaust, S. Julke, T. Lilja, G. Bonilla-Rosso, M. Karlsson, A. Shevchenko, V. Dhandapani, S. R. Choi, H. G. Kim, J. Y. Park, Y. P. Lim, J. Ludwig-Muller, and C. Dixelius. 2015. 'The *Plasmodiophora brassicae* genome reveals insights in its life cycle and ancestry of chitin synthases', *Sci Rep*, 5: doi:10.1038/srep11153.
Sędzielewska Toro, Kinga, and Andreas Brachmann. 2016. 'The effector candidate repertoire of the arbuscular mycorrhizal fungus *Rhizophagus clarus*', *BMC Genomics*, 17: 101.
Selosse, Marc-André, Alain Bessis, and María J. Pozo. 2014. 'Microbial priming of plant and animal immunity: symbionts as developmental signals', *Trends in Microbiology*, 22: 607-13.
Sessitsch, Angela, and Birgit Mitter. 2014. '21st century agriculture: integration of plant microbiomes for improved crop production and food security', *Microbial Biotechnology*, 8: 32-33.
Shachar-Hill, Y., P. E. Pfeffer, D. Douds, S. F. Osman, L. W. Doner, and R. G. Ratcliffe. 1995. 'Partitioning of intermediary carbon metabolism in vesicular-arbuscular mycorrhizal leek', *Plant Physiol*, 108: 7-15.
Shibata, Reiko, and Katsuya Yano. 2003. 'Phosphorus acquisition from non-labile sources in peanut and pigeonpea with mycorrhizal interaction', *Applied Soil Ecology*, 24: 133-41.
Siciliano, Valeria, Andrea Genre, Raffaella Balestrini, Gilda Cappellazzo, Pierre J. G. M. deWit, and Paola Bonfante. 2007. 'Transcriptome analysis of arbuscular mycorrhizal roots during development of the prepenetration apparatus', *Plant Physiol*, 144: 1455-66.
Sieberer, Björn J., Mireille Chabaud, Joëlle Fournier, Antonius C. J. Timmers, and David G. Barker. 2012. 'A switch in Ca2+ spiking signature is concomitant with endosymbiotic microbe entry into cortical root cells of *Medicago truncatula*', *Plant J*, 69: 822-30.
Singh, S, K Katzer, J Lambert, MR Cerri, and M Parniske. 2014. 'CYCLOPS, a DNA-binding transcriptional activator, orchestrates symbiotic root nodule development', *Cell Host Microbe*, 15: 139-52.
Slusarenko, Alan J., and Nikolaus L. Schlaich. 2003. 'Downy mildew of *Arabidopsis thaliana* caused by *Hyaloperonospora parasitica* (formerly *Peronospora parasitica*)', *Molecular Plant Pathology*, 4: 159-70.
Smith, S. E., F. A. Smith, and I. Jakobsen. 2004. 'Functional diversity in arbuscular mycorrhizal (AM) symbioses: the contribution of the mycorrhizal P uptake pathway is not correlated with mycorrhizal responses in growth or total P uptake', *New Phytol*, 162: 511-24.

Smith, Sally E., Iver Jakobsen, Mette Gronlund, and F. Andrew Smith. 2011. 'Roles of arbuscular mycorrhizas in plant phosphorus nutrition: interactions between pathways of phosphorus uptake in arbuscular mycorrhizal roots have important implications for understanding and manipulating plant phosphorus acquisition', *Plant Physiol*, 156: 1050-57.

Smith, Sally E., and F. Andrew Smith. 2011. 'Roles of arbuscular mycorrhizas in plant nutrition and growth: New paradigms from cellular to ecosystem scales', *Annual Review of Plant Biology*, 62: 227-50.

Smith, SE. , and DJ. Read. 2008. *Mycorrhizal Symbiosis* (Academic Press London).

Solaiman, M, T Ezawa, T Kojima, and M. Saito. 1999. 'Polyphosphates in intraradical and extraradical hyphae of an arbuscular mycorrhizal fungus, *Gigaspora margarita*', *Appl Environ Microbiol*, 65.

Soylu, E. M., and S. Soylu. 2003. 'Light and electron microscopy of the compatible interaction between *Arabidopsis* and the downy mildew pathogen *Peronospora parasitica*', *Journal of Phytopathology*, 151: 300-06.

Spanu, Pietro D., James C. Abbott, Joelle Amselem, Timothy A. Burgis, Darren M. Soanes, Kurt Stüber, Emiel Ver Loren van Themaat, James K. M. Brown, Sarah A. Butcher, Sarah J. Gurr, Marc-Henri Lebrun, Christopher J. Ridout, Paul Schulze-Lefert, Nicholas J. Talbot, Nahal Ahmadinejad, Christian Ametz, Geraint R. Barton, Mariam Benjdia, Przemyslaw Bidzinski, Laurence V. Bindschedler, Maike Both, Marin T. Brewer, Lance Cadle-Davidson, Molly M. Cadle-Davidson, Jerome Collemare, Rainer Cramer, Omer Frenkel, Dale Godfrey, James Harriman, Claire Hoede, Brian C. King, Sven Klages, Jochen Kleemann, Daniela Knoll, Prasanna S. Koti, Jonathan Kreplak, Francisco J. López-Ruiz, Xunli Lu, Takaki Maekawa, Siraprapa Mahanil, Cristina Micali, Michael G. Milgroom, Giovanni Montana, Sandra Noir, Richard J. O'Connell, Simone Oberhaensli, Francis Parlange, Carsten Pedersen, Hadi Quesneville, Richard Reinhardt, Matthias Rott, Soledad Sacristán, Sarah M. Schmidt, Moritz Schön, Pari Skamnioti, Hans Sommer, Amber Stephens, Hiroyuki Takahara, Hans Thordal-Christensen, Marielle Vigouroux, Ralf Weßling, Thomas Wicker, and Ralph Panstruga. 2010. 'Genome expansion and gene loss in powdery mildew fungi reveal tradeoffs in extreme parasitism', *Science*, 330: 1543-46.

Spatafora, J. W., Y. Chang, G. L. Benny, K. Lazarus, M. E. Smith, M. L. Berbee, G. Bonito, N. Corradi, I. Grigoriev, A. Gryganskyi, T. Y. James, K. O'Donnell, R. W. Roberson, T. N. Taylor, J. Uehling, R. Vilgalys, M. M. White, and J. E. Stajich. 2016. 'A phylum-level phylogenetic classification of zygomycete fungi based on genome-scale data', *Mycologia*, 108: 1028-46.

Stassen, Joost H. M., and Guido Van den Ackerveken. 2011. 'How do oomycete effectors interfere with plant life?', *Current Opinion in Plant Biology*, 14: 407-14.

Stracke, Silke, Catherine Kistner, Satoko Yoshida, Lonneke Mulder, Shusei Sato, Takakazu Kaneko, Satoshi Tabata, Niels Sandal, Jens Stougaard, Krzysztof Szczyglowski, and Martin Parniske. 2002. 'A plant receptor-like kinase required for both bacterial and fungal symbiosis', *Nature*, 417: 959-62.

Sun, Jongho, J. Benjamin Miller, Emma Granqvist, Audrey Wiley-Kalil, Enrico Gobbato, Fabienne Maillet, Sylvain Cottaz, Eric Samain, Muthusubramanian Venkateshwaran, Sébastien Fort, Richard J. Morris, Jean-Michel Ané, Jean Dénarié, and Giles E.D. Oldroyd. 2015. 'Activation of symbiosis signaling by arbuscular mycorrhizal fungi in legumes and rice', *Plant Cell*, 27: 823-38.

Takeda, Naoya, Yoshihiro Handa, Syusaku Tsuzuki, Mikiko Kojima, Hitoshi Sakakibara, and Masayoshi Kawaguchi. 2015. 'Gibberellins interfere with symbiosis signaling and gene expression and alter colonization by arbuscular mycorrhizal fungi in *Lotus japonicus*', *Plant Physiol*, 167: 545-57.

Takeda, Naoya, Takaki Maekawa, and Makoto Hayashi. 2012. 'Nuclear-localized and deregulated calcium- and calmodulin-dependent protein kinase activates rhizobial and mycorrhizal responses in *Lotus japonicus*', *Plant Cell*, 24: 810-22.

Tamura, Yosuke, Yoshihiro Kobae, Toyotaka Mizuno, and Shingo Hata. 2012. 'Identification and expression analysis of arbuscular mycorrhiza-inducible phosphate transporter genes of soybean', *Bioscience, Biotechnology, and Biochemistry*, 76: 309-13.

Tanaka, Yoko, and Katsuya Yano. 2005. 'Nitrogen delivery to maize via mycorrhizal hyphae depends on the form of N supplied', *Plant, Cell & Environment*, 28: 1247-54.

Tang, Nianwu, Hélène San Clemente, Sébastien Roy, Guillaume Bécard, Bin Zhao, and Christophe Roux. 2016. 'A survey of the gene repertoire of *Gigaspora rosea* unravels conserved features among glomeromycota for obligate biotrophy', *Front Microbiol*, 7: doi: 10.3389/fmicb.2016.00233.

Teichmann, B., U. Linne, S. Hewald, M. A. Marahiel, and M. Bolker. 2007. 'A biosynthetic gene cluster for a secreted cellobiose lipid with antifungal activity from *Ustilago maydis*', *Mol Microbiol*, 66: 525-33.

Thines, Marco. 2018. 'Oomycetes', *Current Biology*, 28: R812-R13.

Thines, Marco, and Sophien Kamoun. 2010. 'Oomycete–plant coevolution: recent advances and future prospects', *Current Opinion in Plant Biology*, 13: 427-33.

Tisserant, E., A. Kohler, P. Dozolme-Seddas, R. Balestrini, K. Benabdellah, A. Colard, D. Croll, C. Da Silva, S. K. Gomez, R. Koul, N. Ferrol, V. Fiorilli, D. Formey, Ph Franken, N. Helber, M. Hijri, L. Lanfranco, E. Lindquist, Y. Liu, M. Malbreil, E. Morin, J. Poulain, H. Shapiro, D. van Tuinen, A. Waschke, C. Azcón-Aguilar, G. Bécard, P. Bonfante, M. J. Harrison, H. Küster, P. Lammers, U. Paszkowski, N. Requena, S. A. Rensing, C. Roux, I. R. Sanders, Y. Shachar-Hill, G. Tuskan, J. P. W. Young, V. Gianinazzi-Pearson, and F. Martin. 2012. 'The transcriptome of the arbuscular mycorrhizal fungus *Glomus intraradices* (DAOM 197198) reveals functional tradeoffs in an obligate symbiont', *New Phytol*, 193: 755-69.

Tisserant, Emilie, Mathilde Malbreil, Alan Kuo, Annegret Kohler, Aikaterini Symeonidi, Raffaella Balestrini, Philippe Charron, Nina Duensing, Nicolas Frei dit Frey, Vivienne Gianinazzi-Pearson, Luz B. Gilbert, Yoshihiro Handa, Joshua R. Herr, Mohamed Hijri, Raman Koul, Masayoshi Kawaguchi, Franziska Krajinski, Peter J. Lammers, Frederic G. Masclaux, Claude Murat, Emmanuelle Morin, Steve Ndikumana, Marco Pagni, Denis Petitpierre, Natalia Requena, Pawel Rosikiewicz, Rohan Riley, Katsuharu Saito, Hélène San Clemente, Harris Shapiro, Diederik van Tuinen, Guillaume Bécard, Paola Bonfante, Uta Paszkowski, Yair Y. Shachar-Hill, Gerald A. Tuskan, Peter W. Young, Ian R. Sanders, Bernard Henrissat, Stefan A. Rensing, Igor V. Grigoriev, Nicolas Corradi, Christophe Roux, and Francis Martin. 2013. 'Genome of an arbuscular mycorrhizal fungus provides insight into the oldest plant symbiosis', *PNAS*: 20117–22.

To, A., J. Joubes, G. Barthole, A. Lecureuil, A. Scagnelli, S. Jasinski, L. Lepiniec, and S. Baud. 2012. 'WRINKLED transcription factors orchestrate tissue-specific regulation of fatty acid biosynthesis in *Arabidopsis*', *Plant Cell*, 24: 5007-23.

Toledo D. , D'Avila H., Melo R.C.N. 2016. 'Host lipid bodies as platforms for intracellular survival of protozoan parasites', *Front Immunol*, 7: doi: 10.3389/mmu.2016.00174.

Trépanier, M, G Bécard, P Moutoglis, C Willemot, S Gagné, TJ Avis, and JA Rioux. 2005. 'Dependence of arbuscular-mycorrhizal fungi on their plant host for palmitic acid synthesis', *Appl Environ Microbiol*, 71: 5341–47.

Triana, S., H. de Cock, R. A. Ohm, G. Danies, H. A. B. Wosten, S. Restrepo, A. F. Gonzalez Barrios, and A. Celis. 2017. 'Lipid metabolic versatility in *Malassezia* spp. yeasts studied through metabolic modeling', *Front Microbiol*, 8: doi: 10.3389/fmicb.2017.01772.

Triana, S., A. Gonzalez, R. A. Ohm, H. A. Wosten, H. de Cock, S. Restrepo, and A. Celis. 2015. 'Draft genome sequence of the animal and human pathogen *Malassezia* pachydermatis strain CBS 1879', *Genome Announc*, 3: doi: 10.1128/genomeA.01197-15.

Tsuzuki, S., Y. Handa, N. Takeda, and M. Kawaguchi. 2016. 'Strigolactone-induced putative secreted protein 1 is required for the establishment of symbiosis by the arbuscular mycorrhizal fungus *Rhizophagus irregularis*', *Mol Plant Microbe Interact*, 29: 277-86.

Uetake, Y., T. Kojima, T. Ezawa, and M. Saito. 2002. 'Extensive tubular vacuole system in an arbuscular mycorrhizal fungus, *Gigaspora margarita*', *New Phytol*, 154: 761-68.

Venkateshwaran, Muthusubramanian, Ana Cosme, Lu Han, Mari Banba, Kenneth A. Satyshur, Enrico Schleiff, Martin Parniske, Haruko Imaizumi-Anraku, and Jean-Michel Ané. 2012. 'The recent evolution of a symbiotic ion channel in the legume family altered ion conductance and improved functionality in calcium signaling', *Plant Cell*, 24: 2528-45.

Venkateshwaran, Muthusubramanian, Dhileepkumar Jayaraman, Mireille Chabaud, Andrea Genre, Allison J. Balloon, Junko Maeda, Kari Forshey, Désirée den Os, Nicholas W. Kwiecien, Joshua J. Coon, David G. Barker, and Jean-Michel Ané. 2015. 'A role for the mevalonate pathway in early plant symbiotic signaling', *PNAS*, 112: 9781.

Visser, Bertanne, Cécile Le Lann, Frank J. den Blanken, Jeffrey A. Harvey, Jacques J. M. van Alphen, and Jacintha Ellers. 2010. 'Loss of lipid synthesis as an evolutionary consequence of a parasitic lifestyle', *PNAS*, 107: 8677-82.

Voelker, T. A., A. C. Worrell, L. Anderson, J. Bleibaum, C. Fan, D. J. Hawkins, S. E. Radke, and H. M. Davies. 1992. 'Fatty acid biosynthesis redirected to medium chains in transgenic oilseed plants', *Science*, 257: 72-74.

Volpe, Veronica, Marco Giovannetti, Xue-Guang Sun, Valentina Fiorilli, and Paola Bonfante. 2015. 'The phosphate transporters LjPT4 and MtPT4 mediate early root responses to phosphate status in non mycorrhizal roots', *Plant, Cell & Environment*, 39: 660-71.

Walder, F., H. Niemann, M. Natarajan, M. F. Lehmann, T. Boller, and A. Wiemken. 2012. 'Mycorrhizal networks: common goods of plants shared under unequal terms of trade', *Plant Physiol*, 159: 789-97.

Wang, B, LH Yeung, JY Xue, Y Liu, Ané. JM, and JL Quiu. 2010. 'Prensece of three mycorrhizal genes in the common ancestor of land plants suggests a key role of mycorrhizas in the colonization of land by plants', *New Phytol*, 186: 514-25.

Wang, Ertao, Sebastian Schornack, JF Marsh, Enrico Gobbato, Benjamin Schwessinger, Peter Eastmond, Michael Schultze, Sophien Kamoun, and GED Oldroyd. 2012. 'A common signaling process that promotes mycorrhizal and oomycete colonization of plants', *Current Biology*, 22: 2242-46.

Wang, Ertao, Nan Yu, S. Asma Bano, Chengwu Liu, Anthony J. Miller, Donna Cousins, Xiaowei Zhang, Pascal Ratet, Million Tadege, Kirankumar S. Mysore, J. Allan Downie, Jeremy D. Murray, Giles E. D. Oldroyd, and Michael Schultze. 2014. 'A H+-ATPase that energizes nutrient uptake during mycorrhizal symbioses in Rice and *Medicago truncatula*', *Plant Cell*.

Weiberg, Arne, Ming Wang, Feng-Mao Lin, Hongwei Zhao, Zhihong Zhang, Isgouhi Kaloshian, Hsien-Da Huang, and Hailing Jin. 2013. 'Fungal small RNAs suppress plant immunity by hijacking host RNA interference pathways', *Science*, 342: 118.

Wewer, Vera, Mathias Brands, and Peter Dörmann. 2014. 'Fatty acid synthesis and lipid metabolism in the obligate biotrophic fungus *Rhizophagus irregularis* during mycorrhization of *Lotus japonicus*', *Plant J*, 79: 398-412.

Whisson, SC, PC Boevink, L Moleleki, AO Avrova, JG Morales, EM Gilroy, MR Armstrong, S Grouffaud, P van West, S Chapman, I Hein, IK Toth, L Pritchard, and PR Birch. 2007. 'A translocation signal for delivery of oomycete effector proteins into host plant cells', *Nature*, 450: 115 - 18.

Wright, D. P., D. J. Read, and J. D. Scholes. 2002. 'Mycorrhizal sink strength influences whole plant carbon balance of *Trifolium repens* L', *Plant, Cell & Environment*, 21: 881-91.

Wu, Guangxi, He Zhao, Chenhao Li, Menaka Priyadarsani Rajapakse, Wing Cheong Wong, Jun Xu, Charles W. Saunders, Nancy L. Reeder, Raymond A. Reilman, Annika Scheynius, Sheng Sun, Blake Robert Billmyre, Wenjun Li, Anna Floyd Averette, Piotr Mieczkowski, Joseph Heitman, Bart Theelen, Markus S. Schröder, Paola Florez De Sessions, Geraldine Butler, Sebastian Maurer-Stroh, Teun Boekhout, Niranjan Nagarajan, and Thomas L. Dawson, Jr. 2015. 'Genus-wide comparative genomics of *Malassezia* delineates its phylogeny, physiology, and niche adaptation on human skin', *PLoS Genetics*, 11: DOI:10.1371/journal.pgen.1005614.

Xie, Xianan, Hui Lin, Xiaowei Peng, Congrui Xu, Zhongfeng Sun, Kexin Jiang, Antian Huang, Xiaohui Wu, Nianwu Tang, Alessandra Salvioli, Paola Bonfante, and Bin Zhao. 2016. 'Arbuscular mycorrhizal symbiosis requires a phosphate transceptor in the *Gigaspora margarita* fungal symbiont', *Molecular Plant*, 9: 1583-608.

Xu, J., C. Saunders, P. Hu, R. Grant, T. Boekhout, E. Kuramae, J. Kronstad, Y. DeAngelis, N. Reeder, K. Johnstone, M. Leland, A. Fieno, W. Begley, Y. Sun, M. Lacey, T. Chaudhary, T. Keough, L. Chu, R. Sears, B. Yuan, and Dawson Jr. T. 2007. 'Dandruff-associated Malassezia genomes reveal convergent and divergent virulence traits shared with plant and human fungal pathogens', *PNAS*, 104: 18730-35.

Xue, L., L. Klinnawee, Y. Zhou, G. Saridis, V. Vijayakumar, M. Brands, P. Dormann, T. Gigolashvili, F. Turck, and M. Bucher. 2018. 'AP2 transcription factor CBX1 with a specific function in symbiotic exchange of nutrients in mycorrhizal *Lotus japonicus*', *PNAS*, 115: E9239-E46.

Xue, Li, Haitao Cui, Benjamin Buer, Vinod Vijayakumar, Pierre-Marc Delaux, Stefanie Junkermann, and Marcel Bucher. 2015. 'Network of GRAS transcription factors involved in the control of arbuscule development in *Lotus japonicus*', *Plant Physiol*, 167: 854-71.

Yang, Shu-Yi, Mette Grønlund, Iver Jakobsen, Marianne Suter Grotemeyer, Doris Rentsch, Akio Miyao, Hirohiko Hirochika, Chellian Santhosh Kumar, Venkatesan Sundaresan, Nicolas Salamin, Sheryl Catausan, Nicolas Mattes, Sigrid Heuer, and Uta Paszkowski. 2012. 'Nonredundant regulation of rice

arbuscular mycorrhizal symbiosis by two members of the PHOSPHATE TRANSPORTER1 gene family', *Plant Cell*, 24: 4236-51.
Yang, Weili, Jeffrey P. Simpson, Yonghua Li-Beisson, Fred Beisson, Mike Pollard, and John B. Ohlrogge. 2012. 'A land-plant-specific Glycerol-3-Phosphate Acyltransferase family in Arabidopsis: Substrate specificity, sn-2 preference, and evolution', *Plant Physiol*, 160: 638-52.
Yano, K, S Yoshida, J Müller, S Singh, M Banba, K Vickers, K Markmann, C White, B Schuller, S Sato, E Asamizu, S Tabata, Y Murooka, J Perry, TL Wang, M Kawaguchi, H Imaizumi-Anraku, M Hayashi, and M Parniske. 2008. 'CYCLOPS, a mediator of symbiotic intracellular accommodation', *PNAS*, 105: 20540-45.
Yeats, Trevor H., Laetitia B. B. Martin, Hélène M. F. Viart, Tal Isaacson, Yonghua He, Lingxia Zhao, Antonio J. Matas, Gregory J. Buda, David S. Domozych, Mads H. Clausen, and Jocelyn K. C. Rose. 2012. 'The identification of cutin synthase: formation of the plant polyester cutin', *Nat Chem Biol*, 8: 609-11.
Yoneyama, Kaori, Xiaonan Xie, Hyun Kim, Takaya Kisugi, Takahito Nomura, Hitoshi Sekimoto, Takao Yokota, and Koichi Yoneyama. 2012. 'How do nitrogen and phosphorus deficiencies affect strigolactone production and exudation?', *Planta*, 235: 1197-207.
Yoneyama, Kaori, Xiaonan Xie, Dai Kusumoto, Hitoshi Sekimoto, Yukihiro Sugimoto, Yasutomo Takeuchi, and Koichi Yoneyama. 2007. 'Nitrogen deficiency as well as phosphorus deficiency in sorghum promotes the production and exudation of 5-deoxystrigol, the host recognition signal for arbuscular mycorrhizal fungi and root parasites', *Planta*, 227: 125-32.
Zhang, Quan, Laura A. Blaylock, and Maria J. Harrison. 2010. 'Two *Medicago truncatula* half-ABC transporters are essential for arbuscule development in arbuscular mycorrhizal symbiosis', *Plant Cell*, 22: 1483-97.
Zhang, Xiaowei, Wentao Dong, Jongho Sun, Feng Feng, Yiwen Deng, Zuhua He, E. D. Oldroyd Giles, and Ertao Wang. 2014. 'The receptor kinase CERK1 has dual functions in symbiosis and immunity signalling', *Plant J*, 81: 258-67.
Zipfel, C., and G. E. Oldroyd. 2017. 'Plant signalling in symbiosis and immunity', *Nature*, 543: 328-36.
Zoeller, M., N. Stingl, M. Krischke, A. Fekete, F. Waller, S. Berger, and M. J. Mueller. 2012. 'Lipid profiling of the *Arabidopsis* hypersensitive response reveals specific lipid peroxidation and fragmentation processes: biogenesis of pimelic and azelaic acid', *Plant Physiol*, 160: 365-78.

XII. List of Figures

XIII. List of Tables

XIV. Acknowledgements

Over the last four years, many people have significantly contributed directly and indirectly to this work and without whom I would have not been able to finish my doctoral thesis.
Foremost, I would like to express my most profound gratitude and thanks to my supervisor Prof. Dr. Caroline Gutjahr. Throughout the years, Caroline has always been a constant source of inspiration, motivation, and support. It has always been fascinating and encouraging for me to witness her lust for science, her thirst for knowledge, and her overall diligence. With her enormous knowledge and expertise, she has always been the most essential support of this work and vital for my education. I am thankful to her for giving me the chance to activly participate in the world of science by inviting many outstanding researchers and enabling me to visit international conferences. Under her provident guidance, the lab has prospered considerably in the last years and she managed to create a fruitful scientific as well as joyful inter-personal environment in the lab. I am extraordinarily grateful for her constant kindness and empathy, even in rush and busy periods. Lastly, I would like to thank her for giving me this fascinating project and for training me substantially in various aspects.

I also would like to deeply thank Prof. Martin Parniske. His multifaceted support was crucial for the outcome of this thesis. His comments on my work have always been of special relevance and impact for the progress of my work. Moreover, he created an inspiring and enjoyable work environment at the LMU Genetics which allowed me to benefit substantially from and to broaden my horizon in numerous ways. I always appreciated his constant effort to train all students for good scientific practices. Finally, I would like to thank him for his time to evaluate my doctoral thesis.

In this line, I also would like to thank the remaining members of my thesis committee Prof. Dr. Thomas Naegele, Dr. Cordelia Bolle, Prof. Dr. Andreas Klingl and Prof. Dr. Nicolas Gompel for giving their valuable time and efforts to asses my research work.

I would like to express my gratitude to all members of the Gutjahr Lab and to all my office mates (Chloe, Corinna, Basti, Peter, Michi, Jose, Flo, and Fan) for the help, kindness, and fun in everyday lab life. Especially, I would like to acknowledge Verena Klingl, Michael Paries and Salar Torabi for becoming true friends outside of the lab.

The success of this work relied on great support from various people.
First of all, I would like to thank especially Dr. Priya Pimprika for her considerable work and the friendly and cooperative collaboration on the AM lipid transfer project. In this line, I am also very grateful for the hands-on support by Verena Klingl and my Hiwi Julia Mayer. Further, I would like to thank Mathias Brands, Dr. Vera Wewer, and Prof. Peter Dörmann for their collaboration throughout of this work. Dr. Claudia Huber and Prof. Wolfgang Eisenreich performed isotopolg profiling and contributed therefore substantially to the outcome of this thesis.
Big thanks to Aline Banhara who trained me in *Hpa* work. In this respect, I would also like to acknowledge the support of my *Hpa* mates FangYu Hwu and Florian Dunker.

I also would like to express my gratitude to the SFB924 for funding this project and my conference visits. Moreover, the SFB924 had valuable impact on this work and my educational progress by organizing conferences, retreats, as well as training courses.

In the end, I would like to thank all my loved ones outside of the science bubble. The support and love of my friends and my family have always been the most essential basis I could build on. Very special thanks and gratitude to my parents, Doris and Dietrich, for their endless nurture as well as to my sister Sonja and my lady Laura for open ears, help, suggestions, understanding, and all the Pizza dates!

XV. Copyright Clearance

Figure 1: (A) Schematic representation of the AMS colonization process of the plant root cell, dissected in five distinct stages. (B) Schematic representation of seven stages of arbuscule development inside a cortical root cell. (modified figure from Pimprikar and Gutjahr 2018)

OXFORD UNIVERSITY PRESS LICENSE TERMS AND CONDITIONS

Nov 08, 2018

This Agreement between LMU Muncih -- Andreas Keymer ("You") and Oxford University Press ("Oxford University Press") consists of your license details and the terms and conditions provided by Oxford University Press and Copyright Clearance Center.

License Number	4464100003172
License date	Nov 08, 2018
Licensed content publisher	Oxford University Press
Licensed content publication	Plant and Cell Physiology
Licensed content title	Transcriptional Regulation of Arbuscular Mycorrhiza Development
Licensed content author	Pimprikar, Priya; Gutjahr, Caroline
Licensed content date	Feb 7, 2018
Type of Use	Thesis/Dissertation
Institution name	
Title of your work	Dependence of lipids for plant microbe interactions
Publisher of your work	n/a
Expected publication date	Jan 2019
Permissions cost	0.00 USD
Value added tax	0.00 USD
Total	0.00 USD
Title	Dependence of lipids for plant microbe interactions
Institution name	n/a
Expected presentation date	Jan 2019
Portions	Figure 1 " Stage-specific gene expression during AM development. "
Requestor Location	LMU Muncih Großhadernerstrasse 2-4 Martinsried, 82152 Germany Attn: LMU Muncih
Publisher Tax ID	GB125506730
Billing Type	Invoice
Billing Address	LMU Muncih Großhadernerstrasse 2-4 Martinsried, Germany 82152 Attn: LMU Muncih
Total	0.00 USD
Terms and Conditions	

Figure 2: Schematic overview of AM signal transduction upon Myc factor perception via the common symbiosis signaling pathway in a root cell (modified figure from Singh and Parniske 2012)

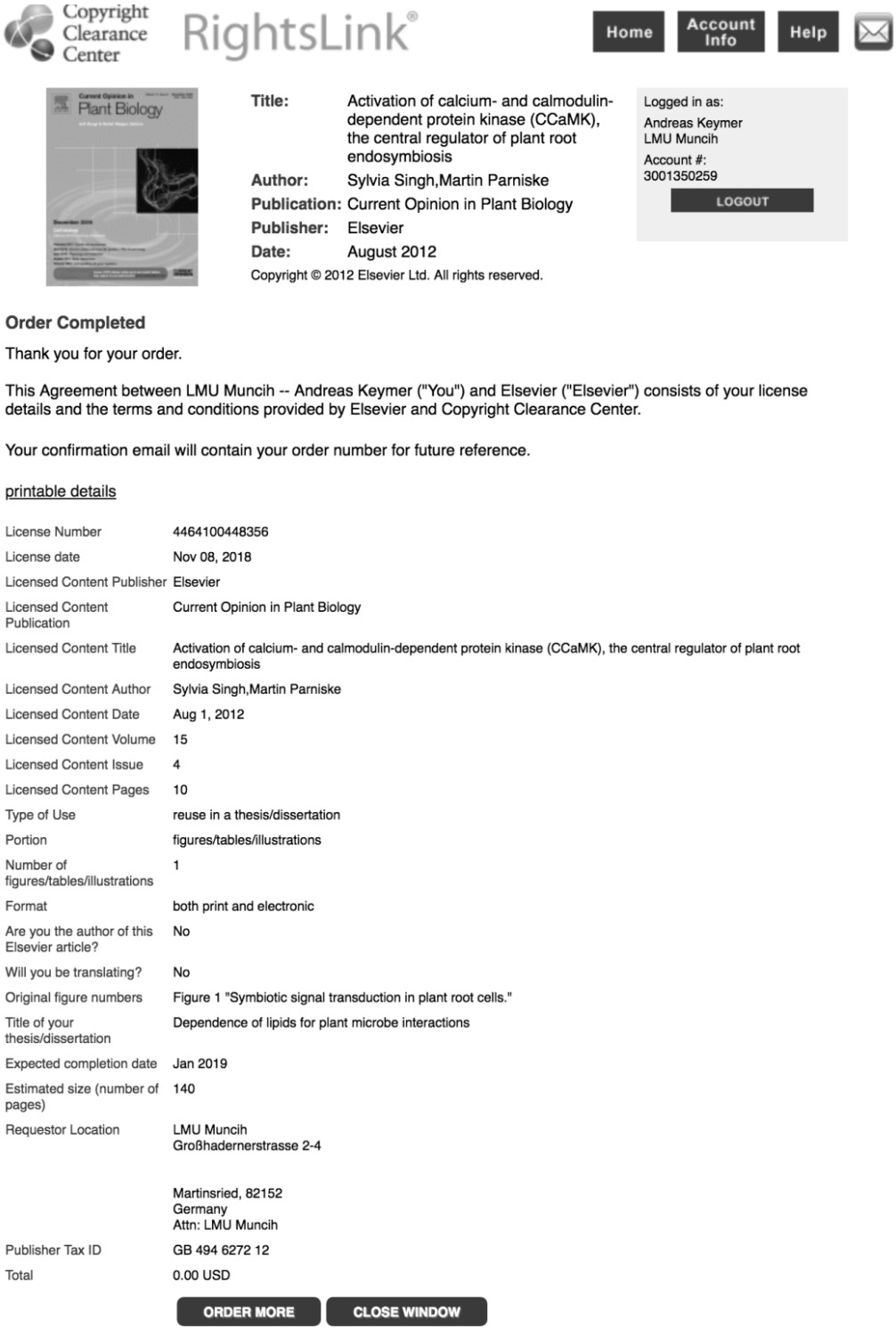

Copyright Clearance Center RightsLink®

Home | Account Info | Help

Title: Activation of calcium- and calmodulin-dependent protein kinase (CCaMK), the central regulator of plant root endosymbiosis
Author: Sylvia Singh,Martin Parniske
Publication: Current Opinion in Plant Biology
Publisher: Elsevier
Date: August 2012
Copyright © 2012 Elsevier Ltd. All rights reserved.

Logged in as:
Andreas Keymer
LMU Muncih
Account #:
3001350259
LOGOUT

Order Completed

Thank you for your order.

This Agreement between LMU Muncih -- Andreas Keymer ("You") and Elsevier ("Elsevier") consists of your license details and the terms and conditions provided by Elsevier and Copyright Clearance Center.

Your confirmation email will contain your order number for future reference.

printable details

License Number	4464100448356
License date	Nov 08, 2018
Licensed Content Publisher	Elsevier
Licensed Content Publication	Current Opinion in Plant Biology
Licensed Content Title	Activation of calcium- and calmodulin-dependent protein kinase (CCaMK), the central regulator of plant root endosymbiosis
Licensed Content Author	Sylvia Singh,Martin Parniske
Licensed Content Date	Aug 1, 2012
Licensed Content Volume	15
Licensed Content Issue	4
Licensed Content Pages	10
Type of Use	reuse in a thesis/dissertation
Portion	figures/tables/illustrations
Number of figures/tables/illustrations	1
Format	both print and electronic
Are you the author of this Elsevier article?	No
Will you be translating?	No
Original figure numbers	Figure 1 "Symbiotic signal transduction in plant root cells."
Title of your thesis/dissertation	Dependence of lipids for plant microbe interactions
Expected completion date	Jan 2019
Estimated size (number of pages)	140
Requestor Location	LMU Muncih Großhadernerstrasse 2-4 Martinsried, 82152 Germany Attn: LMU Muncih
Publisher Tax ID	GB 494 6272 12
Total	0.00 USD

ORDER MORE | CLOSE WINDOW

Figure 3: Metabolic fluxes and long-distance transport in arbuscular mycorrhiza symbiosis (modified figure from Parniske 2008)

Figure 4: Arbuscule phenotype of AM-specific lipid mutant plants and schematic representation of experimental approaches, which demonstrated lipid transfer from plant to fungus. (Figure from Keymer & Gutjahr 2018)

Table 1: Organisms associated with their host in order to exploit lipids. Bright colors indicate interactions, with reported lipid scavenging from the host. Faint colors indicate interactions, for which circumstantial evidence suggest lipid dependence or lipid parasitism. The ability to produce FA is based on the presence of fatty acid synthase genes in respective genomes. (modified table from Keymer & Gutjahr 2018)